# Modelling the Removal of Airborne Contaminants in Swine Facilities by a Biotrickling Filter

A Thesis Submitted to the

College of Graduate Studies and Research

In Partial Fulfillment of the Requirements

For the Degree of Doctor of Philosophy (Ph.D.)

In the Department of Chemical and Biological Engineering

University of Saskatchewan, Canada

By

Myra Martel

## PERMISSION TO USE

In presenting this thesis in partial fulfillment of the requirements for a doctorate of philosophy from the University of Saskatchewan, I agree that the Libraries of this University may make it freely available for inspection. I further agree that permission for copying of this thesis in any manner, in whole or in part, for scholarly purposes may be granted by Dr. Stéphane P. Lemay and Dr. Bernardo Predicala who supervised my thesis work or, in their absence, by the Head of the Department or the Dean of the College of Engineering. It is understood that any copying or publication or use of this thesis or parts thereof for financial gain shall not be allowed without my written permission. It is also understood that due recognition shall be given to me and to the University of Saskatchewan in any scholarly use which may be made of any material in my thesis. Requests for permission to copy or to make other use of material in this thesis in whole or part should be addressed to:

Head of the Department of Chemical and Biological Engineering

University of Saskatchewan

57 Campus Drive

Saskatoon, Saskatchewan

Canada S7N 5A9

## ABSTRACT

The overall objective of this dissertation work was to optimize the performance of biotrickling filters in reducing emissions of odour and harmful substances from swine facilities. The parameters and operating conditions that have significant impact on the treatment process were identified through a modelling study.

Key odour components were selected to serve as model pollutants, which were identified from linear relationships between the logarithm of odour emission and the logarithm of pollutant emission/odour intensity and from odour indices. The potential model pollutants identified were ammonia, dimethyl sulphide, and *p*-cresol.

Different sets of shake-flask experiments were conducted to assess different inocula, to determine the optimum pH, and to estimate the biokinetic parameters for the biodegradation of ammonia and *p*-cresol. Among the three inocula evaluated, the complex inoculum taken from an existing biotrickling filter showed the best performance in terms of *p*-cresol and ammonium reduction. The results also showed that the highest *p*-cresol uptake and reduction rates and $NO_3^-$ production rate were at pH 7. Moreover, it was found that the biodegradation of *p*-cresol was better described by the Monod equation ($R^2 = 0.96$) with estimated values of 0.10 $h^{-1}$ for $\mu_m$ and 103.4 mg $L^{-1}$ for $K_s$. The biodegradation of ammonia, on the other hand, was better described by the Haldane equation ($R^2 = 0.72$) with estimated values of 0.17 $h^{-1}$ for $\mu_m$, 11.9 mg $L^{-1}$ for $K_s$, and 617.9 mg $L^{-1}$ for $K_i$.

Mass balance equations were formulated to describe the processes occurring in the gas, liquid, and biofilm phases of the treatment system. The differential equations were solved using the finite difference numerical analysis method. A one-at-a-time sensitivity analysis was conducted to identify parameters that have significant impact on ammonia removal. Calibration

and validation results showed good agreement between predicted and measured values; based on the fractional bias (FB) results, the normalized model's prediction errors were within ±1 to 7%. After model calibration and validation, a simulation study was conducted using the model to evaluate the impacts of selected process and design parameters for a biotrickling filter system.

## ACKNOWLEDGEMENTS

I am immensely grateful to my supervisors, Dr. Stéphane P. Lemay and Dr. Bernardo Predicala, for their valuable inputs to my thesis as well as for the guidance and compassion they have given me throughout this doctorate program. I am also indebted to Dr. Lope Tabil, the chair of my advisory committee, and to all the members, Dr. Huiqing Guo, Dr. Darren Korber, and Dr. John Feddes, for their comments and for the time spent in reading my thesis. I also would like to thank Dr. Michèle Heitz for serving as the external examiner during my defence.

I am also very thankful for the wonderful experience I had at the Research and Development Institute for the Agri-Environment (IRDA) in Quebec City, Quebec and for the help and support of its researchers, technicians, and staff, in particular, Dr. Matthieu Girard and Dr. Richard Hogue for reading and providing comments and inputs to my thesis, and Martin Belzile, Thomas Jean, Lise Potvin, Michèle Grenier, and Dr. Patrick Dubé for their contributions to my research work.

My special thanks also go to my family and friends for their prayers and encouragement, which made the daily struggles bearable.

Above all, I thank the Almighty God for all the graces He bestowed upon me each and every day of this doctoral journey and for making this great endeavor a successful one.

## TABLE OF CONTENTS

## LIST OF TABLES

## LIST OF FIGURES

## LIST OF SYMBOLS AND ABBREVIATIONS

| | |
|---|---|
| a | Mass transfer area ($m^2$) |
| $a_t$ | Total specific surface area ($m^{-1}$) |
| A | Filter bed cross-sectional area ($m^2$) |
| $A_G$ | Cross-sectional area perpendicular to gas flow ($m^2$) |
| $A_L$ | Cross-sectional area perpendicular to liquid flow ($m^2$) |
| $A_S$ | Wetted specific surface area in Mpanias and Baltzis model ($m^{-1}$) |
| ANOVA | Analysis of variance |
| ASTM | American Society for Testing and Materials |
| ATCC | American Type Culture Collection |
| b | Distance along biofilm depth (μm); $b = 0$ at liquid-biofilm interface; $b = B_t$ at support |
| $B_t$ | Biofilm thickness (μm) |
| $C_A$ | Concentration of substance *A* (g $m^{-3}$), |
| $C_{AG}$ | Concentration of substance *A* at the gas film (g $m^{-3}$) |
| $C_{AGb}$ | Concentration of substance *A* in the bulk gas phase (g $m^{-3}$) |
| $C_{AL}$ | Concentration of substance *A* at the liquid film (g $m^{-3}$) |
| $C_{ALb}$ | Concentration of substance *A* in the bulk liquid phase (g $m^{-3}$) |
| $C_{AG}^*$ | Gas phase concentration of substance *A* that is in equilibrium with the bulk liquid phase concentration $C_{ALb}$ (g $m^{-3}$), |
| $C_{AL}^*$ | Liquid phase concentration of substance *A* that is in equilibrium with the bulk gas phase concentration $C_{AGb}$ (g $m^{-3}$) |
| $C_{AGi}$ | Gas concentration of substance *A* at the gas-liquid interface (g $m^{-3}$) |
| $C_{ALi}$ | Liquid-interfacial concentration of substance *A* at the gas-liquid interface (g $m^{-3}$) |
| $C_B$ | Ammonia concentration in the biofilm (g $NH_4^+$-N $m^{-3}$) |
| cfu | Colony-forming unit |
| $C_G$ | Contaminant concentration in the gas phase (g $m^{-3}$ or $ppm_v$); ammonia concentration in the gas phase (g $NH_3$-N $m^{-3}$ or $ppm_v$) |
| $C_{Gout}$ | Gas exhaust concentration (g $m^{-3}$) or ammonia gas exhaust concentration (g $NH_3$-N $m^{-3}$) |
| $C_{Gin}$ | Gas inlet concentration (g $m^{-3}$) or ammonia gas inlet concentration (g $NH_3$-N $m^{-3}$) |
| $C_L$ | Contaminant concentration in the liquid phase (g $m^{-3}$); ammonia concentration in liquid phase (g TAN $m^{-3}$) |
| $C_L^*$ | Equilibrium concentration of contaminant in the liquid phase (g $m^{-3}$) |
| $C_{Lout}$ | Liquid outlet concentration of ammonia (g TAN $m^{-3}$) |
| $C_{Lin}$ | Liquid inlet concentration of ammonia (g TAN $m^{-3}$) |

| | |
|---|---|
| $C_m$ | Measured concentration (g $m^{-3}$) |
| $\overline{C}_m$ | Mean measured concentration (g $m^{-3}$) |
| $C_p$ | Predicted concentration (g $m^{-3}$) |
| $\overline{C}_p$ | Mean predicted concentration (g $m^{-3}$) |
| $C_{odour}$, C | Odour concentration (OU $m^{-3}$) |
| $CaCl_2.2H_2O$ | Calcium chloride dihydrate |
| $CH_4$ | Methane |
| CIS | Cooled injection system |
| $CO_2$ | Carbon dioxide |
| CRIQ | Centre de Recherche Industrielle du Québec |
| $d_p$ | Nominal packing diameter (m) |
| $D_A$ | Diffusion coefficient of substance *A* ($m^2$ $h^{-1}$) |
| $D_{AG}$ | Diffusion coefficient of substance *A* in the gas phase ($m^2$ $h^{-1}$) |
| $D_{AL}$ | Diffusion coefficient of substance *A* in the liquid phase ($m^2$ $h^{-1}$) |
| $D_{AS}$ | Diffusion coefficient of substance *A* in porous solid ($m^2$ $h^{-1}$) |
| $D_L$, $D_W$ | Diffusion coefficient in water ($m^2$ $h^{-1}$) |
| $D_G$ | Diffusion coefficient in air ($m^2$ $h^{-1}$) |
| DGGE | Denaturing gradient gel electrophoresis |
| DO | Dissolved oxygen |
| DSMZ | German Collection of Microorganisms and Cell Cultures |
| $E_G$ | Gas emission rate (µg $min^{-1}$ $kg^{-1}_{pig}$) |
| $E_{odour}$ | Odour emission rate (OU $h^{-1}$ $kg^{-1}_{pig}$) |
| EC | Elimination capacity (g $m^{-3}_{bed}$ $h^{-1}$) |
| EBRT | Empty bed residence time (s) |
| ELISA | Enzyme-linked immunosorbent assay |
| $f_{NH3}$ | Unionized fraction of total ammonia (-) |
| $f_w$ | Wetted fraction of packing material's surface area (-) |
| $f_{Xv}$ | Correction factor for diffusion coefficient (-) |
| $FeSO_4$ .$7H_2O$ | Ferrous sulfate heptahydrate |
| FB | Fractional bias (-) |
| FIA | Flow injection analysis |
| $g_c$ | Gravitational constant (m $h^{-2}$) |
| GC-MS/O | Gas chromatograph coupled with a mass spectrometer and an olfactory detection port |
| h | Distance along the height of biotrickling filter (m); $h = 0$ at the top; $h = H_t$ at the bottom |
| H | Hedonic tone (-) |
| $H^+$ | Hydrogen ion |
| $H_t$ | Total filter bed height (m) |
| $H_2O$ | Water |

| | |
|---|---|
| $H_2S$ | Hydrogen sulfide |
| $HNO_2$ | Nitrous acid |
| I | Odour intensity (-) |
| IRDA | Research and Development Institute for the Agri-Environment |
| $J_A$ | Mass flux of substance *A* (g $m^{-2}$ $h^{-1}$) |
| $J_{AG}$ | Mass flux of component *A* from the bulk gas-phase to the interface (g $m^{-2}$ $h^{-1}$) |
| $J_{AL}$ | Mass flux of component *A* from the interface to the bulk liquid-phase (g $m^{-2}$ $h^{-1}$) |
| k | Orifice coefficient (-) |
| $k_d$ | Microbial decay coefficient ($h^{-1}$) |
| $k_{AG}$ | Individual gas phase mass transfer coefficient of component *A* (m $h^{-1}$) |
| $k_{AL}$ | Individual liquid phase mass transfer coefficient of component *A* (m $h^{-1}$) |
| $k_H$ | Henry's law constant (-) |
| $k_{Heff}$ | Effective Henry's law constant (-) |
| $K_a$ | Acid (or $NH_4^+$) ionization constant (mol $L^{-1}$) |
| $K_b$ | Base (or $NH_3$) ionization constant (mol $L^{-1}$) |
| $K_{AG}$ | Overall gas phase mass transfer coefficient of component *A* (m $h^{-1}$) |
| $K_{AL}$ | Overall liquid phase mass transfer coefficient of component *A* (m $h^{-1}$) |
| $K_i$ | Inhibition constant (g $m^{-3}$ or mg $L^{-1}$ or g $NH_4^+$-N $m^{-3}$) |
| $K_{i1}$, $K_{i2}$, $K_{h1}$, $K_{h2}$ | Coefficients related to intensity and hedonic tone (-) |
| $K_s$ | Half-saturation constant (g $m^{-3}$ or mg $L^{-1}$ or g $NH_4^+$-N $m^{-3}$) |
| KCl | Potassium chloride |
| l | Distance along the length of biotrickling filter (m); $l = 0$ at entrance; $l = L$ at exit |
| L | Total filter bed length (m) |
| LEAA | Laboratoire d'Expertises et d'Analyses Alimentaires |
| m | Number of divisions in gas domain; partition coefficient between gas and liquid in Mpanias and Baltzis model (-) |
| $M_{pig}$ | Mass of pigs (kg) |
| $MgSO_4.7H_2O$ | Magnesium sulfate heptahydrate |
| n | Number of divisions in liquid domain; number of data pairs |
| N | Nitrogen |
| NaCl | Sodium chloride |
| $NaHCO_3$ | Sodium bicarbonate |
| $NaH_2PO_4$ | Sodium dihydrogen phosphate |
| $Na_2HPO_4$ | Disodium hydrogen phosphate |
| NDIR | Non-dispersive infrared |
| $NH_3$ | Ammonia |
| $NH_4^+$ | Ammonium |
| $NH_4^+$-N | Ammonium nitrogen |

| | |
|---|---|
| $(NH_4)_2SO_4$ | Ammonium sulfate |
| NMSE | Normalized mean square error (-) |
| $NO_2^-$ | Nitrite |
| $NO_2^-$ -N | Nitrite nitrogen |
| $NO_3^-$ | Nitrate |
| $NO_3^-$ -N | Nitrate nitrogen |
| $O_2$ | Oxygen |
| OD | Optical density |
| $OH^-$ | Hydroxide |
| OI | Odour index (-) |
| OU | Odour unit |
| pH | Negative logarithm of hydrogen ion concentration |
| $pK_a$ | Negative logarithm of acid ionization constant $K_a$ |
| $pK_b$ | Negative logarithm of base ionization constant $K_b$ |
| P | Pressure (in. $H_2O$); model parameter |
| $P_d$ | Default parameter |
| PBS | Phosphate buffer solution |
| PCR | Polymerase chain reaction |
| $q_s$ | Specific rate of substrate utilization (mg substrate $mg^{-1}$ biomass $h^{-1}$) |
| $Q_A$ | Mass transfer rate of substance *A* (g $h^{-1}$) |
| $Q_G$ | Air flow rate ($m^3$ $h^{-1}$ or $ft^3$ $min^{-1}$) |
| $Q_L$ | Liquid flow rate ($m^3$ $h^{-1}$) |
| $R^2$ | Coefficient of determination |
| RE | Removal efficiency (%) |
| RNA | Ribonucleic acid |
| S | Growth-limiting substrate concentration (g $m^{-3}$ or mg $L^{-1}$) |
| t | Time (h) |
| T | Temperature ($^oC$) |
| TAN | Total ammonia nitrogen (g $m^{-3}$) |
| TDS | Thermal desorption system |
| $U_G$ | Gas superficial velocity (m $h^{-1}$) |
| $U_L$ | Liquid superficial velocity (m $h^{-1}$) |
| UV-Vis | Ultraviolet-visible |
| V | Simulated variable |
| $V_d$ | Default variable |
| $V_f$ | Empty filter bed volume ($m^3$) |
| $V_L$ | Volume of recirculating liquid ($m^3$) |
| VBA | Visual Basic for Applications |
| VOC | Volatile organic compound |
| x | Distance of diffusion (m); distance along biofilm depth (µm; Mpanias and Baltzis model) |

| | |
|---|---|
| $X$ | Biomass concentration (g $m^{-3}$ or mg $L^{-1}$) |
| $X_a$ | Active biomass concentration (g $m^{-3}$) |
| $X_v$ | Biofilm density (kg $m^{-3}$ or g $m^{-3}$) |
| $Y$ | Biomass yield coefficient (g biomass formed $g^{-1}$ of contaminant or substrate consumed) |
| $z$ | Film thickness (m) |
| $z_G$ | Gas film thickness (m) |
| $z_L$ | Liquid film thickness (m) |
| $\sigma_p$ | Surface tension of packing material (N $m^{-1}$) |
| $\sigma_L$ | Surface tension of water (N $m^{-1}$) |
| $\rho_L$ | Density of water (kg $m^{-3}$) |
| $\rho_G$ | Density of air or density of $NH_3$ or $H_2S$ (kg $m^{-3}$) |
| $\mu$ | Specific growth rate ($h^{-1}$) |
| $\mu_G$ | Viscosity of air (kg $m^{-1}$ $h^{-1}$) |
| $\mu_L$ | Viscosity of water (kg $m^{-1}$ $h^{-1}$) |
| $\mu_m$ | Maximum specific growth rate ($h^{-1}$) |
| $\delta$ | Effective biofilm thickness in Mpanias and Baltzis model (μm) |
| $\xi_1$, $\xi_2$ | Correction factors for mass transfer coefficients (-) |

# Chapter 1
# General Introduction

## 1.1 PROBLEM DEFINITION

The hog industry is an important component of the Canadian agriculture (CPI 2012). In 2011, it contributed $9.28 billion to its agricultural economy (CPC 2012a). A study showed that the exportation of pork created 45,000 jobs, generated $1.98 billion in income and benefits and $318 million in taxes, and contributed $3.5 billion in gross domestic product (CPC 2012a).

However, sustainability has now become a global issue, and the swine industry has been challenged to play its part. Honeyman (1996) indicated that a sustainable swine production system is one that enhances profits for the producers without jeopardizing the quality of the pork produced and maintains or improves the ecological and socioeconomic conditions of the communities through application of combined production and management techniques.

Emissions of malodorous gases, as well as of dust and microorganisms, threaten the social and environmental sustainability of swine production (Blanes-Vidal et al. 2009). Several reports (Blanes-Vidal et al. 2009; Donham 2000) have cited the negative impacts of these emissions on the local economy, human health, the quality of life of neighbouring communities, and the environment. For example, ammonia emanating from pig manure can cause eutrophication and soil acidification; hydrogen sulphide can have harmful effects on barn workers and surrounding communities; methane produced from decomposing manure becomes an important greenhouse gas; and dust generated can cause various respiratory diseases on workers (Donham 2000). Above all, the largest public concern, and which has been the source of many complaints, is the emission of odour (Rappert and Muller 2005).

Over the past few decades, odour complaints and other environmental, health, and social-related issues have been increasing with the intensification of pig production. In Canada, for example, as of January 1, 2012, the total number of pigs on farms was reported to be approximately 12 million (CPC 2012b). Though this number was smaller compared to 15 million pigs in 2006, the estimated number of farms in that year was 12,320 compared to only 6820 in 2012 (CPC 2012b). This implies that pig production has become concentrated in fewer but larger farms. As swine production intensifies, concerns about the higher risk of negative impacts and the unwillingness of neighbouring communities to accept swine odours also increase (Hogberg et al. 2005).

Considerable efforts have already been made over the years to make the swine industry environmentally and socially sustainable. Odour and gas emission abatement techniques such as altering the protein diet of pigs (Kerr et al. 2006), introducing waste additives (McCrory and Hobbs 2001), and employing different swine manure handling and management strategies (Ndegwa et al. 2002) have been applied to minimize production of malodourous gases. Apart from these source reduction and waste management techniques, treating off-gases from livestock buildings is also recently considered a potential air treatment strategy.

One of the end-of-pipe air treatment techniques which has gained interest recently for the treatment of air exhausted from swine facilities is biotrickling filtration. Though some studies (Jensen and Hansen 2006; Melse and Mol 2004) have revealed that this technique can effectively reduce odour and gas emissions from pig buildings, this approach has not yet been efficiently applied in barn systems (Ozis et al. 2005). Despite its advantages over other methods, it is still limited by some operational problems (e.g. biomass accumulation, mass transfer limitation, and product or substrate inhibition). Nevertheless, the impact of these limitations can be reduced by

using mathematical models, which serve not only to describe and predict process performance but also to identify relevant parameters for better design and process optimization.

Thus, this study was aimed at developing a mathematical model that could predict and simulate the performance of biotrickling filters in removing odour and gaseous pollutants exhausted from pig buildings. The main objective of which was to identify relevant processes and design parameters that could help optimize the system to make it environmentally, socially, and economically sustainable.

This chapter describes the background information gathered from the literature regarding swine barn emissions, waste gas treatment techniques, and existing models. The information obtained from the literature review was used as a base in the formulation of the hypothesis, the specific objectives, and the content of the current study.

## 1.2 LITERATURE REVIEW

### 1.2.1 Origin and nature of airborne emissions from swine operation

The odour emitted from swine operation mainly come from livestock facilities (animal housing and feed storage areas), manure storage facilities, and land application of manure (Sheridan et al. 2002b; Powers 1999). According to Mackie et al. (1998), most of the offensive odour is produced from the decomposition of manure during collection and subsequent handling and management. Lemay (1999) cited that 22% of the total odour complaints were from animal production buildings, 17% from manure storage facilities, 52% from manure spreading, 8% from feed production, and 1% from silage clamps. It is quite evident, based on the figures given above, that the main responsible for the malodour associated with swine production is the pig manure.

Pig manure, which contains undigested feed, metabolic products, and indigenous bacteria, is a combination of urine and feces (Sutton et al. 1999). The odour emanating from manure is caused by various odorous substances produced from the breakdown of organic materials, particularly protein and carbohydrates, by the different microorganisms present in the manure (Rappert and Muller 2005; Lemay 1999). The overall impact of odour depends on each of the compounds odour character and concentration (Lemay 1999).

Most of the odorous compounds have been reported to be generated from the anaerobic degradation of manure, where most of them have low odour thresholds, thus, they become odour nuisances even at very low concentrations (Rappert and Muller 2005). Schiffman et al. (2001) identified a total of 331 gaseous compounds in pig production facilities. Several studies (Rappert and Muller 2005; Zhu 2000; Mackie et al. 1998) categorized these compounds into four general groups:

(1) Volatile fatty acids (VFAs, i.e. branched and straight chain VFAs)

Some of the volatile fatty acids found in swine air include acetic, propionic, butyric, iso-butyric, valeric, iso-valeric, caproic, capric, iso-caproic, iso-capric, hexanoic, and heptanoic acids (Zhu 2000; Mackie et al. 1998). These acids are generated from the deamination of amino acids, which are formed from the breakdown of protein and carbohydrates (Zhu 2000).

(2) Aromatic compounds

Some of the important aromatic compounds are indole, skatole, *p*-cresol, phenol, and 4-ethlylphenol, which are formed from the breakdown of aromatic amino acids (Rappert and Muller 2005).

(3) Nitrogen-containing compounds

The nitrogen-containing compounds emanating from animal wastes are mainly ammonia and volatile amines. Volatile amines, which include putrescine, cadaverine, methylamine, and

ethylamine, are generated from amino acid decarboxylation that occurs in the gastrointestinal tract and during storage of fresh manure (Rappert and Muller 2005; Zhu 2000). Ammonia, on the other hand, is produced from amino acid deamination and urea hydrolysis (Rappert and Muller 2005).

(4) Sulfur-containing compounds

The typical sulfur-containing compounds that belong to this group are the sulphides and the methyl- and ethyl-mercaptans, which are generated through sulfate reduction and breakdown of sulfur-containing amino acids by anaerobic bacteria (Zhu 2000; Mackie et al. 1998).

Table 1.1 shows the reported average concentrations and odour thresholds of some of the important odorants of pig barn air.

**Table 1.1 Average concentrations and odour thresholds of some pig barn air odorants.**

| Name | Concentration ($ppb_v$) | Odour threshold ($ppb_v$) | Characteristic odour |
|---|---|---|---|
| Ammonia | $5 \times 10^3$-$18 \times 10^3$[a] | $5.75 \times 10^3$ | Sharp, pungent |
| Dimethyl sulphide | 1.5-12[b] | 2.24 | Decayed vegetables, putrid |
| Hydrogen sulfide | 20-146[c] | 17.80 | Rotten eggs |
| *p*-Cresol | 9 | 1.86 | Faecal, barnyard |
| Butanoic acid | 60 | 3.89 | Sweaty, rancid |
| 2-Methylbutanoic acid | 3 | 1.86 | Irritant, stench |
| Isovaleric acid | 15 | 2.46 | Rancid, cheese, stench |

Source: Schiffman et al. (2001); otherwise, [a]Groot Koerkamp et al. (1998), [b]Kim et al. (2007), [c]Thorne et al. (2009).

Emissions of dust and bioaerosols also pose health concerns. Donham et al. (1989) have shown significant correlation between these types of air contaminants to respiratory illnesses (e.g. cough, bronchitis) experienced by swine workers. Dust particles, which come from animal feed, bedding materials, dried manure, animal skin, and building materials, are important carriers of swine odours (Lemay 1999). Hoff et al. (1997), as cited by Lemay (1999), found 23 to 76%

odour threshold reduction resulting from 47 to 98% dust particle removal. Bioaerosols, which are dust particles carrying pathogenic bacteria, viruses, and endotoxin, can impose risk of infection in the barn as well as in the neighbouring animal houses (Takai et al. 1998). Predicala et al. (2001) measured 2.13 mg $m^{-3}$ inhalable dust, 0.11 mg $m^{-3}$ respirable dust, $17x10^3$ cfu $m^{-3}$ total viable particles, and $4.5x10^3$ cfu $m^{-3}$ respirable viable particles from a mechanically ventilated pig barn. The same authors cited that the suggested limits for total dust and respirable dust are 2.4 mg $m^{-3}$ and 0.23 mg $m^{-3}$, respectively.

### 1.2.2 Design and control of ventilation system of swine buildings

As discussed in the preceding section, pig barn air contains gases and microorganisms originating from feces and urine as well as dusts from feeds, feces, skin particles, and building materials. Additionally, pigs release moisture, heat, and carbon dioxide. In order to dilute the air and eliminate these air contaminants from pig buildings and to maintain sufficient oxygen levels, ventilation is therefore required. Ventilation can be accomplished either by natural means, where air moves through the building by wind and thermal convection, or by mechanical means (the one more common in colder climates), where air is moved by fans (FAO 2011).

Maintaining good air quality and optimum environmental conditions within pig barns is of primary importance because it affects the health and productivity of pigs as well as of barn workers. The important environmental parameters in a barn include temperature, humidity, air speed, and indoor air quality (Jacobson 2012). Lambert et al. (2001) cited that relative humidity should be kept below 80% to lower risk of fungal infection. Air speeds at floor level should not exceed 0.15 m $s^{-1}$ for smaller pigs and 0.2 m $s^{-1}$ for larger ones during cold weather to prevent cold drafts (Meyer 2002). The time-weighted average exposure threshold limit values recommended by the American Conference of Governmental Industrial Hygienists for gases

such as $H_2S$, $NH_3$, $CH_4$, and $CO_2$ are 1, 25, 1000, and 5000 ppm, respectively (CCOHS 2013). For maximum pig performance, barn temperature should be kept within 16 to 21°C for 70 to 100 kg hogs, 17 to 23°C for 20 to 59 kg hogs, 23 to 28°C for younger pigs, and 30 to 32°C for piglets of up to two weeks of age (ASHRAE 1993).

Depending on barn indoor and outdoor conditions, ventilation rates may fluctuate over a year or even over a day. Ventilation rates applied in a barn are estimated by performing sensible heat balance during hot weather and moisture balance during cold weather (FAO 2011). Figure 1.1 shows an example of a ventilation curve for both temperature and moisture control (FAO 2011). Ventilation rates normally vary from 1 L $s^{-1}$ $animal^{-1}$ for 5 to 14 kg piglets in winter to 240 L $s^{-1}$ $animal^{-1}$ for sows and litters in summer (Jacobson 2012). It is important to note that ventilation rates do not depend only on outside weather and barn design conditions but also on age, type, and number of pigs and on other factors such as diet, floor type, and manure management.

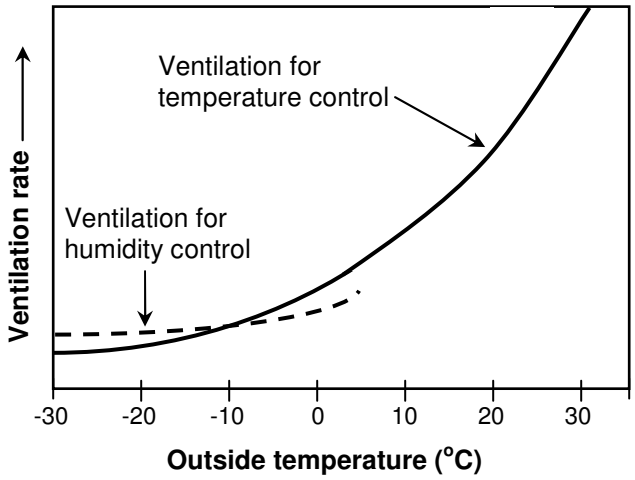


**Figure 1.1 An example of a ventilation curve applied in pig buildings.**
Adapted from FAO (2011).

### 1.2.3 Techniques for waste gas treatment

Various approaches have been used to treat waste gases. These control technologies (Figure 1.2) can be categorized into physico-chemical and biological. The important factors that are considered in selecting an effective control technique are the characteristics of the compounds to be treated and the conditions of the waste stream (Revah and Morgan-Sagastume 2005).

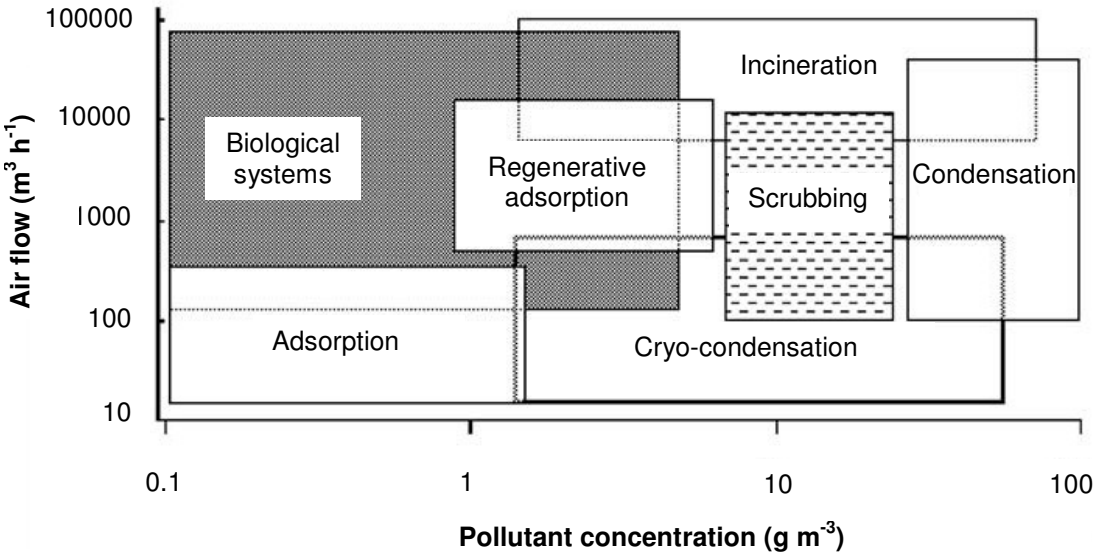


**Figure 1.2 Various control technologies based on air flow rates and concentrations of waste streams.**
Adapted from Revah and Morgan-Sagastume (2005).

#### 1.2.3.1 Physico-chemical methods

Air treatment technologies are mostly based on physico-chemical processes as shown in Figure 1.2. Treatments under this category include condensation, adsorption, absorption or scrubbing, membrane systems, oxidation, and incineration.

***Condensation***. Pollutant vapors are condensed from the waste gas by lowering the temperature of the gas at constant pressure or increasing its pressure at constant temperature (Revah and Morgan-Sagastume 2005). This method is found cost-effective for the treatment of highly concentrated air streams (around 100 g $m^{-3}$) composed of a condensable contaminant vapor and a non-condensable gas (Revah and Morgan-Sagastume 2005; Shareefdeen et al. 2005).

***Adsorption.*** In adsorption, the waste air stream is brought in contact with an adsorbent (e.g. activated carbon, silica gel, alumina, and zeolite) and the contaminants are removed from the air stream due to the weak intermolecular attractions that are formed at the surface of the adsorbent (Revah and Morgan-Sagastume 2005). This method is effective for low concentrated air streams (up to 1 g $m^{-3}$); however, the high cost of recovering the compounds and the spent adsorbents that need to be disposed limit the application of this method (Shareefdeen et al. 2005).

***Absorption/scrubbing***. This method is accomplished by absorbing pollutants from the air into a scrubbing liquid such as water (Shareefdeen et al. 2005), although sometimes an acid or alkali is added to the solvent to enhance absorption. This process is normally carried out in a large contactor where gaseous pollutants are allowed to come in contact with the liquid phase through the use of a packed or bubble column, or a venturi contactor (Devinny et al. 1999). The affinity of the gaseous contaminant for the liquid largely dictates the success of the treatment (Devinny et al. 1999). The drawbacks of this method are the high cost of chemicals and the treatment of spent liquid.

***Membrane system***. In this technique, the air pollutants are removed from the waste gas stream through the use of a semi-permeable membrane, which is permeable to the pollutants but not to air (Revah and Morgan-Sagastume 2005).

***Oxidation.*** This process is carried out by absorbing first the pollutant in a scrubbing tower. The absorbed pollutant is then oxidized by an oxidizing agent such as chlorine, ozone, potassium permanganate, and hydrogen peroxide (Revah and Morgan-Sagastume 2005). Ultraviolet light is sometimes introduced to enhance the process (Revah and Morgan-Sagastume 2005).

***Incineration***. This method involves combustion of pollutants at relatively higher temperatures. Thermal incineration is carried out at temperatures between 700 and 1400$^{o}$C while catalytic incineration is between 300 and 700$^{o}$C and uses catalysts such as platinum, palladium, and rubidium (Devinny et al. 1999). This method is primarily applied for the control of hazardous and odorous volatile organic compounds (Revah and Morgan-Sagastume 2005). Although this method is highly efficient, it is not economical for low-concentration high-flow air streams due to its high energy requirements (Shareefdeen et al. 2005).

#### 1.2.3.2 Biological methods

Although biological systems have already been widely used in wastewater treatment, they are just recently applied in the treatment of off-gases containing biodegradable compounds (Hodge and Devinny 1995). This technology is cost-effective for the treatment of high-flow, low-concentration waste gas streams (up to 100,000 $m^3$ $h^{-1}$ flow rate and concentrations of not more than 10 g $m^{-3}$) of readily biodegradable contaminants (Park and Jung 2006; Iliuta and Larachi 2004; Abumaizar et al. 1997). Thus, it is a promising method for the treatment of waste air exhausted from farm facilities (Sheridan et al. 2002a).

Biotechnology offers several advantages over the conventional physical and chemical methods. These include lower treatment costs since no chemical addition is required and reduced environmental impact for it has no harmful by-products (Streese et al. 2005). It is a low-capital

technology and since biodegradation usually occurs at ambient temperature and pressure, it is also energy-efficient and has low operational cost (Park and Jung 2006; Iliuta and Larachi 2004).

Biological treatments involve transformation of pollutants into less harmful and odourless substances (e.g. carbon dioxide, water, sulfate, and nitrate) under the action of microorganisms (Deshusses 1997b). These pollutants are used by the microorganisms as food and energy sources for growth and cell maintenance (Revah and Morgan-Sagastume 2005). Since microorganisms grow in the process, more biomass is also produced (Revah and Morgan-Sagastume 2005).

Biological methods have been found efficient for the treatment of highly soluble and low molecular weight organic (e.g. methanol, ethanol, aldehydes, acetates, ketones, and some aromatic hydrocarbons) and inorganic (e.g. hydrogen sulphide and ammonia) compounds (Shareefdeen et al. 2005).

Air-phase bioreactors widely used for the control of odour and gas emissions are biofilters, biotrickling filters, and bioscrubbers. Although these bioreactors differ in configuration (microbes may be suspended or fixed and the liquid may be flowing or stationary), they all employ the same basic principle: the contaminants are transferred from the gas stream to the aqueous phase where microbial degradation occurs.

***Biofilter.*** This system (Figure 1.3) traditionally employs naturally bioactive media (e.g. wood chips, soil, compost, peat), which possess a high water retention capacity and bioavailable nutrients (e.g. nitrogen, phosphorus, and trace minerals) for microorganisms (Govind and Narayan 2005). Aside from nutrients, the packing media also provide a pH buffer and a support for biofilm (Chou and Huang 1997). Due to the characteristics of the packing material described above, the system does not need continuous flow of nutrients and moisture (Govind and Narayan

2005). However, once the packing material is exhausted, it can be regenerated by adding a buffer or nutrients in the irrigation liquid or it can be replaced with new one (Chou and Huang 1997).

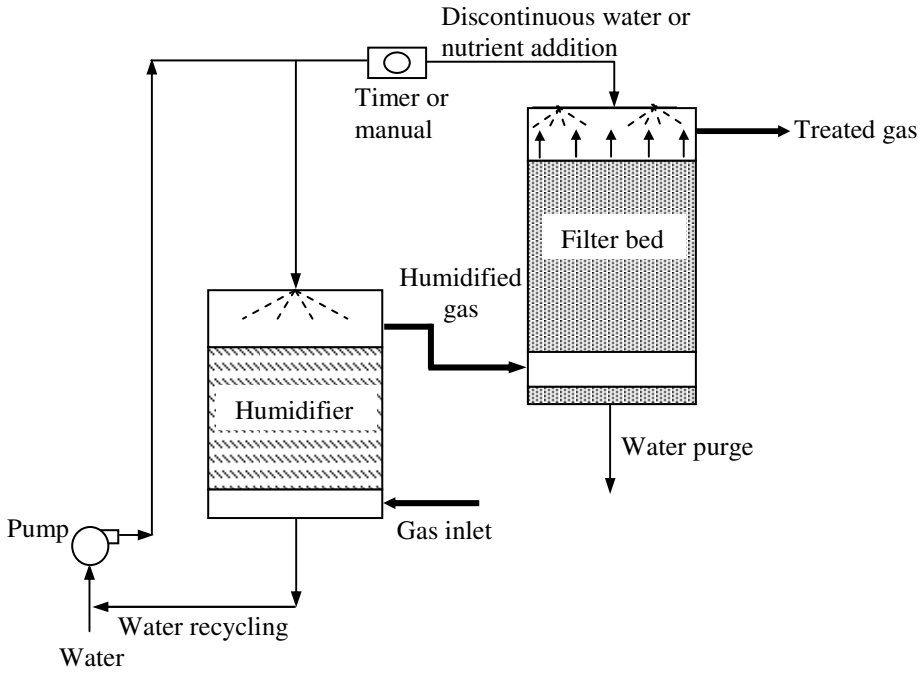


**Figure 1.3 Schematic diagram of a biofilter.**
Adapted from Revah and Morgan-Sagastume (2005).

As shown in Figure 1.3, as the contaminated air passes through the filter bed, the contaminants in the gas phase are transferred into the biofilm where they are biodegraded. However, to avoid the filter media from drying, the contaminated airstream is humidified first before it enters into a biofilter (Swanson and Loehr 1997). The humidity in the filter bed is one of the important parameters in achieving an optimum performance since microbial activity highly depends on water content (Revah and Morgan-Sagastume 2005). In instances where humidification seems insufficient, periodic liquid irrigation may be applied to the filter bed (Devinny et al. 1999).

Aside from water retention capacity and nutrient availability of the packing medium, other properties such as porosity, degree of compaction, ability to host microbial populations, and environmental factors such as pH and temperature also largely affect the overall performance of biofilters (Devinny et al. 1999). Moreover, pollutant concentration and loading are also important parameters that influence process efficiency (Deshusses 1997a).

Although biofilters are found efficient in treating waste gases, problems such as pressure drop due to excessive biomass accumulation and high moisture content and liquid flow rate limit their performance (Shareefdeen et al. 2005). Moreover, maintaining pH in biofilters is also a challenge, especially when dealing with compounds containing chlorine and sulfur since the acids produced from the reactions can lower the pH and the buffering capacity of the filter medium (Choi et al. 2004).

Treating off-gases by biofilters was first conceptualized in 1923 when Bach (1923, cited by Leson and Winer 1991) suggested this method for the control of $H_2S$ emitted from sewage treatment plants. Application of this technique was first reported in the United States and in Germany in the 1950s (Leson and Winer 1991). However, Nicolai and Janni (1997) cited that the use of biofilters for livestock operation started in Germany in 1960s. In the United States, its application to livestock facilities began only in the 1990s when Nicolai and Janni (1997) explored the feasibility of using biofilters in treating pit exhaust air from a swine farrowing barn. Recently, more biofilters were investigated and developed for the treatment of swine facility air (Sheridan et al. 2002b; Hartung et al. 2001; Martens et al. 2001).

***Biotrickling filter.*** The operating principle of this system is similar to that of biofilters wherein a contaminated air stream passes through a filter bed where biofilm is attached (Figure 1.4). However, unlike biofilters, biotrickling filters utilize synthetic/inert packing media (e.g. random

or structured plastic packing, polyurethane foam, and lava rocks). Since this type of media has no or low water retention capacity, the filter bed is continuously irrigated to provide sufficient moisture (Govind and Narayan 2005). The packing media provides surface not only for biofilm attachment but for gas-liquid contact as well (Cox and Deshusses 1998). Contaminants and oxygen transfer to the aqueous phase or directly to the biofilm as polluted air passes through the filter bed (Cox and Deshusses 1998).

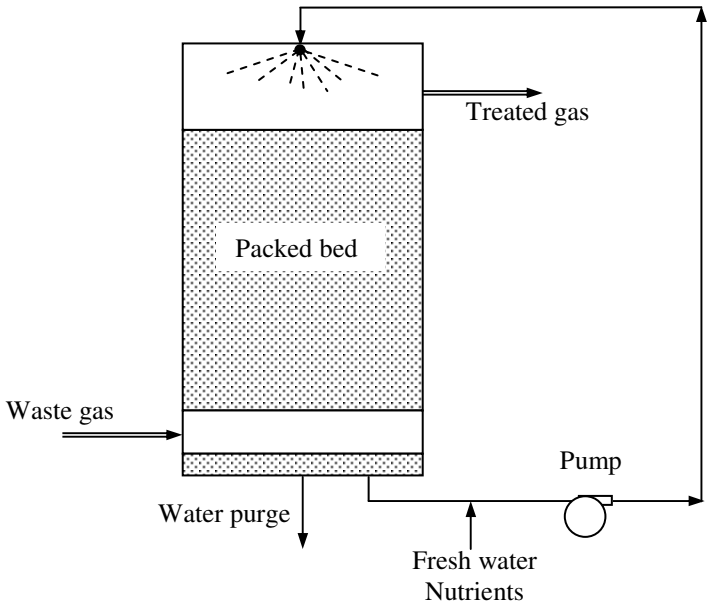


**Figure 1.4 Schematic diagram of a biotrickling filter.**
Adapted from Revah and Morgan-Sagastume (2005).

The construction and operation of biotrickling filters are more complex than those of biofilters (Shareefdeen et al. 2005); however, this system avoids some of the limitations of biofilters, such as channelling and filter media compaction and degradation (Chou and Huang 1997). Although problems such as excessive biomass growth and clogging are sometimes encountered in biotrickling filters, their inert packing material can be cleaned by regular backwashing. The continuous liquid flow in biotrickling filters does not only provide moisture

but also removes excess biomass from the filter bed, provides nutrients for the microorganisms, and controls pH (Govind and Narayan 2005).

Due to the advantages of biotrickling filters, application of this system to swine facilities have been explored by several laboratory and field studies over the past few years. Full-scale biotrickling filters have been installed in some pig production facilities in Europe to reduce ammonia and odour emissions (Melse et al. 2012; Jensen and Hansen 2006; Melse and Mol 2004).

A number of studies have also been conducted to assess the economic feasibility of this technique. Grimm (2005) compared the total cost (investment and operating costs) of different techniques for the treatment of swine facility air. The total costs (€ per pig delivered) were found to be 3.2 to 4.7, 2.5 to 4.4, and 2.0 to 3.1 for chemical scrubber, biotrickling filter, and biofilter, respectively. Deshusses and Cox (1999) listed reactor cost and costs of ducts, controls, and installation as part of capital costs while operating costs could include electricity, water, nutrients, labor, and those related to the control of biomass accumulation. An average of 9 L $pig^{-1}$ $day^{-1}$ of water was consumed in a biotrickling filter operation conducted by Lemay (2013) for the treatment of air exhausted from the pig barns of Prairie Swine Centre, Inc. in Saskatoon, Saskatchewan, Canada. This water consumption has been found relatively high, thus, further studies are still required to address this limitation. Since the recirculation liquid is high in nitrogen and other nutrients, it should be treated before discharge or could be potentially used as a fertilizer.

***Bioscrubber.*** This system is composed of two units: a scrubber or absorber column and a liquid-phase bioreactor (Figure 1.5). Contaminants are removed from the air in the scrubber or absorber by a scrubbing liquid, usually water, which are then treated in the liquid-phase bioreactor

containing suspended cultures (Shareefdeen et al. 2005). Absorption in the absorber unit is generally carried out using a packed column, a spray tower, or a bubble column (Devinny et al. 1999). Generally, the effluent from the liquid-phase bioreactor is recirculated to the absorber column. Sufficient oxygen is supplied to the bioreactor to obtain optimum microbial activity (Shareefdeen et al. 2005). Nutrients can also be added to the liquid phase and the pH can be controlled to maintain high level of biodegradation. The liquid phase also helps in eliminating toxic by-products (Devinny et al. 1999). Another important advantage of this system is its ability to handle varying contaminant loading (Shareefdeen et al. 2005). However, the wastewater generated in the bioreactor due to the accumulation of biomass and dissolved by-products may require further treatment. Since evaporation of water or disposal of concentrated effluent may occur, fresh water needs to be added regularly (Singh et al. 2005).

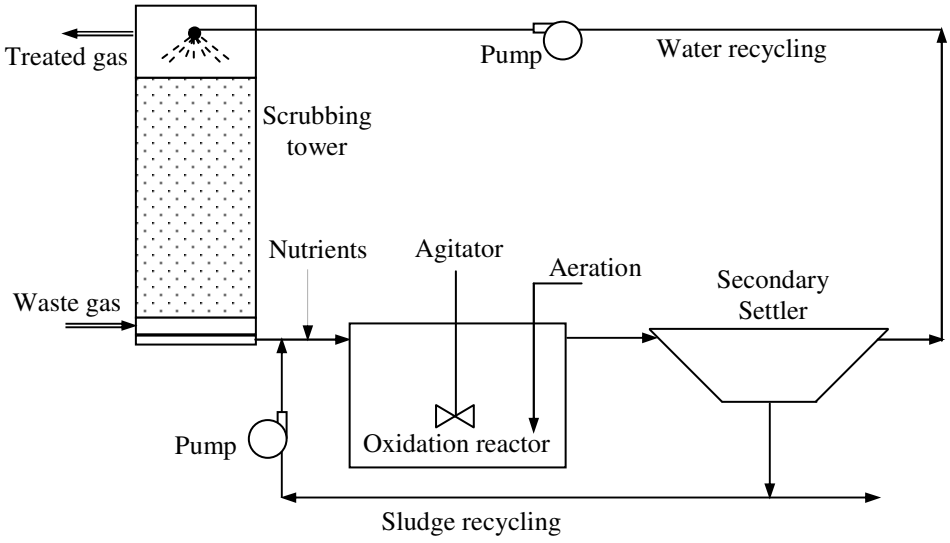


**Figure 1.5 Schematic diagram of a bioscrubber.**
Adapted from Revah and Morgan-Sagastume (2005).

Lais et al. (1997) investigated the applicability of bioscrubbers in removing ammonia and odour from pig barns. They found the system not feasible due to the additional cost needed for the treatment of the effluent.

While both biotrickling filters and bioscrubbers seem comparable in overcoming some of the limitations of biofilters (e.g. filter degradation, compaction of filter material, poor control of pH and removal of reaction wastes), biotrickling filters appear to be more attractive than bioscrubbers. Biotrickling filters have smaller space requirement since absorption and biodegradation occur in the same reactor, produce lesser amount of wastewater, and do not need aeration.

### 1.2.4 Underlying principles governing biotrickling filter operation

Biotrickling filter technology relies on the ability of the microorganisms to degrade contaminants in the air. The success of its operation depends on many factors, which include pH of the trickling liquid, temperature, moisture and oxygen contents, among others. This section presents the mechanisms of its operation, its design and operation considerations, and challenges to its operation.

#### 1.2.4.1 Mechanisms for the removal and degradation of gas contaminants

The elimination of a gaseous pollutant in a biotrickling filter is a result of a complex combination of different physico-chemical and biological phenomena. This, generally, involves three steps: the transfer of the contaminant from the gas phase to the liquid phase, the subsequent transfer to the biofilm, and the biodegradation in the biofilm. In addition, contaminant degradation may also take place in the liquid phase (Shareefdeen et al. 2005). Since packing

media utilized in biotrickling filters are usually made of inert materials, adsorption onto the media is generally negligible (Cox and Deshusses 1998).

***Mass transfer.*** The contaminant in the air is moved by advection and eddy diffusion (convection), since the bulk air flows in a turbulent motion (Devinny et al. 1999). When the contaminant comes in contact with the liquid, it is then absorbed and transferred into the liquid phase. The process of absorption can be described by Whitman's two-film theory illustrated in Figure 1.6, where $C_{AGb}$ and $C_{ALb}$ are the concentrations of substance *A* in the bulk gas and liquid, respectively (g $m^{-3}$); $C_{AG}$ and $C_{AL}$ are the concentrations of substance *A* at the gas and liquid films, respectively (g $m^{-3}$), which are functions of film thickness *z* (m); and $C_{AGi}$ and $C_{ALi}$ are the gas and liquid interfacial concentrations of substance *A*, respectively (g $m^{-3}$).

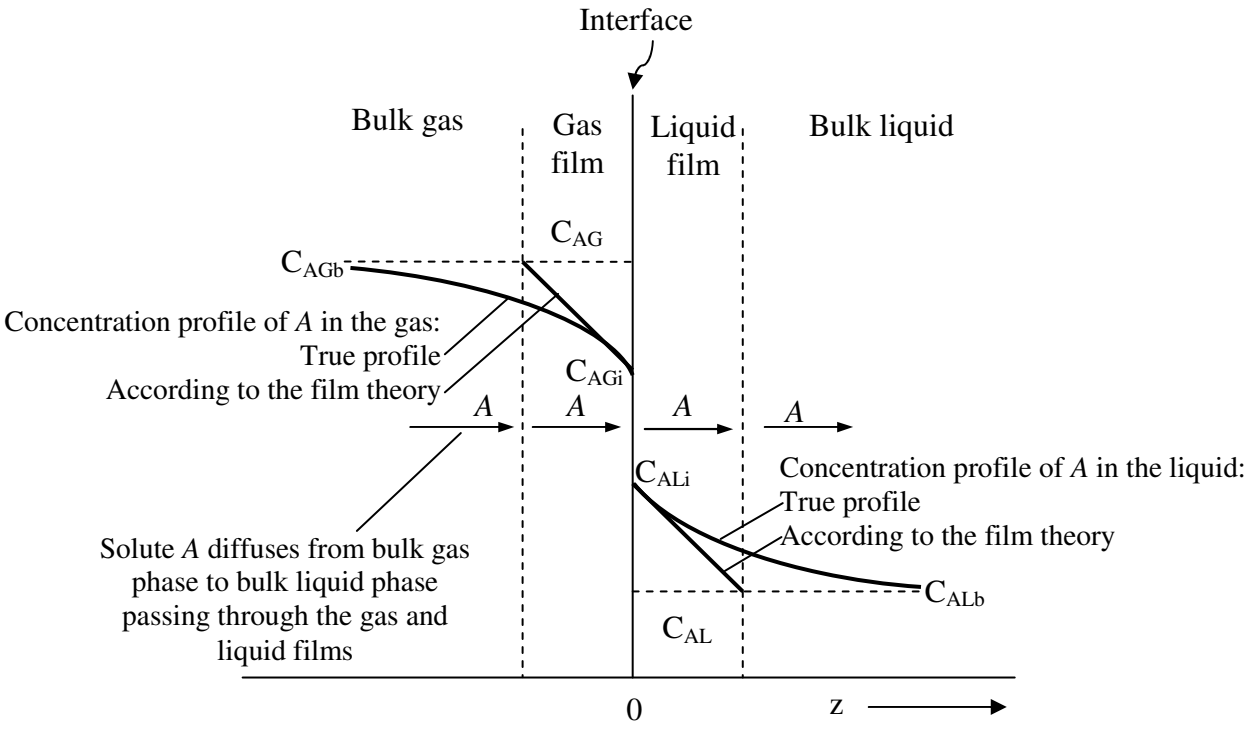


**Figure 1.6 Concentration profile for absorbed component *A*.**
Adapted from Dutta (2007).

According to the Whitman's two-film theory, the mass transfer of the contaminant involves transport from the bulk gas phase to the phase boundary or interface, and then from the interface to the bulk liquid phase (Dutta 2007). This theory states that a fluid film or mass-transfer boundary layer is formed wherever two phases are brought in contact (Doran 1995). Away from this film (at the bulk phases), each fluid is assumed to be well-mixed and in fully developed turbulent flow (Doran 1995). Thus, it is further assumed that at the bulk phases, there is no resistance to mass transfer and concentration gradients are negligible (Dunn 2003). However, at the fluid films, concentration difference exists and turbulent flow ceases (Coulson et al. 2002). It is also assumed that there is no mass transfer resistance at the interface, and all the resistance to mass transfer exists only within the two films located at each side of the interface (Dunn 2003). In each of these films, the flow is assumed to be stagnant, and the transport of mass occurs only by molecular diffusion, which can be described by Fick's first law, as presented in equation 1.1 (Dunn 2003):

$$J_A = -D_A \frac{dC_A}{dz} \tag{1.1}$$

where $J_A$ = mass flux of substance *A* (g $m^{-2}$ $h^{-1}$),

$D_A$ = diffusion coefficient of substance *A* ($m^2$ $h^{-1}$),

$C_A$ = concentration of substance *A* (g $m^{-3}$);

z = film thickness (m).

Equation 1.1 shows that the flux of substance *A* ($J_A$) goes from a region of higher concentration to a region of lower concentration, with a magnitude that is proportional to the concentration gradient.

In a steady-state process of absorption, the flux through the gas film is equal to the flux through the liquid film. Applying the concept described in equation 1.1 and integrating over the

linear concentration gradient at each film, the mass transfer across the two films can be then represented by equation 1.2:

$$J_A = D_{AG}\frac{C_{AGb} - C_{AGi}}{z_G} = D_{AL}\frac{C_{ALi} - C_{ALb}}{z_L} \tag{1.2}$$

where subscripts *G* and *L* stand for gas and liquid phases, respectively.

In terms of the volumetric mass transfer coefficient ($k_G$ or $k_L$), the total rate of mass transfer can be given by equation 1.3:

$$Q_A = k_{AG}a\left(C_{AGb} - C_{AGi}\right) = k_{AL}a\left(C_{ALi} - C_{ALb}\right) \tag{1.3}$$

where $Q_A$ = mass transfer rate of substance *A* (g $h^{-1}$),

$k_{AG}$ = individual gas phase mass transfer coefficient of substance *A* (m $h^{-1}$),

$k_{AL}$ = individual liquid phase mass transfer coefficient of substance *A* (m $h^{-1}$),

a = mass transfer area ($m^2$).

It is assumed that at the interface mass transfer resistance is negligible and equilibrium exists according to the film theory. Generally, equilibrium relationships at low concentrations are described by Henry's law; thus, interfacial concentrations $C_{AGi}$ and $C_{ALi}$ can be related by equation 1.4:

$$k_H = \frac{C_{AGi}}{C_{ALi}} \tag{1.4}$$

where $k_H$ is the Henry's law constant (dimensionless).

However, since $C_{AGi}$ and $C_{ALi}$ cannot be measured, mass transfer rate equations are defined based on overall mass transfer coefficients ($K_G$ and $K_L$). Thus, equation 1.3 can be expressed in a form given in equation 1.5, where interfacial concentrations are replaced by equilibrium concentrations that correspond to the bulk concentrations:

$$Q_A = K_{AG}a\left(C_{AGb} - C_{AG}^{\ *}\right) = K_{AL}a\left(C_{AL}^{\ *} - C_{ALb}\right) \tag{1.5}$$

where $K_{AG}$ = overall gas phase mass transfer coefficient of substance *A* (m $h^{-1}$),

$K_{AL}$ = overall liquid phase mass transfer coefficient of substance *A* (m $h^{-1}$),

$C_{AG}$* = gas phase concentration that is in equilibrium with the bulk liquid phase concentration $C_{ALb}$ (g $m^{-3}$),

$C_{AL}$* = liquid phase concentration that is in equilibrium with the bulk gas phase concentration $C_{AGb}$ (g $m^{-3}$).

Applying the same principle (Henry's law) described in equation 1.4, $C_{AG}^{*}$ can be then calculated using equation 1.6:

$$C_{AG}^{*} = k_H C_{ALb} \tag{1.6}$$

The performance of biotrickling filters also depends on the Henry's law constant of the target compound since a higher value of this constant indicates lower affinity of the contaminant with the liquid and biofilm phases where absorption and microbial degradation occur (Datta and Allen 2005). In general, gaseous compounds with Henry's law constant of less than 0.1 are believed to be effectively removed in biotrickling filters (Mohseni 2005). For gases which are less soluble in water (those with high Henry's law constant e.g. oxygen), the mass transfer is generally controlled by the liquid phase; whereas, for compounds which are very soluble in water (e.g. ammonia), mass transfer resistance is from the gas side (Tchobanoglous et al. 2003).

***Microbial biodegradation***. The contaminant absorbed in the liquid phase is transported by molecular diffusion to the biofilm where microbial degradation occurs. A biofilm is a gel-like material composed of microorganisms and degradation by-products (Alley 1998). Since the water within the biofilm is stationary, the only mode of transport is molecular diffusion (Devinny et al. 1999).

In stationary liquids like in biofilm where velocity is zero and when diffusion is assumed to be at unsteady state, Fick's second law of diffusion is generally applied (Bird et al. 2002; Fogler 1986). This law describes how concentration varies with time due to diffusion. For one-directional diffusion (e.g. in *x* direction), Fick's second law of diffusion can be described by equation 1.7:

$$\frac{\partial C_A}{\partial t} = -D_A\left(\frac{\partial^2 C_A}{\partial x^2}\right) \tag{1.7}$$

where t = time (h),

x = distance of diffusion (m).

Diffusion in porous media, such as in a biofilm, is generally slower than in water due to the retardant effect caused by the gelatinous property of the biofilm (Abumaizar et al. 1997). One of the empirical equations used to estimate effective diffusivity in biofilm is the one developed by Fan et al. (1990) given in equation 1.8:

$$f_{Xv} = 1 - \frac{0.43 X_v^{0.92}}{11.19 + 0.27 X_v^{0.99}} \tag{1.8}$$

where $f_{Xv}$ = correction factor for diffusion coefficient (dimensionless),

$X_v$ = biofilm density (kg $m^{-3}$).

***Microbial growth.*** Knowledge of microbial kinetics and contaminant degradation rate is important in designing a biological treatment system. Designing a system without sufficient information on these processes may only impair the feasibility and effectiveness of the system (Alley 1998).

Typical microbial growth in a batch system occurs in four phases as shown in Figure 1.7. Each of these phases is described by Alley (1998) and Shuler and Kargi (1992). The first phase,

which is characterized by a period of adjustment, is called the lag phase. This occurs when microorganisms are exposed to new substrates or to the same substrates but of different concentrations. This phase involves formation of new microorganisms or a change in the rate at which microorganisms are produced. Once the cells get adjusted to their new environment, a balanced growth takes place, in which the cells grow at an exponential and a constant rate. During this phase, the specific growth rate determined either from cell number or from cell mass is the same. Rapid growth continues until substrate or nutrients limitation or toxic metabolic product inhibition occurs, where growth rate starts to decrease until it approaches zero. The microbial population at this phase is said to be in stationary growth. After this period, the cells begin to die at an exponential rate.

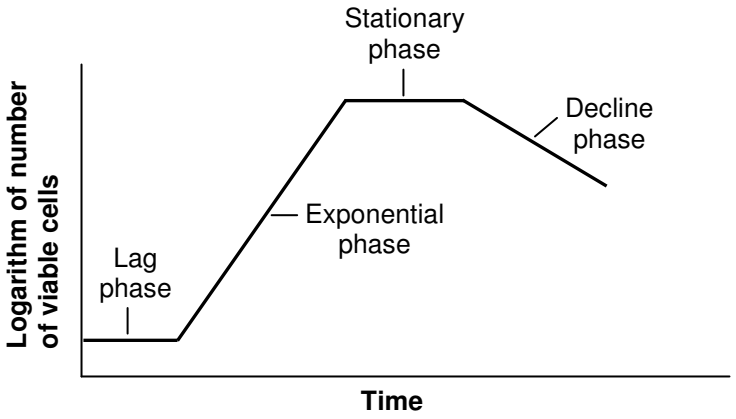


**Figure 1.7 Generalized growth curve of a bacterial culture.**
Adapted from Alley (1998).

During exponential stage, where all growth requirements are met, the growth rate is assumed to be of first order with respect to the concentration of active microorganisms (Pavlostathis 2006). As shown in equation 1.9, the growth rate of the microorganisms is directly

proportional to the concentration of the active microorganisms ($X_a$, g $m^{-3}$) with the specific growth rate ($\mu$, $h^{-1}$) as the proportionality constant:

$$\frac{dX_a}{dt} = \mu X_a \tag{1.9}$$

Further, during exponential growth phase, biomass growth and substrate utilization are interrelated and the rates of these two activities are directly related through the yield coefficient (Y) as presented in equation 1.10 (Dunn 2003; Pavlostathis 2006):

$$\frac{dX_a}{dt} = Y\left(\frac{-dS}{dt}\right) \tag{1.10}$$

where Y = biomass yield coefficient (g biomass formed $g^{-1}$ of substrate consumed),

S = growth-limiting substrate concentration (g $m^{-3}$).

***Microbial growth rate expressions.*** One of the most widely used relationships to represent microbial growth kinetics is the Monod equation (Rittman and McCarty 2001) described in equation 1.11:

$$\mu = \frac{\mu_m S}{K_s + S} \tag{1.11}$$

where $\mu_m$ = maximum specific growth rate ($h^{-1}$),

$K_s$ = half-saturation constant (g $m^{-3}$).

This equation best represents substrate-limited growth with a smooth transition from first order kinetics at low subtrate concentration to zero-order kinetics at high substrate concentration (Shuler and Kargi 1992). This is also generally applicable for degradation kinetics of non-toxic compounds (Lodha et al. 2007).

However, for the growth kinetics of inhibitory compounds (especially at very high substrate concentrations), the Haldane equation (Eq. 1.12) may be used (Devinny et al. 1999):

$$\mu = \frac{\mu_m S}{K_s + S + \left(S^2 / K_i\right)} \tag{1.12}$$

where $K_i$ is the inhibition constant (g $m^{-3}$). The Haldane equation is widely accepted because it is simple and represents growth kinetics with substrates inhibition quite well (Kumar et al. 2005).

There are other microbial growth rate equations. Some of these are discussed by Raghuvanshi and Babu (2010) and Mulchandani and Luong (1989). Some of these models describe the effects of multiple substrates on the growth of either single or mixed bacterial cultures (Okpokwasili and Nweke 2005; Reardon et al. 2002; Kovarova et al. 1997; Bae et al. 1995); however, they have not yet been validated extensively.

***Microbial decay.*** Utilization of substrate produces energy; however, a fraction of this energy is used for endogenous processes such as cell maintenance and decay (Rittman and McCarty 2001). Endogenous decay is assumed to be of first order with respect to the concentration of the active microorganisms (Rittman and McCarty 2001). Thus, considering the amount of energy that is utilized for these processes, the net microbial growth can be then calculated using equation 1.13 (Rittman and McCarty 2001):

$$\frac{dX_a}{dt} = Y\left(\frac{-dS}{dt}\right) - k_d X_a \tag{1.13}$$

where $k_d$ is the decay coefficient ($h^{-1}$).

The first term at the right side of equation 1.13 represents the growth from substrate utilization described in equation 1.10, while the second term represents the microbial decay.

### 1.2.4.2 Performance parameters for biotrickling filter sytems

***Empty bed residence time (EBRT).*** This parameter relates the air flow rate to the size of the bioreactor as described by equation 1.14 (Devinny et al. 1999) and is defined as the empty filter bed volume ($V_f$, $m^3$) divided by the air flow rate ($Q_G$, $m^3\ h^{-1}$):

$$EBRT = \frac{V_f}{Q_G} \tag{1.14}$$

***Surface, volumetric, and loading rates.*** These parameters refer to the amount of air or of contaminant that is fed to the system. Since these are normalized parameters, these would allow comparison of loading rates between reactors of different sizes (Devinny et al. 1999):

$$Surface\ loading = \frac{Q_G}{A} \tag{1.15}$$

$$Volumetric\ loading = \frac{Q_G}{V_f} \tag{1.16}$$

$$Mass\ loading\ (surface) = \frac{Q_G \times C_{Gin}}{A} \tag{1.17}$$

$$Mass\ loading\ (volumetric) = \frac{Q_G \times C_{Gin}}{V_f} \tag{1.18}$$

where A = filter bed cross-sectional area ($m^2$),

$C_{Gin}$ = gas inlet concentration ($g\ m^{-3}$).

***Removal efficiency and elimination capacity.*** These terms are used to describe bioreactor performance. Removal efficiency (RE), as presented in equation 1.19, measures the amount of contaminant removed by the reactor. Since it varies according to contaminant concentration, airflow rate, and filter bed size and only reflects the conditions under which it is evaluated, it cannot be always used to compare performance of different reactors (Devinny et al. 1999):

$$RE = \frac{C_{Gin} - C_{Gout}}{C_{Gin}} \times 100 \quad (1.19)$$

where $C_{Gout}$ = gas exhaust concentration (g $m^{-3}$).

Elimination capacity (EC), on the other hand, measures the mass of contaminant degraded per unit volume of filter material per unit time (equation 1.20). Since this parameter is normalized with respect to the airflow and reactor volume, it can be used to compare performance of two different reactors (Devinny et al. 1999).

$$EC = \frac{(C_{Gin} - C_{Gout}) \times Q_G}{V_f} \quad (1.20)$$

#### 1.2.4.3 Design and operation considerations of biotrickling filters

***Packing media.*** Since microorganisms are important element in the biodegradation of the contaminants, choosing a packing material that would enhance bacterial attachment is essential (Devinny et al. 1999). The desirable characteristics of packing materials include high surface area for biofilm attachment, long-term physical stability, low pressure drop, good moisture retention capacity, and high porosity (Datta and Allen 2005; Devinny et al. 1999).

Biotrickling filters generally use synthetic or inert packing materials such as lava rocks, polypropylene packing, and polyurethane foam. Unlike organic packing materials, inert materials are stable, lighter, and stronger; thus, deeper (with smaller footprint) units can be constructed without fear of compaction (Ozis et al. 2005). These highly-engineered synthetic materials are known to have longer life span, although they can be much more expensive than the naturally available materials.

***Moisture content.*** Water is essential for microorganisms to carry out their normal metabolic activities; thus, low moisture content may result in a low biodegradation rate (Datta and Allen

2005). However, too much water in the bed may also have negative impacts for it hinders transfer of oxygen and hydrophobic pollutants to the biofilm and reduces void volume of the bed causing gas channelling and pressure drop increases (Datta and Allen 2005). For aerobic microorganisms, the optimum moisture content is between 38 and 81% of the pore space of the filter material (Le Cloirec et al. 2005).

***Microorganisms and inoculation.*** The air that goes through the biotrickling filter units also carries aerosols and dust, which in turn carry various types of microorganisms (Devinny et al. 1999). The two most common groups of microorganisms found in air-phase bioreactors are bacteria and fungi. Bacteria generally have rapid substrate uptake and growth under favourable conditions, while fungi normally grow slowly (Devinny et al. 1999). Since fungi can survive in harsher conditions and are able to degrade a larger variety of pollutants (Devinny et al. 1999), they are found more efficient for the treatment of hydrophobic compounds (Singh and Ward 2005).

Microbial population is selected based on the properties of the contaminant to be treated. Heterotrophic microorganisms, which derive energy from the oxidation of organic molecules, are found suitable for the treatment of volatile organic compounds (Singh and Ward 2005). Hydrogen sulphide, ammonia, and other inorganic pollutants are treated with autotrophic microorganisms, which use inorganic molecules as energy source and carbon dioxide as a carbon source (Singh and Ward 2005).

For bioreactors that use organic packing materials such as compost, inoculation may not be needed since these organic materials carry with them large variety of vigorous and well-developed microorganisms, which can be used as initial inoculum (Devinny et al. 1999). However, for biotrickling filters, inoculation may be necessary since their packing media are

generally made of synthetic/inert materials. A microbial culture obtained from an environment similar to the one that exists in the bioreactor could be an effective inoculum (Devinny et al. 1999). While some studies found that inoculation does not directly affect removal efficiencies but only hasten acclimation process, others obtained higher elimination capacities from inoculated bioreactors than from non-inoculated ones (Devinny et al. 1999). Thus, the success of inoculation probably depends on the choice and preparation of the inoculum.

***Nutrients.*** Although the gas contaminants may be used by the microorganisms as carbon and energy sources, nutrients such as nitrogen, phosphorus, minerals, and trace elements should be provided to microorganisms to achieve optimum microbial activity (Datta and Allen 2005).

***Temperature.*** Temperature is also a critical factor for achieving optimum microbial performance. Microorganisms are classified according to their optimum temperature range: (1) psychrophilic microorganisms are those which achieve highest growth rates below 20$^{o}$C; (2) mesophilic microorganisms are those which grow best at 20 to 40$^{o}$C; and (3) thermophilic microorganisms are those which have optimum temperatures above 40$^{o}$C (Datta and Allen 2005).

***pH***. A neutral environment is generally favourable for the growth of many bacterial species. Optimum microbial activity generally exists at pH between 5 to 9 (Le Cloirec et al. 2005). The production of acidic or basic by-products in bioreactors leads to pH changes; however, these pH variations can be controlled in biotrickling filters by continuous wash-out of these by-products or by addition of pH buffer to the liquid phase.

***Oxygen content***. Oxygen is essential to the operation of aerobic biological systems (those that employ aerobic microorganisms). For aerobic heterotrophic bacteria to survive, they require at least 5 to 15% oxygen at the inlet gas stream (Datta and Allen 2005).

#### 1.2.4.4 Challenges to operation and design

***Transient conditions.*** The variability of contaminant load affects microbial activity. During low contaminant load, starvation could occur because of insufficient supply of food and energy for microorganisms (Devinny et al. 1999). On the other hand, since microbial growth is proportional to substrate concentration, microorganisms grow rapidly at high loads, as long as a favourable environment exists (Devinny et al. 1999). However, there will be a point where a further increase in concentrations will no longer correspond to an increase in the removal efficiency, thus, resulting in a performance drop.

Transient conditions in terms of gas concentrations and air flow rates are particularly significant in hog production. Ventilation rates applied in pig barns may vary from 1 L $s^{-1}$ $animal^{-1}$ during winter to 240 L $s^{-1}$ $animal^{-1}$ during summer (Jacobson 2012). Aside from seasonal variations in gas concentrations and flow rates of air emitted from pig barns, diurnal variations may also occur. Thus, designing a biotrickling filter that could efficiently handle these fluctuating conditions is a great challenge.

***Pressure drop and biomass accumulation.*** The biomass formed from the degradation of contaminants tends to accumulate in the filter bed and causes pressure drop. Morgan-Sagastume et al. (2001) observed that at a given air flow rate, the pressure drop increases exponentially with increased biomass. When biofilms get too thick, its deeper regions become inactive because diffusion of contaminants and oxygen becomes restricted (Ozis et al. 2005). Significant

microbial activity is believed to occur only at the outer 100 μm (Ozis et al. 2005). The microelectrode measurements conducted by Masic et al. (2010) on a nitrifying biofilm showed that oxygen content started to drop to 1 g $mL^{-1}$ (the critical dissolved oxygen for nitrification according van Haandel and Van der Lubbe 2012) at portions underneath the 150 μm outer layer thickness.

### 1.2.5 Modelling studies on biotrickling filter

Several models have already been developed for biotrickling filters used for waste air treatment and while they are useful tools in understanding processes, they also have certain limitations and challenges.

#### 1.2.5.1 Model advantages, challenges, and limitations

The different physical, chemical, and biological phenomena occuring in a biological air treatment system can be described through mathematical models. These models can predict process performance and understand relationships between different design and process parameters. Thus, mathematical models become important tools in performing engineering tasks such as sizing and designing bioreactors and optimizing processes (Revah and Morgan-Sagastume 2005; Devinny et al. 1999). Deshusses and Shareefdeen (2005) enumerated some of the advantages of mathematical modelling. According to these authors, by using models one can obtain insight into a given process, acquire quantitative information on parameters that may be difficult or impossible to measure (e.g. contaminant concentration in the biofilm), assess conditions that cannot be tested, and automatically conduct numerous simulations to optimize processes. Furthermore, model simulation is cost-effective and facilitates performance of virtual experiments.

However, there are also significant challenges in modelling biological air treatment systems since they are dynamic systems involving various complex phenomena. Devinny et al. (1999) listed a number of difficulties that exist in defining the model equations for biofilters and biotrickling filters. According to this author, biological systems are still relatively not well-defined, where no agreement has yet been established in the scientific community regarding their operation principles. Since these are tubular reactors, conditions prevailing at the top may be different from those at the bottom of the reactor, which means that calculation involves integration from one end of the reactor to the other. Kinetic relationships on attached growth system are not well-understood yet. Microscopic observation of biofilms is a difficult and expensive task. Model equations involved cannot be solved analytically and model parameters that actually exist in the system are difficult to determine.

The resulting model equations describing physical, chemical, and biological processes are generally a complex set of partial differential equations. Most often, the complexity of the equations could be significantly reduced by applying justifiable assumptions such as equilibrium at phase interface, ideal mixing in liquid phase, plug flow conditions, constant biofilm thickness or biomass density, steady-state conditions, availability of excess oxygen and nutrients, and use of simple microbial kinetics (Shareefdeen et al. 2005; Deshusses and Shareefdeen 2005). However, application of these assumptions may pose certain limitations to the performance and validity of the model. Deshusses and Shareefdeen (2005) listed some of these limitations. According to these authors, models will work only based on the concepts and the assumptions at which they are developed. There are also risks involved in the application of a model outside its calibrated and validated data as uncertainties and discrepancies may increase.

#### 1.2.5.2 Existing mathematical models

One of the earliest mathematical models found in the literature that was specifically developed for gas-phase biofilters was that of Ottengraf and Van der Oever (1983). In this model, the biofilter was divided into three phases: bulk gas, biofilm, and packing. It assumes constant biofilm thickness, plug flow for the gas phase, and negligible gas phase mass transfer resistance. It was adapted from the model of Jennings et al. (1976), which was developed for the removal of a biodegradable substrate in a submerged biological filter.

Recently, more models have been developed for both biofilters and biotrickling filters. Some models describe steady-state condition either in terms of contaminant concentration or of biofilm thickness (Diks and Ottengraf 1991; Sharvelle et al. 2008) while others calculate transient contaminant concentration (Baquerizo et al. 2005; Kim and Deshusses 2003; Deshusses et al. 1995) or account for biological growth and biomass accumulation (Li et al. 2002; Okkerse et al. 1999; Alonso et al. 1998). Mpanias and Baltzis (1998) and Shareefdeen et al. (1993) account for oxygen limitation, which is often neglected in most models. Interactions among multiple contaminants and biofilm species are investigated in some models (Baltzis et al. 2001). Most biotrickling filter models assume that the transfer of contaminant into the liquid phase occurs first prior to the transport to the biofilm, whereas Kim and Deshusses (2003) account for direct transfer of contaminant into non-wetted portion of the biofilm. Dispersion, which is neglected in most models, is considered in the model of Hodge and Devinny (1995). Sharvelle et al. (2008) and Baquerizo et al. (2005) take into account the pH dependence of the reactions. Though the existing different models vary in terms of the processes that are considered or neglected from the model, they all describe the fundamental processes: mass transfer of contaminant from the gas phase into the liquid phase and subsequent mass transfer into the biofilm where microbial degradation occurs (Sharvelle et al. 2008).

One of the models developed for biotrickling filters is by Mpanias and Baltzis (1998). This model accounts for the mass transfer and kinetic effects based on volatile organic compound (VOC) and oxygen availability under steady-state condition. It describes VOC and oxygen concentration profiles in all three phases: gas, trickling liquid, and biofilm as shown in Figure 1.8.

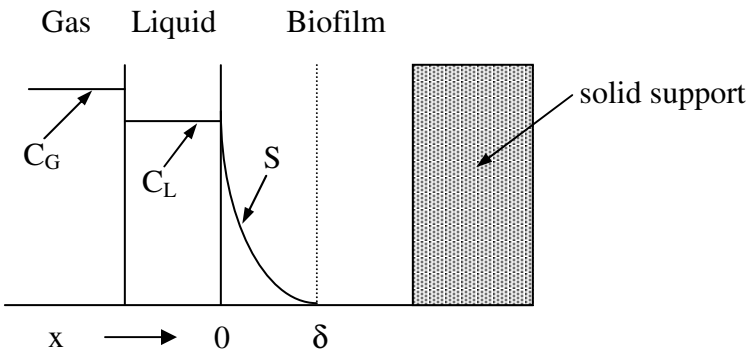


**Figure 1.8 Schematic representation of the model of Mpanias and Baltzis (1998).**

The mass balance equations for VOC and oxygen in the biofilm are given in equations 1.21 and 1.22, respectively:

$$f(X_v)D_{Wj}\frac{d^2S_j}{dx^2} = \frac{X_v}{Y_j}\mu_j(S_j)f(S_O) \tag{1.21}$$

$$f(X_v)D_{WO}\frac{d^2S_O}{dx^2} = \frac{X_v}{Y_{Oj}}\mu_j(S_j)f(S_O) \tag{1.22}$$

where $D_W$ is the diffusion coefficient in water, S is the VOC concentration in the biofilm, x is the distance along biofilm depth, and the subscripts *j* and *O* refer to VOC and oxygen, respectively. The product of $\mu_j(S_j)$ and $f(S_O)$ represents the dependence of the microbial growth rate to the concentrations of the VOC and oxygen. Equations 1.21 and 1.22 simply imply that the changes in VOC and oxygen concentrations in the biofilm are due to their degradation in the biofilm.

In the liquid phase, the changes in VOC and oxygen concentrations are the net results of the two processes: absorption from the gas phase and diffusion to the biofilm, as described in equations 1.23 and 1.24:

$$U_L \frac{dC_{Lj}}{dh} = K_{Lj}\left(\frac{C_{Gj}}{m_j} - C_{Lj}\right) + f(X_v) D_{Wj} A_S \left[\frac{dS_j}{dx}\right]_{x=0} \tag{1.23}$$

$$U_L \frac{dC_{LO}}{dh} = K_{LO}\left(\frac{C_{GO}}{m_O} - C_{LO}\right) + f(X_v) D_{WO} A_S \left[\frac{dS_O}{dx}\right]_{x=0} \tag{1.24}$$

where $U_L$ is the liquid superficial velocity, h is the height of filter bed, m is the distribution coefficient between air and water, and $A_S$ is the wetted biolayer surface area.

Equations 1.25 and 1.26 predict the concentration profiles of VOC and oxygen in the gas phase, which according to the equations, are influenced by the amount that goes into the liquid phase. The sign of the right-side term of the equations depends on the gas flow direction (upward or downward):

$$U_G \frac{dC_{Gj}}{dh} = \pm K_{Lj}\left(\frac{C_{Gj}}{m_j} - C_{Lj}\right) \tag{1.25}$$

$$U_G \frac{dC_{GO}}{dh} = \pm K_{LO}\left(\frac{C_{GO}}{m_O} - C_{LO}\right) \tag{1.26}$$

where $U_G$ is the gas superficial velocity.

The model was validated using mono-chlorobenzene. An independent kinetic study with suspended cultures was performed to describe the biodegradation kinetics of mono-chlorobenzene. The model was used to evaluate process performance under a variety of operating conditions concerning inlet mono-chlorobenzene concentration, flow rate of the air stream, and flow rate of the trickling liquid. This model assumes a planar geometry for the biolayer, plug flows for both gas and liquid streams, an existence of an effective biofilm layer (δ),

which is determined by the depletion of either mono-chlorobenzene or oxygen, and a constant biofilm density and void fraction of the filter bed. The concentrations of mono-chlorobenzene and oxygen at the gas-liquid interface were assumed to be related via Henry's law. It also assumes negligible biodegradation in the liquid phase and negligible mass transfer resistances at the gas-liquid and liquid-biofilm interfaces. The diffusivities of mono-chlorobenzene and oxygen in the biofilm were assumed equal to those in water multiplied by a correction factor. An improved version of this model, which is presented in the study by Baltzis et al. (2001), accounts for the kinetic interactions among pollutants during biodegradation.

## 1.3 CURRENT STUDY

The information gathered from the literature review was used as basis in developing the hypothesis, objective, and methodology of this current study, which are presented in the succeeding sub-sections.

### 1.3.1 Hypothesis

A large number of experimental and research studies have demonstrated the efficiency and potential of biological reactors to treat pollutants in air emissions. However, studies dealing with bioreactor modelling are relatively limited. Mathematical models are known to be useful tools in developing a fundamental understanding of a process and to accomplish engineering tasks such as reactor design, scale-up, and process optimization.

Based on the literature review conducted, no model has yet been developed for a biotrickling filter used for the removal of pollutants emitted from pig barns. Thus, this study was carried out in order to produce mathematical equations that could describe the important processes involved in the removal of pig barn air contaminants in biotrickling filters. The

hypothesis of this research was that if the parameters that play important roles in the removal of contaminants in biotrickling filters could be properly identified and their effects clearly understood by using the developed model, then a better understanding of the process could be achieved, which could eventually lead to a better design and process optimisation.

### 1.3.2 Objective

The main goal of this research was to optimize the performance of biotrickling filters in reducing emission of odour and toxic substances from swine facilities by identifying parameters and operating conditions that have significant impact on the treatment process. To achieve this objective, a steady-state mathematical model that describes the physical, chemical, and biological phenomena taking place in a biotrickling filter unit was developed.

This study consists of two parts:

i) Determination of model parameters

The parameters were determined either from published literature or from small-scale laboratory experiments.

ii) Model development, sensitivity analysis, calibration, validation, and simulations

Model development entails establishing of equations that describe the different physical, chemical, and biological reactions involved in the treatment of a pollutant in a biotrickling filter. Sensitivity analysis helps identify the key parameters that have great impact on the removal of a pollutant. Calibration involves adjustment of model parameters within physically reasonable ranges until the resulting predictions give the best fit to the observed data. Validation involves assessment of the reliability of the model's performance under a variety of operating conditions and ensures that the model closely simulates what the real system does. Model simulation is the application of the developed model to

evaluate how various process and design parameters relate to the reactor's performance or how these parameters relate to each other.

Both model calibration and validation used the data obtained from the bench-scale biotrickling filter operations conducted at the laboratory of the Research and Development Institute for the Agri-Environment (IRDA) at Deschambault, Quebec, Canada. Initially, the model was to be calibrated and validated using at least two key odour components of swine facility air. However, due to limitations encountered in monitoring the odour components in the waste air, only ammonia was used for these steps. Ammonia was chosen as the model contaminant because it is a very significant swine barn gas contaminant, comprising more than 50% of the total emissions as reported in the literature (Armeen et al. 2008). Thus, being emitted from swine production facilities, its removal in the biotrickling filter could be a potential indicator of the reactor's performance in removing odorous gases from the waste air.

Simulations were conducted using the validated model to predict the removal of ammonia at different operating modes of the biotrickling filter under steady-state conditions. Simulations were also performed to identify key design parameters and operating conditions that could be adjusted to further improve the performance of the bioreactor.

### 1.3.3 Methodology

The goal of this research was achieved by performing the specific steps listed below, which are also presented in the flow diagram in Figure 1.9.

1. Conduct a literature review;

2. Develop mass balance equations for the pollutant in the gas, liquid, and biofilm phases of a biotrickling filter system under steady-state conditions;
3. Determine the model parameters using empirical equations or obtain them from small-scale experiments or published literature;
4. Solve the partial differential equations by a numerical method;
5. Perform a parametric sensitivity analysis to determine the relative influence of each of the model parameters for various operating conditions;
6. Calibrate and validate the model using field measurements;
7. Perform simulations under different operating conditions (e.g. residence time, gas and liquid flow rates, gas and liquid inlet concentrations).

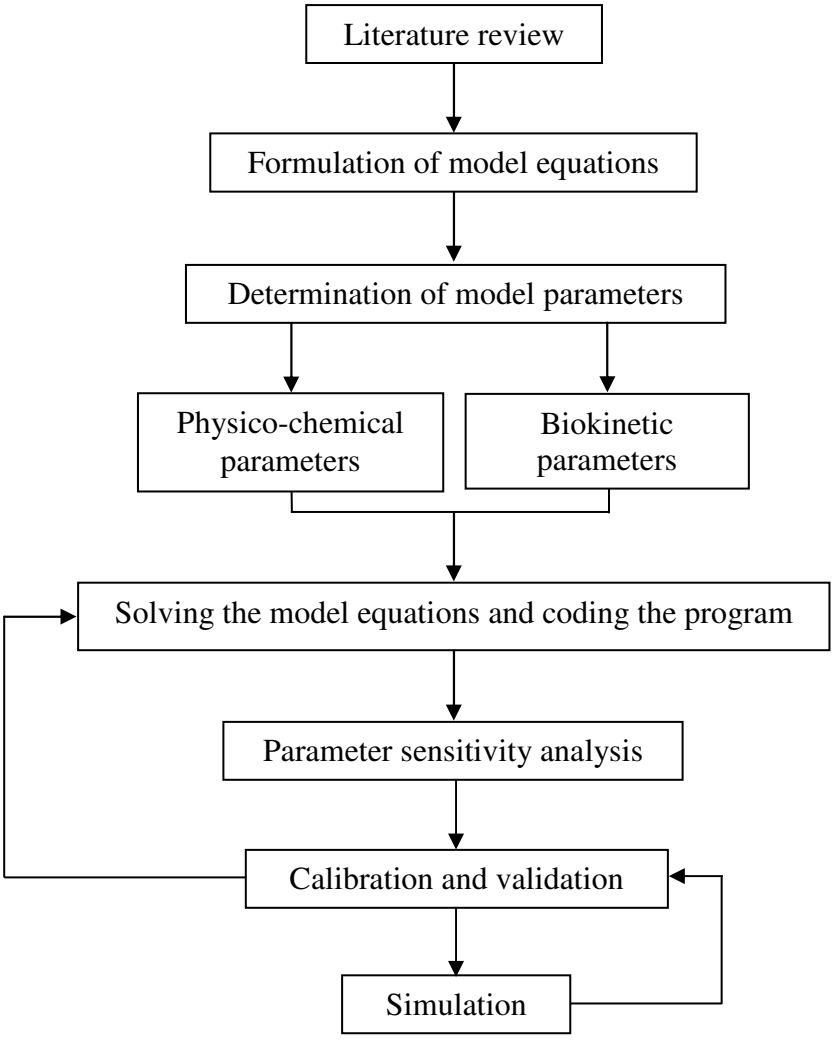


**Figure 1.9 Flow diagram of the research study.**

### 1.3.4 Thesis outline

Chapter 2 presents the study on determining the key odour components of swine barn air, which could be potentially used as model pollutants for a modelling study. Chapter 3 describes a kinetic study conducted using suspended mixed cultures to assess the ability of different microbial cultures in degrading substances found in swine facility air. Chapter 4 describes three kinetic studies, also conducted using suspended mixed cultures, whose objectives were to evaluate the effects of pH and to determine the kinetic parameters associated with the

biodegradation of *p*-cresol and ammonia (two of the key odour components identified in Chapter 2). Chapter 5 focuses on the development, sensitivity analysis, calibration and validation of the model describing ammonia removal in a biotrickling filter under steady-state conditions. Chapter 6 presents the simulation study on ammonia removal using the developed model. Chapter 7 presents the general discussion as well as the conclusions of the thesis.

## 1.4 REFERENCES


Abumaizar, R.J., E.H. Smith and W. Kocher. 1997. Analytical model of dual-media biofilter for removal of organic air pollutants. *Journal of Environmental Engineering* 123: 606-614.

Alley, R.E. Jr. 1998. Biofiltration of gaseous compounds. In *Air Quality Control Handbook*, ed. E. Roberts Alley & Associates, 23.1-23.31. USA: McGraw-Hill.

Alonso, C., M.T. Suidan, B.R. Kim and B.J. Kim. 1998. Dynamic mathematical model for the biodegradation of VOCs in a biofilter: Biomass accumulation study. *Environmental Science and Technology* 32: 3118-3123.

Armeen, A., J.J.R. Feddes, J.J. Leonard and R.N. Coleman. 2008. Biofilters to treat swine facility air: Part 1. Nitrogen mass balance. *Canadian Biosystems Engineering* 50: 6.21-6.27.

ASHRAE. 1993. *ASHRAE Handbook: Fundamentals*. USA: American Society of Heating, Refrigerating and Air Conditioning Engineers.

Bach, H. 1923. Schwefel im abwasser. *Gesundheits-Ingenieur* 46: 370.

Bae, B.H., R.L. Autenrieth and J.S. Bonner. 1995. Kinetics of multiple phenolic compounds degradation with a mixed culture in a continuous-flow reactor. *Water Environment Federation* 67(2): 215-223.

Baltzis, B.C., C.J. Mpanias and S. Bhattacharya. 2001. Modeling the removal of VOC mixtures in biotrickling filters. *Biotechnology and Bioengineering* 72: 389-401.

Baquerizo, G., J.P. Maestre, T. Sakuma, M.A. Deshusses, X. Gamisans, D. Gabriel and J. Lafuente. 2005. A detailed model of a biofilter for ammonia removal: Model parameters analysis and model validation. *Chemical Engineering Journal* 113: 205-214.

Bird, R.B., W.E. Stewart and E.N. Lightfoot. 2002. *Transport Phenomena*, 2nd edition. USA: John Wiley & Sons, Inc.

Blanes-Vidal, V., M.N. Hansen, A.P.S. Adamsen, A. Feilberg, S.O. Petersen and B.B. Jensen. 2009. Characterization of odor released during handling of swine slurry: Part 1. Relationship between odorants and perceived odor concentrations. *Atmospheric Environment* 43(18): 2997-3005.

CCOHS (Canadian Centre for Occupational Health and Safety). 2013. OSH Answers. http://www.ccohs.ca (2013/04/09).

Choi, D.S., J.S. Devinny and M.A. Deshusses. 2004. Behavior of field-scale biotrickling filter under nonsteady state conditions. *Journal of Environmental Engineering* 130(3): 322-328.

Chou, M.S. and J.J. Huang. 1997. Treatment of methylethylketone in air stream by biotrickling filters. *Journal of Environmental Engineering* 123:569-576.

Coulson, J.M., J.F. Richardson, J.R. Backhurst and J.H. Harker. 2002. *Coulson and Richardson's Chemical Engineering – Particle Technology and Separation Processes*, 5th edition, Vol. 2. Massachusettes, USA: Elsevier Science.

Cox, H.H.J. and M.A. Deshusses. 1998. Biological waste air treatment in biotrickling filters. *Current Opinion in Biotechnology* 9: 256-262.

CPC (Canadian Pork Council). 2012a. Canadian Hog Production and Pork Exports Contribute $9.28 Billion to the Economy**.** http://www.cpc-ccp.com/news.php? rev=e&ID=306& article=1&year=2012&da=0&incl=0 (2012/7/30).

CPC (Canadian Pork Council). 2012b. Description of Canadian Hog Farms. http://www.cpc-ccp.com/statistics-farms-e.php (2012/5/28).

CPI (Canada Pork International). 2012. Hog Production in Canada. http://www.canadapork.com/en/industry-information/hog-production-in-canada (2012/7/30).

Datta, I. and D.G. Allen. 2005. Biofilter technology. In *Biotechnology for Odour and Air Pollution Control*, ed. Z. Shareefdeen and A. Singh, 125-145. Germany: Springer-Verlag.

Deshusses, M.A. 1997a. Transient behavior of biofilters: Start-up, carbon balances, and interactions between pollutants. *Journal of Environmental Engineering* 123: 563-568.

Deshusses, M.A. 1997b. Biological waste air treatment in biofilters. *Current Opinion in Biotechnology* 8: 335-339.

Deshusses, M.A. and H.H. J. Cox. 1999. A cost benefit approach to reactor sizing and nutrient supply for biotrickling filters for air pollution control. *Environmental Progress* 18: 188-196.

Deshusses, M.A., G. Hamer and I.J. Dunn. 1995. Behavior of biofilters for waste air biotreatment. 1. Dynamic model Development. *Environmental Science Technology* 29: 1048-1058.

Deshusses, M.A. and Z. Shareefdeen. 2005. Modeling of biofilters and biotrickling filters for odour and VOC control applications. In *Biotechnology for Odour and Air Pollution Control*, ed. Z. Shareefdeen and A. Singh, 213-231. Germany: Springer-Verlag.

Devinny, J.S., M.A. Deshusses and T.S. Webster. 1999. *Biofiltration for Air Pollution Control.* USA: CRC Press LLC.

Diks, R.M.M. and S.P.P. Ottengraff. 1991. Verification studies of a simplified model for the removal of dichloromethane from waste gases using a biological trickling filter (Part I). *Bioprocess Engineering* 6: 93-99.

Donham, K.J. 2000. The concentration of swine production: Effects on swine health, productivity, human health, and the environment. *Veterinary Clinics of North America: Food Animal Practice* 16(3): 559-597.

Donham, K., P. Haglind, Y. Peterson, R. Rylander and L. Belin. 1989. Environmental and health studies of farm workers in Swedish swine confinement buildings. *British Journal of Industrial Medicine* 46(1): 31–37.

Doran, P.M. 1995. *Bioprocess Engineering Principles*. USA: Academic Press Limited.

Dunn, I.J. 2003. *Biological Reaction Engineering: Dynamic Modelling Fundamentals*. Weinheim, Germany: Wiley-VCH Verlag.

Dutta, B.K. 2007. *Principles of Mass Transfer and Separation Processes.* New Delhi, India: Prentice-Hall of India Private Limited.

Fan, L.S., R. Leyva-Ramos, K.D. Wisecarver and B.J. Zehner. 1990. Diffusion of phenol through a biofilm grown on activated carbon particles in a draft-tube three-phase fluidized-bed bioreactor. *Biotechnology and Bioengineering* 35: 279-286.

FAO. 2011. *Rural structures in the tropics. Design and development.* Rome: Food and Agriculture Organization of the United Nations.

Fogler, H.S. 1986. *Elements of Chemical Reaction Engineering*. USA: Prentice-Hall, Inc.

Govind, R. and S. Narayan. 2005. Selection of bioreactor media for odour control. In *Biotechnology for Odour and Air Pollution Control*, ed. Z. Shareefdeen and A. Singh, 65-100. Germany: Springer-Verlag.

Grimm, E. 2005. State-of-the-art of waste air purification systems for application in animal husbandry facilities. *Landtechnik* 60: 36-37.

Groot Koerkamp, P.W.G., J.H.M. Metz, G.H. Uenk, V.R. Phillips, M.R. Holden, R.W. Sneath, J.L. Short, R.P.P. White, J. Hartung, J. Seedorf, M. Schroder, K.H. Linkert, S. Pedersen, H. Takai, J.O. Johnsen and C.M. Wathes. 1998. Concentrations and emissions of ammonia in livestock buildings in northern Europe. *Journal of Agricultural Engineering Research* 70 (1): 79-85.

Hartung, E., T. Jungbluth and W. Buscher. 2001. Reduction of ammonia and odor emissions from a piggery with biofilters. *Transactions of the ASAE* 44(1): 113-118.

Hodge, D.S. and J.S. Devinny. 1995. Modeling removal of air contaminants by biofiltration. *Journal of Environmental Engineering* 121: 21-32.

Hoff, S.J., D.S. Bundy and X.W. Li. 1997. Dust effects on odor and odor compounds. In *Proceedings of the International Symposium on Ammonia and Odour Control from Animal Production facilities*, 101-110. Vinkeloord, The Netherlands: International Commission of Agricultural and Biosystems Engineering.

Hogberg, M.G., S.L. Fales, F.L. Kirschenmann, M.S. Honeyman, J.A. Miranowski and P. Lasley. 2005. Interrelationships of animal agriculture, the environment, and rural communities. *Journal of Animal Science* 83: E13-E17.

Honeyman, M.S. 1996. Sustainability issues of U.S. swine production. *Journal of Animal Science* 74: 1410-1417.

Iliuta, I. and F. Larachi. 2004. Transient biofilter aerodynamics and clogging for VOC degradation. *Chemical Engineering Science* 59:3293-3302.

Jacobson, L.D. 2012. 21st Century Ventilation and Energy Management. http://nationalhog farmer.com/facilities/21st-century-ventilation-and-energy-management (2013/03/29).

Jennings, P.A., V.L.Snoeyink, E.S.K. Chian. 1976. Theoretical model for a submerged biological filter. *Biotechnology and Bioengineering* 18: 1249-1273.

Jensen, T.L. and M.J. Hansen. 2006. A biotrickling filter for removing ammonia and odour in ventilation air from a unit with growing-finishing pigs. In *Proceedings Workshop on Agricultural Air Quality*, 844-846. Washington, D.C., USA. June 5-8.

Kerr, B.J., C.J. Ziemer, S.L. Trabue, J.D. Crouse and T.B. Parkin. 2006. Manure composition as affected by dietary protein and cellulose concentrations. *Journal of Animal Science* 84: 1584-1592.

Kim, S. and M.A. Deshusses. 2003. Development and experimental validation of a conceptual model for biotrickling filtration of $H_2S$. *Environmental Progress* 22(2): 119-128.

Kim, K.Y., H.J. Ko, H.T. Kim, Y.S. Kim, Y.M. Roh, C.M. Lee, H.S. Kim and C.N. Kim. 2007. Sulfuric odorous compounds emitted from pig-feeding operations. *Atmospheric Environment* 41: 4811-4818.

Kovarova, K., A. Kach, A.J.B. Zehnder and T. Egli. 1997. Cultivation of *Escherichia coli* with mixtures of 3-phenylpropionic acid and glucose: Steady-state growth kinetics. *Applied and Environmental Microbiology* 63(7): 2619-2624.

Kumar, A., S. Kumar and S. Kumar. 2005. Biodegradation kinetics of phenol and catechol using *Pseudomonas. Biochemical Engineering Journal* 22: 151-159.

Lais, S., E. Hartung and T. Jungbluth**.** 1997. Reduction of ammonia and odour emissions by bioscrubbers. In *Proceedings of the International Symposium on Ammonia and Odour Control from Animal Production Facilities*, 533-536. Vinkeloord, The Netherlands: International Commission of Agricultural and Biosystems Engineering.

Lambert, M., S.P. Lemay, E.M. Barber, T.G. Crowe and L. Chénard. 2001. Humidity control for swine buildings in cold climate - Part I: Modelling of three control strategies. *Canadian Biosystems Engineering* 43: 5.29-5.36.

Le Cloirec, P., Y. Andres, C. Gerente and P. Pre. 2005. Biological treatment of waste gases containing volatile organic compounds. In *Biotechnology for Odour and Air Pollution Control*, ed Z. Shareefdeen and A. Singh, 281-302. Germany: Springer-Verlag.

Lemay, S.P. 1999. Barn management and control of odours. *Advances in Pork Production* 10: 81-91.

Lemay, S.P. 2013. Development of an innovative air cleaning system for swine buildings. Canadian Swine Research and Development Cluster Project 1009. Quebec City, Quebec, Canada: Research and Development Institute for the Agri-Environment.

Leson, G. and A.M. Winer. 1991. Biofiltration: an innovative air pollution control technology for VOC emissions. *Journal of the Air & Waste Management Association* 41(8): 1045-1054.

Li, H., J.C. Crittenden, J.R. Mihelcic and H. Hautakangas. 2002. Optimization of biofiltration for odor control: Model development and parameter sensitivity. *Water Environment Research* 74(1): 5-16.

Lodha, B., P. Bhat, M.S. Kumar, A.N. Vaidya, S. Mudliar, D.J. Killedar and T. Chakrabarti. 2007. Bioisomerization kinetics of γ-HCH and biokinetics of *Pseudomonas aeruginosa* degrading technical HCH. *Biochemical Engineering Journal* 35: 12-19.

Mackie, R.I., P.G. Stroot and V.H. Varel. 1998. Biochemical identification and biological origin of key odour components in livestock waste. *Journal of Animal Science* 76: 1331-1342.

Martens, W., M. Martinec, R. Zapirain, M. Stark, E. Hartung and U. Palmgren. 2001. Reduction potential of microbial, odour and ammonia emissions from a pig facility by biofilters. *International Journal of Hygiene and Environmental Health* 203(4): 335-345.

Masic, A., J. Bengtsson and M. Christensson. 2010. Measuring and modeling the oxygen profile in a nitrifying moving bed biofilm reactor. *Mathematical Biosciences* 227: 1-11.

McCrory, D.F. and P.J. Hobbs. 2001. Additives to reduce ammonia and odor emissions from livestock wastes: A review. *Journal of Environmental Quality* 30: 345-355.

Melse, R.W. and G. Mol. 2004. Odour and ammonia removal from pig house exhaust air using a biotrickling filter. *Water Science and Technology* 50(4): 275-282.

Melse, R.W., J.P.M. Ploegaert and N.W.M. Ogink. 2012. Biotrickling filter for the treatment of exhaust air from a pig rearing building: Ammonia removal performance and its fluctuations. *Biosystems Engineering* 113: 242-252.

Meyer, S. 2002. Comfort Drives Pig Efficiency. http://nationalhogfarmer.com/mag/farming_ comfort _drives_pig (2013/03/29).

Mohseni, M. 2005. Biological treatment of waste gases containing inorganic compounds. In *Biotechnology for Odor and Air Pollution Control*, ed. Z. Shareefdeen and A. Singh, 253-280. Germany: Springer-Verlag.

Morgan-Sagastume, F., B.E. Sleep and D.G. Allen. 2001. Effects of biomass growth on gas pressure drop in biofilters. *Journal of Environmental Engineering* 127(5): 388-396.

Mpanias, C.J. and B.C. Baltzis. 1998. An experimental and modeling study on the removal of mono-chlorobenzene vapor in biotrickling filters. *Biotechnology and Bioengineering* 59: 328-343.

Mulchandani, A. and J.H.T. Luong. 1989. Microbial inhibition kinetics revisited. *Enzyme and Microbial Technology* 11: 66-73.

Ndegwa, P.M., J. Zhu and A. Luo. 2002. Stratification of solids, nitrogen and phosphorus in swine manure in deep pits under slatted floors. *Bioresource Technology* 83: 203-211.

Nicolai, R.E., and K.A. Janni. 1997. Development of a low cost biofilter on swine production facilities. ASAE Paper No. 974040. St. Joseph, MI: ASABE.

Okkerse, W.J.H., S.P.P. Ottengraf, B. Osinga-Kuipers and M. Okkerse. 1999. Biomass accumulation and clogging in biotrickling filters for waste gas treatment. Evaluation of a dynamic model using dichloromethane as a model pollutant. *Biotechnology and Bioengineering* 63: 418-430.

Okpokwasili, G.C. and C.O. Nweke. 2005. Microbial growth and substrate utilization kinetics. *African Journal of Biotechnology* 5(4): 305-317.

Ottengraf, S.P.P. and A.H.C. Van Den Oever. 1983. Kinetics of organic compound removal from waste gases with a biological filter. *Biotechnology and Bioengineering* 25(12): 3089-3102.

Ozis, F., A. Bina and J.S. Devinny. 2005. Future prospects of biotechnology for odor control. In *Biotechnology for Odour and Air Pollution Control*, ed. Z. Shareefdeen and A. Singh, 383-401. Germany: Springer-Verlag.

Park, O.H. and I.G. Jung. 2006. A model study based on experiments on toluene removal under high load conditions in biofilters. *Biochemical Engineering Journal* 28: 269-274.

Pavlostathis, S.G. 2006. Basic concepts of biological processes. In *Advanced Biological Treatment Processes for Industrial Wastewaters: Principles and Applications*, ed F.J. Cervantes, S.G. Pavlostathis and A.C. Van Haandel, 16-46. UK: IWA Publishing.

Powers, W.J. 1999. Odour control for livestock systems. *Journal of Animal Science* 77: 169-176.

Predicala, B.Z., R.G. Maghirang, S.B. Jerez, J.E. Urban and R.D. Goodband. 2001. Dust and bioaerosol concentrations in two swine–finishing buildings in Kansas. *Transactions of the ASAE* 44(5): 1291-1298.

Raghuvanshi, S. and B.V. Babu. 2010. Biodegradation kinetics of methyl iso-butyl ketone by acclimated mixed culture. *Biodegradation* 21: 31-42.

Rappert, S. and R. Muller. 2005. Odour compounds in waste gas emissions from agricultural operations and food industries. *Waste Management* 25: 887-907.

Reardon, K.F., D.C. Mosteller, J.B. Rogers, N.M. DuTeau and K.H. Kim. 2002. Biodegradation kinetics of aromatic hydrocarbon mixtures by pure and mixed bacterial cultures. *Environmental Health Perspectives* 110(6): 1005-1011.

Revah, S. and J.M. Morgan-Sagastume. 2005. Methods of odour and VOC control. In *Biotechnology for Odour and Air Pollution Control*, ed. Z. Shareefdeen and A. Singh, 29-63. Germany: Springer-Verlag.

Rittmann, B.E. and P.L. McCarty. 2001. *Environmental Biotechnology: Principles and Applications*. USA: McGraw-Hill.

Schiffman, S.S., J.L. Bennett and J.H. Raymer. 2001. Quantification of odors and odorants from swine operations in North Carolina. *Agricultural and Forest Meteorology* 108(3): 213-240.

Shareefdeen, Z., B.C. Baltzis, Y.S. Oh and R. Bartha. 1993. Biofiltration of methanol vapor. *Biotechnology and Bioengineering* 41: 512-524.

Shareefdeen, Z., B. Herner and A. Singh. 2005. Biotechnology for air pollution control – An overview. In *Biotechnology for Odour and Air Pollution Control*, ed. Z. Shareefdeen and A. Singh, 3-15. Germany: Springer-Verlag.

Sharvelle, S., M. Arabi, E. McLamore and M.K. Banks. 2008. Model development for biotrickling filter treatment of graywater simulant and waste gas. I. *Journal of Environmental Engineering* 134(10): 813-824.

Sheridan, B.A., T.P. Curran and V.A. Dodd. 2002a. Assessment of the influence of media particle size on the biofiltration of odourous exhaust ventilation air from a piggery facility. *Bioresource Technology* 84: 129-143.

Sheridan, B., T. Curran, V. Dodd and J. Colligan. 2002b. Biofiltration of odour and ammonia from a pig unit – A pilot-scale study. *Biosystems Engineering* 82: 441-453.

Shuler, M.L. and F. Kargi. 1992. *Bioprocess Engineering: Basic Concepts*. USA: PTR Prentice – Hall, Inc.

Singh, A., Z. Shareefdeen and O.P. Ward. 2005. Bioscrubber technology. In *Biotechnology for Odour and Air Pollution Control*, Z. Shareefdeen and A. Singh, 169-193. Germany: Springer-Verlag.

Singh, A. and O. Ward. 2005. Microbiology of bioreactors for waste gas treatment. In *Biotechnology for Odour and Air Pollution Control*, ed. Z. Shareefdeen and A. Singh, 101-121. Germany: Springer-Verlag.

Streese, J., M. Schlegelmilch, K. Heining and R. Stegmann. 2005. A macrokinetic model for dimensioning of biofilters for VOC and odour treatment. *Waste Management* 25: 965-974.

Sutton, A.L., K.B. Kephart, M.W.A. Verstegen, T.T. Canh and P.J. Hobbs. 1999. Potential for reduction of odorous compounds in swine manure through diet modification. *Journal of Animal Science* 77: 430-439.

Swanson, W.J., and R.C. Loehr. 1997. Biofiltration: Fundamentals, design and operations, principles, and applications. *Journal of Environmental Engineering* 123: 538-546.

Takai, H., S. Pedersen, J.O. Johnsen, J.H.M. Metz, P.W.G. Groot Koerkamp, G.H. Uenk, V.R. Phillips, M.R. Holden, R.W. Sneath, J.L. Short, R.P. White, J. Hartung, J. Seedorf, M. Schroder, K.H. Linkert and C.M. Wathes. 1998. Concentrations and emissions of airborne

dust in livestock buildings in northern Europe. *Journal of Agricultural Engineering Research* 70: 59-77.

Tchobanoglous, G., F.L. Burton, H.D. Stensel and Metcalf & Eddy. 2003. *Wastewater Engineering: Treatment and Reuse*. USA: McGraw-Hill.

Thorne, P.S., A.C. Ansley and S.S. Perry. 2009. Concentrations of bioaerosols, odors, and hydrogen sulfide inside and downwind from two types of swine livestock operations. *Journal of Occupational and Environmental Hygiene* 6(4): 211-220.

van Haandel, A.C. and J.G.M. van der Lubbe. 2012. *Handbook of Biological Wastewater Treatment: Design and Optimisation of Activated Sludge Systems*, 2nd edition. London, UK: IWA Publishing.

Zhu, J. 2000. A review of microbiology in swine manure odour control. *Agriculture, Ecosystems and Environment* 78: 93-106.

# Chapter 2
# Identification of Key Odour Components of Swine Facility Air for a Modelling Study of a Biotrickling Filter

## 2.1 VERSION PRESENTED IN A CONFERENCE

A similar version of this chapter was presented at the joint conference of the International Commission of Agricultural and Biosystems Engineering (CIGR) and the Canadian Society for Bioengineering (CSBE) in June 2010 in Quebec City, Quebec, Canada.

- Martel, M., S.P. Lemay, M. Belzile, J. Feddes and S. Godbout. 2010. Identification of Key Odour Components from Pig Buildings for Modelling Purposes. Presented at the XVII$^{th}$ World Congress of the International Commission of Agricultural and Biosystems Engineering (CIGR). Quebec City, Quebec. June 13-17, 2010.

## 2.2 CONTRIBUTION OF THE PH.D. CANDIDATE

This study resulted in the identification of the key odour components of pig barn air. Knowledge of these key odour components can help develop cost effective strategies for reducing odour nuisances from livestock production. The data analysis and manuscript writing were performed by the candidate while most of the sample collection was conducted by the research associates and technicians of the Research and Development Institute for the Agri-Environment (IRDA). Dr. Stéphane P. Lemay and Dr. Bernardo Predicala, as well as Dr. Matthieu Girard of IRDA, provided editorial inputs while Dr. John Feddes provided suggestions on the analysis of data.

## 2.3 CONTRIBUTION OF THIS PAPER TO THE OVERALL STUDY

Mathematical models are useful tools for describing and simulating performance of reactors; yet, simulating the removal of hundreds of odour components of pig barn air in biotrickling filters poses a significant challenge. However, it has been hypothesized that modelling the removal of certain key odour components, those that are mainly responsible for the unpleasant odour, might be sufficient to describe the overall odour reduction. Thus, in this study, the key odour components of swine facility air were identified using field data. The identified key odour components could then be used as model pollutants for the mathematical modelling portion of the overall research.

## 2.4 ABSTRACT

The key odour components of pig barn air were identified using the data collected from the inlet and exhaust of three pilot-scale biotrickling filters treating waste air from three bench-scale pig chambers. Ammonia ($NH_3$) and hydrogen sulphide ($H_2S$) concentrations were measured inline while the volatile organic compounds (VOCs) were collected using adsorption tubes and analyzed by a gas chromatograph coupled with a mass spectrometer and an olfactory detection port (GC-MS/O). A total of 176 VOCs were identified in 60 samples, each with corresponding odour intensity and odour character. Samples for odour measurements were also collected in Nalophan bags and analyzed using a dynamic olfactometer. The key odorants were determined through linear regression analysis and from calculated odour indices. The compounds that had the highest $R^2$ were butanoic acid, 3-methylbutanoic acid, and $NH_3$ with corresponding values of 0.47, 0.37, and 0.35. The VOCs that had the highest odour indices at the inlet of the bioreactors include butanoic acid, 3-methylbutanoic acid, *p*-cresol, and dimethyl sulphide with corresponding odour index values of 6.6, 6.3, 5.8, and 5.2. While the result indicates that these

substances could be mainly responsible for the unpleasant odour, most of them were almost completely eliminated in the biotrickling filters, except *p*-cresol and dimethyl sulphide. This implies that optimizing the removal of *p*-cresol and dimethyl sulphide could further improve the performance of biotrickling filters in treating swine odours. Thus, *p*-cresol and dimethyl sulphide, together with $NH_3$, were considered as potential model pollutants for a modelling study of swine odour removal in biotrickling filters.

## 2.5 INTRODUCTION

Odour emissions from livestock operations have become a significant social problem due to their negative impact on the local economy, human health, and quality of life (Blanes-Vidal et al. 2009). As swine production intensifies, concerns about the higher risk of negative impacts and the unwillingness of neighbouring communities to accept swine odours also increase (Hogberg et al. 2005). Although concerns have been directed to most livestock production operations, the hog industry got the highest attention from both public health and public policy perspectives (Thu 2002). An increase in public awareness has stimulated the development of more stringent legislation (Sheridan et al. 2003) and technologies to control the release of malodorous gases from swine facilities.

Although many technologies exist for odour control, biological treatment (e.g. biofilters, biotrickling filters, and bioscrubbers) has been found to be cost-effective for the treatment of high-volume waste gases containing readily biodegradable contaminants in relatively low concentrations such as those emitted from farm facilities (Park and Jung 2006; Iliuta and Larachi 2004; Sheridan et al. 2002). However, bioreactors have not yet been efficiently integrated into barn systems (Ozis et al. 2005). Despite its advantages over other methods, biological treatment is limited by some operational problems (e.g. biomass accumulation, mass transfer limitation,

and product and substrate inhibition). The development of mathematical models for predicting and simulating the performance of bioreactors could help reduce the impact of these limitations by optimizing reactor design and operation (Devinny et al. 1999).

One of the challenges of simulating odour and gas removal from swine facility air in treatment units is the presence of numerous odour components. Schiffman et al. (2001) identified 331 gaseous compounds from swine operations in North Carolina. These compounds include alcohols, aldehydes, amides, amines, aromatics, esters, ethers, hydrocarbons, ketones, nitrogen-containing compounds, sulphur-containing compounds, and volatile fatty acids. This myriad of components makes it difficult, if not nearly impossible, to simulate their removal in biotrickling filters. However, simulation of the removal of key odour components, those that are mainly responsible for the malodour, might be sufficient to describe the overall odour reduction. Blanes-Vidal et al. (2009) cited that in order to develop cost effective approaches for reducing odour emissions from livestock operations, it is important to determine the compounds that are mainly responsible for the unpleasant odour. With this, analysis could therefore focus on a small number of substances, thereby simplifying odour measurement. Though the odour perceived by humans in livestock buildings cannot be directly related to the concentration of individual contaminants in the waste air due to the interaction effects among different contaminants (Blanes-Vidal et al. 2009), using the key odour components to describe the overall odour impact might be an adequate approach.

Several studies have attempted to identify the key odorants responsible for the malodour emitted from pig buildings. O'Neill and Phillips (1992) cited that the compounds which are frequently reported as main responsible for the malodour in swine facilities are *p*-cresol, ammonia, volatile fatty acids, and phenol. Of the substances identified by Schiffman et al. (2001), those that exceeded the standardized odour threshold were *p*-cresol, *n*-butanoic acid,

isovaleric acid, 2-methylbutanoic acid, and indole. Other studies (Bulliner et al. 2006; Wright et al. 2005; Spoelstra 1980) also identified *p*-cresol as an important key odour indicator of swine facility air. Blanes-Vidal et al. (2009) found a strong correlation between odour concentration and sulphur-containing compounds. Though some studies have shown contradictory results regarding the relationship between ammonia and odour concentration (Aarnink et al. 2007), in terms of quantity, ammonia accounts for more than 50% of the odourants in swine facilities (Armeen et al. 2008).

Thus, the objective of this study was to select the key odour components of pig barn air, which could be used as potential model pollutants for a modelling study of a biotrickling filter treating waste air exhausted from pig buildings.

## 2.6 MATERIALS AND METHODS

### 2.6.1 Pig chambers

Three independent environmentally-controlled bench-scale pig chambers located at one of the laboratories of the Research and Development Institute for the Agri-Environment (IRDA) in Deschambault, Quebec, Canada were used to supply the contaminated air in this experiment. Each chamber (1.14 m wide, 2.44 m long, and 2.44 m high; Figure 2.1) housed 4 to 5 grower/finisher pigs with weights ranging from 30 to 60 kg. The pigs were distributed in a manner that each chamber had similar average weight. The set-point temperatures in the chambers were set according to the pigs' weight, which were varied from 22 to 18$^{o}$C as the pigs grew older. The feeders were refilled approximately every two days, and the pigs had free access to feed 24 h a day. The liquid manure was stored in a shallow pit underneath the fully-slatted floor and was removed by a vacuum pump on average two times during every trial. The

ventilation system was composed of an air inlet and an exhaust fan (14 to 100 L $s^{-1}$) mounted on the ceiling of each chamber.


**Figure 2.1 Inside view of one of the pig chambers.**

### 2.6.2 Biotrickling filters

Three cross-flow biotrickling filters were installed to treat the air exhausted from the three bench-scale pig chambers, one filter unit for each chamber. The three units served as three replicates in each trial. As shown in the schematic diagram presented in Figure 2.2, the exhaust duct of the pig chamber was connected to the treatment unit. Booster fans (Model 415; Delhi Industries, Inc., Delhi, Ontario, Canada) were used to compensate for the pressure loss across the biotrickling filters.

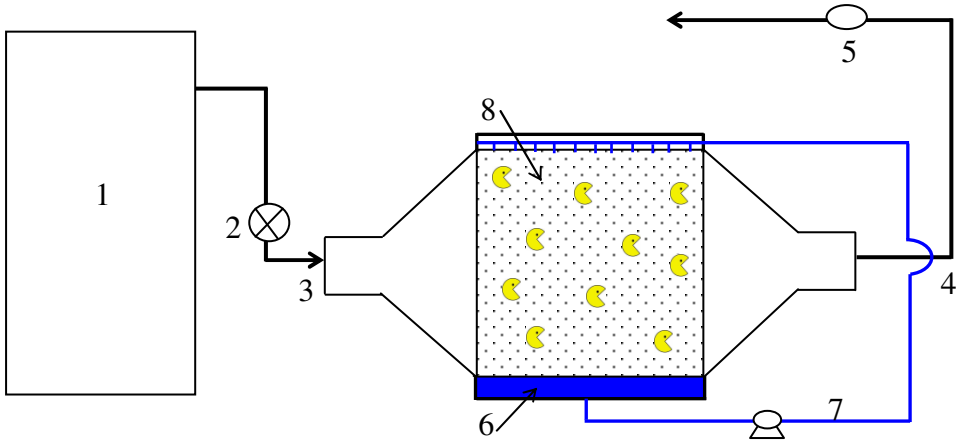


**Figure 2.2 Schematic diagram of the biotrickling filter system. (1) pig chamber; (2) booster fan; (3) air inlet to the treatment unit; (4) air outlet; (5) iris damper; (6) liquid sump; (7) recirculating liquid; and (8) packing media.**

The biotrickling filters were made of galvanized steel with internal dimensions of 1.1 m by 1.2 m by 1.1 m. Each treatment unit was filled with structured polypropylene packing media with a total volume of approximately 0.8 $m^3$. The packing material (purchased from Lantec Products, Inc., California, USA) had a specific surface area of 980 $m^2$ $m^{-3}$, a void fraction of 87.8%, and a standard module size of approximately 0.3 m x 0.3 m x 0.3 m (Figure 2.3; Lantec Products, Inc. 2013).

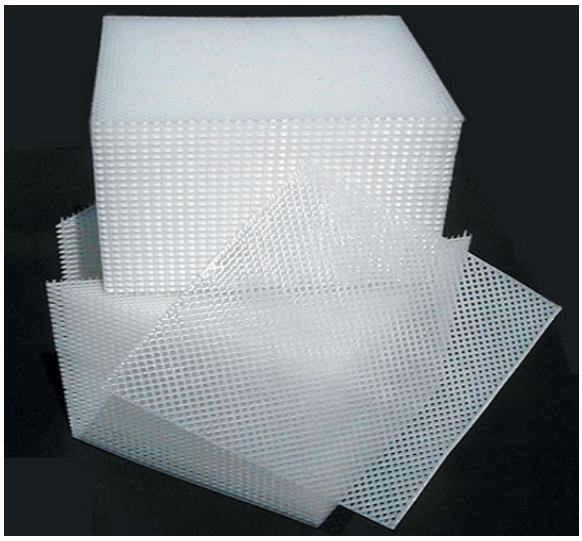

**Figure 2.3 Photo of the structured packing material.**

Each biotrickling filter was equipped with a liquid recirculation system holding a total liquid volume of 130 L. A liquid composed of a dilute nutrient solution was continuously recirculated over the packing material at a flow rate of 60 L $min^{-1}$ to provide sufficient filter bed moisture.

The air exhausted from the treatment unit was directed to a 204-mm iris orifice damper (Model 200; Continental Fan Manufacturer Inc., Buffalo, New York, USA; ± 5% accuracy). The differential pressure across the orifice plate, which was measured by a transducer (Model 694; Huba Control, Switzerland; ± 0.5% accuracy), was used to calculate the air flow rate.

### 2.6.3 Experimental trials

Two sets of trials were conducted: one in fall/winter (November-December 2008) and one in spring/summer (May-June 2009), where each trial lasted for four weeks. No amount of liquid was bled out from the unit during the entire trial. Any liquid that was lost through evaporation was periodically replaced by tap water to keep the total volume constant. Before each trial, the whole unit (including the packing media) was washed and sterilized with a sodium hypochlorite solution to avoid any contamination.

### 2.6.4 Sample collection and measurements

Samples for $NH_3$, $H_2S$, and odour measurements were collected during the entire four-week trial, while those for VOCs were collected only during the last two weeks of each trial.

#### 2.6.4.1 $NH_3$ and $H_2S$

The concentrations of $NH_3$ and $H_2S$ before and after the biotrickling filter unit were monitored inline every four hours. Thus, the data reported for a certain day were the average of the six measurements taken on that day.

The air samples were pumped to a mobile laboratory through Teflon tubing. The $NH_3$ was measured using a non-dispersive infrared (NDIR) analyzer (Ultramat 6E; Siemens, Germany) with detection limit of 1 $ppm_v$. The $H_2S$ was measured through semi-quantitative evaluation with an ultraviolet (UV) fluorescence analyzer (M101E; Teledyne API, USA); however, the detection limit of the analyzer was not quantified. The analyzers were supplied with certified calibration gases every two days for quality control purposes.

#### 2.6.4.2 Volatile organic compounds

The VOC samples were collected using carbotrap-300 multi-bed thermal desorption tubes purchased from GERSTEL Inc., USA. Each tube contained a total of approximately 423 mg of three different types of carbon adsorbents placed in three adjacent beds.

The samples were collected once every week (consistently every Wednesday) during the last two weeks of each trial when removal efficiencies were at maximum. The samples were collected from both the inlet and the exhaust of each bioreactor. A total of 72 samples were collected from the two trials; yet, 12 of them were disregarded due to problems encountered during sample injection at the GC-MS. Three samples were collected simultaneously at each sampling point to obtain three replicates (Figure 2.4); however, the sample collection at each sampling point was performed one at a time due to limited availability of pumps. The air was pumped through the tubes at an average flow rate of 0.2 L $min^{-1}$ for two hours using Sidepak personal sampling pumps (TSI SP330/SP350; TSI Inc., USA), which were calibrated before

sample collection. The air was passed through a filter to remove humidity and particles before going to the carbotrap tube. After collection, the tubes were placed in an ice box while being transported to the laboratory and were kept refrigerated at 4°C until analysis by GC-MS/O.

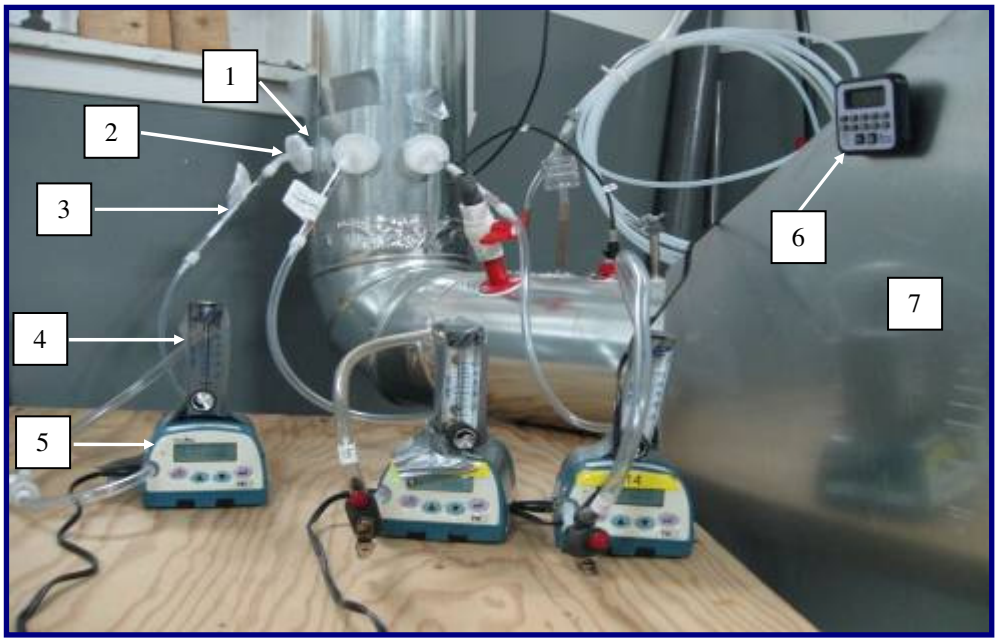


**Figure 2.4 VOC sample collection at one of the biotrickling filter sampling points. (1) sampling port; (2) filter; (3) carbotrap tube; (4) flow meter; (5) pump; (6) timer; (7) biotrickling filter unit.**

The GC-MS/O analysis was performed by the *Centre de Recherche Industrielle du Québec* (CRIQ) in Quebec City, Quebec, Canada. The system consisted of a gas chromatograph (Agilent Model 6890N; Agilent Technologies, Inc., USA) coupled with a mass spectrometer detector (Agilent Model 5975; Agilent Technologies, Inc., USA) and an olfactory detector port (GERSTEL ODP 2; GERSTEL Inc., USA). The VOCs were desorbed from the tubes at 325°C by means of a thermal desorption system (TDS) and then pre-concentrated at -150°C by a cooled injection system (CIS). The oven temperature was initially set at 35°C and was programmed by certain increments until the final temperature reached 325°C. The sample was then injected at

325$^{o}$C and separated at the GC capillary column (DB-5MS of 60 m by 0.32 mm by 1 µm). Helium gas, which was supplied at a flow rate of 2 mL min$^{-1}$, was used as the carrier gas. As the compounds exited the GC column, they were simultaneously directed to two detectors: the mass spectrometer and the olfactory detection port. The mass spectrometer identified the different odour components while the olfactory detection port allowed three experts to rate (from 1 to 10) the odour intensity of each component as well as to identify each component's odour character. The odour intensity reported was the average of the intensities of the three replicates.

#### 2.6.4.3 Odour measurement

Another set of samples for odour concentration measurement was collected in Nalophan bags once every week during the four-week trial. Sixty litres of air was collected each from the inlet and the exhaust of the biotrickling filter using the sampling lung technique at a flow rate of approximately 1 L s$^{-1}$. No replicates were made at each sampling point; however, as mentioned earlier, the three biotrickling filter units already served as replicates for the experimental treatment. The sample collection was conducted on the same day as for the GC-MS/O analysis (every Wednesday), though, not exactly at the same time due to the difference in the duration of sample collection. The odour sample collection lasted only around one minute while the VOC sample collection lasted for around two hours. The samples for odour measurement were analysed within 24 h of sampling in a six-port mobile olfactometer (Odile Olfactometer; Odotech Inc., Montreal, Quebec, Canada; Figure 2.5) using the dynamic olfactometry standard (CEN 2003). Following this technique, a sample of odorous air was diluted with clean non-odorous air and was presented to trained panelists at an increasing concentration. The number of dilutions at which 50% of the panellists could detect the odour was reported as the odour detection threshold or the odour concentration expressed as odour unit per cubic meter of air (OU m$^{-3}$). The hedonic

tone values of the air samples (original samples diluted 60 times) were also determined using an 11-point (-5 to +5) scale, with -5 for the most disagreeable odour, +5 for the most agreeable odour, and 0 for neutral.

**Figure 2.5 Odour sniffing in one of the ports of the olfactometer.**

### 2.6.5 Emission calculation

The pressure differentials across the iris damper were used to calculate the air flow rates using equation 2.1. As shown in equation 2.1, the flow rate of the air ($Q_G$, $ft^3\ min^{-1}$) flowing through the orifice of the damper is proportional to the pressure drop ($\Delta P$, in. $H_2O$). The value of the orifice coefficient (k, dimensionless, and provided by Continental Fan Manufacturer Inc., Buffalo, New York, USA) was dependent on the damper setting.

$$Q_G = k(\Delta P)^{0.5} \tag{2.1}$$

Using the calculated air flow rates and measured gas and odour concentrations, the gas and odour emission rates were then calculated using equations 2.2 and 2.3, respectively:

$$E_G = \left( \frac{C_G \rho_G Q_G}{M_{pig}} \right) \left( \frac{10^3}{60} \right) \quad (2.2)$$

$$E_{odour} = \frac{C_{odour} Q_G}{M_{pig}} \quad (2.3)$$

where $E_G$ = $NH_3$ or $H_2S$ emission rates ($\mu g\ min^{-1}\ kg^{-1}_{pig}$),

$E_{odour}$ = odour emission rate ($OU\ h^{-1}\ kg^{-1}_{pig}$),

$C_G$ = $NH_3$ or $H_2S$ concentrations ($ppm_v$),

$\rho_G$ = $NH_3$ or $H_2S$ gas densities ($kg\ m^{-3}$),

$M_{pig}$ = total mass of pigs in a room (kg),

$C_{odour}$ = odour concentration ($OU\ m^{-3}_{air}$).

$Q_G$ in equations 2.2 and 2.3 were expressed in $m^3\ h^{-1}$.

### 2.6.6 Key odour component selection techniques

Two techniques were employed to identify the key odour components, namely, linear regression analysis and calculation of odour index values. However, the odour indices were calculated only for VOCs.

#### 2.6.6.1 Linear regression

Regression analysis was the first method employed to select the key odour components. Several studies (Qu et al. 2010; Segura and Feddes 2005; Zhang et al. 2002) have shown that odour intensity (the perceived strength of the odour) is a logarithmic function of human olfactory response to odour (expressed as odour concentration). Thus, a plot of these two measurements in a log-log scale would produce a linear relationship. In this study, linear regression analyses were conducted between the logarithm of odour emissions and that of the odour intensities (and gas

concentrations) of the components, instead of the odour intensities of the gas mixtures. Though some studies (Blanes-Vidal et al. 2009) have cited that the odour perceived by humans cannot be easily predicted from the concentrations of the individual compounds due to the interaction effects among compounds, it is worthwhile to evaluate which of the odour components make a strong correlation with the perceived odour. Since the data obtained for $NH_3$ and $H_2S$ were the gas emissions only and for the VOCs were the odour intensities of the individual components, the linear regressions for $NH_3$ and $H_2S$ were made between the logarithm of odour emission and the logarithm of gas emissions, while for the VOCs, the regressions were established between the logarithm of odour emission and the logarithm of VOC odour intensity.

#### 2.6.6.2 Odour index

The key odour components were also identified based on their odour indices. Several studies have attempted to develop equations that describe the qualitative and quantitative perception of human receptor to odour using a single parameter such as an odour index. According to Qu et al. (2010), the olfactory response of humans to odour can be described by the following five parameters: concentration, intensity, hedonic tone, persistence, and character. Odour concentration, as described in section 2.6.4.3, refers to the number of dilution of an odorous gas with a clean non-odorous gas at the detection threshold. Intensity is defined as the perceived strength of an odour, hedonic tone is the measure of the pleasantness or unpleasantness of odour, persistence is the rate at which odour's perceived intensity decreases as the odour is diluted, and odour character is the quality of odour defined by descriptive quality terms. Though, in this study, the odour character of each VOC was the one used to obtain the hedonic tone value (as described below), odour character is purely qualitative without any mathematical basis (Qu et al. 2010). Persistence, on the other hand, is a function of both odour concentration and intensity

(Qu et al. 2010). Thus, on the basis of the above-mentioned arguments, odour character and persistence may be excluded in the odour index equation. Qu et al. (2010) developed equations (Eqs. 2.4 and 2.5) that relate the remaining three parameters namely odour concentration, odour intensity, and hedonic tone. Using equations 2.4 and 2.5, an equation for odour index (Eq. 2.6) was obtained:

$$I = K_{i1} * C^{K_{i2}} \tag{2.4}$$

$$H = K_{h1} * C^{K_{h2}} \tag{2.5}$$

$$OI = \sqrt{I * |H|} \tag{2.6}$$

where I = odour intensity (dimensionless),

H = hedonic tone (dimensionless),

OI = odour index (dimensionless),

C = odour concentration (OU $m^{-3}$),

$K_{i1}$, $K_{i2}$, $K_{h1}$, $K_{h2}$ = coefficients related to intensity and hedonic tone (dimensionless).

The odour index, as described in equation 2.6, is the geometric mean of odour intensity and hedonic tone and is defined as a power function of odour concentration as implicitly expressed in equations 2.4 and 2.5.

Though the equation for odour index was applied by Qu et al. (2010) to mixtures of odorous gases and not to individual components, it was assumed that applying this equation in this study would still give odour indices that would adequately identify the key odour components.

Equation 2.6 indicates that for a component to be considered a key odorant, it should be significant both in intensity and hedonic tone. High odour intensity does not always necessarily indicate a malodour. A component could be present in high odour intensity but with a non-

offensive odour, thus, contributing less to the overall severity of the malodour. In this regard, the hedonic tone must also be taken into consideration. It should be noted, however, that the intensity and hedonic tone of a particular component may be altered by the presence of other components.

The odour intensities applied here were the relative intensities of the individual VOC determined from the GC-MS/O analysis. The value for the hedonic tone, on the other hand, was determined by assigning numerical value to the odour character of the VOC, which was also identified from the GC-MS/O analysis. Using the odour wheels presented by Sheffield and Ndegwa (2008) and McGinley et al. (2000) as guides, values were assigned to the different types of odour. A value of 1 was given to the natural pleasant odours (e.g. fruity, vegetable-like, floral); 2 to the earthy odours (e.g. mushroom, grassy, peaty); 3 to the chemical odours (e.g. plasticizer, solvent, metallic, paint); 4 to the disinfectant or medicinal odours (e.g. alcohol, vinegar, ammonia, phenolic, chlorinous); and 5 to the unpleasant or offensive odours (e.g. sulphide, fishy, rancid, faecal, burnt, manure, sour, vomit, rotten eggs). The values for the hedonic tone applied here were different from the conventional ones where negative values are assigned for unpleasant odours and positive values for the pleasant ones. As indicated by equation 2.6, an unpleasant odour would result in a higher positive odour index.

Since the odour intensity and the odour character, which was used to calculate the hedonic tone, were determined from the GC-MS/O analysis, the odour indices were calculated for the VOCs only and not for $NH_3$ and $H_2S$.

## 2.7 RESULTS AND DISCUSSION

### 2.7.1 $NH_3$ and $H_2S$ emissions

The $NH_3$ and $H_2S$ concentrations measured throughout the trials ranged from 2 to 25 $ppm_v$ and 3 to 1300 $ppb_v$, respectively, while room temperatures ranged from 16 to 31$^oC$. Part of the data collected is presented in Appendix D. Figures 2.6 and 2.7 show the calculated average $NH_3$ and $H_2S$ emission rates, respectively, at the inlet and exhaust of the three biotrickling filters for the fall/winter and spring/summer trials. These were the average $NH_3$ and $H_2S$ emissions during the days when odour concentrations were also measured. As shown in Figures 2.6 and 2.7, the $NH_3$ and $H_2S$ emissions from the pig chambers (emissions measured at the inlet of the reactors) during spring/summer were relatively higher than those during fall/winter. The average $NH_3$ and $H_2S$ emissions during spring/summer were 66±18 and 0.49±0.45 $\mu g\ min^{-1}\ kg^{-1}_{pig}$, respectively, while those during fall/winter were 44±10 and 0.29±0.1 $\mu g\ min^{-1}\ kg^{-1}_{pig}$, respectively. From the t-test analysis conducted, there was a significant difference ($P < 0.05$) in $NH_3$ emissions between spring/summer and fall/winter while no significant difference was found for $H_2S$. Jacobson et al. (2005) and Sun (2005) observed no specific seasonal effects on $NH_3$ and $H_2S$ emissions. Since emission rates are calculated as a product of gas concentrations and ventilation rates, the high gas concentrations during winter are compensated by the low ventilation rates while the low gas concentrations during summer are compensated by the high ventilation rates, thus resulting in relatively constant emission rates. The relatively higher emission rates observed in this study during spring/summer could be due to the higher variability in ventilation rates during this period. The effect of the high variability in ventilation rates can also be observed in the high values of the standard deviations, particularly from the spring/summer trial.

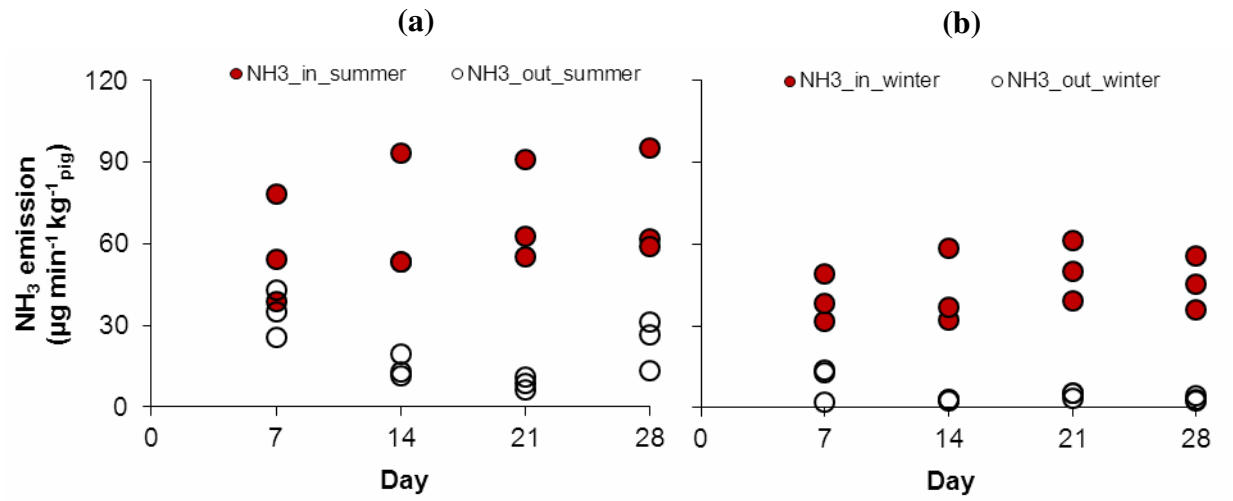


**Figure 2.6 Average $NH_3$ emission rates for the day when odour measurements were taken: (a) spring/summer; (b) fall/winter (in and out represent inlet and exhaust of bioreactors, respectively).**

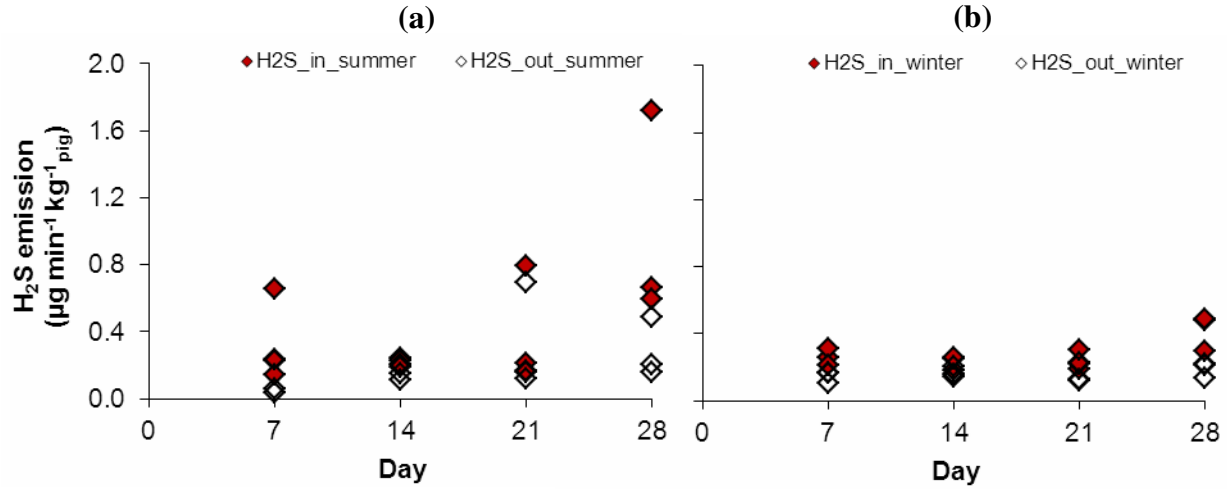


**Figure 2.7 Average $H_2S$ emission rates for the day when odour measurements were taken: (a) spring/summer; (b) fall/winter (in and out represent inlet and exhaust of bioreactors, respectively).**

On average, the air treatment resulted in $NH_3$ and $H_2S$ removal efficiencies of 67±20% and 50±29%, respectively, during spring/summer and 88±9% and 40±13%, respectively, during fall/winter. The higher removal efficiency for $NH_3$ as compared with $H_2S$ could be due to $NH_3$'s

relatively higher solubility in water as well as to its higher concentration in the pig barn air. The $NH_3$ removal efficiencies achieved in this study were comparable to the 79 and 82% obtained by Melse and Mol (2004) and Sheridan et al. (2002), respectively. Both studies were also conducted using swine waste air. For the $H_2S$, the removal efficiencies obtained were lower compared to the 100% obtained by Aroca et al. (2007) and 90% obtained by Abdehagh et al. (2011). Both studies used $H_2S$ inlet concentrations which were a lot higher than those observed in this current study. Also, both related studies used biotrickling filters inoculated with $H_2S$ degrading bacteria, the *Thiobacillus thioparus* and the *Acidithiobacillus thiooxidans*.

There was a significant difference ($P < 0.05$) in the removal efficiencies for $NH_3$ between fall/winter and spring/summer, but none for $H_2S$. The observed difference in the $NH_3$ removal efficiencies between the two trials could be again due to the high variation in ventilation rates during spring/summer or to the higher $NH_3$ concentrations during fall/winter.

### 2.7.2 Volatile organic compounds

The results of the GC-MS/O analysis are shown in Table 2.1. A total of 176 different VOCs were identified from the 60 samples considered in this study. Table 2.1 also presents the frequency of appearance and the average intensities of the compounds at the inlet and exhaust of the bioreactors. The maximum number of times that a certain VOC was detected at the inlet or the exhaust of the bioreactor is ten, since a similar compound that appeared in replicate samples was counted only once. The maximum possible value for intensity is also ten since this is the maximum value given by the experts who conducted the GC-MS/O analysis.

**Table 2.1 Frequency of appearance and intensity of the compounds identified in the samples collected at the inlet and exhaust of the biotrickling filters.**

| Compounds | Frequency[1] | | Intensity[2] | | Compounds | Frequency | | Intensity | |
|---|---|---|---|---|---|---|---|---|---|
| | In[3] | Out[4] | In | Out | | In | Out | In | Out |
| 1,3-Di-tert-butylbenzene | 2 | 0 | 0.6 | 0.0 | 6-Methyl-5-heptene-2-one | 10 | 9 | 6.7 | 4.5 |
| 111-Trichloroethane | 1 | 0 | 0.2 | 0.0 | Acetaldehyde | 10 | 9 | 5.1 | 2.8 |
| 1-Butanol | 3 | 1 | 0.4 | 0.1 | Acetic acid | 10 | 2 | 6.0 | 0.5 |
| 1-Dodecene | 1 | 2 | 0.3 | 0.4 | Acetic formic anhydride | 0 | 1 | 0.0 | 0.4 |
| 1-Heptanol | 0 | 1 | 0.0 | 0.2 | Acetone | 5 | 0 | 1.1 | 0.0 |
| 1-Methoxy-2-propylacetate | 1 | 2 | 0.1 | 0.6 | Acetonitrile | 3 | 0 | 0.7 | 0.0 |
| 1-Octene | 1 | 0 | 0.1 | 0.0 | Acetophenone | 7 | 4 | 4.5 | 1.2 |
| 1-Phenyl-1-butene | 0 | 1 | 0.0 | 0.1 | Acetyl valerate | 2 | 0 | 1.6 | 0.0 |
| 1-Propanol | 4 | 0 | 0.5 | 0.0 | Alpha-cumyl alcohol | 7 | 4 | 4.5 | 1.7 |
| 1-Tetralone | 0 | 2 | 0.0 | 0.5 | *a*-Pinene | 10 | 10 | 3.9 | 2.0 |
| 2,3-Butanedione | 10 | 3 | 7.2 | 1.3 | Benzaldehyde | 1 | 5 | 0.5 | 2.6 |
| 2,4-Dimethylheptene | 0 | 9 | 0.0 | 2.7 | Benzene | 2 | 3 | 0.5 | 0.3 |
| 2,6-Dimethylheptane | 2 | 3 | 1.1 | 1.1 | Benzoquinone | 1 | 0 | 0.5 | 0.0 |
| 2-Butanone | 2 | 6 | 0.3 | 1.9 | Bicyclohexyl | 0 | 3 | 0.0 | 1.2 |
| 2-Butoxyethanol | 1 | 3 | 0.3 | 0.9 | *b*-Pinene | 1 | 2 | 0.7 | 0.8 |
| 2-Butylacetate | 1 | 0 | 0.3 | 0.0 | Butanoic acid | 10 | 2 | 8.8 | 0.7 |
| 2-Ethylhexanal | 0 | 1 | 0.0 | 0.1 | Butylacetate D3 | 1 | 0 | 0.6 | 0.0 |
| 2-Ethylhexanol | 2 | 4 | 0.7 | 0.7 | Camphene | 0 | 1 | 0.0 | 0.2 |
| 2-Hexyl-4,5-dimethyloxazole | 4 | 0 | 1.6 | 0.0 | Carbon disulphide | 4 | 2 | 0.8 | 0.5 |
| 2-Isobutyl-4,5-dimethyloxazole | 1 | 0 | 0.5 | 0.0 | Carbonyl sulphide | 5 | 1 | 1.4 | 0.1 |
| 2-Methyl-1-pentene | 0 | 2 | 0.0 | 0.3 | Carveol | 0 | 2 | 0.0 | 0.9 |
| 2-Methyl-3-oxobutyronitrile | 1 | 0 | 0.4 | 0.0 | Cumene | 8 | 6 | 3.2 | 1.4 |
| 2-Methyl-benzaldehyde | 0 | 1 | 0.0 | 0.2 | Cyclohexanone | 1 | 0 | 0.2 | 0.0 |
| 2-Methylbutanoic acid | 10 | 0 | 7.1 | 0.0 | Cyclopentane | 1 | 0 | 0.2 | 0.0 |
| 2-Methylbutanol | 1 | 0 | 0.1 | 0.0 | D4 siloxane | 3 | 2 | 1.2 | 0.6 |
| 2-Methylpropionic acid | 10 | 1 | 6.2 | 0.5 | D5 siloxane | 7 | 7 | 4.1 | 3.2 |
| 2-Nitro-p-cresol | 2 | 0 | 0.5 | 0.0 | D6 siloxane | 0 | 2 | 0.0 | 0.2 |
| 2-Nitrophenol | 4 | 0 | 2.3 | 0.0 | D7 siloxane | 8 | 6 | 3.7 | 2.2 |
| 2-Octene | 1 | 0 | 0.4 | 0.0 | Decahydro-2-methylnaphthalene | 0 | 1 | 0.0 | 0.1 |
| 2-Pentanone | 3 | 0 | 0.5 | 0.0 | Decanal | 2 | 2 | 0.0 | 0.5 |
| 2-Pentylfurane | 5 | 4 | 2.9 | 1.8 | DEMB | 0 | 1 | 0.0 | 0.6 |
| 3-Methylbutanal | 2 | 2 | 0.7 | 0.2 | Dichlorobenzene | 3 | 0 | 0.4 | 0.0 |
| 3-Acetyl-4-hydroxy-6-methylpyridone | 1 | 1 | 0.2 | 0.1 | Dimethylsulphide | 10 | 9 | 5.5 | 3.5 |
| 3-Carene | 1 | 1 | 0.3 | 0.1 | Dimethyldisulphide | 5 | 5 | 1.7 | 1.1 |
| 3-Methylbutanoic acid | 10 | 1 | 7.9 | 0.6 | Dimethylethoxybenzene | 1 | 2 | 0.7 | 0.7 |
| 3-Methylbutanol | 1 | 0 | 0.1 | 0.0 | Dimethylstyrene | 2 | 3 | 1.2 | 0.9 |
| 3-Methylbutanol propanoate | 1 | 0 | 0.5 | 0.0 | Dimethylsulfone | 6 | 0 | 3.6 | 0.0 |
| 3-Methylhexane | 1 | 0 | 0.2 | 0.0 | Dimethylsulfoxide | 1 | 0 | 0.2 | 0.0 |
| 3-Octene | 0 | 2 | 0.0 | 0.4 | Dimethyltrisulphide | 3 | 2 | 1.6 | 1.2 |
| 3-Pentanenitrile | 0 | 1 | 0.0 | 0.2 | *D*-Limonene | 8 | 4 | 2.6 | 1.1 |
| 3-Propylacetate | 0 | 1 | 0.0 | 0.1 | DMEB | 2 | 1 | 0.8 | 0.4 |
| 5-Methyl-indene | 1 | 0 | 0.7 | 0.0 | Dodecanal | 0 | 5 | 0.0 | 1.5 |

[1]Frequency of appearance of the compound in the samples (dimensionless; maximum is ten at either inlet or exhaust of the bioreactor); [2]Mean intensity (dimensionless; maximum is ten); [3]Inlet of the bioreactor; [4]Exhaust of the bioreactor.

**Table 2.1 (continued). Frequency of appearance and intensity of the compounds identified in the samples collected at the inlet and exhaust of the biotrickling filters.**

| Compounds | Frequency[1] | | Intensity[2] | | Compounds | Frequency | | Intensity | |
|---|---|---|---|---|---|---|---|---|---|
| | In[3] | Out[4] | In | Out | | In | Out | In | Out |
| Dodecane | 2 | 0 | 0.3 | 0.0 | Naphthalene | 8 | 8 | 2.4 | 2.0 |
| Dodecanol | 7 | 7 | 2.4 | 3.1 | N-ethyl propanamide | 1 | 0 | 0.6 | 0.0 |
| Ethanol | 3 | 0 | 0.6 | 0.0 | Nitrilbenzyl | 1 | 0 | 0.2 | 0.0 |
| Ethoxyacetylene | 0 | 1 | 0.0 | 0.2 | Nitrosodimethylamine | 1 | 0 | 0.1 | 0.0 |
| Ethylacetate | 0 | 1 | 0.0 | 0.1 | Nitrostyrene | 2 | 0 | 0.5 | 0.0 |
| Ethylanisol | 0 | 1 | 0.0 | 0.2 | N-methyl-3-nitrobenzamine | 1 | 0 | 0.2 | 0.0 |
| Ethylbenzene | 4 | 9 | 2.6 | 2.0 | N-methylnitrobenzamide | 2 | 1 | 0.4 | 0.2 |
| Ethylbutyrate | 0 | 2 | 0.0 | 0.6 | N-methylnitrobenzamine | 1 | 0 | 0.1 | 0.0 |
| Ethylhexylethanoate | 2 | 1 | 0.7 | 0.3 | NN-dimethylacetamide | 1 | 0 | 0.2 | 0.0 |
| Ethyl-m-cresol | 0 | 2 | 0.0 | 1.1 | NN-dimethylpropamide | 2 | 0 | 1.0 | 0.0 |
| Ethylphenol | 8 | 4 | 4.9 | 2.1 | Nonanal | 0 | 1 | 0.0 | 0.5 |
| Ethylpropylbenzene | 0 | 1 | 0.0 | 0.3 | Nonenal | 1 | 0 | 0.4 | 0.0 |
| Ethylvalerate | 1 | 0 | 0.1 | 0.0 | Octanal | 5 | 7 | 2.4 | 2.1 |
| Ethylxylene | 2 | 0 | 0.8 | 0.0 | Octanoic acid | 1 | 0 | 0.5 | 0.0 |
| Freon11 | 1 | 0 | 0.3 | 0.0 | *o*-Xylene | 4 | 1 | 1.3 | 0.5 |
| Freon142 | 4 | 1 | 0.6 | 0.2 | *p*-Cresol | 10 | 7 | 6.7 | 3.2 |
| Furfural | 1 | 0 | 0.6 | 0.0 | *p*-Cresol acetate | 2 | 0 | 1.4 | 0.0 |
| Heptanoic acid | 2 | 0 | 0.8 | 0.0 | *p*-Cymene | 3 | 2 | 1.1 | 0.8 |
| Hexahydrocumene | 1 | 0 | 0.1 | 0.0 | Pentanal | 1 | 0 | 0.4 | 0.0 |
| Hexanal | 2 | 9 | 1.5 | 4.0 | Pentanoic acid | 10 | 0 | 6.3 | 0.0 |
| Hexanoic acid | 5 | 0 | 2.3 | 0.0 | Pentyl benzene | 0 | 1 | 0.0 | 0.3 |
| Hexanone | 0 | 1 | 0.0 | 0.3 | Pentylacetate | 0 | 2 | 0.0 | 0.7 |
| Indane | 2 | 0 | 0.5 | 0.0 | Phenol | 3 | 0 | 1.4 | 0.0 |
| Indanol | 1 | 0 | 0.1 | 0.0 | Phenylethyl alcohol | 3 | 0 | 1.2 | 0.0 |
| Indene | 1 | 0 | 0.3 | 0.0 | *p*-Menthatriene | 1 | 0 | 0.5 | 0.0 |
| Indole | 1 | 2 | 0.1 | 0.6 | Propanoic acid | 10 | 1 | 4.3 | 0.5 |
| Isobutyl acetate | 1 | 0 | 0.3 | 0.0 | Propenylbenzene | 2 | 2 | 0.7 | 0.7 |
| Isopropanol | 2 | 0 | 0.4 | 0.0 | Propylacetate | 0 | 1 | 0.0 | 0.2 |
| Isothiocyanatocyclohexane | 3 | 3 | 0.5 | 0.6 | Propylbenzene | 1 | 2 | 0.2 | 0.4 |
| *m*-Cresol | 0 | 1 | 0.0 | 0.4 | Propylbutyrate | 1 | 0 | 0.6 | 0.0 |
| *m*-Cymene | 1 | 2 | 0.3 | 0.9 | Propylcyclohexane | 1 | 1 | 0.9 | 0.1 |
| Menth-8-ene | 0 | 1 | 0.0 | 0.2 | Propylmethylbenzene | 1 | 0 | 0.2 | 0.0 |
| Menthane | 1 | 0 | 0.6 | 0.0 | Propylpropionate | 0 | 1 | 0.0 | 0.3 |
| Methanamide | 1 | 0 | 0.1 | 0.0 | Sec-butyl-methylbenzene | 0 | 1 | 0.0 | 0.2 |
| Methanamine | 3 | 0 | 0.8 | 0.0 | Styrene | 6 | 9 | 3.3 | 3.0 |
| Methanesulphonyl chloride | 2 | 0 | 0.6 | 0.0 | Tetrachloroethylene | 1 | 6 | 0.4 | 1.4 |
| Methanethiol | 0 | 1 | 0.0 | 0.1 | Tetrahydrofuran | 0 | 1 | 0.0 | 0.2 |
| Methylformate | 1 | 0 | 0.6 | 0.0 | Tetrahydronaphthalene | 0 | 1 | 0.0 | 0.1 |
| Methylindole | 3 | 2 | 1.4 | 1.0 | Tetralin | 3 | 1 | 0.7 | 0.1 |
| Methylmercaptan | 5 | 3 | 2.0 | 0.7 | Tetralin2 | 0 | 1 | 0.0 | 0.2 |
| Methylmetacrylate | 0 | 1 | 0.0 | 0.2 | TMB | 3 | 0 | 1.0 | 0.0 |
| Methylpropanal | 1 | 0 | 0.1 | 0.0 | Tolualdehyde | 0 | 1 | 0.0 | 0.6 |
| Methylpyrimidine | 0 | 1 | 0.0 | 0.5 | Toluene | 4 | 9 | 2.5 | 3.5 |
| Methylstyrene | 2 | 0 | 1.2 | 0.0 | Trimethyl silanol | 1 | 0 | 0.1 | 0.0 |
| *m*-Nitrocresol | 2 | 0 | 0.5 | 0.0 | Trimethylamine | 3 | 0 | 1.5 | 0.0 |
| *m,p*-Xylene | 6 | 10 | 3.3 | 2.7 | Trimethylcyclohexane | 0 | 1 | 0.0 | 0.3 |

[1]Frequency of appearance of the compound in the samples (dimensionless; maximum is ten at either inlet or exhaust of the bioreactor); [2]Mean intensity (dimensionless; maximum is ten); [3]Inlet of the bioreactor; [4]Exhaust of the bioreactor.

Out of the 176 VOCs, only a few could be considered significant based on the frequency of their appearance in the samples (frequency ≥ 5) and odour intensity (odour intensity ≥ 5). As can be seen in Table 2.1, some compounds were only occasionally present in the samples. Some even appeared only at the exhaust of the bioreactors, which could indicate that these compounds were produced during the biological treatment process. The variations in the composition of the pig barn air might have affected the quality of the odour emitted as well as the odour removal efficiency since different compounds have different odour and removal properties.

The compounds that were always present in the pig barn air (air samples taken at the inlet of the bioreactors) were the volatile fatty acids (e.g. butanoic acid, propanoic/propionic acid, pentanoic acid, acetic acid), 2,3-butanedione, 6-methyl-5-heptene-2-one, acetaldehyde, *a*-pinene, dimethyl sulphide, and *p*-cresol. Except *a*-pinene, these compounds were also present in high intensity (odour intensity > 5).

However, the volatile fatty acids were almost completely removed in the biotrickling filters as they seldom appeared in the samples collected at the exhaust of the reactors. This observation could be due to the relatively high solubility of these compounds in water which enhanced their removal by the recirculating liquid in the biotrickling filters. Most of the compounds that were frequently present at the exhaust of the bioreactors were the relatively less water-soluble compounds (e.g. dimethyl sulphide, *p*-cresol).

### 2.7.3 Odour emissions

The odour emission rates, which were calculated from the odour concentrations measured once per week from both the inlet and exhaust of the three biotrickling filters, are shown in Figure 2.8. The corresponding odour concentrations are presented in Appendix D.

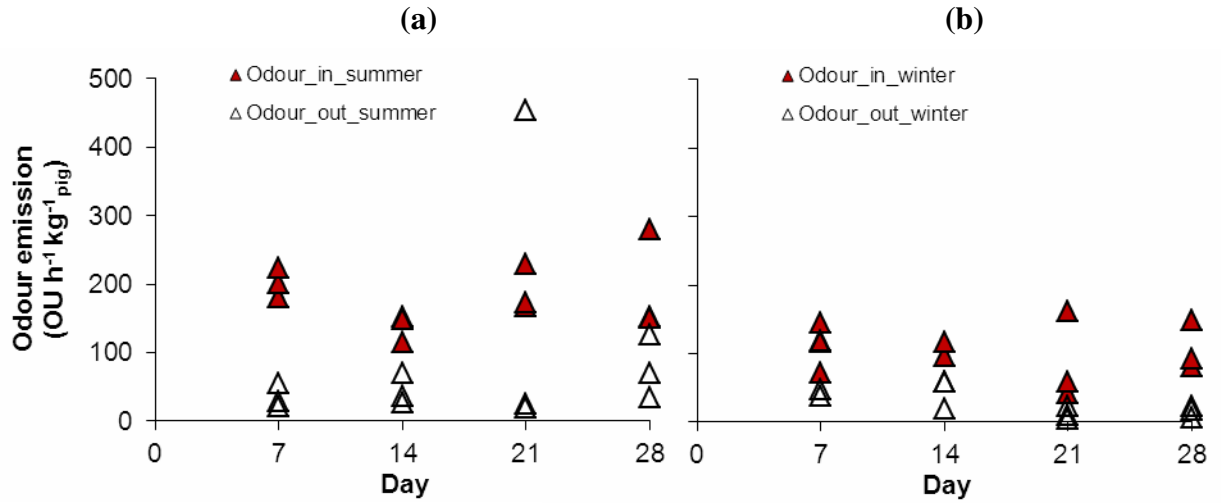


**Figure 2.8 Average odour emission rates measured once every week for four weeks during (a) spring/summer; (b) fall/winter (in and out represent inlet and exhaust of bioreactors, respectively).**

The odour emissions from the pig chambers from the fall/winter and spring/summer trials were 103±38 and 181±45 OU $h^{-1}$ $kg^{-1}_{pig}$, respectively. Similar to the $NH_3$ emissions, odour emissions during spring/summer were significantly higher ($P < 0.05$) than those during fall/winter. Though in some studies (Guo et al. 2006; Sun 2005) odour emissions have not been found to be significantly different between different seasons, the relatively higher odour emissions measured in this study during spring/summer could be again due to the relatively higher variation in the ventilation rates during this period. However, the odour removal efficiencies between fall/winter (69±25%) and spring/summer (74±14%) were not significantly different ($P > 0.05$). This implies that the performance of the biotrickling filters was not affected by the initial odour emissions. This is contrary to the observation of Jensen and Hansen (2006) where reduced odour removal efficiency in a biotrickling filter was observed during summer due to the reduced gas retention time caused by increased ventilation rate during this period. The odour removal efficiencies obtained in this study were within the average of 49, 90, and 76%

removal efficiencies reported by Melse and Mol (2004), Sheridan et al. (2002), and Chen et al. (2009), respectively.

### 2.7.4 Selection of key odour components

The key odour components were identified using the $R^2$ values from the linear regression analysis and the odour index values.

#### 2.7.4.1 Linear regression

Figure 2.9 shows the results of the regression analysis for $NH_3$, $H_2S$, and some VOCs (butanoic acid, 3-methyl butanoic acid, *p*-cresol, and dimethyl sulphide). The $R^2$ values were relatively low (ranging from 0.07 to 0.47), although some of them (those for $NH_3$, $H_2S$, butanoic acid, and 3-methylbutanoic acid) were found to be statistically significant ($\alpha = 0.05$). One factor that could explain the results is the difference in the time in which the $NH_3$, $H_2S$, VOCs, and odour samples were collected. As mentioned earlier, though the samples were taken on the same day, the $NH_3$ and $H_2S$ were measured every four hours and the values used were the average of the six measurements taken in a day, the VOCs were sampled for a period of two hours, while the odour samples were collected in approximately one minute only. Since the composition and/or the concentrations of the components of pig barn air vary continuously throughout the day, the time difference on sample collection possibly affected the results. The low $R^2$ values for the VOCs could also be due to the limited measurements taken. The results could also imply that the odour perceived by humans cannot be simply associated to any particular component, as cited in the literature (Blanes-Vidal et al. 2009).

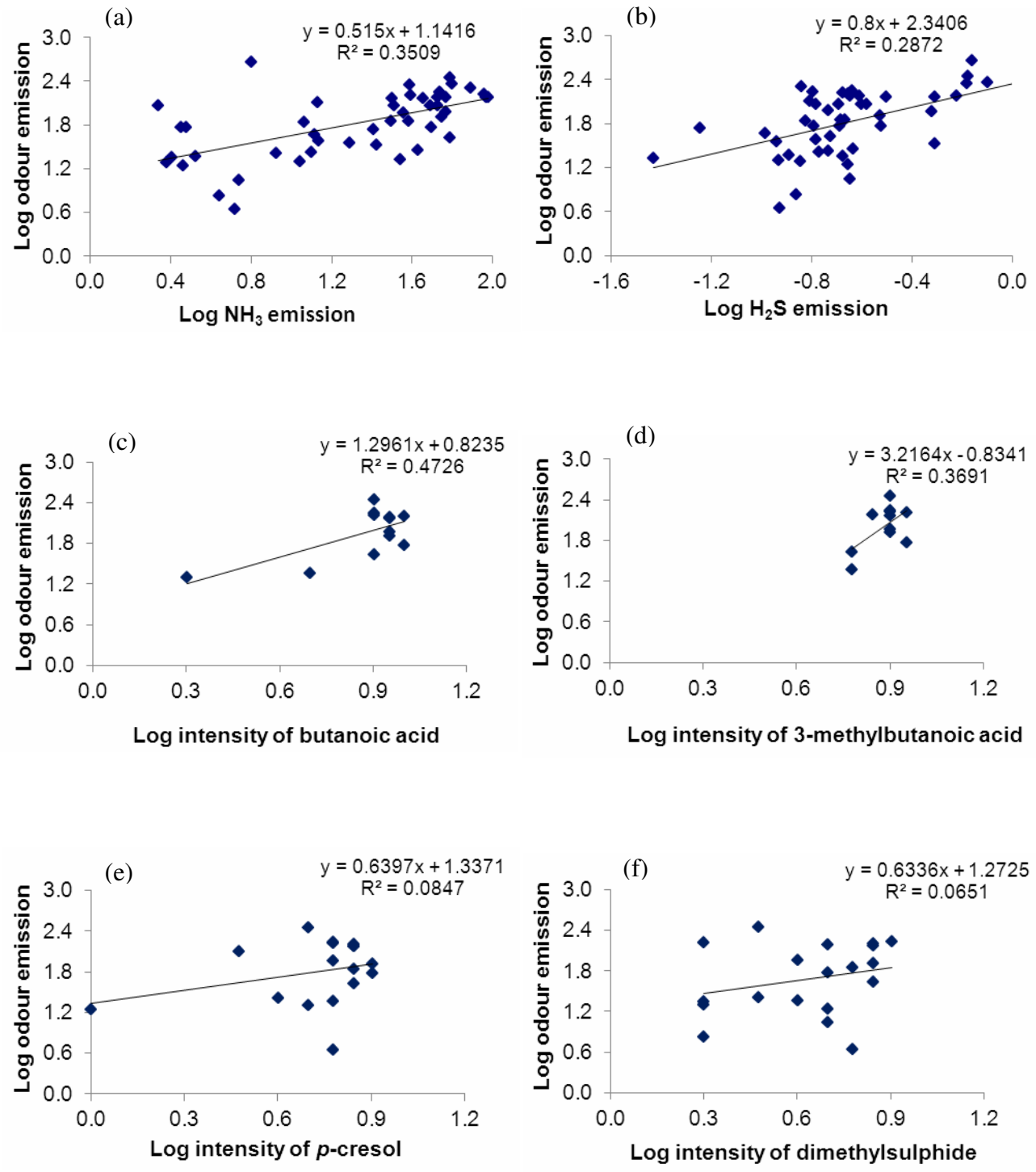


**Figure 2.9 Results of regression analysis between the logarithm of odour emission and the logarithm of $NH_3$ or $H_2S$ emissionn or VOC odour intensity. (a) $NH_3$; (b) $H_2S$; (c) butanoic acid; (d) 3-methylbutanoic acid; (e) *p*-cresol; (f) dimethyl sulphide.**

Among the odour components studied, those that showed relatively higher $R^2$ values were $NH_3$, butanoic acid, and 3-methyl butanoic acid. Aarnink et al. (2007) cited studies (Verdoes and Ogink 1997; Miner 1995; Liu et al. 1993; Schulte et al. 1985), which have contradictory results regarding the relationship between $NH_3$ and odour emissions from pig houses; Miner (1995) and Schulte et al. (1985) found good correlations while Verdoes and Ogink (1997) and Liu et al. (1993) observed low correlations.

The volatile fatty acids were cited by O'Neill and Phillips (1992) and Spoelstra (1980) as good indicators of swine odour. However, in this current study, the volatile fatty acids (e.g. butanoic acid, 3-methyl butanoic acid) found in the air exhausted from the pig chambers were almost completely removed in the biotrickling filters as shown in Table 2.1. Thus, these components might not present any challenge to the treatment process, and therefore, not suitable model pollutants for this study.

#### 2.7.4.2 Odour index

Table 2.2 presents the odour components which appeared five times or more at the inlet of the biotrickling filters. Being frequently present in the samples, they could be considered as the main components of pig barn air. Among these compounds, those which had higher odour intensities (intensity > 5) were 2,3-butanedione, 2-methylbutanoic acid, 2-methylpropionic acid, 3-methylbutanoic acid, 6-methyl-5-heptene-2-one, acetaldehyde, acetic acid, butanoic acid, dimethyl sulphide, *p*-cresol, and pentanoic acid. However, as previously mentioned, a high odour intensity is not a sufficient criterion to consider a component a significant odorant. An odour index, which also considers the hedonic tone, could be a better criterion.

**Table 2.2 Average odour indices of components frequently identified at the inlet of the biotrickling filters.**

| Volatile organic compound | Odour index[1] | |
|---|---|---|
| | Inlet | Exhaust |
| 2,3-Butanedione | 5.4 | 2.3 |
| 2-Methylbutanoic acid | 6.0 | 0.0 |
| 2-Methylpropionic acid | 5.6 | 1.6 |
| 2-Pentylfurane | 3.8 | 3.0 |
| 3-Methylbutanoic acid | 6.3 | 1.7 |
| 6-Methyl-5-heptene-2-one | 3.7 | 3.0 |
| Acetaldehyde | 3.9 | 2.9 |
| Acetic acid | 4.9 | 1.4 |
| Acetone | 1.8 | 0.0 |
| Acetophenone | 4.2 | 2.2 |
| Alpha-cumyl alcohol | 4.2 | 2.6 |
| *a*-Pinene | 4.4 | 3.2 |
| Butanoic acid | 6.6 | 1.9 |
| Carbonyl sulphide | 2.6 | 0.7 |
| Cumene | 4.0 | 2.6 |
| D5 siloxane | 3.5 | 3.1 |
| D7 siloxane | 3.3 | 2.6 |
| Dimethyl sulphide | 5.2 | 4.2 |
| Dimethyl disulphide | 2.9 | 2.3 |
| Dimethyl sulfone | 4.2 | 0.0 |
| *D*-Limonene | 3.6 | 2.3 |
| Dodecanol | 2.7 | 3.0 |
| Ethylphenol | 3.8 | 2.5 |
| Hexanoic acid | 2.6 | 0.0 |
| Methylmercaptan | 3.2 | 1.9 |
| *m,p*-Xylene | 3.1 | 2.8 |
| Naphthalene | 3.1 | 2.8 |
| Octanal | 3.1 | 2.9 |
| *p*-Cresol | 5.8 | 4.0 |
| Pentanoic acid | 5.6 | 0.0 |
| Propanoic acid | 4.1 | 1.4 |
| Styrene | 2.6 | 2.4 |

[1]Dimensionless; maximum possible value is 7.1 (for maximum possible value of 10 for intensity and 5 for hedonic tone).

As shown in Table 2.2, out of the components which were frequently present in the pig barn air, 2,3-butanedione, 2-methylbutanoic acid, 2-methylpropionic acid, 2-pentylfurane, 3-

methylbutanoic acid, acetophenone, alpha-cumyl alcohol, butanoic acid, dimethyl sulphide, dimethylsulfone, *p*-cresol, and pentanoic acid have the highest odour indices (OI > 5.0). This indicates that these compounds were mainly responsible for the unpleasant odour emitted from the experimental pig chambers.

The findings of this study are in agreement with those obtained by other studies. O'Neill and Phillips (1992) cited that 2-methylpropanoic, butanoic, 3-methylbutanoic, pentanoic, *p*-cresol, indole, 3-methylindole, dimethyl sulphide, dimethyl disulphide, butanol, and 3-methylbutanol produced an odour very similar to swine odour. Eniola et al. (2006) identified *p*-cresol, ethylphenol, and 3-methylbutanoic acid as the most persistent and main responsible for the malodour of swine exhaust air. In addition, Spoelstra (1980) stated that *p*-cresol and volatile fatty acids are the key odour indicators of swine gas. The study by Wright et al. (2005) showed *p*-cresol to be the key odour character of pig barn air. Blanes-Vidal et al. (2009) and Noble et al. (2001) found that odour concentrations were strongly related to sulphur-containing compounds.

However, most of these significant malodorous components were almost completely removed by the biotrickling filters except *p*-cresol and dimethyl sulphide. These two compounds still appeared to have high odour indices at the exhaust of the bioreactors (Table 2.2). On the other hand, the volatile fatty acids (e.g. butanoic acid, 3-methylbutanoic acid, 2-methylbutanoic acid, pentanoic acid) were almost completely removed by the treatment system, which could be due to their high solubility in water.

Since the ultimate goal is to reduce the odour nuisance of the air released to the environment from swine facilities, it is important to study the optimum conditions for the removal of *p*-cresol and dimethyl sulphide, which probably still have significant contributions to the malodour of the treated air from the bioreactors. By doing this, the performance of the biotrickling filters in reducing odour emissions could be further improved. Though the reduction

in the concentrations of individual components might not be necessarily directly correlated to the overall odour reduction, the removal of *p*-cresol and dimethyl sulphide from the exhaust air of swine facilities might have significant impact on the overall odour reduction.

## 2.8 SUMMARY AND CONCLUSIONS

The key odour indicators of swine exhaust air were identified through two techniques: (1) linear regression analysis between the logarithm of odour emissions and logarithm of gas concentrations or odour indices of selected components, and (2) odour index values of the VOCs. The odour components with relatively higher $R^2$ values were $NH_3$, butanoic acid, and 3-methyl butanoic acid. Though some of the $R^2$ values were statistically significant, they were not very strong (ranging only from 0.07 to 0.50). The results could be due to the time difference in sample collection or could also mean that the perceived odour might not be directly associated with any particular component.

The VOC components which had higher odour indices before the filters were 2,3-butanedione, 2-methylbutanoic acid, 2-methylpropionic acid, 2-pentylfurane, 3-methylbutanoic acid, acetophenone, alpha-cumyl alcohol, butanoic acid, dimethyl sulphide, dimethyl sulfone, *p*-cresol, and pentanoic acid. However, most of these components, especially the volatile fatty acids, were almost completely removed by the treatment units, except *p*-cresol and dimethyl sulphide. This indicates that optimizing the removal of *p*-cresol and dimethyl sulphide might improve the performance of biotrickling filters in reducing odour emitted from swine facilities.

Thus, the results of this study show that *p*-cresol, dimethyl sulphide, and $NH_3$ could be considered as potential model pollutants for a modelling study on the removal of odorous components of pig barn air in biotrickling filters. Though different studies had contradictory results on the relationship between $NH_3$ and odour emissions and a relatively low correlation was

also obtained in this study, the high concentration of $NH_3$ in pig barn air could be a justifiable reason to consider $NH_3$ a model pollutant for this study as well.

## 2.9 REFERENCES


Aarnink, A.J.A., A.L. Sutton, T.T. Canh, M.W.A. Verstegen and D.J. Langhout. 2007. Dietary Factors Affecting Ammonia and Odour Release from Pig Manure. http://en.engormix.com/ MA-pig-industry/articles/dietary-factors-affecting-ammonia-t716/ p0.htm (2013/01/01).

Abdehagh, N., M.T. Namini, S.M. Heydarian, B. Bonakdarpour and D. Zare. 2011. Performance of a biotrickling filter employing *Thiobacillus thioparus* immobilized on polyurethane foam for hydrogen sulfide removal. *Iranian Journal of Environmental Health Science & Engineering* 8(3): 245-254.

Armeen, A., J.J.R. Feddes, J.J. Leonard and R.N. Coleman. 2008. Biofilters to treat swine facility air: Part 1. Nitrogen mass balance. *Canadian Biosystems Engineering* 50: 6.21-6.27.

Aroca, G., H. Urrutia, D. Núñez, P. Oyarzun, A. Arancibia and K. Guerrero. 2007. Comparison on the removal of hydrogen sulfide in biotrickling filters inoculated with *Thiobacillus thioparus* and *Acidithiobacillus thiooxidans*. *Electronic Journal of Biotechnology* 10(4): 514-520.

Blanes-Vidal, V., M.N. Hansen, A.P.S. Adamsen, A. Feilberg, S.O. Petersen and B.B. Jensen. 2009. Characterization of odor released during handling of swine slurry: Part 1. Relationship between odorants and perceived odor concentrations. *Atmospheric Environment* 43: 2997-3005.

Bulliner, E.A., J.A. Koziel, L. Cai and D. Wright. 2006. Characterization of livestock odors using steel plates, solid-phase microextraction, and multidimensional gas chromatography-

mass spectrometry-olfactometry. *Journal of the Air and Waste Management Association* 56(10): 1391-1403.

CEN (Communauté Européen de Normalisation). 2003. Air quality – Determination of odour concentration by dynamic olfactometry. Standard No. EN 13725:2003 F. Brussels, Belgium: European Committee for Standardization.

Chen, L., S. Hoff, L. Cai, J. Koziel and B. Zelle. 2009. Evaluation of wood chip-based biofilters to reduce odor, hydrogen sulfide, and ammonia from swine barn ventilation air. *Journal of the Air & Waste Management Association* 59(5): 520-530.

Devinny, J.S., M.A. Deshusses and T.S. Webster. 1999. *Biofiltration for Air Pollution Control*. USA: CRC Press LLC.

Eniola, B., Z. Perschbacher-Buser, E. Caraway, N. Ghosh, M. Olsen and D. Parker. 2006. Odor control in waste management lagoons via reduction of *p*-cresol using horseradish peroxidase. ASAE Paper No. 064044. Saint Joseph, MI: ASABE.

Guo, H., W. Dehod, J. Agnew, C. Lague, J.R. Feddes and S. Prang. 2006. Annual odor emission rate from different types of swine production buildings. *American Society of Agricultural and Biological Engineers* 49(2): 517-525.

Hogberg, M.G., S.L. Fales, F.L. Kirschenmann, M.S. Honeyman, J. Miranowski and P. Lasley. 2005. Interrelationships of animal agriculture, the environment, and rural communities. *Journal of Animal Science* 83: E13-E17.

Iliuta, I. and F. Larachi. 2004. Transient biofilter aerodynamics and clogging for VOC degradation. *Chemical Engineering Science* 59(16): 3293-3302.

Jacobson, L.D., B.P. Hetchler, V.J. Johnson, R.E. Nicolai and D.R. Schmidt. 2005. Seasonal variations in $NH_3$, $H_2S$, and $PM_{10}$ emissions from pig and poultry buildings from a multi-

state project. ASAE Meeting Paper No. ___. Saint Joseph, MI: ASABE.

Jensen, T.L. and M.J. Hansen. 2006. A biotrickling filter for removing ammonia and odour in ventilation air from a unit with growing-finishing pigs. In *Proceedings Workshop on Agricultural Air Quality*, 844-846. Washington, D.C., USA. June 5-8.

Lantec Products, Inc. 2013. Plastic packing. http://www.lantecp.com/products/ (2013/09/06).

Liu, Q., D.S. Bundy and S.J. Hoff. 1993. Utilizing ammonia concentrations as an odor threshold indicator for swine facilities. In *Proceedings of the IVth International Livestock Environment Symposium*, 678–685. Coventry, England. July 6-9.

McGinley, C.M., M.A. McGinley and D.L. McGinley. 2000. "Odor basics", Understanding and Using Odor Testing. http://www.fivesenses.com/ Documents/ Library/33%20%20Odor%20 Basics.pdf (2010/02/05).

Melse, R.W. and G. Mol. 2004. Odour and ammonia removal from pig house exhaust air using a biotrickling filter. *Water Science and Technology* 50(4): 275-282.

Miner, J.R. 1995. A review of the literature on the nature and control of odors from pork production facilities. Washington, D.C., USA: National Pork Producers Council.

Noble, R., P.J. Hobbs, A. Dobrovin-Pennington, T.H. Misselbrook and A. Mead. 2001. Olfactory response to mushroom composting emissions as a function of chemical concentration. *Journal of Environmental Quality* 30: 760-767.

O'Neill, D.H. and V.R. Phillips. 1992. A review of the control of odour nuisance from livestock buildings: Part 3. Properties of the odorous substances which have been identified in livestock wastes or in the air around them. *Journal of Agricultural Engineering Research* 53(1): 23-50.

Ozis, F., A. Bina and J.S. Devinny. 2005. Future prospects of biotechnology for odor control. In *Biotechnology for Odour and Air Pollution Control*, ed. Z. Shareefdeen and A. Singh, 383-

402. Germany: Springer-Verlag.

Park, O.H. and I.G. Jung. 2006. A model study based on experiments on toluene removal under high load conditions in biofilters. *Biochemical Engineering Journal* 28(3): 269-274.

Qu, G., I.E. Edeogu and J.J.R. Feddes. 2010. Odor index: An integration of odor parameters for swine slurry odors. *Transactions of the ASABE* 53(1): 219-223.

Schiffman, S.S., J.L. Bennett and J.H. Raymer. 2001. Quantification of odors and odorants from swine operations in North Carolina. *Agricultural and Forest Meteorology* 108: 213-240.

Schulte, D.D., D.A. Kottwitz and C.B. Gilbertson. 1985. Nitrogen content of scraped swine manure. In *Proceedings of the Vth International Symposium on Agricultural Waste*, 321-328. St. Joseph, MI: ASABE.

Segura, J.C. and J.J.R. Feddes. 2005. Relationship between odour intensity and concentration of *n*-butanol. CSAE/SCGR Paper No. 05-020. Manitoba, Canada: CSAE/SCGR.

Sheffield, R.E. and P. Ndegwa. 2008. Sampling agricultural odors. http://www.cals.uidaho.edu/edComm/pdf/PNW/PNW595.pdf (2010/02/05).

Sheridan, B.A., T.P. Curran and V.A. Dodd. 2003. Biofiltration of n-butyric acid for the control of odour. *Bioresource Technology* 89(2): 199-205.

Sheridan, B., T. Curran, V. Dodd and J. Colligan. 2002. Biofiltration of odour and ammonia from a pig unit – A pilot-scale study. *Biosystems Engineering* 82: 441-453.

Spoelstra, S.F. 1980. Origin of objectionable odourous components in piggery wastes and the possibility of applying indicator components for studying odour development. *Agriculture and Environment* 5: 241-260.

Sun, G. 2005. Monitoring and modelling diurnal and seasonal odour and gas emission profiles for swine grower/finisher rooms. Unpublished M.Sc. thesis. Saskatoon, Saskatchewan,

Canada. Department of Agricultural and Bioresource Engineering, University of Saskatchewan.

Thu, K.M. 2002. Public health concerns for neighbors of large-scale swine production operations. *Journal of Agricultural Safety and Health* 8(2): 175-184.

Verdoes, N. and N.W.M. Ogink. 1997. Odour emission from pig houses with low ammonia emission. In *International Symposium on Ammonia and Odour Control from Animal Production Facilities*, 317-325. Vinkeloord, The Netherlands. October 6-10.

Wright, D.W., D.K. Eaton, L.T. Nielsen, F.W. Kuhrt, J.A. Koziel, J.P. Spinhirne and D.B. Parker. 2005. Multidimensional gas chromatography – olfactometry for the identification and prioritization of malodors from confined animal feeding operations. *Journal of Agricultural and Food Chemistry* 53(22): 8663-8672.

Zhang, Q., J.J.R. Feddes, I.K. Edeogu and X.J. Zhou. 2002. Correlation between odour intensity assessed by human assessors and odour concentration measured with olfactometers. *Canadian Biosystems Engineering* 44: 6.27-6.32.

# Chapter 3
# Assessing Different Microbial Cultures for Their Ability to Degrade Mixtures of Pig Barn Air Key Odour Components

## 3.1 CONTRIBUTION OF THE PH.D. CANDIDATE

This present study resulted in the identification of the microbial culture that was most capable of degrading the key odour components of pig barn air. Employing suitable and effective microorganisms is one of the factors that determine the success of biotrickling filter operation. All the experiments, data analysis, and manuscript writing were performed by the candidate while editorial inputs were provided by Dr. Stéphane P. Lemay and Dr. Bernardo Predicala as well as by Dr. Matthieu Girard of the Research and Development Institute for the Agri-Environment (IRDA). Valuable suggestions pertaining to the experimental design were also provided by Dr. Richard Hogue of IRDA.

## 3.2 CONTRIBUTION OF THIS PAPER TO THE OVERALL STUDY

The key odour components of pig barn air selected in Chapter 2 as model pollutants were *p*-cresol, dimethyl sulphide, and ammonia. It was hypothesized that optimizing the removal of these three odour components could improve the performance of biotrickling filters in reducing odour emitted from pig buildings. Since biodegradation of contaminants is one of the core processes in biotrickling filter operation and considering the fact that different compounds are degraded by different types of microorganisms at different degrees, it is therefore important to choose the right microbial strains that produce optimum degradation of target components. Thus, in this paper, different strains of microorganisms were assessed for their ability to degrade mixtures of the above-mentioned model pollutants.

## 3.3 ABSTRACT

Three different inocula were assessed for their ability to degrade mixtures of *p*-cresol, dimethyl sulphide, and ammonia under a suspended growth system. The three inocula were (1) a complex inoculum taken from an existing biotrickling filter; (2) a pure culture of *Pseudomonas putida*; and (3) a mixture of *Thiobacillus thioparus*, *Nitrosomonas europaea* and *Nitrobacter vulgaris*. Above 90% *p*-cresol reduction and 10% $NH_4^+$-N reduction were observed in samples with inoculum 1 (complex inoculum). No significant reduction of *p*-cresol and only 2% reduction of $NH_4^+$-N were obtained in samples with inoculum 2. Above 90% reduction of *p*-cresol and 5% reduction of $NH_4^+$-N were achieved in samples with inoculum 3. It was not possible to calculate the reduction of dimethyl sulphide in the samples since concentrations of this compound in the liquid phase were below the instrument's detection limit. Based on *p*-cresol and $NH_4^+$ reductions, the complex inoculum was found to have the best degradation performance.

## 3.4 INTRODUCTION

One of the promising techniques for the treatment of odour emitted from swine production facilities is biotrickling filtration. In this system, contaminated air passes through a packed bed where microorganisms are immobilized, while an aqueous phase is recirculated over the packing to provide moisture and nutrients to the microorganisms (Cox and Deshusses 1998). The contaminants are utilized by the microorganisms as sources of carbon, nutrients, and energy for growth and cell maintenance, producing more biomass and less toxic substances such as carbon dioxide, water, nitrate, and sulfate (Revah and Morgan-Sagastume 2005; van Groenestijn and Hesselink 1993).

The air that goes through the biotrickling filter units also carries aerosols and dust, which in turn carry various types of microorganisms (Devinny et al. 1999). The two most common groups of microorganisms found in air-phase bioreactors are bacteria and fungi. Bacteria generally have rapid substrate uptake and growth under favourable conditions, while fungi normally grow slowly (Devinny et al. 1999). Since fungi can survive harsher conditions and are able to degrade a larger variety of pollutants (Devinny et al. 1999), they are found more suitable for the treatment of hydrophobic compounds (Singh and Ward 2005).

The air that goes through the biotrickling filter units carries aerosols and dust, which in turn carry various types of microorganisms (Devinny et al. 1999). The two most common groups of microorganisms found in air-phase bioreactors are bacteria and fungi (Devinny et al. 1999). Bacteria generally demonstrate faster substrate uptake and growth under favourable conditions, while fungi normally grow relatively slower because of their bigger size, which give them a smaller surface-to-volume ratio for substrate uptake (Devinny et al. 1999). Fungi can survive in harsher conditions and are able to degrade a wider variety of contaminants (Devinny et al. 1999); thus, they are found more suitable for the treatment of hydrophobic compounds (Singh and Ward 2005).

The relevance of inoculating biotrickling filters has been questioned because the microbial strains present in the waste air may overwhelm the inoculated species; yet, for biotrickling filters with synthetic packing materials, inoculation may be important. Though inoculation may not directly affect removal efficiencies, it may speed up the start-up period and acclimation stage (Devinny et al. 1999).

The microbial population is selected based on the properties of the contaminant to be treated (Singh and Ward 2005). Heterotrophic microorganisms (e.g *Pseudomonas putida)*, which derive energy from the oxidation of organic molecules, are found suitable for the treatment of VOCs

(Singh and Ward 2005). Different species of *Pseudomonas* have been used in several studies (Jang et al. 2005; Zilli et al. 2004; Zilli et al. 1993) for the treatment of VOCs. Hydrogen sulphide, ammonia, and other inorganic pollutants are treated with autotrophic microorganisms, which use the inorganic molecules as energy source and carbon dioxide as a carbon source (Singh and Ward 2005). The widely studied autotrophs used for nitrification of ammonia are the *Nitrosomonas* and *Nitrobacter*. *Nitrosomonas* oxidizes ammonium to nitrite while *Nitrobacter* subsequently oxidizes nitrite to nitrate (Melse and Mol 2004). *Nitrosomonas europaea*, for example, has been used in many biofilter and biotrickling filter studies (Ramirez et al. 2009a; Chung and Huang 1998) for the treatment of ammonia. Oxidation of sulphides, on the other hand, can be carried out by autotrophs such as *Thiobacillus*. Several biofiltration studies (Ramirez et al. 2009b; Duan et al. 2005; Hirai et al. 1990) have utilized *Thiobacillus sp.* for the treatment of sulphur-containing compounds. However, some studies have shown that inorganic compounds can also be treated with heterotrophic bacteria. Chung et al. (2001) have shown that ammonia and hydrogen sulphide can be oxidized by *Arthrobacter* and *Pseudomonas spp.*, respectively, while Pol et al. (1994) have found that dimethyl sulphide contaminated air could be effectively treated with *Hyphomicrobium sp*.

Instead of inoculating the bioreactors with pure cultures, some studies use mixed microbial cultures to start-up the system (Cox et al. 1997). Sakuma et al. (2008) and Jiang et al. (2009) used activated sludge that were already exposed to the contaminants of interest. In this study, three inocula were evaluted for their ability to degrade mixtures of three key odour components identified in Chapter 2, namely, *p*-cresol, dimethyl sulphide, and ammonia. The best inoculum identified would be the one utilized in the succeeding shake-flask and biotrickling filtration experiments.

## 3.5 MATERIALS AND METHODS

### 3.5.1 Microorganisms

The three inocula employed were (1) a complex inoculum; (2) a pure culture of *Pseudomonas putida*; and (3) a mixture of *Thiobacillus thioparus*, *Nitrosomonas europaea* and *Nitrobacter vulgaris*.

The complex inoculum (inoculum 1) was taken from the biotrickling filters treating waste air exhausted from the bench-scale pig chambers of the Research and Development Institute for the Agri-Environment (IRDA) in Dechambault, Quebec. Several studies (Delhoménie et al. 2008; Jorio et al. 2005; Veiga et al. 1999) also utilized inocula extracted from bioreactors already in operation. According to Jorio et al. (2005), this approach offers a good representation of the real kinetics that are taking place in bioreactors since the microorganisms in these inocula have already been exposed to the contaminants in the air and to the reactions occurring in bioreactors.

Inoculum 1 contained various microbial strains, both autotrophic and heterotrophic. The initial polymerase chain reaction-denaturing gradient gel electrophoresis (PCR-DGGE) analysis conducted at the microbiological laboratory of IRDA showed that the dominant species of the complex inoculum were *Sphingobacteriales sp.*, *Bacteroides sp.*, *Sphingomonas sp.*, *Stenotrophomonas sp.*, *Methylophaga sp.*, and two *Rhodanobacter sp.*, with the last three being the most dominant.

The complex inoculum was preserved by placing 25 mL of the inoculum in 50 mL plastic tubes, each added with approximately 15 mL of pure glycerol, which served as cryoprotectant. The tubes were stored at -80$^{o}$C until utilization (Doelle 1994).

Inoculum 2 was a pure culture of *Pseudomonas putida*. Some studies showed that *P. putida* is capable of degrading organic compounds (Basu and Phale 2008; Nikakhtari and Hill 2006), ammonia (Daum et al. 1998), and sulphide (Chung et al. 1996).

Inoculum 3 was a defined mixed culture of *Nitrosomonas europaea* and *Nitrobacter vulgaris* for nitrogen removal, and *Thiobacillus thioparus* for sulphide removal. This microbial consortium was similar to the one used by Park et al. (2009), except that there was no inclusion of *P. putida* in this study.

*Pseudomonas putida* (DSM 291), *T. thioparus* (DSM 505) and *N. vulgaris* (DSM 10236) were purchased from the German Collection of Microorganisms and Cell Cultures (DSMZ) in Braunschweig, Germany while *N. europaea* (ATCC 19718) was obtained from the American Type Culture Collection (ATCC) in Virginia, USA. To obtain sufficient quantity, all these cultures were independently cultivated according to companies' specifications (appendix A). *Pseudomonas putida*, *T. thioparus*, and *N. vulgaris* were grown in DSM medium 1 (DSMZ 2007a), DSM medium 36 (DSMZ 2009), and DSM medium 756a (DSMZ 2007b), respectively, while *N. europaea* was enriched using ATCC medium 2265 (ATCC 2012).

### 3.5.2 Mineral media

Since the three inocula are composed of different microbial species, which have different nutrient requirements, three different mineral media were utilized: medium 1 for inoculum 1, medium 2 for inoculum 2, and medium 3 for inoculum 3. The composition of the three liquid media are presented in Table 3.1.

**Table 3.1 Composition of mineral media.**

| Component | Amount (g $L^{-1}$ of phosphate buffer solution) | | |
|---|---|---|---|
| | **Medium 1** | **Medium 2** | **Medium 3** |
| $CaCl_2.2H_2O$ | 0.050 | 0.050 | 0.004 |
| KCl | 0.200 | 0.200 | 0.200 |
| $MgSO_4.7H_2O$ | 0.050 | 0.040 | 0.050 |
| $FeSO_4 .7H_2O$ | 0.001 | 0.001 | 0.001 |
| NaCl | 5.000 | - | - |
| $CuSO_4.5H_2O$ | - | $3.0x10^{-5}$ | - |

Medium 1 was based on DSM medium 951 (DSMZ 2007c), but with some modifications (e.g. no addition of vitamins and different concentrations of some nutrients). This medium is for a *Methylophaga sp.*, which was found to be the most dominant in the complex inoculum. Since most members of the genus *Methylophaga* are found in marine environments, medium 1 was high in salt content. This mineral medium also contained the necessary nutrients for the other two dominant species (the two *Rhodanobacter sp.*) in the complex inoculum. Media 2 and 3 were based on the ones used by Daum et al. (1998) and Park et al. (2009), respectively. Except NaCl, the three media were not very different in terms of composition. All the three mineral media were prepared at pH 7.

Since it was observed during preliminary experiments that the pH of the solutions changed significantly to below seven during the course of the experiment, a phosphate buffer solution (PBS) was used in lieu of distilled water. To make a litre of PBS of pH 7, 5.38 g of $NaH_2PO_4.H_2O$ and 8.66 g of $Na_2HPO_4$ were added to one litre of distilled water (Gomori 1955).

### 3.5.3 Preparation of the inocula

The tube containing the frozen complex microbial culture (inoculum 1) was thawed in a water bath at 20°C. When completely thawed, the culture was centrifuged at 3500 rpm for 10 min at 20°C. Preliminary trials showed that this speed and duration are sufficient to completely collect the solid particles. After centrifugation, the pellets were suspended in approximately 20 mL of fresh mineral medium 1 and were again centrifuged at the same conditions. This cell washing process was conducted two times to thoroughly eliminate traces of glycerol and other substances. After the second washing, the pellets were again suspended in fresh mineral medium 1 to make a final volume of 40 mL and were then directly utilized in the batch experiment.

Inoculum 2, which was composed of *P. putida* only, was prepared by taking 25 mL of *P. putida* culture from the flasks where it was cultivated during its exponential growth phase. The microbial culture was then centrifuged at 3500 rpm for 10 min at 20°C. The cells were washed using medium 2 following the same procedure applied to inoculum 1. After the second washing, the pellets were again suspended in fresh mineral medium 2 to obtain a volume of 40 mL and were then directly utilized in the batch experiment.

Inoculum 3 was prepared in the same manner as inoculum 2. Cell suspensions of each of the three strains *(N. europaea*, *N. vulgaris*, and *T. thioparus)* were taken from the flasks where they were grown. However, these strains grew very slowly, especially *N. europaea* and *N. vulgaris*, a condition normal for autotrophs (Ni 2013); thus, larger volumes of cell suspensions (~ 50 to 100 mL) were used. The cells of each strain were washed with medium 3 following the same procedure applied to inocula 1 and 2. After the second washing, approximately 13 mL of medium 3 were added to the pellets of each strain before they were all mixed together (which resulted to a final volume of around 39 mL) for utilization in the batch experiment.

The summary of the preparation of the different inocula is presented in Figure 3.1.

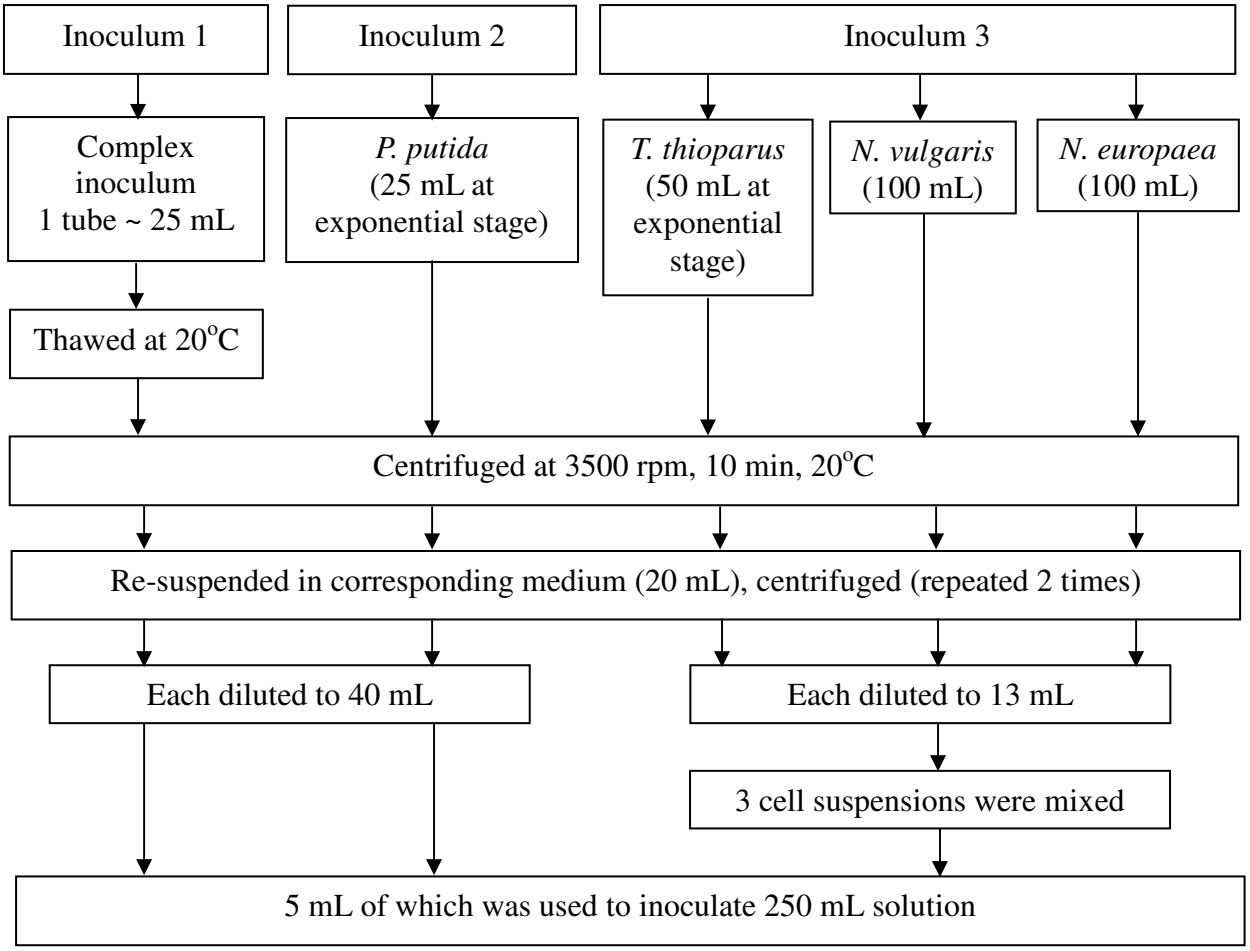


**Figure 3.1 Preparation steps for the different inocula.**

### 3.5.4 Odour components

Ammonia as $(NH_4)_2SO_4$, *p*-cresol, and dimethyl sulphide were added to each culture medium to obtain liquid concentrations of 850 ppm $NH_4^+$-N, 10 ppm *p*-cresol, and 20 ppb dimethyl sulphide. The $NH_4^+$-N concentration employed was the average concentration of $NH_4^+$-N measured in the recirculating liquid of the biotrickling filters in Deschambault, Quebec. On the other hand, the *p*-cresol and dimethyl sulphide liquid concentrations utilized in this study were estimated using their average concentrations in pig barn air as published in the literature (Blanes-Vidal et al. 2009; Schiffman et al. 2001) and Henry's law constants (Sander 2011). All

the chemicals used in the experiment were of laboratory grade purchased from Sigma-Aldrich Co., Missouri, USA.

### 3.5.5 Batch experiments

The different mineral media were placed in 500-mL glass bottles, which were silanized using 5% dimethyldichlorosilane in toluene (purchased from Sigma-Aldrich Co., Missouri, USA) to minimize adsorption of dimethyl sulphide onto the glassware's surfaces (Yang et al. 1996). The silanization procedure (appendix B) was provided by Sigma-Aldrich Co.

The volume of the culture medium placed in each bottle was adjusted such that the total volume after the addition of the contaminants and inoculum would be approximately 250 mL. The bottles containing the media with the $(NH_4)_2SO_4$, and the other unsterilized materials were autoclaved for 15 min at 121$^{o}$C. The *p*-cresol and dimethyl sulphide were not autoclaved as they are very volatile. Considering that these two substances are toxic at high concentrations as reported in the literature (Singh et al. 2008; Sercu et al. 2005), it was assumed that no microorganisms were present in the concentrated solutions, hence, autoclaving was deemed not necessary. However, the water used for dilution and the bottles used to hold the stock solutions were all sterilized. After autoclaving, the culture bottles were allowed to cool to room temperature, after which they were sealed with rubber caps.

The inoculum and the other two model contaminants (i.e. *p*-cresol and dimethyl sulphide) were injected into the bottles using disposable sterilized syringes or Hamilton gastight syringes for low volume solutions. Five millilitres of inoculum was used to inoculate 250-mL culture solution. Each treatment was conducted in three replicates.

The bottles were agitated at 100 rpm in a rotary shaker, which was placed in a temperature-controlled room to maintain the temperature at 20$^{o}$C. At the start and end of the

experiment, 10 mL samples were taken from the bottles using disposable sterilized syringes to measure the optical density (OD), pH, dissolved oxygen, and concentrations of $NH_4^+$, $NO_3^-$, *p*-cresol, and dimethyl sulphide. During the course of the experiments, only 2-mL samples were taken to monitor the OD and pH.

### 3.5.6 Analytical methods

The microbial growth was monitored by reading the OD of the cell suspensions at 600 nm (Yan et al. 2006) using a UV-Vis spectrophotometer (LKB Ultrospec II; LKB Biochrom Ltd, Cambridge, UK). The corresponding medium of the culture was used as blank.

The $NH_4^+$ and $NO_3^-$ concentrations were analyzed in the chemistry laboratory of IRDA using colorimetric method, employing the enzyme-linked immunosorbent assay (ELISA) technique. The detection limit for $NH_4^+$ and $NO_3^-$ were 10 and 7 ppb, respectively. The *p*-cresol and dimethyl sulphide concentrations in the liquid phase were analyzed by the *Laboratoire d'Expertises et d'Analyses Alimentaires* (LEAA) in Quebec City, Quebec, Canada. Samples of the headspace gas above the liquid samples were injected into a gas chromatograph and analyzed with a mass spectrometer. The detection limits of the instrument were 3 ppb for both *p*-cresol and dimethyl sulphide. The internal standards used were naphthalene D8, *p*-dichlorobenzene D4, 4-tert-amyl-phenol, and fluorobenzene.

The dissolved oxygen and pH were monitored using a Thermo Orion 862A dissolved oxygen meter (Cole-Parmer, USA) and a UB10 pH meter (Denver Instrument, USA), respectively.

## 3.6 RESULTS AND DISCUSSION

The average initial $OD_{600}$ of the samples with inoculum 1, 2, and 3 were 0.195, 0.004, and 0.007, respectively (Table 3.2). Only the samples with inoculum 1 (complex inoculum) and inoculum 3 exhibited evident biomass growth. The $OD_{600}$ readings of the samples with the complex inoculum were almost 0.5 after 45 h while those with inoculum 3 were in the range of 0.02 to 0.03 after 77 h. Since the $OD_{600}$ were monitored over a relatively wide time interval, it is difficult to assume that these were the maximum values in the growth curve of the microorganisms for it would be possible that maximum growth rates had already been surpassed during these periods. However, if these values were used for the calculation of the growth rates, the two inocula would have comparable growth rates (0.020 $h^{-1}$ for inoculum 1 and 0.017 $h^{-1}$ for inoculum 3) despite the difference in the initial biomass concentrations. A longer acclimation period was observed in samples with inoculum 3, which could be due to the relatively low initial biomass concentrations or to the lack of prior acclimation with *p*-cresol. Unlike inoculum 3, inoculum 1 had already been exposed to various organic compounds, including *p*-cresol, in the bioreactor where it was taken.

**Table 3.2 Optical density readings of the samples taken over time.**

| **Sample** | **Optical density at 600 nm (dimensionless)** | | | | | | | |
|---|---|---|---|---|---|---|---|---|
| | Time (h) | | | | | | | |
| | 0 h | 17 h | 45 h | 77 h | 101 h | 149 h | 221 h | 245 h |
| Inoculum 1 - A | 0.192 | 0.317 | 0.483 | 0.443 | 0.442 | (-) | (-) | (-) |
| Inoculum 1 - B | 0.198 | 0.292 | 0.470 | 0.418 | 0.423 | (-) | (-) | (-) |
| Inoculum 2 - A | 0.002 | 0.005 | 0.010 | 0.001 | (-) | 0.002 | 0.000 | 0.004 |
| Inoculum 2 - B | 0.005 | 0.006 | 0.008 | 0.012 | (-) | 0.001 | -0.001 | 0.026 |
| Inoculum 2 - C | 0.004 | 0.000 | 0.005 | -0.003 | (-) | -0.004 | -0.004 | 0.007 |
| Inoculum 3 - A | 0.009 | -0.002 | -0.007 | 0.032 | 0.033 | 0.013 | 0.016 | 0.009 |
| Inoculum 3 - B | 0.005 | -0.006 | -0.004 | 0.019 | 0.015 | 0.025 | 0.018 | 0.011 |

Note: A, B, and C were replicate samples; (-) means no measurement was taken.

On the other hand, the $OD_{600}$ of the samples with inoculum 2 almost remained unchanged all throughout the experiment which lasted for about ten days (245 h). This implies that no microbial growth occurred in samples inoculated with inoculum 2. This seems surprising since other studies (Mathur et al. 2010; Hutchinson and Robinson 1988) were able to grow *P. putida* in *p*-cresol solutions. The low initial biomass concentration should not be the reason for the absence of growth in these samples. A separate trial with inoculum 2 having an initial $OD_{600}$ of 0.136 still obtained no remarkable growth after nine days when using *p*-cresol as the source of carbon as compared to the one supplied with glucose, which was able to achieve an $OD_{600}$ of 0.883 after nine days.

The initial and final concentrations of dimethyl sulphide, *p*-cresol, $NH_4^+$, and $NO_3^-$ were measured in selected samples. Due to the cost of the analyses, the initial concentrations of the above-mentioned components were measured only in the samples containing inoculum 2. It was assumed that the other samples would have more or less the same initial concentrations considering that the same initial quantities of analytes were injected into all the sample bottles.

In terms of the reduction of the target components (Table 3.3), above 90% of the *p*-cresol and 10% of the $NH_4^+$-N were biodegraded in samples containing inoculum 1 after 101 h. It should be noted that the calculation for *p*-cresol reduction was based on the target initial concentration of 10 ppm (the calculated amount initially placed on each bottle) and not on the average measured concentration of 20 ppm. This is because *p*-cresol was suspected to form residues on the column of the GC after each injection as can be noticed in the results presented in Table 3.3, where initial concentrations of replicates were relatively different (15 and 24 ppm). Results from control samples (data not shown) also indicated depostion of *p*-cresol residues on the column.

**Table 3.3 Measured concentrations of target components.**

| Sample | Dimethyl sulphide (ppm) | | *p*-Cresol (ppm) | | $NH_4^+$-N (ppm) | | $NO_3^-$-N (ppm) | |
|---|---|---|---|---|---|---|---|---|
| | Initial[c] | Final[c] | Initial | Final | Initial | Final | Initial | Final |
| Inoculum 1 - A | $2.2 \times 10^{-4}$[a] | $1.7 \times 10^{-4}$ | 20[a] | <1[b] | 842[a] | 744 | 0.47[a] | 1.31 |
| Inoculum 1 - B | | $1.4 \times 10^{-4}$ | | <1[b] | | 773 | | 0.87 |
| Inoculum 2 - A | $2.4 \times 10^{-4}$[c] | $3.8 \times 10^{-4}$ | 15[b] | 15[b] | 812 | 800 | 0.36 | 0.17 |
| Inoculum 2 - B | $2.0 \times 10^{-4}$[c] | $4.1 \times 10^{-4}$ | 24[b] | 26[b] | 882 | 853 | 0.47 | 0.25 |
| Inoculum 2 - C | (-) | (-) | (-) | (-) | 833 | (-) | 0.57 | (-) |
| Inoculum 3 - A | $2.2 \times 10^{-4}$[a] | 0[d] | 20[a] | <1[b] | 842[a] | 810 | 0.47[a] | 0.24 |
| Inoculum 3 - B | | 0[d] | | <1[b] | | 800 | | 0.13 |

Note: A, B, and C were replicate samples; [a]average of the initial values measured from inoculum 2; [b]*p*-cresol measurements suspected to be contaminated by residues in the column; [c]values below the detection limit of the instrument; [d]ratio or retention time is incorrect; (-) means no measurement was taken.

No reduction of *p*-cresol was observed in samples inoculated with inoculum 2 and only 2% reduction of $NH_4^+$-N was obtained after 245 h. This reduction in $NH_4^+$ concentration was very low that it could be even attributed to errors caused by the instrument or the method. This result supported the absence of biomass growth observed in samples inoculated with inoculum 2.

Above 90% reduction of *p*-cresol (based on calculated initial value of 10 ppm) and 5% reduction of $NH_4^+$-N were achieved in samples containing inoculum 3 after 245 h. The nitrifiers in inoculum 1 seemed to perform better than the *N. europaea* and *N. vulgaris* strains in inoculum 3. The performance of these two autotrophic nitrifiers was possibly affected by the presence of *p*-cresol, which is an organic carbon source (Texier and Gomez 2007; Zhu and Chen 2001; Lauchnor et al. 2011). Texier and Gomez (2007) found a decrease in the specific rate of ammonium consumption when *p*-cresol was added to a nitrifying mixed culture. The authors

cited that the inhibory effect of *p*-cresol on ammonia oxidation might be due to a competing effect on the active site of the enzyme.

Moreover, the reactions in samples containing inoculum 1 and 3 were already limited by *p*-cresol (concentrations < 1 ppm), thus, no further growth had occurred after 45 h for inoculum 1 and 101 h for inoculum 3 even if levels of $NH_4^+$ were still very high (> 700 ppm). The reduction of *p*-cresol in samples inoculated with inoculum 3 might have been carried out by all the three strains present, namely *N. europaea*, *N. vulgaris* and *T. thioparus*. Though these microbial species are known to be autotrophs, which normally use carbon dioxide as source of carbon, some studies (Taylor and Bottomley 2006; Hommes et al. 2003; Keunen and Veldkamp 1973) have revealed that *N. europaea* and *T. thioparus* could also utilize organic carbon either as a source of energy or for cell growth. In addition, the *Nitrobacter* species utilized in this experiment is a mixotrophic (see Appendix A), which is capable of utilizing carbon from either organic or inorganic compounds.

The ability of *T. thioparus* to oxidize dimethyl sulphide was not determined since this compound was not detected in the liquid samples. Due to its very high Henry's law constant, most of the dimethyl sulphide probably stayed in the gas phase. The concentrations of dimethyl sulphide at the beginning of the experiment was expected to be above the detection limit of the instrument (based on Henry's law), yet, the resulting concentrations in the liquid phase were still undetectable.

In terms of $NO_3^-$, only a very slight production was observed in samples with inoculum 1, which could be due to the low reduction of $NH_4^+$. However, it was surprising that a slight decrease in $NO_3^-$ levels was observed in samples containing inocula 2 and 3. This could be an indication of aerobic denitrification; however, this process usually occurs at higher C/N ratios (Feng et al. 2011; Kim et al. 2008), a condition contrary to what had existed in this study.

The dissolved oxygen at the start of the experiment measured between 8 to 9 ppm for all the samples. At the end of the batch experiment, the dissolved oxygen in the samples inoculated with inoculum 1, 2, and 3 were found to be around 1, 9, and 7 ppm, respectively. It seems that the reaction in samples containing inoculum 1 was not only substrate-limited but was also limited by oxygen. The reported critical value for dissolved oxygen is around 0.5 to 1 ppm for the biodegradation of organic materials and 1 to 2 ppm for nitrification (van Haandel and Van der Lubbe 2012). The low dissolved oxygen content in the samples with inoculum 1 might have affected the nitrification process. Ruiz et al. (2003) found an accumulation of nitrite at a dissolved oxygen of 1.4 ppm and a decreased in ammonia consumption when the dissolved oxygen reached 0.5 ppm.

The pH, on the other hand, never went down below 6.8 in all samples until the end of the experiment. In this trial, no samples were employed to verify any loss of contaminants through bottle leakage or during sample extraction as well as the effect of volume reduction due to sample withdrawal. However, subsequent experiments showed no leakage of contaminants during an entire course of any experiment as well as no noticeable difference on the degradation rates in the bottles being sampled regularly and in those which were sampled only at the beginning and at the end of the experiment.

Based on the results, the complex inoculum (inoculum 1) was shown to have the best performance among the three inocula tested. Since it was taken from a bioreactor that had already been treating air exhausted from a pig barn, the different microbial species in inoculum 1 have already developed the adaptability and robustness to degrade the contaminants tested in this study.

## 3.7 SUMMARY AND CONCLUSIONS

Three inocula were assessed for their ability to degrade mixtures of key odour components of pig barn air, namely ammonia, *p*-cresol, and dimethyl sulphide. The three inocula were (1) a complex inoculum; (2) a pure culture of *Pseudomonas putida*; and (3) a mixture of *Thiobacillus thioparus*, *Nitrosomonas europaea* and *Nitrobacter vulgaris*. Above 90% *p*-cresol reduction and 10% $NH_4^+$-N reduction were observed in samples inoculated with inoculum 1. No significant reduction of *p*-cresol and only 2% reduction of $NH_4^+$-N were obtained in samples containing inoculum 2. Above 90% reduction of *p*-cresol and 5% reduction of $NH_4^+$-N were achieved in samples inoculated with inoculum 3.

Among the three inocula, it was shown that the complex inoculum (inoculum 1) had the best performance in terms of *p*-cresol and ammonia reduction. Moreover, the difficulty of cultivating *N. europaea* and *N. vulgaris* reinforced the choice of using inoculum 1 for the subsequent tests. Due to the instrument's detection limit for dimethyl sulphide, this contaminant was omitted in the subsequent experiments. Since oxygen limitation occurred in the reactions with inoculum 1, Erlenmeyer flasks capped with cotton plugs were used in the subsequent trials instead of sealed bottles.

## 3.8 REFERENCES

ATCC. 2012. ATCC Medium 2265. http://www.atcc.org/Attachments/ 3402.pdf (2012/01/05).

Basu, A. and P.S. Phale. 2008. Conjugative transfer of preferential utilization of aromatic compounds from *Pseudomonas putida* CSV86. *Biodegradation* 19: 83-92.

Blanes-Vidal, V., M.N. Hansen, A.P.S. Adamsen, A. Feilberg, S.O. Petersen and B.B. Jensen. 2009. Characterization of odor released during handling of swine slurry: Part 1.

Relationship between odorants and perceived odor concentrations. *Atmospheric Environment* 43: 2997-3005.

Chung Y.C. and C. Huang. 1998. Biotreatment of ammonia in air by an immobilized *Nitrosomonas europaea* biofilter. *Environmental Progress* 17(1): 70-76.

Chung, Y.C., C. Huang and C.P. Tseng. 1996. Biodegradation of hydrogen sulphide by a laboratory-scale immobilized *Pseudomonas putida* CH11 biofilter. *Biotechnology Progress* 12: 773-778.

Chung, Y.C., C. Huang and C.P. Tseng. 2001. Biological elimination of $H_2S$ and $NH_3$ from wastegases by biofilter packed with immobilized heterotrophic bacteria. *Chemosphere* 43: 1043-1050.

Cox, H.J.J. and M.A. Deshusses. 1998. Biological waste air treatment in biotrickling filters. *Current Opinion in Biotechnology* 9: 256-262.

Cox, H.H., R.E. Moerman, S. van Baalen, W.N. van Heiningen, H.J. Doddema and W. Harder. 1997. Performance of a styrene-degrading biofilter containing the yeast *Exophiala jeanselmei*. *Biotechnology and Bioengineering* 53(3): 259-266.

Daum, M., W. Zimmer, H. Papen, K. Kloos, K. Nawrath and H. Bothe. 1998. Physiological and molecular biological characterization of ammonia oxidation of the heterotrophic nitrifier *Pseudomonas putida*. *Current Microbiology* 37: 281-288.

Delhoménie, M.C., J. Nikiema, L. Bibeau and M. Heitz. 2008. A new method to determine the microbial kinetic parameters in biological air filters. *Chemical Engineering Science* 63(16): 4126-4134.

Devinny, J.S., M.A. Deshusses and T.S. Webster. 1999. *Biofiltration for Air Pollution Control*. USA: CRC Press LLC.

Doelle, H.W. 1994. *Microbial Process Development*. Singapore: World Scientific Publishing Co. Pte. Ltd.

DSMZ. 2007a. DSM Medium 1. http://www.dsmz.de/ microorganisms/ medium/pdf/ DSMZ_ Medium1.pdf (2012/01/05).

DSMZ. 2007b. DSM Medium 756a. http://www.dsmz.de/ microorganisms/ medium/pdf/ DSMZ_ Medium756a.pdf (2012/01/05).

DSMZ. 2007c. DSM Medium 951. http://www.dsmz.de/ microorganisms/ medium/pdf/ DSMZ_Medium951.pdf (2012/01/05).

DSMZ. 2009. DSM Medium 36. http://www.dsmz.de/ microorganisms/ medium/pdf/ DSMZ Medium36.pdf (2012/01/05).

Duan, H., L.C.C. Koe and R. Yan. 2005. Treatment of $H_2S$ using a horizontal biotrickling filter based on biological activated carbon: reactor setup and performance evaluation. *Environmental Biotechnology* 67: 143-149.

Feng, Q., J.S. Cao, L.N. Chen, C.Y. Guo, J.Y. Tan and H.L. Xu. 2011. Simultaneous nitrification and denitrification at variable C/N ratio in aerobic granular sequencing batch reactors. *Journal of Food, Agriculture & Environment* 9(3&4): 1131-1136.

Gomori, G. 1955. Preparation of buffers for use in enzyme studies. *Methods in Enzymology* 1: 138-146.

Hirai, M., M. Ohtake and M. Shoda. 1990. Removal kinetics of hydrogen sulfide, methanethiol and dimethyl sulfide by peat biofilters. *Journal of Fermentation and Bioengineering* 70(5): 334-339.

Hommes, N.G., L.A. Sayavedra-Soto and D.J. Arp. 2003. Chemolithoorganotrophic growth of *Nitrosomonas europaea* on Fructose. *Journal of Bacteriology* 185(23): 6809-6814.

Hutchinson, D.H. and C.W. Robinson. 1988. Kinetics of the simultaneous batch degradation of *p*-cresol and phenol by *Pseudomonas putida. Applied Microbiology and Biotechnology* 29: 599-604.

Jang, J.H., M. Hirai and M. Shoda. 2005. Performance of a styrene-degrading biofilter inoculated with *Pseudomonas sp*. SR-5. *Journal of Bioscience and Bioengineering* 100(3): 297-302.

Jiang, X., R. Yan and J.H. Tay. 2009. Transient-state biodegradation behavior of a horizontal biotrickling filter in co-treating gaseous $H_2S$ and $NH_3$. *Applied Microbiology and Biotechnology* 81: 969-975.

Jorio, H., R. Brzezinski and M. Heitz. 2005. A novel procedure for the measurement of the kinetics of styrene biodegradation in a biofilter. *Journal of Chemical Technology and Biotechnology* 80: 796-804.

Kim, M., S.Y. Jeong, S.J. Yoon, S.J. Cho, Y.H. Kim, M.J. Kim, E.Y. Ryu and S.J. Lee. 2008. Aerobic denitrification of *Pseudomonas putida* AD-21 at different C/N ratios. *Journal of Bioscience and Bioengineering* 106(5): 498-502.

Kuenen, J.G. and H. Veldcamp. 1973. Effects of organic compounds on growth of chemostat cultures of *Thiomicrospira pelophila*, *Thiobacillus thioparus* and *Thiobacillus neapolitanus*. *Archives of Microbiology* 94: 173-190.

Lauchnor, E.G., T.S. Radniecki and L. Semprini. 2011. Inhibition and gene expression of *Nitrosomonas europaea* biofilms exposed to phenol and toluene. *Biotechnology and Bioengineering* 108(4): 750-757.

Mathur, A.K., S. Bala, C.B. Majumder and S. Sarkar. 2010. Kinetics studies of *p*-cresol biodegradation by using *Pseudomonas putida* in batch reactor and in continuous bioreactor packed with calcium alginate beads. *Water Science and Technology* 62(12): 2920-2929.

Melse, R.W. and G. Mol. 2004. Odour and ammonia removal from pig house exhaust air using a biotrickling filter. *Water Science and Technology* 50(4): 275-282.

Ni, B.J. 2013. *Formation, Characterization, and Mathematical Modeling of the Aerobic Granular Sludge*. Germany: Springer-Verlag.

Nikakhtari, H. and G.A. Hill. 2006. Continuous bioremediation of phenol-polluted air in an external loop airlift bioreactor with a packed bed. *Journal of Chemical Technology and Biotechnology* 81: 1029-1038.

Park, B.G., W.S. Shin and J.S. Chung. 2009. Simultaneous biofiltration of $H_2S$, $NH_3$ and toluene using cork as a packing material. *Korean Journal of Chemical Enginnering* 26: 79-85.

Pol, A., H.J. Op den Camp, S.G. Mees, M.A. Kersten and C. van der Drift. 1994. Isolation of a dimethylsulfide-utilizing *Hyphomicrobium* species and its application in biofiltration of polluted air. *Biodegradation* 5(2): 105-112.

Ramirez, M., J.M. Gomez, G. Aroca and D. Cantero. 2009a. Removal of ammonia by immobilized *Nitrosomonas europaea* in a biotrickling filter packed with polyurethane foam. *Chemosphere* 74: 1385-1390.

Ramirez, M., J.M. Gomez, G. Aroca and D. Cantero. 2009b. Removal of hydrogen sulfide by immobilized *Thiobacillus thioparus* in a biotrickling filter packed with polyurethane foam. *Bioresource Technology* 100: 4989-4995.

Revah, S. and J.M. Morgan-Sagastume. 2005. Methods of odour and VOC control. In *Biotechnology for Odour and Air Pollution Control*, ed. Z. Shareefdeen and A. Singh, 29-63. Germany: Springer-Verlag.

Ruiz, G., D. Jeison and R. Chamy. 2003. Nitrification with high nitrite accumulation for the treatment of wastewater with high ammonia concentration. *Water Research* 37: 1371-1377.

Sakuma, T., S. Jinsiriwanit, T. Hattori and M.A. Deshusses. 2008. Removal of ammonia from contaminated air in a biotrickling filter – denitrifying bioreactor combanation system. *Water Research* 42: 4507-4513.

Sander, R. 2011. Henry's Law Constants. In *NIST Chemistry WebBook, NIST Standard Reference Database Number 69,* ed. P.J. Linstrom and W.G. Mallard. USA: National Institute of Standards and Technology. http://webbook.nist.gov (2013/01/15).

Schiffman, S.S., J.L. Bennett and J.H. Raymer. 2001. Quantification of odors and odorants from swine operations in North Carolina. *Agricultural and Forest Meteorology* 108: 213-240.

Sercu, B., D. Nunez, G. Aroca, N. Boon, W. Verstraete and H. Van Langenhove. 2005. Inoculation and start-up of a biotricking filter removing dimethyl sulfide. *Chemical Engineering Journal* 113: 127-134.

Singh, A. and O. Ward. 2005. Microbiology of bioreactors for waste gas treatment. In *Biotechnology for Odour and Air Pollution Control*, ed. Z. Shareefdeen and A. Singh, 101-121. Germany: Springer-Verlag.

Singh, R.K., S. Kumar, S. Kumar and A. Kumar. 2008. Biodegradation kinetic studies for the removal of *p*-cresol from wastewater using *Gliomastix indicus* MTCC 3869. *Biochemical Engineering Journal* 40: 293-303.

Taylor, A.E. and P.J. Bottomley. 2006. Nitrite production by *Nitrosomonas europaea* and *Nitrosospira* sp. AV in soils at different solution concentrations of ammonium. *Soil Biology and Biochemistry* 38(4): 828-836.

Texier, A.C. and J. Gomez. 2007. Simultaneous nitrification and *p*-cresol oxidation in a nitrifying sequencing batch reactor. *Water Research* 41: 315-322.

van Groenestijn, J.W. and P.G.M. Hesselink. 1993. Biotechniques for air pollution control. *Biodegradation* 4: 283-301.

van Haandel, A.C. and J.G.M. van der Lubbe. 2012. *Handbook of Biological Wastewater Treatment: Design and Optimisation of Activated Sludge Systems*, 2nd edition. London, UK: IWA Publishing.

Veiga, M.C., M. Fraga, L. Amor and C. Kennes. 1999. Biofilter performance and characterization of a biocatalyst degrading alkylbenzene gases. *Biodegradation* 10: 169-176.

Yan, J., W. Jianping, B. Jing, W. Daoquan and H. Zongding. 2006. Phenol biodegradation by the yeast *Candida tropicalis* in the presence of *m*-cresol. *Biochemical Engineering Journal* 29: 227-234.

Yang, G., Z. Zhang, L. Liu and X. Liu. 1996. Study on the analysis and distribution of dimethyl sulphide in the East China Sea. *Chinese Journal of Oceanology and Limnology* 14(2): 141-147.

Zhu, S. and S. Chen. 2001. Effects of organic carbon on nitrification rate in fixed film biofilters. *Aquacultural Engineering* 25: 1–11.

Zilli, M., A. Converti, A. Lodi, M. Del Borghi and G. Ferraiolo. 1993. Phenol removal from waste gases with a biological filter by *Pseudomonas putida.* *Biotechnology and Bioengineering* 41(7): 693-699.

Zilli, M., D. Daffonchio, R. Di Felice, M. Giordani and A. Converti. 2004. Treatment of benzene-contaminated airstreams in laboratory-scale biofilters packed with raw and sieved sugarcane bagasse and with peat. *Biodegradation* 15(2): 87-96.

# Chapter 4
# Kinetic Studies on *p*-Cresol and Ammonia Biodegradation

## 4.1 CONTRIBUTION OF THE PH.D. CANDIDATE

The kinetic parameters on the biodegradation of certain pig barn key odour components (i.e. ammonia and *p*-cresol) were estimated in this study. These parameters are important in modelling studies as well as in understanding the biodegradation kinetics of these substances. All the experiments, data analysis, and manuscript writing were performed by the candidate while editorial inputs were provided by Dr. Stéphane P. Lemay and Dr. Bernardo Predicala as well as by Dr. Matthieu Girard of the Research and Development Institute for the Agri-Environment (IRDA). Valuable suggestions pertaining to the experimental design were also provided by Dr. Richard Hogue of IRDA.

## 4.2 CONTRIBUTION OF THIS PAPER TO THE OVERALL STUDY

One of the main concerns in mathematical modelling is the determination of the unknown model parameters such as biokinetic, physical, and chemical parameters (Alonso et al. 2000). Although some of these values can be taken from published literature, results from one study cannot be always applied to another due to the differences in certain conditions applied among different studies. The model parameters are often unique to a specific application or process, and thus, they have to be estimated using experimental data. In biological systems, which are living and dynamic, determination of these parameters is a great challenge. The parameters related to microbial kinetics are of greater concern since microorganisms are very sensitive to environmental factors. Thus, this study aimed to determine the biokinetic parameters involved in

the degradation of two key pig barn odour components (*p*-cresol and ammonia) identified in Chapter 2 using the best inoculum (a mixed microbial culture) chosen in Chapter 3. The biokinetic parameters estimated from this study were used as input parameters for the model developed in the next chapter.

## 4.3 ABSTRACT

The effect of pH on simultaneous nitrification and *p*-cresol oxidation was evaluated in shake-flask experiments using a mixed microbial culture. The highest *p*-cresol uptake and reduction rates and $NO_3^-$ production rate were observed at pH 7; thus, the kinetic studies on the biodegradation of *p*-cresol and ammonia at different concentrations were investigated at this pH level. The growth kinetics data were then fitted to the Monod and Haldane models to obtain the different kinetic parameters. The biodegradation of *p*-cresol over the studied concentration range was better described by the Monod equation ($R^2 = 0.96$) with estimated values of 0.10 $h^{-1}$ for $\mu_m$ and 103.4 mg $L^{-1}$ for $K_s$. The biodegradation of ammonia, on the other hand, was better described by the Haldane equation ($R^2 = 0.72$) with estimated values of 0.17 $h^{-1}$ for $\mu_m$, 11.9 mg $L^{-1}$ for $K_s$, and 617.9 mg $L^{-1}$ for $K_i$. The values obtained for ammonia were relatively higher compared to those reported in the literature. The utilization of glucose as a carbon source supplement might have affected the results.

## 4.4 INTRODUCTION

There has been an increasing concern on the odour emitted from swine production facilities. Though the exhaust air contains hundreds of substances, the offensive odour is hypothesized to be caused by only a few of these substances as well as by their interactions. Two of these key odour components identified in Chapter 2 were ammonia and *p*-cresol. Concerns

have been raised regarding the odour nuisance caused by these substances as well as their health and environmental impacts. The $NH_3$ released from livestock operation has become an important environmental concern because of its contribution to soil acidification and eutrofication (Melse and Mol 2004). Ammonia is also a severe respiratory tract irritant, which becomes noticeable by smell at concentrations as low as 0.6 $ppm_v$ (CCOHS 1998). On the other hand, *p*-cresol is highly toxic and corrosive, and causes nervous system depression. It has a fecal characteristic odour with an odour threshold of 1.9 $ppb_v$ (Schiffman et al. 2001). The reported average $NH_3$ concentration in pig barns is about 10 $ppm_v$ (Armeen et al. 2008), while that of *p*-cresol ranges between 9 to 59 $ppb_v$ (Blanes-Vidal et al. 2009; Schiffman et al. 2001).

Several techniques are available to reduce odour emissions from swine production. One of these is biological treatment, which is cost-effective for the treatment of high-volume waste gas streams containing readily biodegradable contaminants at relatively low concentrations such as those emitted from farm facilities (Park and Jung 2006; Iliuta and Larachi 2004; Sheridan et al. 2002). This technique relies on the ability of the microorganisms to degrade the pollutants in the waste air.

In processes where microorganisms are used to degrade the substances, the removal rate of the contaminants is inevitably linked to the microbial activity. Thus, sufficient knowledge of the microbial growth kinetics is important to understand the degradation capacities of the microorganisms and the factors that influence the success of the treatment operations (Kumar et al. 2005).

The growth rates of the microorganisms are influenced by several factors such as osmotic pressure, ionic strength, pH, temperature, and substrate concentration (Mulchandani and Luong 1989). Several studies have shown a strong influence of substrate concentration on microbial growth and a number of kinetic growth models that relate these two parameters have been

developed and studied. Some of these models are discussed in the works of Raghuvanshi and Babu (2010) and Mulchandani and Luong (1989). Most of the models developed relate utilization of a single substrate to the growth of a single population, although in some cases, they are applied to mixed cultures taken as a single entity (Marrot et al. 2006; Jorio et al. 2005; Veiga et al. 1999). There are also a few models that describe the effects of multiple substrates on the growth of either single or mixed bacterial cultures (Okpokwasili and Nweke 2005; Reardon et al. 2002; Kovarova et al. 1997; Bae et al. 1995); however, these models have not yet been validated extensively.

Two of the widely used kinetic growth models are the Monod and Haldane equations described in equations 1.11 and 1.12, respectively. The Monod model describes the transition from a first order reaction at low substrate concentration to a zero-order reaction at high substrate concentration (Rittman and McCarty 2001). Kermanshahi Pour et al. (2006) and Reardon et al. (2002) successfully applied this model to describe the biodegradation kinetics of benzene, toluene, and *p*-xylene.

The Haldane model, on the other hand, describes microbial growth where the substrate is also an inhibitor of microbial reaction (Marrot et al. 2006). This model was used to describe the biodegradation kinetics of inhibitory substances such as phenol, catechol, cresols, and styrene (Singh et al. 2008; Yan et al. 2006; Kumar et al. 2005; Jorio et al. 2005). Park and Bae (2009) used this model to describe the kinetics of ammonium and nitrite oxidation with inhibition by free ammonia and free nitrous acid.

In this study, a series of experiments were conducted to study the biodegradation of $NH_3$ and *p*-cresol, which were identified in Chapter 2 as key odour components of pig barn air. The kinetic studies were performed using suspended cells of the best inoculum (a mixed microbial culture) chosen in Chapter 3. Since pH is one of the significant factors affecting microbial

activity, the effect of pH on the simultaneous nitrification and *p*-cresol oxidation was evaluated. Using the optimum pH identified, the kinetics of the biodegradation of *p*-cresol and ammonia at different concentrations were then evaluated. The kinetic parameters were estimated by fitting the data to the Monod and Haldane models. The parameters obtained from this study were used as input parameters for the modelling study conducted in Chapter 5.

## 4.5 MATERIALS AND METHODS

### 4.5.1 Microbial culture

The source of the mixed microbial culture utilized in the experiments was the biofilm taken from the packing media of biotrickling filters used to treat the air exhausted from the bench-scale pig chambers of the Research and Development Institute for the Agri-Environment (IRDA) in Deschambault, Quebec, Canada. This inoculum provided the highest *p*-cresol and ammonium reductions as discussed in Chapter 3. Using a microbial consortium taken from existing bioreactors that are treating the target contaminants has also been adopted by other studies (Delhoménie et al. 2008; Jorio et al. 2005; Veiga et al. 1999). According to Jorio et al. (2005), this approach offers a good representation of the real kinetics that are taking place in bioreactors since the microorganisms in these inocula have already been exposed to the contaminants in the air and to the reactions occurring in bioreactors.

The dominant species found in the inoculum through the initial polymerase chain reaction-denaturing gradient gel electrophoresis (PCR-DGGE) and 16S rRNA gene sequence analysis conducted at the microbiological laboratory of IRDA were *Sphingobacteriales sp.*, *Bacteroides sp.*, *Sphingomonas sp.*, *Stenotrophomonas sp.*, *Methylophaga sp.*, and two *Rhodanobacter sp.*, with the last three being the most dominant.

The inoculum was preserved by placing 25 mL of mixed microbial suspension and approximately 15 mL of pure glycerol, which served as cryoprotectant, in 50 mL plastic tubes. The tubes were then stored at -80$^{o}$C until utilization (Doelle 1994). When needed, the frozen mixed culture in the tube was thawed in a water bath at 20$^{o}$C. When completely thawed, the culture was centrifuged at 3500 rpm for 10 min at 20$^{o}$C. After centrifugation, the pellets were suspended in approximately 20 mL of fresh mineral medium at pH 7 and were again centrifuged at the same conditions. This cell washing process was conducted two times to thoroughly eliminate traces of glycerol and other substances. After the second washing, the pellets were again suspended in fresh mineral medium to make a final volume of 45 mL and were then directly utilized in the batch experiments.

### 4.5.2 Mineral media

The mineral medium used was based on DSMZ (German Collection of Microorganisms and Cell Cultures) medium 951 (DSMZ 2007), but with some slight modifications such as no addition of vitamins and different dosage levels of nutrients. Though this medium was for a *Methylophaga* species, which was found to be one of the most dominant species in the mixed microbial culture based on the initial PCR-DGGE analysis, it also contained the nutrients needed by the other species in the inoculum. Components of this mineral medium are also found in the media utilized by other studies (Raghuvanshi and Babu 2010; Jácome et al. 2006) for mixed microbial culture.

The medium was composed of 0.040 g of $CaCl_2.2H_2O$, 0.200 g of KCl, 0.050 g of $MgSO_4.7H_2O$, 0.001 g of $FeSO_4 .7H_2O$, 3.000 g of NaCl, and 1.000 g of $NaHCO_3$ in one litre of phosphate buffer solution (PBS). The PBS was composed of $NaH_2PO_4.H_2O$ and $Na_2HPO_4$, the ratios of which in solution were varied depending on the desired pH of the solution. To make

solutions of pH 6, 7, and 8, the amount of $NaH_2PO_4.H_2O$ (in g $L^{-1}$) were 12.10, 5.38, and 0.73, respectively; while that of $Na_2HPO_4$ (in g $L^{-1}$) were 1.75, 8.66, and 13.45, respectively (Gomori 1955). PBS was used in lieu of distilled water since it had been observed in preliminary trials that the pH of the solutions varied significantly during the course of the experiment.

### 4.5.3 Batch experiments

Different sets of experiments were carried out to evaluate the effect of pH on nitrification, *p*-cresol oxidation, and microbial diversity as well as the effect of ammonia and *p*-cresol concentrations on microbial growth rate.

#### 4.5.3.1 Effect of pH on nitrification, *p*-cresol oxidation, and microbial diversity

Three pH values were tested in this study, namely, pH 6, 7, and 8. Two concentration levels (low and high) of *p*-cresol and $NH_4^+$-N [supplied as $(NH_4)_2SO_4$] were used to assess the effect of pH on the nitrification and biodegradation of *p*-cresol. For the low concentration level, 40 mg $L^{-1}$ *p*-cresol and 60 mg $L^{-1}$ $NH_4^+$-N were utilized while the *p*-cresol and $NH_4^+$-N concentrations employed for the high level concentration were 100 mg $L^{-1}$ and 500 mg $L^{-1}$, respectively. The $NH_4^+$-N concentrations utilized in this study were within the range of the $NH_4^+$-N concentrations measured in the recirculating liquid of the biotrickling filters where the mixed microbial culture was taken. The *p*-cresol concentrations, on the other hand, were the corresponding liquid phase concentrations, as estimated by Henry's law, of the published range of pig barn air *p*-cresol concentrations (Blanes-Vidal et al. 2009; Schiffman et al. 2001; Zahn et al. 1997). The Henry's law constant (defined as ratio between gas and liquid phase concentrations) used for *p*-cresol was $2.3 \times 10^{-5}$ at $20^oC$ (Sander 2011).

Approximately 250-mL liquid medium was placed in 500-mL Erlenmeyer flasks. After capping the flasks with cotton plugs, they were autoclaved for 15 min at 121°C. The $(NH_4)_2SO_4$ stock solution was autoclaved separately. The *p*-cresol stock solution was not autoclaved, assuming that no microorganisms could grow in a concentrated toxic solution. All the other materials used in this study were sterilized.

Three millilitres of the inoculum, prepared as described in section 4.5.1, was used to inoculate the growth medium. Each experimental treatment was done in triplicate. The flasks were agitated at 100 rpm in a rotary shaker, which was placed in a temperature-controlled room (Figure 4.1) to maintain the temperature at 20°C, which was the approximate average temperature of the air exhausted from the pig chambers and the temperature of the room where the bioreactors are placed. It was assumed that at the start of the operation the temperature of the recirculating liquid had already equilibrated to the room temperature and that temperature changes from liquid replenishment were negligible due to the small volume added. This means that more or less a constant temperature of about 20°C existed in the filter bed.


**Figure 4.1 Shake-flask experiment set-up inside a temperature-controlled chamber.**

It is important to note that *p*-cresol was added in two steps in the biodegradation study involving low substrate concentration since it was difficult to observe the exponential growth of the microorganisms. At the start of the experiment, 20 mg $L^{-1}$ of *p*-cresol and 60 mg $L^{-1}$ of $NH_4^+$-N were added to the liquid medium in the flask. After 20 h of incubation, another 25 mg $L^{-1}$ of *p*-cresol was added to the medium, which resulted in a *p*-cresol concentration of approximately 40 mg $L^{-1}$. After the lag phase period, the microorganisms consumed *p*-cresol rapidly, thus, it was difficult to obtain enough data points during exponential growth phase. Addition of *p*-cresol after the lag phase ensured that the exponential growth phase would be captured sufficiently. However, the $(NH_4)_2SO_4$ was added only once since there was a relatively lower $NH_4^+$ uptake by the microorganisms. At high substrate concentrations, *p*-cresol was added only once since the amount was high enough to adequately observe the exponential growth phase.

Two-millilitre samples were taken from each flask at different time intervals to monitor the biomass, *p*-cresol, $NH_4^+$, $NO_3^-$, and $NO_2^-$ concentrations. Another 2-mL sample was withdrawn from each flask once a day for pH measurement. Selected samples (54 out of 162 samples) were analyzed to observe the microbial diversity in the mixed culture. To confirm that the reactions were not limited by oxygen, the dissolved oxygen was measured at the start and at end of the experiment.

Control samples were also employed to verify the efficiency of the experimental method. The control samples consisted of (1) inoculated mineral media without *p*-cresol and $(NH_4)_2SO_4$ to verify if there were traces of carbon and nitrogen compounds that remained in the inoculum after cell washing, where a "no growth" in these control samples would indicate absence of these compounds; and (2) non-inoculated mineral media with *p*-cresol and $(NH_4)_2SO_4$ to check if there was contamination or volatilization of *p*-cresol or $NH_3$ that had occurred during the experiment.

#### 4.5.3.2 Effect of *p*-cresol concentration on microbial growth rate

The kinetic study on the biodegradation of *p*-cresol was carried out at pH 7 (the optimum pH found in the previous experiment) and at various initial concentrations of *p*-cresol: 20, 60, 95, 130, and 170 mg $L^{-1}$. To provide nitrogen to the microorganisms, 1.5 g $L^{-1}$ of $(NH_4)_2SO_4$ (equivalent to 318 mg $L^{-1}$ $NH_4^+$-N) was added to the mineral medium before it was autoclaved for 15 min at 121$^o$C. Previous trials showed that with this $NH_4^+$-N concentration, the biodegradation of *p*-cresol at the above-mentioned range of concentrations would not be limited by nitrogen.

Three millilitres of the mixed microbial suspension, which was prepared following the method described in section 4.5.1, was used to inoculate a 250-mL sterilized growth medium placed in a 500-mL Erlenmeyer flask. The incubation was initiated by adding 20 mg $L^{-1}$ of *p*-

cresol to all the flasks, which were then agitated at 100 rpm in a rotary shaker for 20 h at 20$^{o}$C (Figure 4.1). After 20 h, various amounts of *p*-cresol stock solution were then added to the flasks to achieve the desired initial *p*-cresol concentrations of approximately 20, 60, 95, 130, and 170 mg $L^{-1}$. The flasks were then re-agitated at the same conditions. For reason similar to the previous experiment, *p*-cresol was added in two steps to adequately observe the exponential growth phase. Each experimental treatment was done in triplicate and control samples similar to those in the previous experiment were also employed.

Two-millilitre samples were withdrawn from each flask every three or four hours to determine the biomass and *p*-cresol concentrations. A microbial analysis was also conducted with some selected samples (20 out of 72 samples). The concentrations of the nitrogen species were not monitored in this experiment. The pH and the dissolved oxygen were monitored the same way as in the previous experiment.

#### 4.5.3.3 Effect of ammonia concentration on microbial growth rate

The biodegradation study of ammonia was conducted at initial concentrations of 10, 30, 60, 85, and 140 mg $L^{-1}$ $NH_4^+$-N at pH 7 (the optimum pH found in the previous experiment). Relatively lower concentrations of $NH_4^+$ (lower than those encountered in the biotrickling filter units where the inoculum was taken) were employed due to very low consumptions of $NH_4^+$ as observed in the previous experiments.

The volumes of the mineral medium placed in 500-mL flasks were adjusted such that the final volume after the addition of the bacterial suspension and substrates was approximately 250 mL. The mineral medium and the $(NH_4)_2SO_4$ and glucose stock solutions were autoclaved separately at 121$^{o}$C for 15 min. Again, the *p*-cresol solution was not autoclaved, consistent with what was done in the previous experiments. After autoclaving and cooling to room temperature,

various quantities of the $(NH_4)_2SO_4$ stock solution were added to the medium to obtain the desired initial $NH_4^+$-N concentrations. Fixed amounts of glucose (3 g $L^{-1}$) and *p*-cresol (70 mg $L^{-1}$), which served as carbon sources, were also added to each of the flasks. Due to *p*-cresol's known toxicity, it cannot be added in large quantities; thus, glucose was added to ensure that the microorganisms were not limited by carbon, although it was recognized that addition of glucose could affect the results.

Three millilitres of the mixed bacterial suspension, prepared as described in section 4.5.1, was used to inoculate a 250-mL culture medium. All the substrates were added to the medium in one step only. The flasks were agitated in a rotary shaker at 100 rpm and 20$^oC$ (Figure 4.1). Each experimental treatment was done in triplicate and control samples were also employed similar to what had been done in the previous experiments.

To monitor the biomass growth, 2-mL samples were taken from each flask every three or four hours during the early stage of the exponential growth and became less frequent towards the end of the exponential growth phase. Selected samples (74 out of 257 samples) were analyzed for $NH_4^+$, $NO_3^-$, and $NO_2^-$ concentrations. A microbial analysis was also conducted to observe changes in microbial diversity. The pH and the dissolved oxygen were monitored the same way as in the other experiments.

### 4.5.4 Analytical and microbiological methods

The biomass concentration was determined by measuring the optical density (OD) of the cell suspension at 600 nm (Yan et al. 2006) using a UV-Vis spectrophotometer (LKB Ultrospec II; LKB Biochrom Ltd, Cambridge, UK). From the measured net OD (raw OD subtracted by that of the medium which served as blank), the biomass concentration, expressed as milligram of dry biomass per litre of culture solution, was estimated using a calibration curve. Two calibration

curves were developed for this purpose: (1) where only *p*-cresol was used as carbon source ($R^2$ = 0.99; Appendix C.1), and (2) where both *p*-cresol and glucose were used as carbon sources ($R^2$ = 0.97; Appendix C.2). The second calibration curve was the one utilized to calculate the biomass concentration in the kinetic study on ammonia biodegradation where both glucose and *p*-cresol were used as carbon sources while the first one was used in the other two sets of experiments (study on the effects of pH and kinetic study on *p*-cresol biodegradation).

After measuring the OD, samples were centrifuged at 13,000 rpm for 15 min using a microcentrifuge (AccuSpin Micro R; Fisher Scientific, USA). The supernatant liquid was analyzed for *p*-cresol concentration by measuring the absorbance at 277 nm (Singh et al. 2008) using the same spectrophotometer utilized in the measurement of the biomass concentration. A calibration curve ($R^2$ = 1.00; Appendix C.3) relating optical density at 277 nm and *p*-cresol concentration was used to estimate the concentration of *p*-cresol. After measuring the absorbance at 277 nm, the same supernatant was used for the $NH_4^+$, $NO_3^-$, $NO_2^-$ analyses, which were conducted at the chemistry laboratory of IRDA using colorimetric method, employing enzyme-linked immunosorbent assay (ELISA) technique. The concentrations of the nitrogen species were determined using calibration curves prepared for concentrations up to 1 mg $L^{-1}$ only since the relationship between optical density and concentrations was no longer linear beyond 1 mg $L^{-1}$. Thus, samples with concentrations above 1 mg $L^{-1}$ had to be diluted to below 1 mg $L^{-1}$. The detection limit for $NH_4^+$, $NO_3^-$, and $NO_2^-$ were 10, 7, and 6 ppb, respectively.

In addition, the pellets removed from centrifugation were analyzed for microbial diversity at the microbiological laboratory of IRDA using PCR-DGGE (Muyzer et al. 1993). The dominant bacterial strains found in the PCR-DGGE were then identified by 16S rRNA gene sequence analysis. Figure 4.2 shows the steps on how the samples were treated for the different analyses.

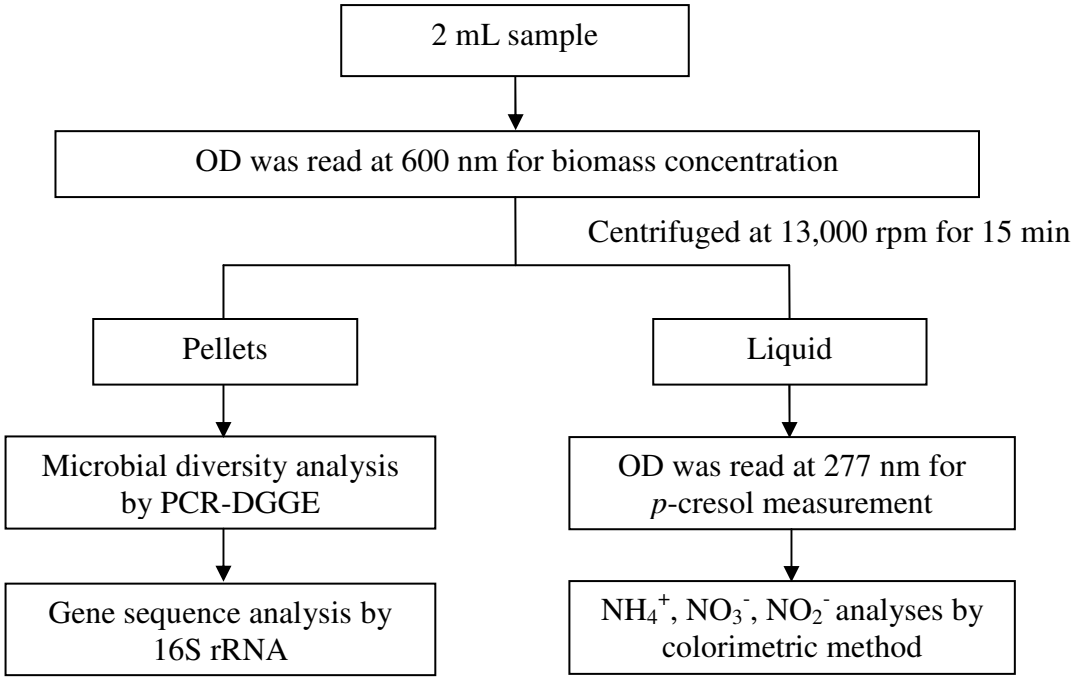


**Figure 4.2 Steps of sample treatment and analyses.**

The dissolved oxygen and pH were monitored using a Thermo Orion 862A dissolved oxygen meter (Cole-Parmer, USA) and a UB10 pH meter (Denver Instrument, USA), respectively.

### 4.5.5 Calculation of kinetic parameters

The different kinetic parameters were estimated using the empirical equations available in the literature.

#### 4.5.5.1 Microbial growth rate

In a batch system, the utilization rate of the substrate is related to the microbial growth rate as described by equation 4.1, while the net microbial growth is defined by equation 4.2 (Kumar et al. 2005):

$$\frac{dS}{dt} = -\frac{dX}{Ydt} \tag{4.1}$$

$$\frac{dX}{dt} = \mu X - k_d X \tag{4.2}$$

where S = substrate concentration (mg $L^{-1}$),

X = biomass concentration (mg $L^{-1}$),

Y = biomass yield coefficient (mg biomass formed $mg^{-1}$ of substrate consumed),

t = time (h),

μ = microbial specific growth rate ($h^{-1}$),

$k_d$ = microbial decay coefficient ($h^{-1}$).

At the exponential growth phase where $k_d$ can be neglected (Singh et al. 2008), equation 4.2 can then be reduced to equation 4.3 in its integrated form:

$$\ln\frac{X}{X_0} = \mu(t - t_0) \tag{4.3}$$

where subscript *0* indicates the condition at the beginning of the exponential growth phase.

Thus, applying equation 4.3, the value of μ in each of the tested initial *p*-cresol or ammonium concentration was estimated as the slope of the line when the logarithm of the biomass concentrations measured during exponential growth phase was plotted against time. The initial substrate concentration and the μ obtained at that concentration were fitted to the Monod (Eq. 4.4) and Haldane (Eq. 4.5) models using SAS PROC NLIN (SAS 2008):

$$\mu = \mu_m \frac{S}{K_s + S} \tag{4.4}$$

$$\mu = \frac{\mu_m S}{K_s + S + \left(S^2 / K_i\right)} \tag{4.5}$$

where $\mu_m$ = maximum microbial specific growth rate ($h^{-1}$),

$K_s$ = half-saturation constant (mg $L^{-1}$),

$K_i$ = inhibition constant (mg $L^{-1}$).

The kinetic parameters $\mu_m$, $K_s$, and $K_i$ were obtained from the non-linear regression employed.

The value of $K_s$ indicates the affinity of the microbial culture for the substrates. A high $K_s$ value indicates low affinity of the microorganisms to the substrate, resulting in a low growth rate (Singh et al. 2008). The value of $K_i$, on the other hand, indicates the inhibition capacity of the substrate and the extent of its toxicity towards the microorganisms, where a higher value indicates that the substrate is less inhibitory and toxic to the microorganisms (Singh et al. 2008).

#### 4.5.5.2 Yield coefficient

The biomass yield coefficient (Y) is defined as the ratio of the mass of biomass formed to the mass of substrate consumed as described in equation 4.6 (Ntwampe and Sheldon 2006):

$$Y = \frac{X - X_0}{S_0 - S} \tag{4.6}$$

In this study, Y was estimated as the slope of the line when the amount of biomass produced during the exponential growth phase was plotted against the corresponding amount of *p*-cresol or ammonium consumed.

#### 4.5.5.3 Utilization, reduction, and production rates

The specific rate of substrate utilization ($q_s$; mg substrate $mg^{-1}$ biomass $h^{-1}$), which is defined as the mass of the substrate removed per unit mass of the biomass produced per unit time, was calculated using equation 4.7 (Rittman and McCarty 2001):

$$q_s = \frac{\mu}{Y} \tag{4.7}$$

The reduction rate of substrate and the production rate of product were estimated as the slopes of the lines when substrate and product concentrations were plotted against time.

## 4.6 RESULTS AND DISCUSSION

### 4.6.1 Effect of pH on nitrification and *p*-cresol oxidation

The specific growth rate of the microorganisms, biomass yield on *p*-cresol, specific rate of *p*-cresol utilization, *p*-cresol reduction rate, and $NO_2^-$ and $NO_3^-$ production rates at different pH are presented in Table 4.1. Due to very low $NH_4^+$ utilization rates, values for this parameter are not presented in this paper; instead, the $NO_2^-$ and $NO_3^-$ production rates are presented to provide information on the nitrification rate.

**Table 4.1 The estimated values of the different parameters on nitrification and *p*-cresol oxidation.**

| pH | Specific growth rate ($h^{-1}$) | Yield on *p*-cresol ($mg_X\ mg_S^{-1}$) | *p*-Cresol utilization rate ($mg_S\ mg_X^{-1}\ h^{-1}$) | *p*-Cresol red. rate ($mg\ L^{-1}\ h^{-1}$) | $NO_2^-$ prod. rate ($mg\ L^{-1}\ h^{-1}$) | $NO_3^-$ prod. rate ($mg\ L^{-1}\ h^{-1}$) |
|---|---|---|---|---|---|---|
| 6(L) | 0.0258 | 0.4737 | 0.0537 | 2.5950 | 0.0081 | 0.0021 |
| 7(L) | 0.0408 | 0.6178 | 0.0662 | 3.9318 | 0.0177 | 0.0040 |
| 8(L) | 0.0568 | 1.0341 | 0.0549 | 3.0742 | 0.0256 | 0.0020 |
| 6(H) | 0.0380 | 0.4897 | 0.0765 | 2.0367 | 0.0011 | 0.0092 |
| 7(H) | 0.0503 | 0.6354 | 0.0803 | 5.0067 | 0.0298 | 0.0133 |
| 8(H) | 0.0331 | 0.5936 | 0.0560 | 3.7200 | 0.0489 | 0.0149 |

L – low substrates concentrations (40 mg $L^{-1}$ *p*-cresol and 60 mg $L^{-1}$ $NH_4^+$-N);
H – high substrates concentrations (100 mg $L^{-1}$ *p*-cresol and 500 mg $L^{-1}$ $NH_4^+$-N);
Subscripts *x* and *s* stand for biomass and substrate, respectively; red. for reduction; prod. for production.

A one-way analysis of variance (ANOVA) using SAS mixed model procedure (SAS 2008) was conducted to determine any significant effects of pH on the different kinetic parameters. However, the effects of pH at low substrate concentrations were not compared with those at high substrate concentrations since there was a slight difference in the experimental procedures applied to both sets of treatments. *p*-Cresol was added in two steps in the

biodegradation study with low substrate concentrations but only in one step for high substrate concentrations.

The results of the ANOVA ($\alpha = 0.05$) showed that the pH had significant effect on the specific growth rate of the microorganisms at low initial substrate concentrations, where the lowest growth rate occurred at pH 6 and the highest at pH 8. At high initial substrate concentrations, no significant difference on specific growth rate was observed at all pH values.

The biomass yield from the tests with *p*-cresol at low initial concentration had no significant difference at pH 6 or 7; however, the yield at pH 8 was significantly higher than those at pH 6 and 7. At high initial *p*-cresol concentration, no significant difference was observed for biomass yield at the three pH values.

The biomass yield from the tests with $NH_4^+$ was not calculated due to the low $NH_4^+$ reductions obtained. Moreover, the measured $NH_4^+$ concentrations throughout the experiment were relatively unstable as shown in Figure 4.3, which was probably due to the method employed to determine the nitrogen species. The dilution made to the samples to reduce the concentrations to 1 mg $L^{-1}$ (to be within the calibration range) might have affected the results. However, if the data obtained were used to calculate the $NH_4^+$ reductions, the highest reduction (7% for high initial $NH_4^+$ and 11% for low initial $NH_4^+$ concentration) would have been at pH 8, which would be consistent with the findings of Ward (1987) and Wahman et al. (2006).

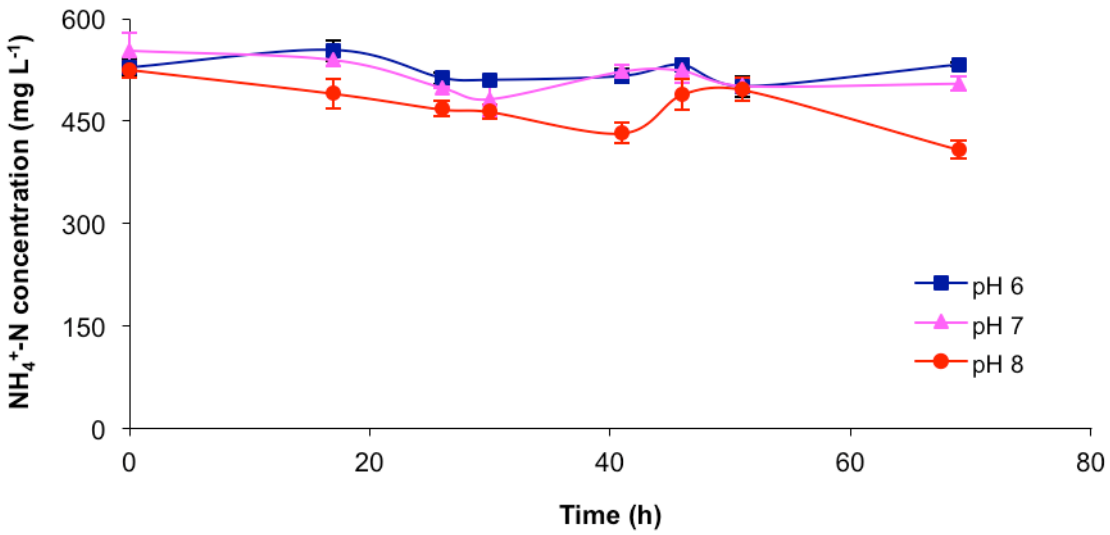


**Figure 4.3 Mean $NH_4^+$ concentrations over time at different pH values with high [H] initial $NH_4^+$ concentration of 500 mg $L^{-1}$.**

At low initial *p*-cresol concentrations, the *p*-cresol utilization rate at pH 7 was significantly higher than at pH 6 and 8, but was not significantly different between pH 6 and 8. At high initial *p*-cresol concentration, the utilization rate at pH 7 was significantly higher than at pH 8, but was not significantly different between pH 6 and 8 and between pH 6 and 7.

The effects of pH on *p*-cresol reduction rate and $NO_2^-$ production rate were significant at all pH levels and in both levels of *p*-cresol concentrations. The highest *p*-cresol reduction rate occurred at pH 7 and lowest at pH 6. The $NO_2^-$ production rate, on the other hand, was highest at pH 8 and lowest at pH 6.

In terms of $NO_3^-$, the production rate at pH 7 was significantly higher than those at pH 6 and 8 at low initial $NH_4^+$ concentration, but no significant difference was observed between pH 6 and 8. At high initial $NH_4^+$ concentration, there were no significant differences in $NO_3^-$ production rate at all pH levels.

The resulting trends for microbial growth rate were consistent with that of the biomass yield on *p*-cresol as shown in Table 4.1, where the maximum values were obtained at pH 8 for

low substrate concentrations and no significant differences were observed at high substrate concentrations. This implies that the observed growth rate was caused only by the growth of the heterotrophs present in the inoculum that were degrading *p*-cresol. Moreover, the nitrifiers, which are mostly autotrophs, generally grow slower (Daims and Wagner 2010). As can be seen in Figures 4.3 to 4.5, ammonium oxidation proceeded slower compared with that of *p*-cresol since nitrification is generally slower than carbon removal (Padin 2009). Furthermore, as shown in Figures 4.4 and 4.5, the microbial growth was more consistent with the degradation of *p*-cresol rather than with ammonia, which remained almost constant and low (Figure 4.3). It can be observed that when almost all of the *p*-cresol was consumed, the growth started to decline. This again indicates that the observed growth rate was due only to the growth of the heterotrophs utilizing *p*-cresol.

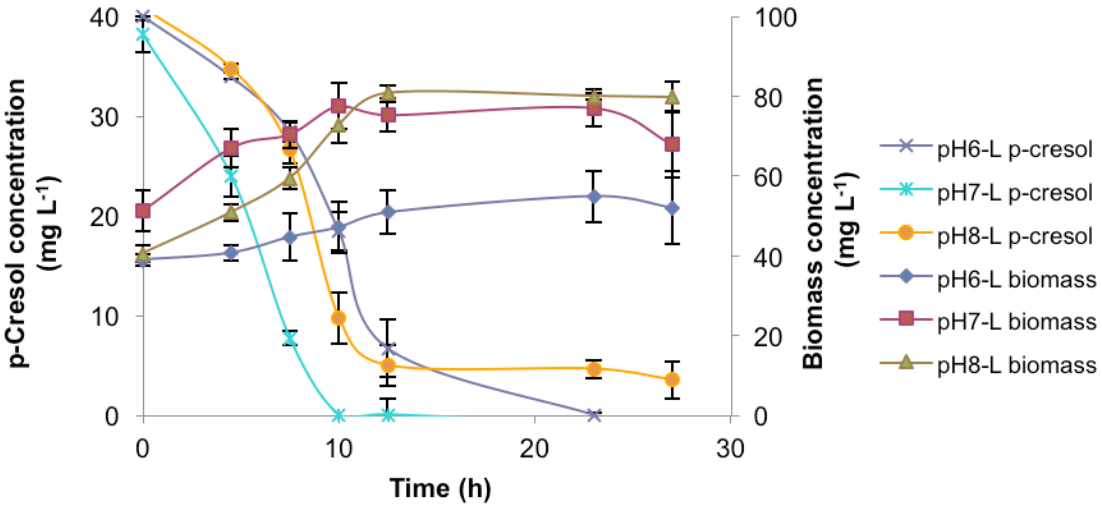


**Figure 4.4 Mean concentrations of *p*-cresol and biomass over time at different pH values with low [L] initial *p*-cresol concentration of 40 mg $L^{-1}$.**

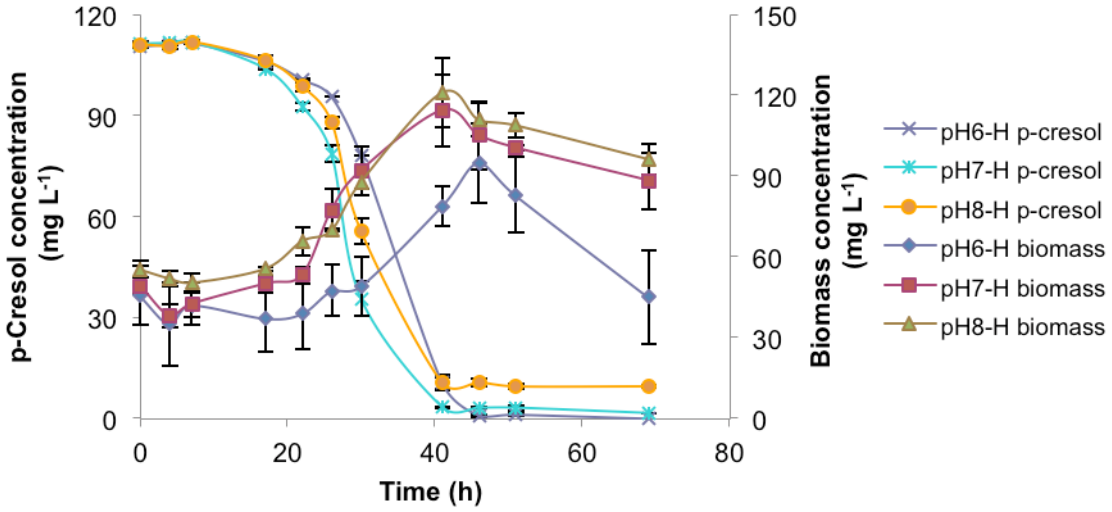


**Figure 4.5 Mean concentrations of *p*-cresol and biomass over time at different pH values with high [H] initial *p*-cresol concentration of 100 mg $L^{-1}$.**

The results show that the uptake rate and reduction rate of *p*-cresol were higher at pH 7 than at pH 6 or 8, for both low and high concentrations. As can be seen in Figures 4.4 and 4.5, the degradation of *p*-cresol occurred soonest at pH 7 than at the other pH levels, particularly for low initial concentrations. Comparing pH 6 and 8, the reduction rate was relatively faster at pH 8 than at pH 6; however, towards the end of the reaction the concentration at pH 8 never went lower than that at pH 6. This was contrary to the observation of Singh et al. (2008) which found the *p*-cresol biodegradation by *Gliomastix indicus* MTCC 3869 to be faster at pH 6 than at other pH values.

As mentioned earlier, due to very low ammonium reductions obtained, the ammonium uptake rate and biomass yield on ammonium were not calculated and the effect of pH was evaluated based only on the production of $NO_2^-$ and $NO_3^-$. As shown in Table 4.1, the $NO_3^-$ production was relatively higher at pH 7 than at the other pH values, particularly for low $NH_4^+$ concentration. The reported optimum pH for nitrification is between 7.5 and 8 (Ward 1987; Wahman et al. 2006). In this study, though there was a relatively better degradation of $NH_4^+$

(Figure 4.3) and a higher $NO_2^-$ production rate at pH 8, there was a relatively low conversion of $NO_2^-$ to $NO_3^-$ at this pH (Figure 4.6; Table 4.1).

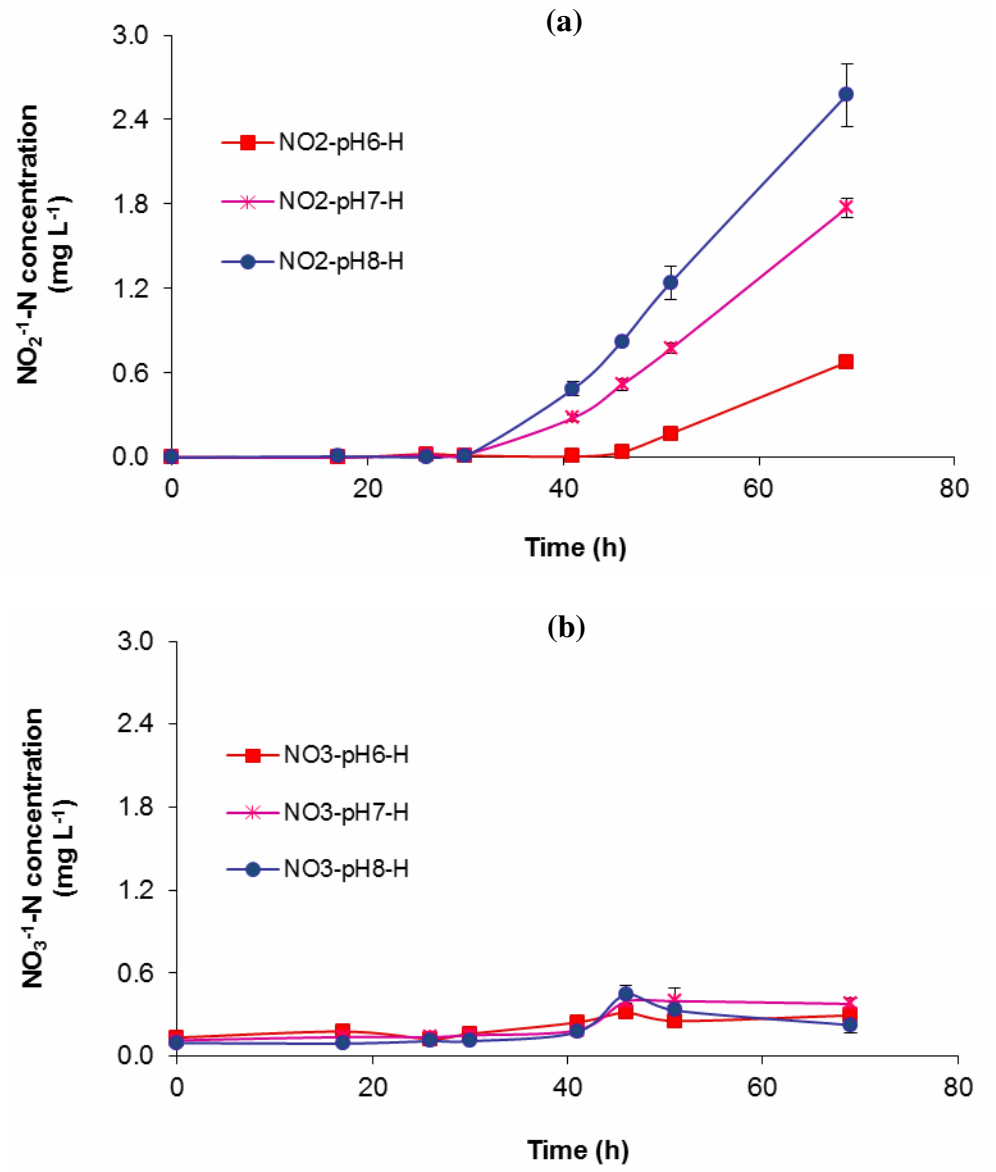


**Figure 4.6 Mean (a) nitrite; (b) nitrate productions over time with high [H] initial $NH_4^+$-N concentration of 500 mg $L^{-1}$.**

Based on the uptake and reduction rates of *p*-cresol and the $NO_3^-$ production rate, the best pH for the degradation of *p*-cresol and ammonia is 7. Thus, the succeeding kinetic studies were conducted at pH 7. Moreover, it would be more cost-effective to maintain the pH at around 7 when the treatment will be adopted in real barn systems.

### 4.6.2. Effect of pH on microbial growth

The 16S rRNA gene sequence analysis conducted on the samples at the start of the experiment showed that the most dominant species in the inoculum were *Arthrobacter sp., Microbacterium sp., and Rhodanobacter sp*. This group of microorganisms was quite different from what was initially found in the inoculum before it was frozen, except for *Rhodanobacter sp.* Keeping the inoculum at -80$^{o}$C for almost a year might have affected the population and diversity of the microorganisms in the inoculum.

*Arthrobacter* are heterotrophic nitrifiers, which perform better under an acidic environment (Mohseni 2005). *Microbacterium* are also heterotrophic bacteria (Maier et al. 2009), while most of the bacteria from the genus *Rhodanobacter* are known to be denitrifiers (Green et al. 2010).

The effects of pH and concentrations of *p*-cresol and $NH_4^+$ on the microbial diversity are shown in Figures 4.7 and 4.8. From the PCR-DGGE analysis conducted on the samples collected at different elapsed time, the population of *Arthrobacter sp.* increased in all pH and concentration levels. *Microbacterium sp.* was not affected by the pH and concentration, while *Rhodanobacter sp.* decreased in all pH levels and a higher decrease was observed at higher concentrations of substrates. This implies that *Arthrobacter sp.* was the main microorganism for the degradation of *p*-cresol and ammonia in the samples. Being heterotrophic nitrifiers, bacteria

from the genus *Arthrobacter* have been used in several studies (Karigar et al. 2006; Ionata et al. 2005; Chung et al. 1997) for the treatment of organic compounds and ammonia.

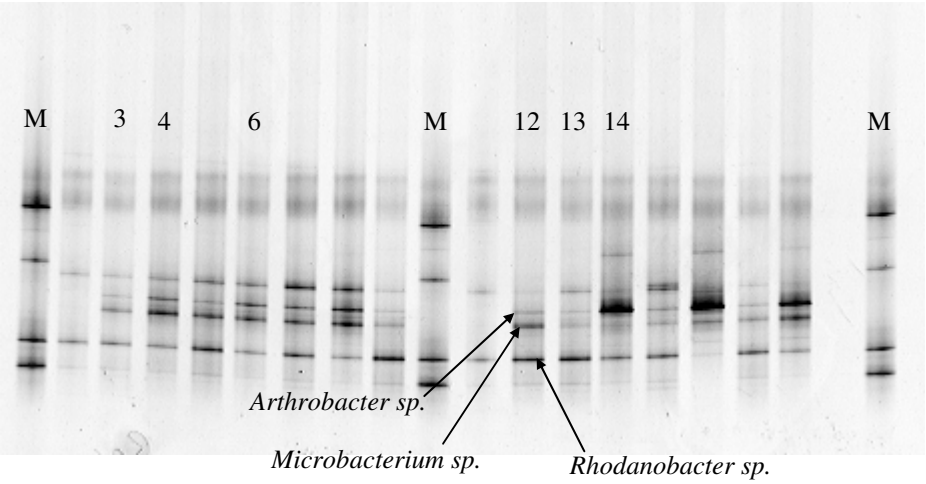


**Figure 4.7 PCR-DGGE results showing the effects of pH at high concentrations (100 mg $L^{-1}$ *p*-cresol; 500 mg $L^{-1}$ $NH_4^+$-N): (M) Marker; (3) No contaminant, pH 6, 22 h; (4) pH 6, 22 h; (6) pH 7, 22 h; (12) pH 6, 41 h; (13) No contaminant, pH 7, 41 h; (14) pH 7, 41 h.**

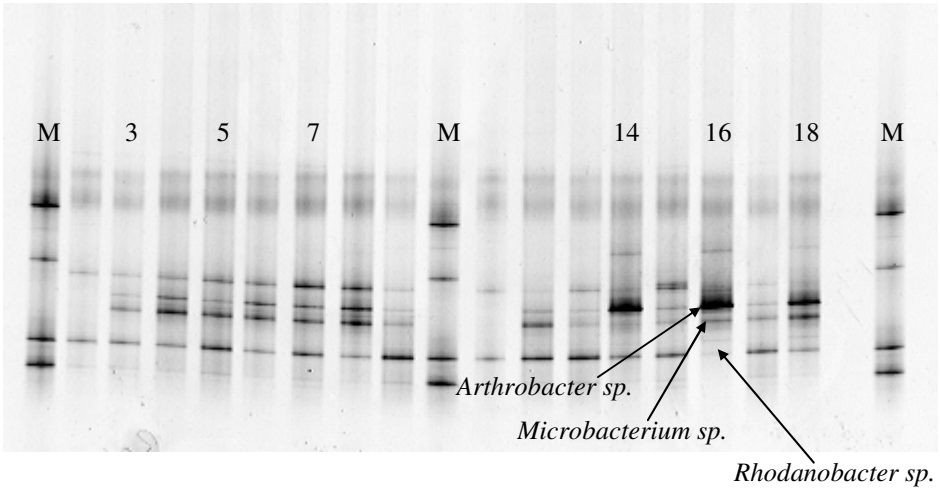


**Figure 4.8 PCR-DGGE results showing the effects of pH at low concentrations (40 mg $L^{-1}$ *p*-cresol; 60 mg $L^{-1}$ $NH_4^+$-N): (M) Marker; (2) No contaminant, pH 6, 22 h; (3) pH 6, 22 h; (5) pH 7, 22 h; (7) pH 8, 22 h; (14) pH 8, 27 h; (16) pH 6, 30 h; (18) pH 7, 30 h.**

The optimum pH observed by Wang et al. (2009) for a *Microbacterium sp.* utilized in the biodegradation of certain polycyclic aromatic hydrocarbons was in the range of 6 to 9. Considering their observation, it was possible that the pH values (pH of 6 to 8) evaluated in this study were also the optimum pH of the *Microbacterium sp.* in the inoculum; hence, there was no difference on the effects of pH on the growth of the *Microbacterium sp.* However, the "no growth" observed for *Microbacterium* in all pH values tested could be due to the relatively low carbon concentration in the samples.

Since most of the *Rhodanobacter* are denitrifiers, which depend on nitrate for their energy requirements, the low nitrate concentration in the samples could be the reason for the decrease in the population of *Rhodanobacter sp.* over time.

Although the pH might have affected the density of the microbial population, it was believed that it did not affect the microbial diversity.

### 4.6.3 Effect of *p*-cresol concentration on microbial growth

The results of the tests on the biodegradation of *p*-cresol at different initial concentrations (20 to 170 mg $L^{-1}$) are presented in Figure 4.9. As expected, biodegradation of higher initial *p*-cresol concentrations took longer time. *p*-Cresol concentrations of 10 and 40 mg $L^{-1}$ were completely degraded after 7 and 10 h, respectively, while initial concentration of 170 mg $L^{-1}$ had only 97% removed after 25 h. This result is comparable to the findings of Singh et al. (2008) and Gallego et al. (2008). Singh et al. (2008) obtained complete degradation of *p*-cresol by *Gliomastix indicus* in 11 h in a solution containing 100 mg $L^{-1}$ of *p*-cresol and 90% after 108 h in a 700 mg $L^{-1}$ solution, while Gallego et al. (2008) observed a 99.8% reduction of cresol mixture (100 mg $L^{-1}$ of each of *o*-, *m*-, and *p*-cresol) within 14 h by a strain of *Pseudomonas putida*.

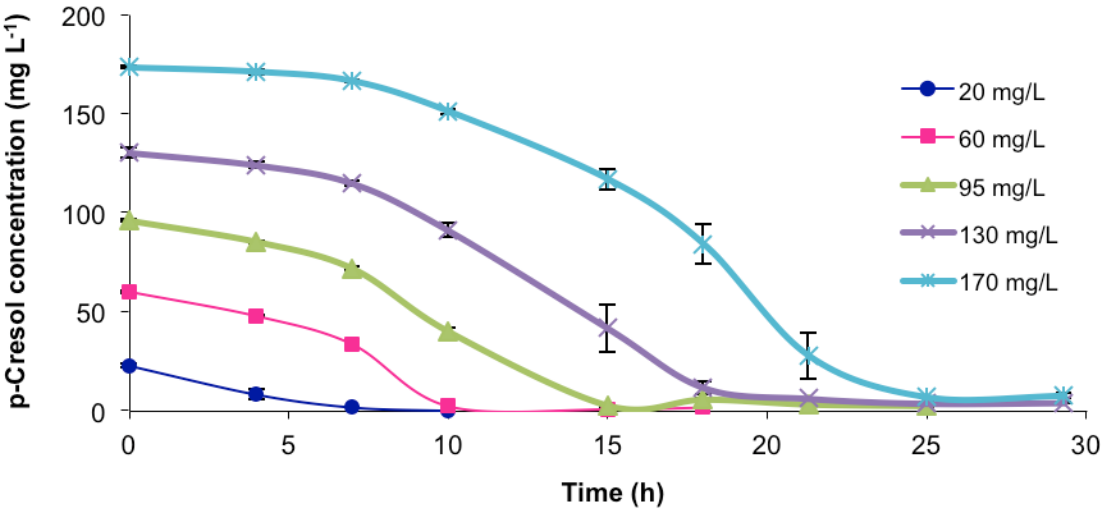


**Figure 4.9 Mean *p*-cresol concentrations over time at different initial *p*-cresol concentrations.**

After a region of exponential *p*-cresol reduction, a lower removal rate was observed towards the end of the *p*-cresol consumption curve (Figure 4.9). According to Kumar et al. (2005), a drop in pH or depletion of oxygen could be probable reasons for this reduction in removal rate, but it was not the case in this study since the measured pH values were around 6.8 and the dissolved oxygen were not less than 5 mg $L^{-1}$. Carbon or nutrient deficiencies could be the cause of the lower removal rate observed towards the end of the reaction.

As shown in Figure 4.10, the exponential growth of the microorganisms occurred when *p*-cresol was consumed, and where higher growth rates were observed at higher concentrations. When the estimated specific growth rates and the corresponding initial *p*-cresol concentrations were fitted to the Monod and Haldane equations, both resulted in an $R^2$ of 0.96 and similar values for the $\mu_m$ and $K_s$, which were 0.1 $h^{-1}$ and 103.4 mg $L^{-1}$, respectively. However, the extremely high value obtained for $K_i$ indicated that no inhibition had occurred at the studied concentrations since as mentioned earlier, a high value of $K_i$ was indicative of low inhibitory effect of the substrate. Based on equation 4.5, when the value of $K_i$ becomes relatively high

compared to substrate concentration, the Haldane equation would be reduced to Monod equation. Thus, in this study, the growth kinetics for the biodegradation of *p*-cresol was best described by the Monod model. Figure 4.11 shows the data fitted to the Monod equation.

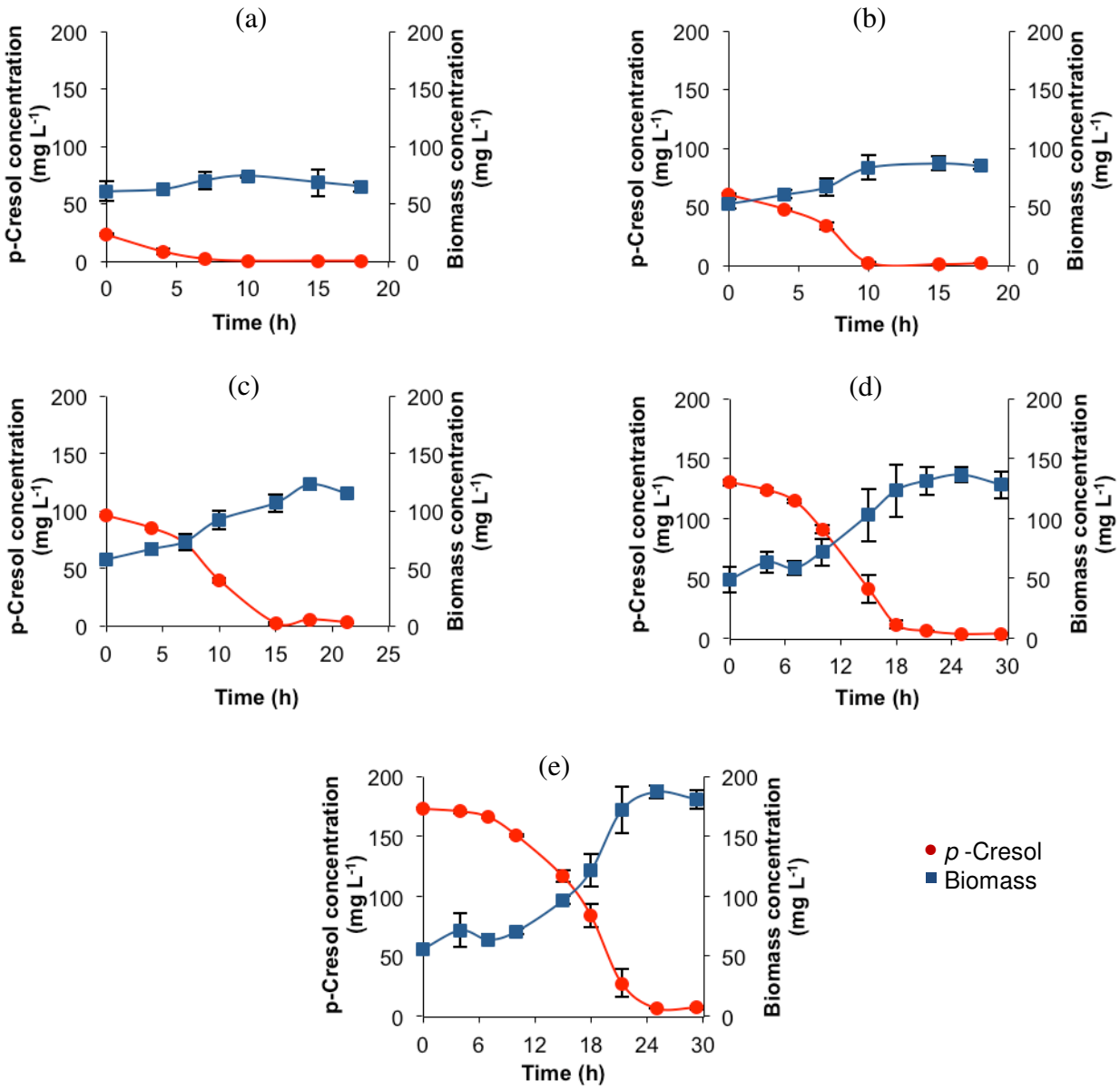


**Figure 4.10 Mean biomass and *p*-cresol concentrations at different initial *p*-cresol concentrations: (a) 20; (b) 60; (c) 95; (d) 130; and (e) 170 mg $L^{-1}$.**

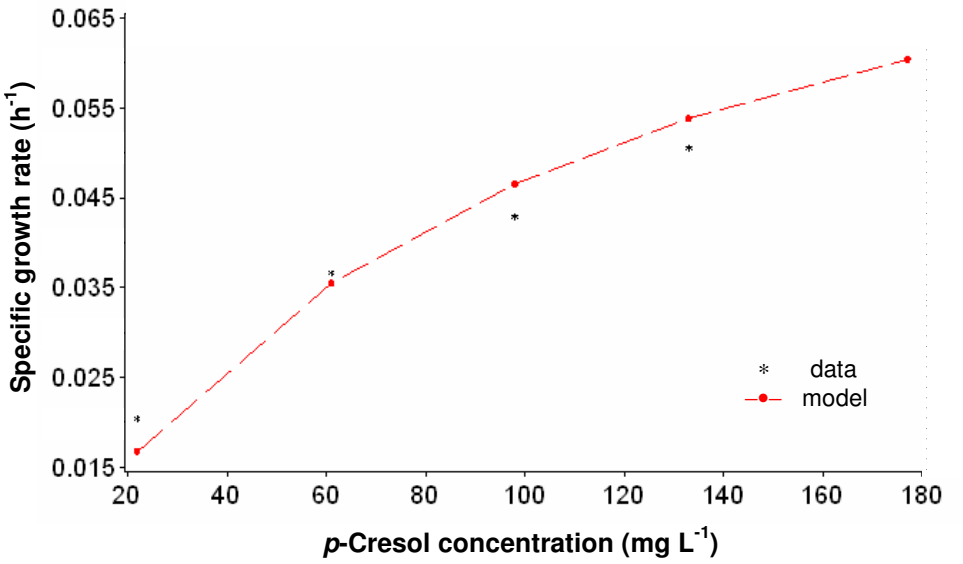


**Figure 4.11 Biodegradation data of *p*-cresol fitted to Monod equation.**

The results showed that *p*-cresol was not inhibitory to the microorganisms utilized in this study even up to a concentration of 170 mg $L^{-1}$. Texier and Gomez (2007) observed that *p*-cresol at an initial concentration of 150 mg $L^{-1}$ could be oxidized by a nitrifying culture in less than an hour. However, there are also several studies (Singh et al. 2008; Yadav et al. 2005) that showed the inhibitory characteristics of *p*-cresol. Singh et al. (2008) found that the inhibition effect of *p*-cresol to *Gliomastix indicus* became predominant above 50 mg $L^{-1}$.

Comparing the estimated kinetic parameters with those obtained by other studies for phenol and other phenol derivatives, including *p*-cresol, the estimated value for $\mu_m$ fell below the published range as presented in Table 4.2 probably because these studies were conducted at higher concentrations (up to 2000 mg $L^{-1}$). However, even if the microorganisms utilized in this study had a relatively lower specific growth rate compared with those used in other studies, their capacity to degrade *p*-cresol were comparable as discussed earlier. On the other hand, though the value of $K_s$ was relatively higher than those reported for *p*-cresol, it was within the published range of $K_s$ for other phenol derivatives. It should be noted that all these biokinetic parameters

are affected by the affinity of the microorganisms to the substrate and by the experimental conditions such as concentration, pH, and temperature, among others.

**Table 4.2 Growth kinetic parameter values for the biodegradation of phenol and other phenol derivatives.**

| Substance | $\mu_m$ ($h^{-1}$) | $K_s$ (mg $L^{-1}$) | $K_i$ (mg $L^{-1}$) | Kinetic model | Microorganisms | Reference |
|---|---|---|---|---|---|---|
| *p*-Cresol | 0.10 | 103.4 | - | Monod | Mixed culture | Present study |
| *p*-Cresol | 0.80 | 42.37 | 43.28 | Haldane | *Gliomastix indicus* | Singh et al. (2008) |
| *p*-Cresol | 1.32 | 17.0 | 542.0 | Haldane | *Pseudomonas sp.* | Yadav et al. (2005) |
| *o*-Cresol | - | 92.4 | 125.2 | Haldane | Mixed culture | Maeda et al. (2005) |
| *m*- Cresol | 2.78 | 866 | 4.42 | Haldane | *Candida tropicalis* | Yan et al. (2006) |
| Phenol | 0.44 | 29.5 | 72.5 | Haldane | Mixed culture | Marrot et al. (2006) |
| Phenol | 0.48 | 11.7 | 208.0 | Haldane | *Candida tropicalis* | Yan et al. (2006) |

In this study, the yield coefficient for *p*-cresol was estimated to be 0.56 milligram of dry biomass per milligram of *p*-cresol.

The results of the PCR-DGGE analysis (Figure 4.12) showed that the populations of some of the microbial strains in the mixed culture were affected by the concentrations of *p*-cresol, although the diversity almost remained constant. An increase in the population of *Arthrobacter sp.* was found, and higher increases were observed at higher *p*-cresol concentrations. The population of *Microbacterium sp.* relatively remained constant, while that of the *Rhodanobacter sp*. was found to decrease with time. These observations agreed with the trends observed from the tests on the effects of pH. The results further supported the hypothesis that *Arthrobacter sp.* was the main species responsible for the biodegradation of *p*-cresol.

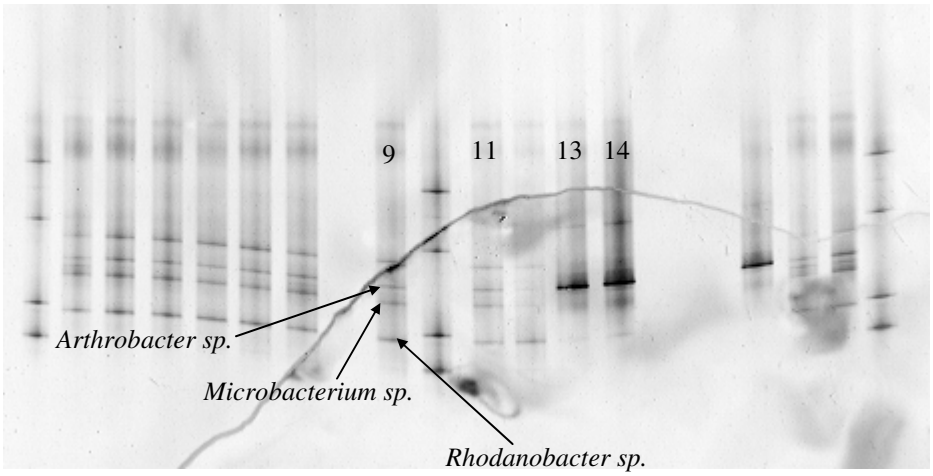


**Figure 4.12 PCR-DGGE results showing the effects of *p*-cresol concentration on microbial diversity and population: (9) 95 mg $L^{-1}$, 0 h; (11) 170 mg $L^{-1}$, 0 h; (13) 130 mg $L^{-1}$, 25 h; (14) 170 mg $L^{-1}$, 29 h.**

### 4.6.4 Effect of $NH_4^+$ concentration on microbial growth

The biodegradation of $NH_4^+$ at various initial concentrations (10 to 140 mg $L^{-1}$) is shown in Figure 4.13. More than 99% of $NH_4^+$ was degraded after 32 h for initial $NH_4^+$ concentrations of 10 and 30 mg $L^{-1}$ and more than 95% of $NH_4^+$ was degraded after 63 h for initial $NH_4^+$ concentrations of 60, 85, and 140 mg $L^{-1}$.

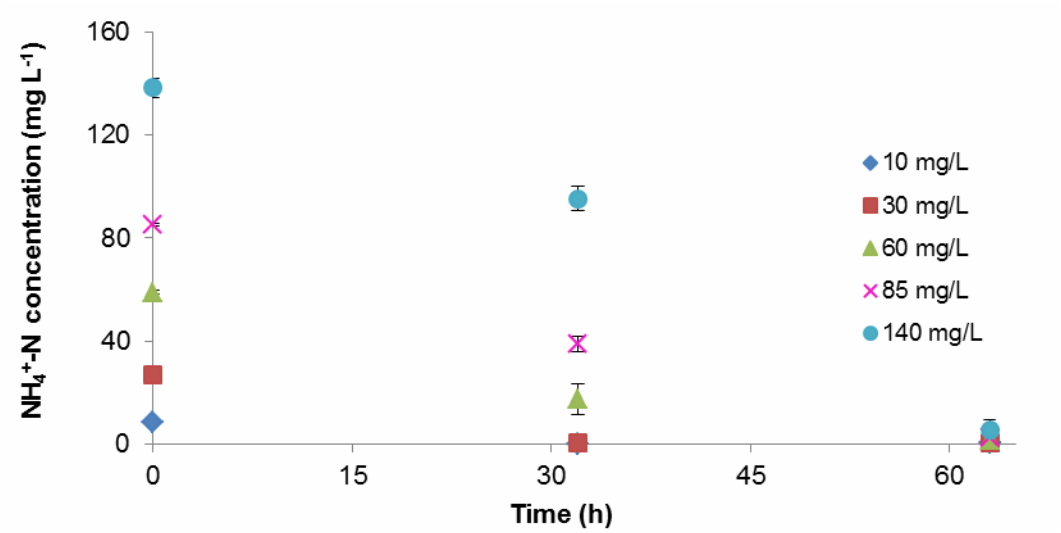


**Figure 4.13 Mean $NH_4^+$ concentrations over time at different initial $NH_4^+$ concentrations.**

Although the different initial $NH_4^+$ concentrations had an effect on the microbial growth as shown in Figure 4.14, the effect was only pronounced at the later part of the exponential phase. Similar growth rates have been observed at the beginning of the exponential phase despite the differences in the initial $NH_4^+$ concentrations. The results would mean that at the earlier stage of the microbial growth, the microorganisms were consuming very minimal amount of $NH_4^+$ and that the amounts of $NH_4^+$ available were even beyond their minimum requirements. Since the microorganisms were also provided with fixed and relatively high concentrations of carbon sources, they were not also carbon-limited, thus, no differences have been observed in their growth rates. However, as the microorganisms grew, their demand for nitrogen increased. Thus, those which still have available $NH_4^+$ continued to grow, while those with $NH_4^+$ already exhausted started to decline. Even if there were only few data collected at the later stage of the exponential growth, the results still show higher growth at higher concentrations, except at initial concentration of 140 mg $L^{-1}$. However, it cannot be concluded that the 140 mg $L^{-1}$ initial

concentration was already inhibitory to the microorganisms since it had similar initial growth rate with the other concentrations.

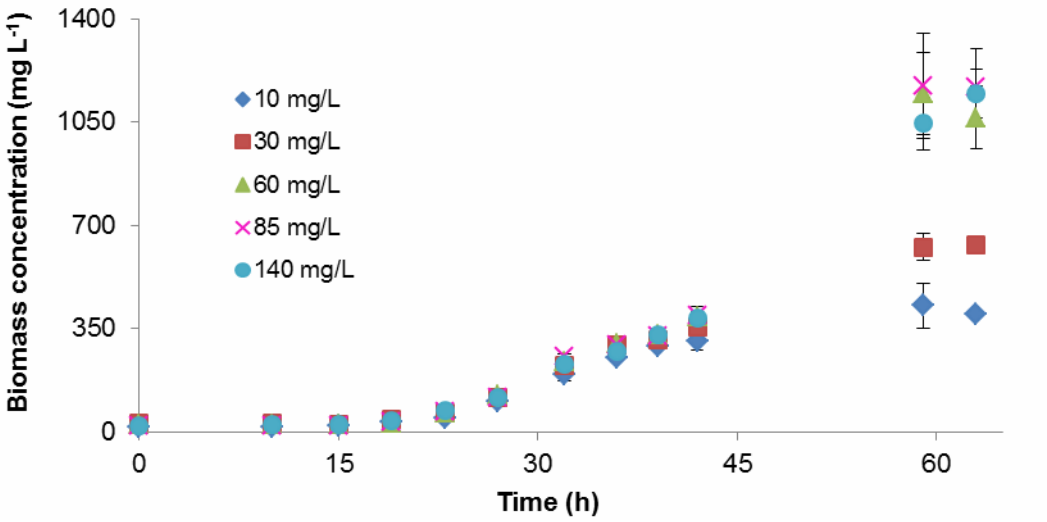


**Figure 4.14 Mean biomass concentrations over time at different initial $NH_4^+$ concentrations.**

The amounts of biomass produced in this trial where both glucose and *p*-cresol were used as carbon sources were relatively higher than those in the previous trials where only *p*-cresol was used. The growth rates obtained in this trial could have been affected by the presence of glucose, a substance which was not found in the bioreactors. Moreover, the results show that the microbial growth was primarily due to the consumption of carbon. It was observed, particularly at 10 and 30 mg $L^{-1}$ initial $NH_4^+$ concentrations, that even if $NH_4^+$ was totally consumed, growth continued for several hours before attaining a stationary phase. This implies that the biomass produced was primarily due to the incorporation of the carbon elements into the cell. This interpretation could be supported by the results of the PCR-DGGE analysis shown in Figure 4.15.

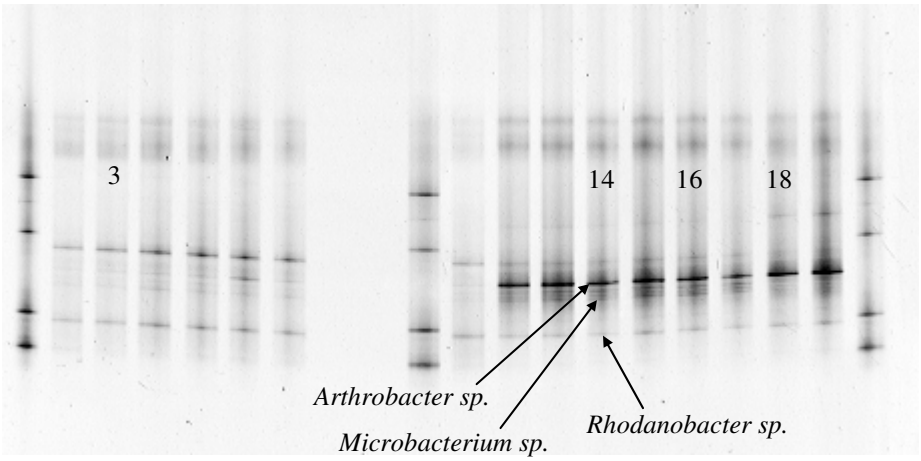


**Figure 4.15 PCR-DGGE results showing the effects of $NH_4^+$ concentration on microbial diversity and population: (3) 10 mg $L^{-1}$, 0 h; (14) 10 mg $L^{-1}$, 23 h; (16) 60 mg $L^{-1}$, 23 h; (18) 140 mg $L^{-1}$, 23 h.**

The populations of *Arthrobacter sp.* and *Microbacterium sp.* increased with time, with higher increases being observed for *Arthrobacter sp.* Due to sufficient amount of carbon compounds provided in this trial, the population of the *Microbacterium sp.* increased, unlike in the previous trials. The increases in population at the different concentration levels were not remarkably different for both species indicating that the biomass production was largely caused by the consumption of carbon compounds by these two heterotrophs. Due to insignificant amount of nitrite or nitrate produced, the *Rhodanobacter sp.* decreased with time. The maximum amount of nitrite obtained was only 0.02 mg $L^{-1}$ while that of nitrate was 0.08 mg $L^{-1}$. Similar to the other previous observations, the microbial diversity almost remained constant from the different experimental trials.

When the estimated values of $\mu$ and the corresponding initial $NH_4^+$-N concentrations were fitted to the Monod and Haldane equations, the resulting $R^2$ values were 0.6 and 0.7, respectively. The estimated $\mu_m$ and $K_s$ values from the Monod equation were 0.14 $h^{-1}$ and 5.8 mg $L^{-1}$, respectively, while the $\mu_m$, $K_s$, and $K_i$ values obtained from the Haldane equation were 0.17

$h^{-1}$, 11.9 mg $L^{-1}$, and 618 mg $L^{-1}$, respectively. Figure 4.16 shows the data fitted to the Haldane model. The yield coefficient obtained on $NH_4^+$ was 0.5 mg biomass per mg of $NH_4^+$-N consumed. The values estimated in this study were 50 to 80% higher than those obtained by other studies (Table 4.3). It was suspected that due to the utilization of glucose as a carbon source, the kinetic parameters obtained in this study mainly described the growth of heterotrophic microorganisms degrading organic carbon, and thus, cannot be used for the nitrifying bacteria. However, they could be used as a starting point for the modelling study where the real values will be determined by fitting the model to the experimental data.

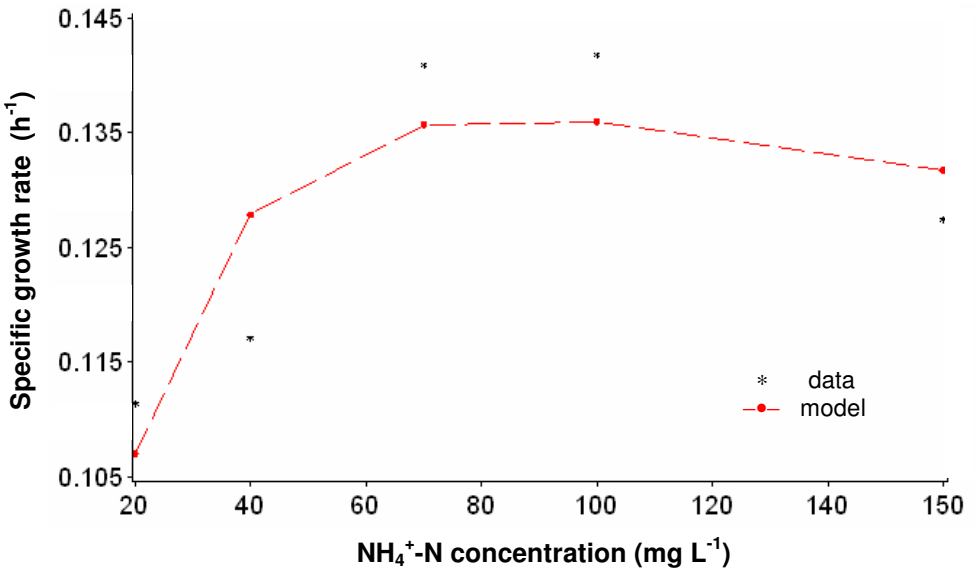


**Figure 4.16 Biodegradation data of ammonia fitted to Haldane equation.**

**Table 4.3 Growth kinetic parameter values for the biodegradation of ammonia.**

| $\mu_m$ ($h^{-1}$) | $K_s$ (mg $L^{-1}$) | $K_i$ (mg $L^{-1}$) | Kinetic model | Microorganisms | Reference |
|---|---|---|---|---|---|
| 0.17 | 11.9 | 618 | Haldane | Mixed culture | Present study |
| 0.03 | 4.8 | 116[a] | Haldane | Nitrifying mixed culture | Baquerizo et al. (2005) |
| - | 5.2 | 340 | Haldane | Nitrifying mixed culture | Sanchez et al. (2005) |
| 0.03 | 2.1 | - | Monod | *Nitrosomonas europaea* | Keen and Prosser (1987) |
| 0.04 | 1.8 | - | Monod | *Nitrobacter sp.* | Keen and Prosser (1987) |
| - | 13.0 | 384 | Haldane | Mixed culture | Carrera et al. (2004) |

[a]Inhibition for free ammonia.

## 4.7 SUMMARY AND CONCLUSIONS

Kinetic studies were conducted to determine the optimum pH, as well as the kinetic parameters, for the biodegradation of *p*-cresol and ammonia. The uptake and reduction rates of *p*-cresol and $NO_3^-$ production rate were highest at pH 7. Thus, the biodegradation study of *p*-cresol and ammonia at various concentrations were carried out at pH 7. The kinetics of the biodegradation of *p*-cresol with initial concentrations up to 170 mg $L^{-1}$ was best described by the Monod equation, indicating that *p*-cresol, at the concentration range tested, was not inhibitory to the growth of the microorganisms utilized in this study. The values for $\mu_m$ and $K_s$ obtained were 0.1 $h^{-1}$ and 103.4 mg $L^{-1}$, respectively. The biodegradation of ammonia was better described by the Haldane equation with values of 0.17 $h^{-1}$, 11.9 mg $L^{-1}$, and 618 mg $L^{-1}$ for $\mu_m$, $K_s$, and $K_i$, respectively. These values are 50 to 80% higher than those reported in the literature. The utilization of glucose as one of the carbon sources was suspected to affect the results for this could favour growth of heterotrophs. However, the results obtained from this study could be used as a starting point for a modelling study. Among the microbial species found in the inoculum, the *Arthrobacter sp.*, a heterotrophic nitrifier, has been found to be the most important in the biodegradation of *p*-cresol and ammonia.

## 4.8 REFERENCES


Alonso, C., X. Zhu and M.T. Suidan. 2000. Parameter estimation in biofilter systems. *Environmental Science and Technology* 34 (11): 2318-2323.

Armeen, A., J.J.R. Feddes, J.J. Leonard and R.N. Coleman. 2008. Biofilters to treat swine facility air: Part 1. Nitrogen mass balance. *Canadian Biosystems Engineering* 50: 6.21-6.27.

Bae, B.H., R.L. Autenrieth and J.S. Bonner. 1995. Kinetics of multiple phenolic compounds degradation with a mixed culture in a continuous-flow reactor. *Water Environment Federation* 67(2): 215-223.

Baquerizo, G., J.P. Maestre, T. Sakuma, M.A. Deshusses, X. Gamisans, D. Gabriel and J. Lafuente. 2005. A detailed model of a biofilter for ammonia removal: Model parameters analysis and model validation. *Chemical Engineering Journal* 113: 205-214.

Blanes-Vidal, V., M.N. Hansen, A.P.S. Adamsen, A. Feilberg, S.O. Petersen and B.B. Jensen. 2009. Characterization of odor released during handling of swine slurry: Part 1. Relationship between odorants and perceived odor concentrations. *Atmospheric Environment* 43: 2997-3005.

Carrera, J., I. Jubany, L. Carvallo, R. Chamy and J. Lafuente. 2004. Kinetic models for nitrification inhibition by ammonium and nitrite in a suspended and an immobilised biomass systems. *Process Biochemistry* 39: 1159-1165.

CCOHS (Canadian Centre for Occupational Health and Safety). 1998. Health Effects of Ammonia Gas. http://www.ccohs.ca/oshanswers/chemicals/chem_profiles/ammonia/health_ammonia.html (2012/02/07).

Chung, Y.C., C. Huang and C.P. Tseng. 1997. Biotreatment of ammonia from air by an immobilized *Arthrobacter oxydans* CH8 biofilter. *Biotechnology Progress* 13: 794-798.

Daims, H. and M. Wagner. 2010. The microbiology of nitrogen removal. In *Microbial Ecology of Activated Sludge*, ed. R. Seviour and P.H. Neilsen, 259-280. London, UK: IWA Publishing.

Delhoménie, M.C., J. Nikiema, L. Bibeau and M. Heitz. 2008. A new method to determine the microbial kinetic parameters in biological air filters. *Chemical Engineering Science* 63(16): 4126-4134.

Doelle, H.W. 1994. *Microbial Process Development*. Singapore: World Scientific Publishing Co. Pte. Ltd.

DSMZ. 2007. DSM Medium 951. http://www.dsmz.de/microorganisms/medium/pdf/ DSMZ_ Medium951.pdf (2012/02/07).

Gallego, A., V.L. Gemini, M.S. Fortunato, P. Dabas, S.L. Rossi, C.E. Gomez, C. Vescina, E.I. Planes and S.E. Korol. 2008. Degradation and detoxification of cresols in synthetic and industrial wastewater by an indigenous strain of *Pseudomonas putida* in aerobic reactors. *Environmental Toxicology* 23: 664-671.

Gomori, G. 1955. Preparation of buffers for use in enzyme studies. In *Methods in Enzymology*, vol. 1, ed. S.P. Colowick and N.O. Kaplan, 138-146. New York, USA: Academic Press.

Green, S.J., O. Prakash, T.M. Gihring, D.M. Akob, P. Jasrotia, P.M. Jardine, D.B. Watson, S.D. Brown, A.V. Palumbo and J.E. Kostka. 2010. Denitrifying bacteria isolated from terrestrial subsurface sediments exposed to mixed-waste contamination. *Applied and Environmental Microbiology* 76(10): 3244-3254.

Iliuta, I. and F. Larachi. 2004. Transient biofilter aerodynamics and clogging for VOC degradation. *Chemical Engineering Science* 59(16): 3293-3302.

Ionata, E., P. De Blasio and F. La Cara. 2005. Microbiological degradation of pentane by immobilized cells of *Arthrobacter* sp. *Biodegradation* 16: 1-9.

Jácome, A., J. Molina, J. Suárez and I. Tejero. 2006. Simultaneous removal of organic matter and nitrogen compounds in autoaerated biofilms. *Journal of Environmental Engineering* 132(10): 1255-1263.

Jorio, H., R. Brzezinski and M. Heitz. 2005. A novel procedure for the measurement of the kinetics of styrene biodegradation in a biofilter. *Journal of Chemical Technology and Biotechnology* 80: 796-804.

Karigar, C., A. Mahesh, M. Nagenahalli and D.J. Yun. 2006. Phenol degradation by immobilized cells of *Arthrobacter citreus*. *Biodegradation* 17: 47-55.

Keen G.A. and J.I. Prosser. 1987. Steady state and transient growth of autotrophic nitrifying bacteria. *Archives of Microbiology* 147: 73-79.

Kermanshahi Pour, A., D. Karamanev and A. Margaritis. 2006. Kinetic modeling of the biodegradation of the aqueous *p*-xylene in the immobilized soil bioreactor. *Biochemical Engineering Journal* 27: 204-211.

Kovarova, K., A. Kach, A.J.B. Zehnder and T. Egli. 1997. Cultivation of *Escherichia coli* with mixtures of 3-phenylpropionic acid and glucose: Steady-state growth kinetics. *Applied and Environmental Microbiology* 63(7): 2619-2624.

Kumar A., S. Kumar and S. Kumar. 2005. Biodegradation kinetics of phenol and cathechol using *Pseudomonas putida* MTCC 1194. *Biochemical Engineering Journal* 22: 151-159.

Maeda, M., A. Itoh and Y. Kawase. 2005. Kinetics for aerobic biological treatment of *o*-cresol containing wastewaters in a slurry bioreactor: biodegradation by utilizing waste activated sludge. *Biochemical Engineering Journal* 22: 97-103.

Maier, R.M., I.L. Pepper and C.P. Gerba. 2009. *Environmental Microbiology*, 2nd edition. USA: Academic Press.

Marrot, B., A. Barrios-Martinez, P. Moulin and N. Roche. 2006. Biodegradation of high phenol concentration by activated sludge in an immersed membrane bioreactor. *Biochemical Engineering Journal* 30: 174-183.

Melse, R.W. and G. Mol. 2004. Odour and ammonia removal from pig house exhaust air using a biotrickling filter. *Water Science and Technology* 50(4): 275-282.

Mohseni, M. 2005. Biological treatment of waste gases containing inorganic compounds. In *Biotechnology for Odor and Air Pollution Control*, ed. Z. Shareefdeen and A. Singh, 253-280. Germany: Springer-Verlag.

Mulchandani, A. and J.H.T. Luong. 1989. Microbial inhibition kinetics revisited. *Enzyme and Microbial Technology* 11: 66-73.

Muyzer, G., E.C. de Waal and A.G. Uitterlinden. 1993. Profiling of complex microbial populations by denaturing gradient gel electrophoresis analysis of polymerase chain reaction-amplified genes coding for 16S rRNA. *Applied and Environmental Microbiology* 59: 695-700.

Ntwampe, S.K.O. and M.S. Sheldon. 2006. Quantifying growth kinetics of *Phanerochaete chrysosporium* immobilised on a vertically orientated polysulphone capillary membrane: Biofilm development and substrate consumption. *Biochemical Engineering Journal* 30: 147-151.

Okpokwasili, G.C. and C.O. Nweke. 2005. Microbial growth and substrate utilization kinetics. *African Journal of Biotechnology* 5(4): 305-317.

Padin, J.R.V. 2009. Autotrophic nitrogen removal in granular sequencing batch reactors. Published Ph.D. dissertation. Spain: Departamento de Ingeniería Química, Universidade de Santiago de Compostela.

Park, O.H. and I.G. Jung. 2006. A model study based on experiments on toluene removal under

high load conditions in biofilters. *Biochemical Engineering Journal* 28(3): 269-274.

Park, S. and W. Bae. 2009. Modeling kinetics of ammonium oxidation and nitrite oxidation under simultaneous inhibition by free ammonia and free nitrous acid. *Process Biochemistry* 44(6): 631-640.

Raghuvanshi, S. and B.V. Babu. 2010. Biodegradation kinetics of methyl iso-butyl ketone by acclimated mixed culture. *Biodegradation* 21: 31-42.

Reardon, K.F., D.C. Mosteller, J.B. Rogers, N.M. DuTeau and K.H. Kim. 2002. Biodegradation kinetics of aromatic hydrocarbon mixtures by pure and mixed bacterial cultures. *Environmental Health Perspectives* 110(6): 1005-1011.

Rittmann, B.E. and P.L. McCarty. 2001. *Environmental Biotechnology: Principles and Applications*. USA: McGraw-Hill.

Sanchez, O., E. Aspe, M.C. Marti and M. Roeckel. 2005. Rate of ammonia oxidation in a synthetic saline wastewater by a nitrifying mixed-culture. *Journal of Chemical Technology and Biotechnology* 80: 1261-1267.

Sander, R. 2011. Henry's Law Constants. In *NIST Chemistry WebBook, NIST Standard Reference Database Number 69,* ed. P.J. Linstrom and W.G. Mallard. USA: National Institute of Standards and Technology. http://webbook.nist.gov (2013/01/15).

SAS. 2008. SAS Institute Inc., North Carolina, USA.

Schiffman, S.S., J.L. Bennett and J.H. Raymer. 2001. Quantification of odors and odorants from swine operations in North Carolina. *Agricultural and Forest Meteorology* 108: 213-240.

Sheridan, B., T. Curran, V. Dodd and J. Colligan. 2002. Biofiltration of odour and ammonia from a pig unit – A pilot-scale study. *Biosystems Engineering* 82: 441-453.

Shuler, M.L. and F. Kargi. 1992. *Bioprocess Engineering: Basic concepts*. USA: PTR Prentice – Hall, Inc.

Singh, R.K., S. Kumar, S. Kumar and A. Kumar. 2008. Biodegradation kinetic studies for the removal of *p*-cresol from wastewater using *Gliomastix indicus* MTCC 3869. *Biochemical Engineering Journal* 40: 293-303.

Texier, A.C. and J. Gomez. 2007. Simultaneous nitrification and *p*-cresol oxidation in a nitrifying sequencing batch reactor. *Water Research* 41: 315-322.

Veiga, M.C., M. Fraga, L. Amor and C. Kennes. 1999. Biofilter performance and characterization of a biocatalyst degrading alkylbenzene gases. *Biodegradation* 10: 169-176.

Wahman, D.G., A.E. Henry, L.E. Katz and G.E. Speitel Jr. 2006. Cometabolism of trihalomethanes by mixed culture nitrifiers. *Water Research* 40: 3349-3358.

Wang, C., D. Li and C. Wang. 2009. Biodegradation of naphthalene, phenanthrene, anthracene and pyrene by *Microbacterium* sp. 3-28. *Chinese Journal of Applied & Environmental Biology* 15(3): 361-366.

Ward, B.B. 1987. Kinetic studies on ammonia and methane oxidation by *Nitrosococcus oceanus*. *Archives of Microbiology* 147: 126-133.

Yadav, K.K., L. Iyengar, N.K. Birkeland and G. Ramanathan. 2005. Transient accumulation of metabolic intermediates of *p*-cresol in the culture medium by a *Pseudomonas* sp. strain A isolated from a sewage treatment plant. *World Journal of Microbiology & Biotechnology* 21: 1529-1534.

Yan, J., W. Jianping, B. Jing, W. Daoquan and H. Zongding. 2006. Phenol biodegradation by the yeast *Candida tropicalis* in the presence of *m*-cresol. *Biochemical Engineering Journal* 29: 227-234.

Zahn, J.A., J.L. Hatfield, Y.S. Do, A.A. DiSpirito, D.A. Laird and R.L. Pfeiffer. 1997. Characterization of volatile organic emissions and wastes from a swine production facility. *Journal of Environmental Quality* 26(6): 1687-1696.

# Chapter 5
# Steady-state Model for Ammonia Removal from Swine Facility Air with a Cross-flow Biotrickling Filter

## 5.1 VERSIONS PRESENTED IN A CONFERENCE

Similar versions of this chapter were presented at the joint conference of the Northeast Agricultural and Biological Engineering Conference (NABEC) and Canadian Society for Bioengineering (CSBE) in July 2012 in Orilla, Ontario, Canada.

- Martel, M., S.P. Lemay, B. Predicala, M. Girard, R. Hogue, M. Belzile, J. Feddes and S. Godbout. 2012. Steady-state model for ammonia removal from swine facility air with a cross-flow biotrickling filter: model development and sensitivity analysis. Paper No. CSBE12-127. Presented at the NABEC-CSBE Joint Meeting and Technical Conference. Orillia, Ontario, Canda. July 15-18, 2012.
- Martel, M., S.P. Lemay, B. Predicala, M. Girard, R. Hogue, M. Belzile, J. Feddes and S. Godbout. 2012. Steady-state model for ammonia removal from swine facility air with a cross-flow biotrickling filter: calibration and validation. Paper No. CSBE12-126. Presented at the NABEC-CSBE Joint Meeting and Technical Conference. Orillia, Ontario, Canada. July 15-18, 2012.

## 5.2 CONTRIBUTION OF THE PH.D. CANDIDATE

A mathematical model for a biotrickling filter used in treating swine exhaust air was developed, calibrated, and validated in this study. This is of paramount importance since based on literature review, no model has yet been developed for biotrickling filters used in the

treatment of air exhausted from pig buildings. All the components of the modelling study and the manuscript writing were performed by the candidate while the collection of data for the model calibration and validation was mostly conducted by the research professionals and technicians of the Research and Development Institute for the Agri-Environment (IRDA). Valuable inputs on the modelling aspect and on the manuscript were provided by Dr. Stéphane P. Lemay and Dr. Bernardo Predicala and as well as by Dr. Matthieu Girard of IRDA.

## 5.3 CONTRIBUTION OF THIS PAPER TO THE OVERALL STUDY

This study is one of the most essential parts of the overall research. The main objective of the overall research was to obtain insights on how to optimize the performance of biotrickling filters for reducing odour emitted from swine facilities. This objective may be achieved by identifying governing processes and optimum design parameters of the treatment system. Though optimum process and design parameters could be identified and obtained by conducting experimental trials using actual biotrickling filters, this would be very costly. Thus, process simulation using a mathematical model that describes the phenomena occurring in biotrickling filters is a cost-effective solution.

Models also have certain limitations because, depending on how extensive they portray the complexities of the real systems, model results could significantly deviate from real values; however, if properly designed and calibrated, they can adequately predict process performance.

Although there are already a number of existing models for biofilters and biotrickling filters, none was developed for application in swine facility air treatment based on literature review. As stated by Sharvelle et al. (2008a), most models are developed specific to the particular applications under investigation; hence, applying these models to other biotrickling filter systems may not be often practical nor useful. In this study, a mathematical model was

developed to simulate the removal of ammonia from pig barn air in biotrickling filters. Simulation results using the developed model could then be utilized to identify the governing processes as well as the optimum operating conditions and design parameters of the system.

## 5.4 ABSTRACT

Biological methods have been found to be cost effective and efficient in treating high-flow, low-concentration waste gas streams containing biodegradable substances such as those emitted from swine production. Yet, despite their advantages, they are limited by some operational problems. The impact of these limitations can be reduced by using mathematical models, which serve not only to describe and predict process performance but also identify relevant parameters for better design and process optimization. Thus, in this study, a model describing important processes involved in the removal of ammonia from pig house exhaust air by a cross-flow biotrickling filter was developed. Mass balance equations in the gas, liquid, and biofilm phases of the treatment system were formulated to describe each of these processes. A one-at-a-time sensitivity analysis of the model showed that the gas diffusion coefficient, the wetted fraction of the surface area, the gas mass transfer coefficient, the gas and liquid flow rates, the empty bed residence time (or bed length), the total surface area, the nominal packing diameter, and the pH of the solution were the parameters that had significant influence on the removal of ammonia from the gas phase. The model was calibrated and validated using different sets of data collected from six pilot-scale biotrickling filters, which were used to treat the air exhausted from six bench-scale pig chambers. Good agreement between predicted and measured values for removal efficiency was obtained; based on the fractional bias (FB) results, the normalized model's prediction errors were within ±1 to 7%.

## 5.5 INTRODUCTION

Odour nuisance and emissions of toxic gases are major challenges in pig production (Clark et al. 2006). Several approaches have already been tested and applied to mitigate these problems. Melse et al. (2009) categorized these approaches into diet manipulation, housing system design, and end-of-pipe air treatment.

One of the end-of-pipe air treatment techniques which has gained interest recently for the treatment of air exhausted from swine facilities is biotrickling filtration. Though some studies have revealed that this technique can effectively reduce odour and gas emissions from pig buildings (Melse and Mol 2004; Jensen and Hansen 2006), this approach has not yet been efficiently integrated into barn systems (Ozis et al. 2005). Despite its advantages over other methods, it is still limited by some operational problems (Devinny et al. 1999) such as biomass accumulation, and product and substrate inhibitions, among others.

To optimize the performance of a reactor, it is important to better understand the processes and the factors affecting its performance. Model simulation has been recognized as a useful and cost-effective tool for accomplishing these tasks (Devinny et al. 1999).

Though a number of mathematical models have already been developed for biotrickling filters, most of them are unique to the application being studied (i.e. they were calibrated and validated for specific applications and operating conditions); thus, it is often not relevant to use these models for other biotrickling filter applications (Sharvelle et al. 2008a; Devinny and Ramesh 2005). For instance, the models developed by Kim and Deshusses (2003) and Mpanias and Baltzis (1998), which were developed for the removal of hydrogen sulfide and mono-chlorobenzene, respectively, cannot be directly applied for the removal of ammonia. Although the model by Sharvelle et al. (2008a) was developed for the removal of ammonia from the waste

gas produced from aerobic digestion of solid waste, the operating conditions by which the model was calibrated and validated were different from those that exist in swine operations.

The different available models also differ in terms of the processes and parameters (e.g. constant biofilm thickness, biomass accumulation, oxygen limitation, and fluid flow characteristics) that are considered or neglected from the model. However, despite these differences they all describe the basic processes: mass transfer of contaminant from the gas phase into the liquid phase and subsequent mass transfer from the liquid phase into the biofilm where microbial degradation takes place (Sharvelle et al. 2008a).

A sensitivity analysis can be performed on mathematical models to identify relevant system parameters. According to Sharvelle et al. (2008b), the most sensitive model parameters require thorough investigation, while those which have minor impact on process performance may not need further investigation.

There are several methods available for doing parametric sensitivity analysis. Sharvelle et al. (2008b) cited techniques such as analytical, screening, and sampling-based methods. Analytical methods need analytical solutions and are established based on Taylor-series expansion of the model's output. Screening methods include one-at-a-time and factorial design techniques. If only the main effects are needed to be determined, the one-at-a-time approach would be sufficient; however, if the interaction effects are desired, the factorial technique is more appropriate. Regionalized sensitivity analysis and multivariate analysis of variance are some of the examples of sampling-based approaches. Nielsen et al. (2007) and Baquerizo et al. (2005) used a sensitivity coefficient, which relates the change of the state variables (predicted variables) to the change of the parameter, to determine the significance of the model parameters.

Moreover, a model must be calibrated and validated before it can be used to provide meaningful results. Calibration is designed to adjust a set of model input parameters so that the

resulting agreement between model predictions and experimental data is maximized (Trucano et al. 2006). Validation, on the other hand, is intended to quantify the predictive capability of a model by comparing model results and experimental data (Trucano et al. 2006).

Statistical tests are often required in model calibration and validation. Martin et al. (2002) calibrated their model by minimizing the value of an objective function, an equation defined by the difference between the experimental and predicted data, as well as by minimizing the sum of the residuals. Sharvelle et al. (2008a) estimated the model parameters by minimizing the sum of squared error (SSE) between the measured and predicted data. The coefficient of determination ($R^2$) was used by Baquerizo et al. (2007) to compare the accuracy of the model fitting. Aside from calculating the $R^2$, Cortus (2006) also used normalized mean square error (NMSE) and fractional bias (FB) in evaluating model results during calibration and validation.

In this study, a mathematical model was developed to predict and simulate the performance of a biotrickling filter in removing ammonia from the air exhausted from pig buildings. This study also presents the calibration and validation of the model.

## 5.6 PROCESS MECHANISMS

The first step involved in the removal of contaminants in biotrickling filters is the transfer of the contaminants from the gas phase to the liquid phase. There are several theories on interphase mass transfer. These include film theory, boundary layer theory, penetration theory, and surface renewal theory (Werth 2005). Among these theories, the Whitman's two-film theory is one of the most widely accepted. The assumptions of the two-film theory are illustrated in Chapter 1 (Figure 1.6) and summarized as follows (Dutta 2007; Dunn 2003; Schnelle and Brown 2002):

1. Concentration differences are negligible in the bulk gas and liquid phases where the material is carried by convection currents;
2. At the vicinity of the gas-liquid interface, the convection currents cease and two fluid films (i.e. gas film and liquid film) are formed;
3. Both films offer resistance to mass transfer. The flow of fluid in each film is assumed to be stagnant, and the mass transfer is assumed to occur only by molecular diffusion. In a steady-state process, the fluxes between these two films are equal. This means that the mass flux of component *A* from the bulk gas phase to the interface ($J_{AG}$; g $m^{-2}$ $h^{-1}$) is equal to its mass flux from the interface to the bulk liquid phase ($J_{AL}$; g $m^{-2}$ $h^{-1}$) as described in equation 5.1:

$$J_{AG} = J_{AL} \tag{5.1}$$

Each of these fluxes can be best described by Fick's first law of diffusion, which states that the mass flux of any component is proportional to its concentration gradient. Thus, equation 5.1 can be expressed as:

$$D_{AG}\frac{C_{AGb} - C_{AGi}}{z_G} = D_{AL}\frac{C_{ALi} - C_{ALb}}{z_L} \tag{5.2}$$

where $D_{AG}$ and $D_{AL}$ = diffusion coefficients of component *A* in the gas and liquid phases, respectively ($m^2$ $h^{-1}$),

$C_{AGb}$ and $C_{ALb}$ = concentrations of component *A* in the bulk gas and liquid phases, respectively (g $m^{-3}$),

$C_{AGi}$ and $C_{ALi}$ = gas and liquid interfacial concentrations of component *A*, respectively (g $m^{-3}$),

$z_G$ and $z_L$ = thickness of gas and liquid films, respectively (m).

Equation 5.2 shows that the mass flux increases as the film thickness becomes smaller. In terms of the volumetric mass transfer coefficient, equation 5.2 can be expressed as:

$$k_{AG}a\left(C_{AGb} - C_{AGi}\right) = k_{AL}a\left(C_{ALi} - C_{ALb}\right) \tag{5.3}$$

where $k_{AG}$ and $k_{AL}$ = individual gas and liquid phase mass transfer coefficients of component *A*, respectively, (m $h^{-1}$),

a = mass transfer area ($m^2$).

However, since interfacial concentrations $C_{AGi}$ and $C_{ALi}$ are not directly measurable quantities, equation 5.3 can be expressed in a form given in equation 5.4, where mass transfer rate equations are defined based on overall coefficients of mass transfer ($K_G$ and $K_L$) and on equilibrium concentrations that correspond to the bulk concentrations:

$$K_{AG}a\left(C_{AGb} - C_{AG}^{*}\right) = K_{AL}a\left(C_{AL}^{*} - C_{ALb}\right) \tag{5.4}$$

where $C_{AG}^{*}$ = gas phase concentration that is in equilibrium with the bulk liquid phase concentration $C_{ALb}$ (g $m^{-3}$),

$C_{AL}^{*}$ = liquid phase concentration that is in equilibrium with the bulk gas phase concentration $C_{AGb}$ (g $m^{-3}$),

$K_{AG}$ and $K_{AL}$ = overall gas and liquid phase mass transfer coefficients of component *A*, respectively (m $h^{-1}$).

4. The interface offers no resistance to mass transfer. Further, interfacial concentrations are in equilibrium; thus, they can be related by Henry's law as described in equation 5.5:

$$k_H = \frac{C_{AGi}}{C_{ALi}} \tag{5.5}$$

where $k_H$ is Henry's law constant (dimensionless). Applying the same principle, $C_{AG}^{*}$ then can be expressed as:

$$C_{AG}^{*} = k_H C_{ALb} \tag{5.6}$$

When a gaseous component is absorbed in a liquid, it forms a solution. For the case of ammonia ($NH_3$), it is a gas that readily dissolves in water forming aqueous $NH_3$ (Eq. 5.7):

$$NH_{3(g)} + H_2O \leftrightarrow NH_{3(aq)} \tag{5.7}$$

In aqueous solution, $NH_3$ acts as a weak base for it deprotonates a small fraction of the water to form ammonium ($NH_4^+$) and hydroxide ($OH^-$) as described in equation 5.8. The production of hydroxide ions when ammonia is dissolved in water gives aqueous solutions of ammonia alkaline properties:

$$NH_{3(aq)} + H_2O_{(l)} \leftrightarrow NH_4^{+}{}_{(aq)} + OH^{-}{}_{(aq)} \tag{5.8}$$

In contrast, the $NH_4^+$ formed acts as a weak acid in aqueous solution because it dissociates into $H^+$ and $NH_3$ as presented in equation 5.9:

$$NH_4^{+}{}_{(aq)} \leftrightarrow NH_{3(aq)} + H^{+}{}_{(aq)} \tag{5.9}$$

As shown in equations 5.8 and 5.9, $NH_3$ and $NH_4^+$ will co-exist in equilibrium in solution. The base ionization constant for ammonia ($K_b$, mol $L^{-1}$) and the acid ionization constant for ammonium ($K_a$, mol $L^{-1}$) are given in equations 5.10 and 5.11, respectively, where $K_b$ is equal to $1.6 \times 10^{-5}$ and $K_a$ to $6.3 \times 10^{-10}$ at 25°C (Clugston and Flemming 2000):

$$K_b = \frac{\left[NH_4^+\right]\left[OH^-\right]}{\left[NH_3\right]} \tag{5.10}$$

$$K_a = \frac{\left[NH_3\right]\left[H^+\right]}{\left[NH_4^+\right]} \tag{5.11}$$

The values of $K_b$ and $K_a$ determine the strength of a weak base and a weak acid, respectively, where larger values of these constants are associated with stronger bases and acids (Cortus 2006). Since, $K_b$ and $K_a$ are constants with negative exponents, the base and acid strengths are

oftentimes expressed in $pK_b$ and $pK_a$ respectively, which are the corresponding negative logarithms of $K_b$ and $K_a$ (Bettelheim et al. 2010). These two sets of expressions are inversely related, e.g. stronger acids have higher $K_a$ values, but smaller $pK_a$ values.

Thus, the total ammonia in aqueous solution exists in two forms: ionized ($NH_4^+$), and un-ionized ($NH_3$), the latter being more toxic (Korner et al. 2001). The un-ionized $NH_3$ is more toxic because it is a neutral molecule, which makes it easier to diffuse across the biological membranes of the microorganisms (EPA 1998). In this paper, ammonia or $NH_3$ in solution refers to total ammonia, unless, otherwise stated as un-ionized. The relative proportion of the two forms largely depends on pH, where the formation of the un-ionized form is favoured at higher pH values. The proportion of the two forms is also dependent on temperature, where higher temperatures favour formation of un-ionized $NH_3$. Salinity also affects $NH_4^+$-$NH_3$ equilibrium, to a lesser degree, since the dissolved salts in solution could affect the equilibrium concentrations of $NH_4^+$ and $NH_3$ (Korner et al. 2001). Equation 5.12 shows how the $pK_a$ value for ammonium varies with temperature *T* (Zhang et al. 1994):

$$pK_a = 0.0897 + \left(\frac{2729.92}{T + 273}\right) \tag{5.12}$$

The fraction of the total $NH_3$ that is un-ionized ($f_{NH3}$, dimensionless), being both pH- and temperature- dependent, can be calculated using the equation (Eq. 5.13) developed by Zhang et al. (1994). Equation 5.13 was estimated using slurry and urine puddles, thus, it is suitable for applications to concentrated solutions such as the recirculating liquid in the biotrickling filter utilized in this study, whose conductivity measured as high as 15,000 μS $cm^{-1}$:

$$f_{NH3} = \frac{10^{pH}}{10^{pH} + 5\left(10^{pKa}\right)} \tag{5.13}$$

Once $NH_3$ is dissolved in the liquid, it is transported into the biofilm. Since the liquid flow at the liquid-biofilm interface is nearly laminar, the dominating mode of transport is molecular diffusion. Subsequently, the $NH_3$ in the biofilm is degraded by the microorganisms. Under aerobic condition, the $NH_4^+$ can be converted to nitrate through a process called nitrification, which proceeds in two steps as shown in equations 5.14 and 5.15 (Melse and Mol 2004): (1) oxidation of $NH_4^+$ to nitrite ($NO_2^-$) by ammonium oxidizing bacteria (e.g. *Nitrosomonas*); (2) subsequent oxidation of $NO_2^-$ to nitrate ($NO_3^-$) by nitrite oxidizing bacteria (e.g. *Nitrobacter*):

$$NH_4^+ + OH^- + 3/2O_2 \rightarrow NO_2^- + H^+ + 2H_2O \quad (5.14)$$

$$NO_2^- + H^+ + 2H_2O + 1/2O_2 \rightarrow NO_3^- + H^+ + 2H_2O \quad (5.15)$$

Since substrate utilization results to biomass growth, these two activities are interrelated to each other as described in equation 5.16 (Pavlostathis 2006):

$$-\frac{dS}{dt} = \frac{dX}{Ydt} = \frac{\mu X}{Y} \quad (5.16)$$

where S and X = substrate and biomass concentrations, respectively (g $m^{-3}$),

Y = biomass yield coefficient (g biomass produced $g^{-1}$ substrate consumed),

μ = microbial specific growth rate ($h^{-1}$),

t = time (h).

A number of growth kinetic models have been developed to describe the specific microbial growth rate as a function of the growth-limiting substrate concentration. The commonly used ones are the Monod and Haldane models given in equations 5.17 and 5.18, respectively. The Haldane equation is particularly useful when substrate is inhibitory to the growth of the microorganisms (Devinny et al. 1999):

$$\mu = \frac{\mu_m S}{K_s + S} \tag{5.17}$$

$$\mu = \frac{\mu_m S}{K_s + S + \left(S^2 / K_i\right)} \tag{5.18}$$

where $\mu_m$ = maximum specific growth rate ($h^{-1}$),

$K_s$ = saturation constant (g $m^{-3}$),

$K_i$ = inhibition constant (g $m^{-3}$).

## 5.7 MATERIALS AND METHODS

### 5.7.1 Pig chamber – biotrickling filter unit and operation

The data used in the calibration and validation of the model were obtained from the experimental trials with the six pilot-scale cross-flow biotrickling filters, which were used to treat the air exhausted from six independent bench-scale pig chambers. The biotrickling filters and the pig chambers were installed at the laboratory of the Research and Development Institute for the Agri-Environment (IRDA) in Deschambault, Quebec, Canada. Each chamber (1.14 m wide, 2.44 m long, and 2.44 m high), shown in Chapter 2 (Figure 2.1), housed 4 to 5 grower/finisher pigs with weights ranging from 30 to 80 kg. The pigs were distributed in a manner such that each chamber would have similar average starting weight. The feeders were refilled approximately every two days, and the pigs had free access to feed 24 h a day. The liquid manure was stored in a shallow pit underneath the fully-slatted chambers and was removed by a vacuum pump, on average, two times in every trial. Since the purpose of the chambers was only to produce swine air, it was assumed that their physical designs did not have significant impact on the quality of the results as all conditions other than the experimental treatments were held constant.

The ventilation system in each chamber was temperature controlled. As shown in Figure 5.1, the air from outside passed through a centralized heating/cooling system, which kept the air temperature at around 15°C, before it was distributed to the different chambers. Each chamber was equipped with its own heating system as well as a ventilation system composed of an air inlet and an exhaust fan mounted on the ceiling. Each chamber was also equipped with temperature and humidity sensors. The temperature in each chamber was controlled between 20 to 30°C (P-band of 10°C) in order to deliver a fixed air flow rate of 302.4 $m^3$ $h^{-1}$ to the treatment units. A fixed flow rate of air in the biotrickling filters was necessary to observe the effects of the operating parameters tested. To assure a constant air flow rate, booster fans (Model 415, Delhi Industries, Inc., Delhi, Ontario, Canada) were used to compensate for any pressure loss in the biotrickling filters. To control the flow rate, a 204-mm iris orifice damper (± 5% accuracy; Model 200; Continental Fan Manufacturer Inc., Buffalo, New York, USA) was used.

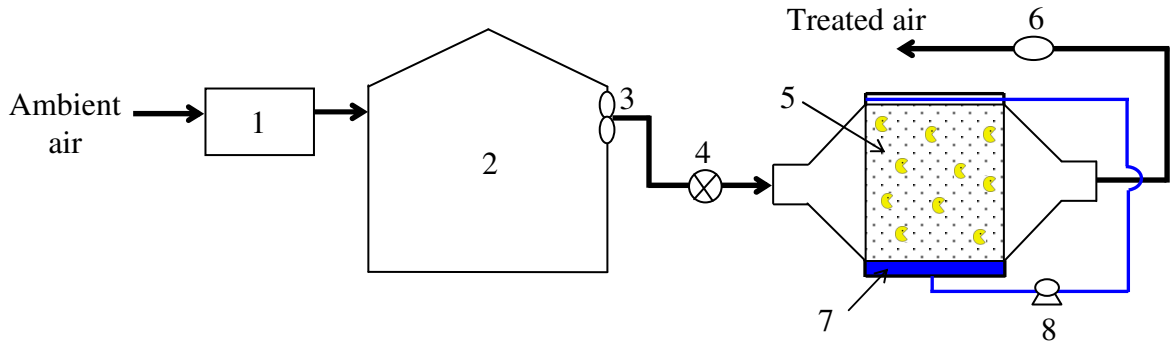


**Figure 5.1 Schematic diagram of the experimental set up.**
**(1) heating/cooling system; (2) pig chamber; (3) exhaust fan; (4) booster fan;**
**(5) packing media; (6) iris damper; (7) liquid sump; and (8) pump.**

The biotrickling filters were made of galvanized steel with internal dimensions of 1.1 m by 1.2 m by 1.1 m (Figure 5.2). Each treatment unit was equipped with liquid recirculation system holding a total liquid volume of 130 L. A liquid composed of a dilute nutrient solution

was continuously recirculated over the packing material to provide sufficient filter bed moisture. No amount of liquid was bled out from the units during the entire trial. Any liquid that was lost through evaporation was automatically replaced by tap water to keep the total volume constant. When necessary, a heater was employed to keep the liquid temperature above 17$^{o}$C. Before each trial, the whole unit was washed and the packing media was sterilized with sodium hypochlorite solution to avoid any contamination.

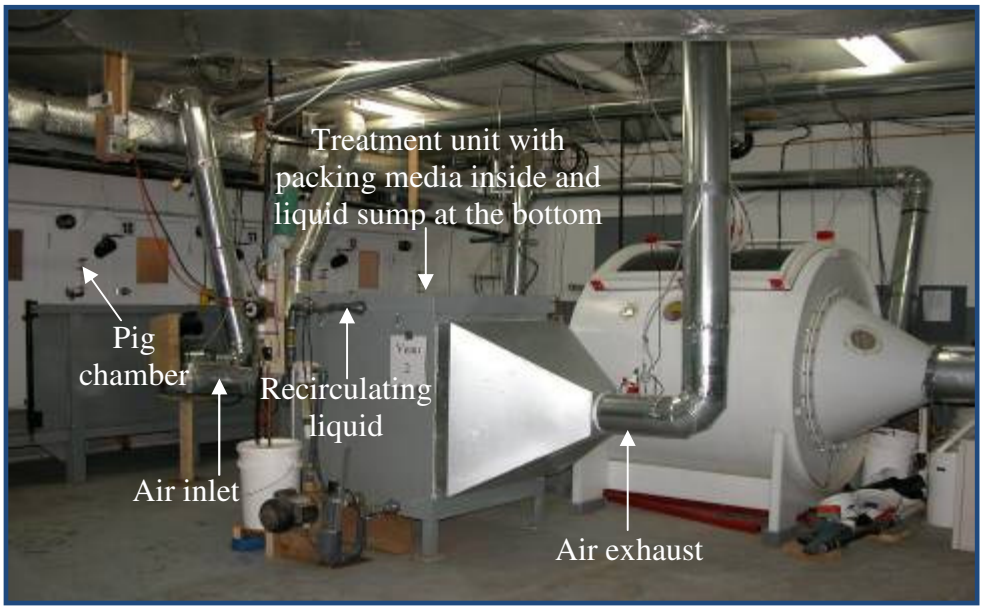


**Figure 5.2 Photo of the actual set-up of the biotrickling filter unit.**

### 5.7.2 Experimental trials

A total of 36 data sets were obtained from the six separate trials, which were completed from March 2011 to February 2012. Each trial ran for seven weeks and employed various operating conditions, i.e. two types of packing media, two liquid recirculation flow rates, and three levels of air residence time (Table 5.1). Each experimental treatment was done in triplicate. For the packing media, both structured and non-structured packing materials were tested. The properties and photos of the packing media (purchased from Lantec Products, Inc., California,

USA) are shown in Table 5.2 and Figure 5.3, respectively. The two liquid superficial velocities were 2.2 and 4.3 m $h^{-1}$ and the three empty bed residence times (EBRT) were 3, 6, and 9 s. These EBRTs were chosen based on the size of the reactor and on the typical EBRTs of biotrickling filter operation. As mentioned earlier, a constant airflow rate of 302.4 $m^3$ $h^{-1}$ was used in all trials. Thus, in order to carry out the different levels of residence time, the length of the bed (the distance the air travelled through the bed) was adjusted instead of the gas flow rate to keep the same gas mass transfer coefficient. At an EBRT of 9 s, the dimension of the bed was 0.9146 m high, 0.9146 m wide, and 0.9146 m long. The bed length was reduced to 2/3 when the residence time was reduced to 6 s, and to 1/3 when it was 3 s.

**Table 5.1 Operating conditions employed in this study.**

| Residence time (s) | Superficial liquid velocity (m $h^{-1}$) | Packing media |
|---|---|---|
| 3<br>6<br>9 | 2.2 | Structured, non-structured |
| 3<br>6<br>9 | 4.3 | Structured, non-structured |

**Table 5.2 Properties of the two types of packing media[a].**

| Parameter | Structured media | Non-structured media |
|---|---|---|
| Product name | HD Q-PAC | LANPAC-XL |
| Material | Polypropylene | Polypropylene |
| Specific surface area ($m^2$ $m^{-3}$) | 984 | 242 |
| Bulk density (kg $m^{-3}$) | 120 | 88 |
| Void fraction (%) | 87.8 | 95 |
| Standard module size (m) | 0.305 x 0.305 x 0.305 | 0.083 x 0.095 |

[a]Source: Lantec Products, Inc. (2013).

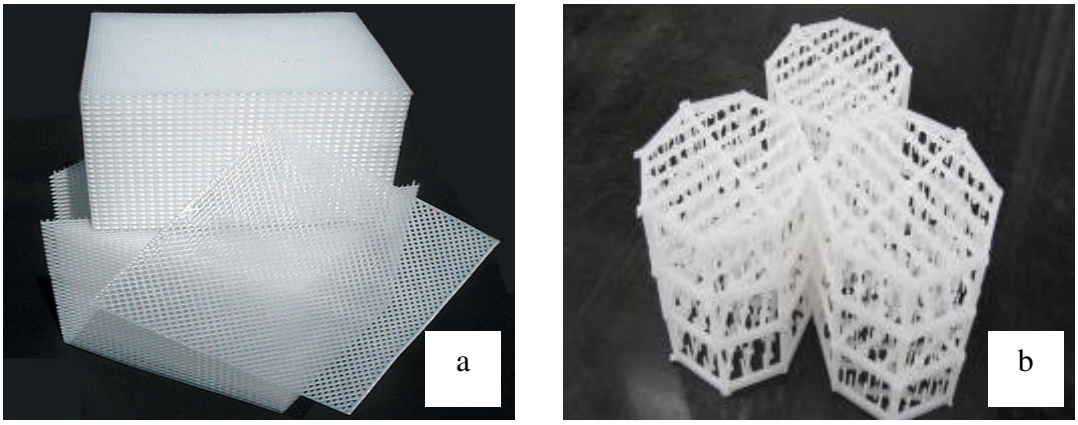


**Figure 5.3 Photos of the packing media utilized:**
**(a) structured media; (b) non-structured media.**

### 5.7.3 Data collection

The $NH_3$ gas was monitored inline using a non-dispersive infrared (NDIR) spectrometer (Ultramat 6E; Siemens, Germany). There were a total of 13 sampling ports: one in each chamber, one at the outlet of each biotrickling filter, and one for ambient air. The $NH_3$ concentration at each sampling port was measured one at a time at 15 min interval. The recirculating liquid were sampled every 1 to 2 weeks for $NH_4^+$, $NO_3^-$, and $NO_2^-$ concentrations, which were analyzed at the chemistry laboratory of IRDA by means of a colorimetric method using flow injection analysis (FIA). The pH, conductivity, and dissolved oxygen (DO) of the recirculating liquid were also monitored using a pH meter (WD-35617, Oakton Instruments, Illinois, USA), a conductivity meter (Model 1056, VWR International, Pennsylvania, USA), and a DO meter (WQ401, Global Water, California, USA), respectively. Each bioreactor was sampled on average every 3 to 4 days for the simultaneous measurements of pH, conductivity, and dissolved oxygen. The air and liquid temperatures in each bioreactor were monitored continuously using a T-type thermocouple. Other parameters such as relative humidity and pressure drop across the reactor were also monitored. Data loggers were employed to record all the measurements every 15 min.

### 5.7.4 Model development

This section discusses the concept on which the model was based, the assumptions made, and the methods of solving the model equations.

#### 5.7.4.1 Model concept

The model developed was a combination of the models of Sharvelle et al. (2008a) and Mpanias and Baltzis (1998). The model of Mpanias and Baltzis (1998), though steady-state, describes the basic processes (e.g. advection, mass transfer, diffusion, and microbial degradation) involved in the removal of mono-chlorobenzene in the gas, liquid, and biofilm phases. The model of Sharvelle et al. (2008a), on the other hand, takes into account the effect of pH on the dissociation of ammonia in solution, which is an important factor in the removal of ammonia. Thus, a model that integrates the above-mentioned components of these two models was deemed appropriate to meet the objectives of this study. Further, since the intended application of the model was to determine the governing processes and design parameters relevant to the treatment of the contaminants, a steady-state model was deemed sufficient to meet this goal (Sharvelle et al. 2008a).

Initially, the plan was to use two or three key odour components (e.g. *p*-cresol, dimethyl sulphide, and ammonia) for model calibration and validation. However, due to some limitations encountered in monitoring *p*-cresol and dimethyl sulphide in the exhaust air (i.e. unavailability of the instruments to measure these components at very low concentrations) only ammonia was finally chosen. Ammonia was the one chosen because of the availability of the technique to monitor ammonia inline, which provides ample measurements for model calibration and validation. Moreover, it was one of the key odour components identified in Chapter 2. Armeen et al. (2008) stated that ammonia accounts for more than 50% of the total emissions from pig

buildings. Since it is often emitted from swine production, its removal in biotrickling filters could be a potential indicator of the reactor's performance in removing odorous gases from the waste air.

#### 5.7.4.2 Model assumptions

The different physico-chemical and biological phenomena that take place in a biotrickling filter are represented by a complex set of differential equations. However, according to Shareefdeen et al. (2005) the complexity of the equations can be significantly reduced with application of justifiable assumptions. Thus, the following assumptions were made to simplify the model equations, yet still depicting the processes relevant in achieving the objective of this study.

1. Plug flow is assumed for both gas and liquid streams, thus, dispersion effects in both fluids are not considered.
2. Consistent with the film theory, there is no resistance to mass transfer at the gas-liquid interface and the phase concentrations at that interface are in equilibrium and are related by Henry's law.
3. There is no resistance to mass transfer from the bulk liquid to the liquid-biofilm interface; thus, concentration at the liquid-biofilm interface is equal to that in the liquid phase.
4. The packing media is not completely wet, consistent with what is usually observed during biotrickling filter operation, and the transfer occurs only in the wetted portion. Further, all the wetted portion is covered with biofilm. The wetted fraction of the packing media can be estimated using the empirical equation (Eq. 5.19; the variables are defined in the list of symbols and abbreviations) developed by Onda et al. (1968). Sharvelle et al. (2008a) found that Onda's (1968) correlation sufficiently predict the wetted fraction of the surface area:

$$f_w = 1 - exp\left\{-1.45\left(\frac{\sigma_p}{\sigma_L}\right)^{0.75}\left[\left(\frac{Q_L\rho_L}{A_L}\right)\left(\frac{1}{a_t\mu_L}\right)\right]^{0.1}\left[\left(\frac{Q_L\rho_L}{A_L}\right)^2\left(\frac{a_t}{\rho_L{}^2 g_c}\right)\right]^{-0.05}\left[\left(\frac{Q_L\rho_L}{A_L}\right)^2\left(\frac{1}{\rho_L\sigma_L a_t}\right)\right]^{0.2}\right\}$$

(5.19)

5. Adsorption of $NH_3$ on the packing material is negligible. Adsorption on the support is usually minimal in biotrickling filters because of the inert property of the support (Cox and Deshusses 1998).
6. Transfer of $NH_3$ directly to the biofilm is insignificant. The $NH_3$ must first enter the liquid phase prior to transport into the biofilm (Sharvelle et al. 2008a).
7. There are no oxygen and nutrient limitations in the biofilm. The components in the waste air are sufficient to provide the necessary nutrients to the microorganisms.
8. Biodegradation occurs mainly in the biofilm. Since only a very small quantity of biomass is present in the recirculating liquid as compared to that attached in the biofilm, biodegradation in the liquid phase can be neglected (Sharvelle et al. 2008a).
9. The biofilm density is constant through the reactor and the biofilm thickness is at steady state. Several other studies (Sharvelle et al. 2008a; Hekmat and Vortmeyer 1994) have assumed that the lysis of aged cells and the constant sloughing of the biofilm due to the shear force of the flowing liquid would occur at approximately the same rate as the growth of the microorganisms. Furthermore, Baltzis et al. (2001) and Okkerse et al. (1999) have shown that a steady-state biofilm assumption is adequate.
10. The diffusion of $NH_3$ from the liquid phase into the biofilm and within the biofilm is described by Fick's law (Dunn 2003). Furthermore, the diffusion coefficient of $NH_3$ in the biofilm is equal to its diffusion coefficient in water multiplied by a correction factor, $f_{Xv}$, estimated by Fan et al. (1990):

$$f_{Xv} = 1 - \frac{0.43 X_v^{0.92}}{11.19 + 0.27 X_v^{0.99}} \quad (5.20)$$

where $X_v$ is biofilm density in kg $m^{-3}$.

11. The microbial growth is described by the Haldane kinetics (Eq. 5.18). As observed from the shake-flask experiment presented in Chapter 4, the biodegradation data of $NH_3$ fitted better to the Haldane equation. Several studies (Baquerizo et al. 2005; Sanchez et al. 2005) have also reported $NH_3$ as an inhibitory substrate, thus, its biodegradation can be well represented by the Haldane equation.

#### 5.7.4.3 Mass balance equations

Based on the above assumptions, three mass balance equations (one each for the gas, liquid, and biofilm phases) and an overall mass balance were formulated to describe the removal of $NH_3$ in a cross-flow biotrickling filter. Ammonia is removed from the gas phase through dissolution in the liquid phase, which in turn is converted into nitrite and nitrate by the microorganisms or remain as unreacted $NH_3$ and $NH_4^+$ in the liquid (Armeen et al. 2008). Thus, the overall nitrogen mass balance of the system can be described by equation 5.21.

$$\left[\left(NH_3\text{-}N\right)_{in} - \left(NH_3\text{-}N\right)_{out}\right]_{(g)} Q_G t = \left[\left(NO_2^-\text{-}N\right) + \left(NO_3^-\text{-}N\right) + \left(NH_4^+\text{-}N\right) + \left(NH_3\text{-}N\right)\right]_{(aq)} V_L \quad (5.21)$$

where $Q_G$ = gas flow rate ($m^3\ h^{-1}$),

t = time (h),

$V_L$ = total volume of liquid ($m^3$),

subscripts *in* and *out* stand for inlet and exhaust of bioreactor, respectively.

Concentrations of all nitrogen species in equation 5.21 are expressed in g N $m^{-3}$. This further assumes that the biofilm is at steady-state (assimilation equals auto-oxidation and lysis), denitrification is negligible, and no $NH_3$ production in the reactor. Equation 5.21 means that the amount of $NH_3$ removed from the gas stream by the system, expressed in terms of nitrogen, is equal to the amount of nitrogen in the liquid solution in the form of $NO_2^-$, $NO_3^-$, $NH_4^+$, and un-ionized $NH_3$.

Using the $NH_3$ gas concentrations at the inlet and exhaust of the bioreactor, the performance of the system could then be evaluated by calculating the removal efficiency (RE) given in equation 5.22:

$$RE = \frac{C_{Gin} - C_{Gout}}{C_{Gin}} = \frac{(NH_3 - N)_{in} - (NH_3 - N)_{out}}{(NH_3 - N)_{in}} \tag{5.22}$$

The differential equations describing the mass balances in the gas, liquid, and biofilm phases, together with the boundary conditions, are described in equations 5.23 to 5.29. As shown in Figure 5.4, the air carrying the contaminant flows horizontally through the length of the filter bed (*l* direction) while the recirculating liquid goes down the height of the bed by gravity (*h* direction).

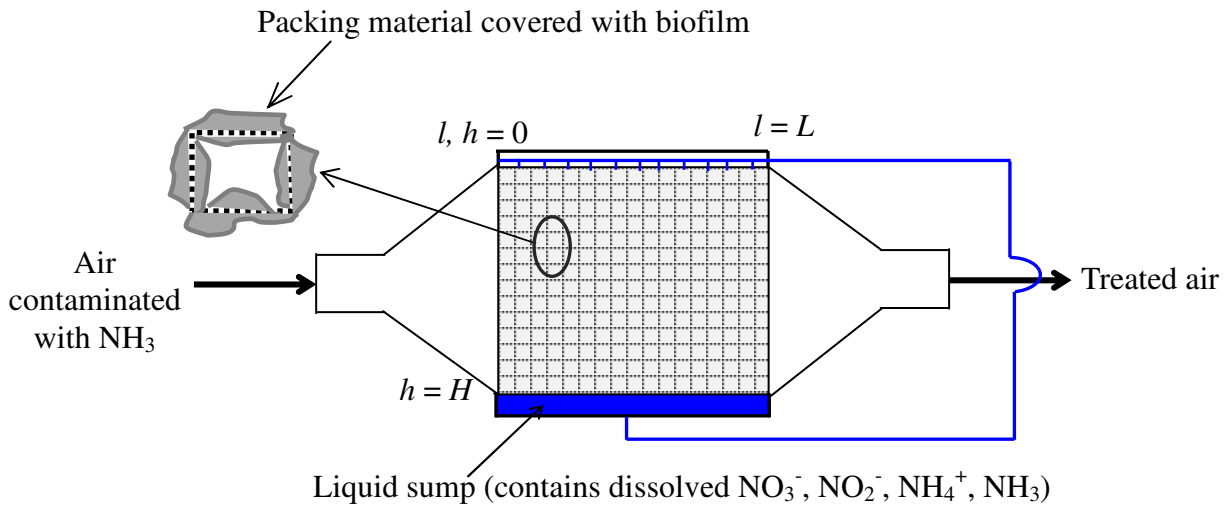


**Figure 5.4 Schematic diagram of the biotrickling filter (*l is* any position along bed length *L* or gas flow direction and *h* is any position along bed height *H* or liquid flow direction).**

1. Mass balance in the gas phase, along the length (*l*) of the column:

$$U_G \frac{dC_G}{dl} = -K_G a_t f_w \left(C_G - k_H f_{NH3} C_L\right) \tag{5.23}$$

with the corresponding boundary equation:

$$C_G = C_{Gin}; \qquad \text{at } l = 0 \tag{5.24}$$

2. Mass balance in the liquid phase, along the height (*h*) of the column:

$$U_L \frac{dC_L}{dh} = K_G a_t f_w \left(C_G - k_H f_{NH3} C_L\right) + f_{X_v} D_L a_t f_w \left(dC_B / db\right)_{b=0} \tag{5.25}$$

Since the liquid is recirculated, the corresponding boundary condition is:

$$C_{L(at\ h=0)} = C_{L(at\ h=Ht)} \tag{5.26}$$

3. Mass balance in the biolayer, at position *(l, h)* of the column and along the depth (*b*) of the biofilm:

$$f_{X_v} D_L \left(\frac{d^2 C_B}{db^2}\right) = \frac{X_v \mu_m C_B}{Y\left[K_s + C_B + \left(C_B^{\,2} / K_i\right)\right]} \tag{5.27}$$

with the corresponding boundary equations:

$$C_B = C_L; \qquad \text{at } b = 0 \tag{5.28}$$

$$dC_b/db = 0; \qquad \text{at } b = B_t \tag{5.29}$$

Equation 5.23 illustrates that the change in gas phase concentration is equal to the amount that is transferred into the liquid phase. The negative sign at the right side of the equation indicates that the concentration decreases as the gas flows along the length of the bed. On the other hand, the change in concentration in the liquid phase, as described in equation 5.25, is equal to the amount that is absorbed from the gas phase less the amount that diffuses into the biofilm. The lower concentration in the biofilm compared to that at the liquid-biofilm interface makes the second term at the right side of the equation positive. Within the biofilm, the change in concentration is only due to the microbial degradation as shown in equation 5.27.

The boundary condition in the gas phase given in equation 5.24 indicates that at the inlet of the reactor ($l = 0$), the $NH_3$ concentration is equal to the gas inlet concentration. Since the liquid is being recirculated within the system, the $NH_3$ concentration in the liquid that goes out from the reactor is equal to that in the liquid that goes into the reactor as described in equation 5.26. Equation 5.28 is based on assumption 3, which states that the concentration at the liquid biofilm interface ($b = 0$) is equal to the bulk liquid concentration. Equation 5.29 means that at the support ($b = B_t$), there is no more change in the concentration.

#### 5.7.4.4 Numerical solution

Since the differential equations 5.23, 5.25, and 5.27 are coupled (i.e. they depend on each other), the only way to solve them is by numerical techniques. Though there are several numerical methods available ranging from simple to sophisticated ones, no method is considered

superior over the others. The selection of an effective method depends on the nature of the problem and on the trade-off between the accuracy of results required and the complexity of the computing process.

Two numerical methods, finite difference and Newton-Raphson, were found adequate to solve the differential equations involved in this study. The implicit finite difference technique was used to approximate the solutions of the three differential equations by transforming them into algebraic equations while the Newton-Raphson method was utilized to solve the resulting non-linear algebraic equation that describes the biofilm. One or both of these techniques have been used by several other studies (Kim and Deshusses 2003; Jorio et al. 2003; Vayenas et al. 1997).

The first step was to discretize the geometric domains of the gas, liquid, and biofilm by dividing each domain into equal intervals to construct a mesh of equally spaced points (uniform grid). The discretization of the gas and liquid domains are shown in Figure 5.5. For $m$ divisions in the gas domain of total length $L$, the mesh width or grid size is $L/m$. Similarly, for $n$ divisions in the liquid domain of total height $H$, the mesh width is $H/n$. $L$ and $H$ are the length and height of the filter bed, respectively. Node ($l_i$, $h_j$), where $i = 1, 2, 3 \ldots m$; $j = 1, 2, 3 \ldots n$; $l$ is any position along bed length or gas flow direction; and $h$ is any position along bed height or liquid flow direction, represent any node in the mesh.

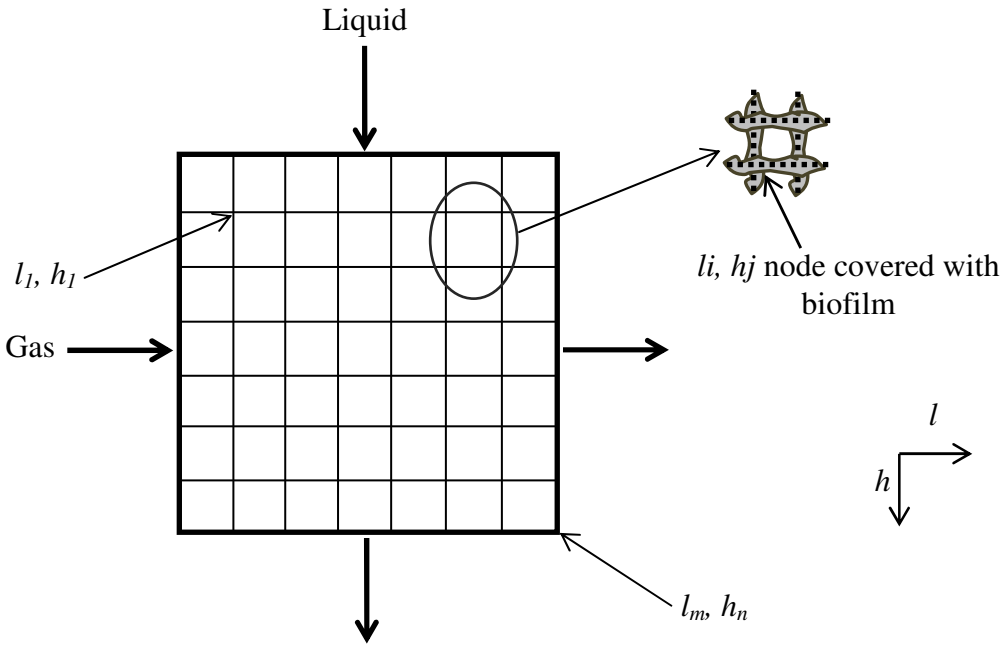


**Figure 5.5 Schematic representation of the discretization in the gas and liquid domains (*l* is any position in the gas flow direction and *h* is any position in the liquid flow direction).**

The code, which was written in Visual Basic for Applications (VBA) in Microsoft Excel to carry out the calculation, allowed the user to divide the gas and liquid domains into different grid sizes. In this study, both the gas and liquid domains were divided into 20 equal divisions. However, the number of divisions in the biofilm domain was fixed at five (not shown in the figure) due to the complexity of the Newton-Raphson method. Since biofilm thickness is generally in micrometer range, five divisions were deemed adequate to provide sufficient accuracy in the results.

The solutions were obtained by first estimating the liquid concentration at node ($l_1$, $h_1$) shown in Figure 5.5 from a simple gas-liquid absorption process. The estimated value of the liquid concentration was then used as the initial guess in estimating the biofilm concentrations at nodes ($l_1$, $h_1$, $b_1$), ($l_1$, $h_1$, $b_2$).....($l_1$, $h_1$, $b_5$) (where $b$ is any position within the biofilm depth) through an iterative process using the Newton-Raphson technique. Since the biofilm thickness

was discretized into five divisions as mentioned earlier, there were five different levels of concentrations in the biofilm corresponding to node $l_i$, $h_j$ in the gas-liquid plane. The five biofilm concentrations ($l_i$, $h_j$, $b_1$ to $l_i$, $h_j$, $b_5$) were solved simultaneously since their equations are coupled. The iteration stopped when the difference between the two consecutive iteration results for all the five concentrations is less than or equal to $1x10^{-12}$ (tolerance limit), or when there was no convergence after 20 iterations.

With the biofilm concentration profile, the gas and liquid concentrations were solved again, this time accounting for the amount that had diffused to the biofilm. This process was repeated until all the gas, liquid, and biofilm concentrations at each node were determined.

#### 5.7.4.5 Model parameters

The biokinetic parameters were determined from the shake-flask experiment described in section 4.5.3.3. The values for $\mu_m$, $K_s$, $K_i$, and Y obtained from the afore-mentioned experiment were 0.17 $h^{-1}$, 11.9 mg $L^{-1}$, 618 mg $L^{-1}$, and 0.5 g biomass $g^{-1}$ $NH_4^+$-N, respectively. However, these values were relatively higher in comparison with those reported in the literature (Baquerizo et al. 2005; Sanchez et al. 2005) for nitrifying biomasses. One reason for this could be the utilization of glucose as carbon source supplement, which enhanced the growth of the heterotrophic microorganisms. Thus, during the model calibration these values were only used as starting point and were adjusted to satisfy the boundary condition given in equation 5.26.

The temperature dependence of the Henry's law constant ($k_H$; dimensionless) was estimated using equation 5.30 (Zhang et al. 1994). Furthermore, to consider the effect of pH and the dissociation of $NH_3$ in solution, an effective Henry's law constant ($k_{Heff}$; dimensionless) was calculated using equation 5.31 (Sharvelle et al. 2008a). Henry's law is applicable for ideal dilute solutions and for solutes whose molecular species are the same both in the gas and liquid phases.

This law may not apply for non-ideal gases and solutions, such as those whose molecules undergo dissociation in solution or those that are highly soluble like $NH_3$ (Halder 2009). The high solubility of $NH_3$ and its dissociation in solution result in a much lower value of Henry's law constant than just due to physical solubility.

$$k_H = 1.1561e^{-4151/(T+273)}\left[\frac{(1000)(17)}{(0.08205)(T)}\right] \tag{5.30}$$

$$k_{Heff} = \left(\frac{K_a k_H}{[H^+]}\right)\left(1+\frac{K_a}{[H^+]}\right)^{-1} \tag{5.31}$$

The overall mass transfer coefficient ($K_G$) was calculated from equation 5.32 (Guo and Roache, 2003):

$$\frac{1}{K_G} = \frac{1}{k_G} + \frac{k_{Heff}}{k_L} \tag{5.32}$$

where the values of the individual mass transfer coefficients ($k_G$ and $k_L$) were estimated using other empirical equations (Eqs. 5.33 and 5.34 ) developed by Onda et al. (1968). Since several studies (Kim and Deshusses 2008; Dvorak et al. 1996)) found that these correlations have some inaccuracies in the predictions, correction factors ($\xi_1$, $\xi_2$) were applied as what Mpanias and Baltzis (1998) have also done to improve the results. Due to $NH_3$'s high solubility in water (having a very low Henry's law constant), the mass transfer resistance is essentially in the gas side, hence, $k_G$ would be approximately equal to $K_G$ (Roustan 2006).

$$k_G\xi_1 = 5.23a_t D_G\left(\frac{Q_G\rho_G}{A_G a_t \mu_G}\right)^{0.7}\left(\frac{\mu_G}{\rho_G D_G}\right)^{1/3}(a_t d_p)^{-2} \tag{5.33}$$

$$k_L\xi_2 = 0.0051\left(\frac{Q_L\rho_L}{A_L f_w a_t \mu_L}\right)^{2/3}\left(\frac{\mu_L}{\rho_L D_L}\right)^{-0.5}\left(\frac{\rho_L}{\mu_L g_c}\right)^{-1/3}(a_t d_p)^{0.4} \tag{5.34}$$

As mentioned earlier, the wetted fraction of the surface area ($f_w$) was calculated from equation 5.19. All the other parameters were taken from the literature.

### 5.7.5 Sensitivity analysis

A sensitivity analysis was conducted to determine the governing processes and the parameters that have significant impacts on the removal of ammonia from the waste gas. Since the objective was to determine the main influence of the individual model parameters, a one-at-a-time (OAT) sensitivity analysis, where parameters were changed in turn, was applied in this study (Sharvelle et al. 2008b). Similar to the approach applied by Baquerizo et al. (2005), the OAT analysis adopted in this study was implemented by changing the default parameters by ± 20% to obtain the upper and lower limit values of the parameters. The model parameters were divided into two groups: intrinsic and design parameters. Intrinsic parameters were those which were inherent to the system, e.g. mass transfer and biokinetic parameters, while design parameters were those which could be controlled by modifying the reactor set-up and operation, e.g. flow rates, inlet concentrations, pH, temperature, residence time or reactor length (Sharvelle et al. 2008b). The equation (Eq. 5.35) employed by Baquerizo et al. (2005) was used to evaluate the impact of each of these parameters on removal efficiency (Eq. 5.22) as their values were changed from the lower to the upper limit.

$$Sensitivity\ coefficient = \frac{\Delta V/V_d}{\Delta P/P_d} \tag{5.35}$$

where ΔV is the difference between the simulated variable (in this case, the removal efficiency) under the new condition and the default value of the variable, $V_d$, and ΔP the difference between the value of the parameter at ±20% and the default value of the parameter, $P_d$.

### 5.7.6 Calibration and validation

Since the purpose of the calibration is to adjust model input parameters to maximize the resulting agreement between the model prediction and experimental data, it was reasonable to calibrate only those parameters that have significant influence on $NH_3$ gas removal. Thus, the parameters adjusted were the ones that showed significant impact on the removal of $NH_3$ based on the results of the sensitivity analysis. However, among the significant parameters identified only the intrinsic ones were calibrated since these parameters were not directly measurable and were only estimated through empirical equations.

As mentioned earlier, the model was calibrated and validated using the data collected from the pilot-scale biotrickling filters, which were installed to treat the air exhausted from the bench-scale pig chambers. In each data set, the $NH_3$ gas concentration selected for the calibration and validation was the 24-h average measurement taken from a period where there was a relatively constant maximum removal rate and a relatively constant $NH_3$ gas inlet concentration (relatively constant means standard deviations were within ±10%). Because of this, only one value could be taken from each run even if there were plenty of data collected from its in-line monitoring. Thus, there were only a total of 36 data sets available. However, only 32 of these were used for calibration and validation due to the availability of pH measurements. Sixteen of these data sets were obtained using the structured packing media and the other 16 from the non-structured packing media. The 16 data sets for each of the packing media were split into a 2/3 – 1/3 ratio (Hagedorn et al. 2011; Blattberg et al. 2008); 2/3 of the data (10 data sets) was used for calibration and the remaining 1/3 (6 data sets) was used for validation. Since these data were collected using two liquid flow rates, this means that at each flow rate only three points were available for validation. The data were grouped according to the experimental treatment, and then from each group, the samples for calibration and those for validation were randomly

selected. The purpose of grouping the samples in this manner was to ensure that even if only few data were used, each treatment combination would be well-represented in both the validation and calibration processes.

The model, both in calibration and validation, was evaluated based on the ASTM D 5157- 97 Standard Guide for Statistical Evaluation of Indoor Air Quality Models (ASTM 2003), which was also used by Cortus (2006). The evaluation parameters and the suggested evaluation limits are listed in Table 5.3.

**Table 5.3 Model evaluation criteria.**

| Evaluation parameter | Equation | Suggested evaluation limit | Equation number |
|---|---|---|---|
| General agreement: Normalized Mean Square Error (NMSE) | $NMSE = \left[\frac{\sum_{k=1}^{n}\left(C_{pk} - C_{mk}\right)^2}{n}\right]\left[\frac{1}{\overline{C_p} \bullet \overline{C_m}}\right]$ | NMSE < 0.25 | (5.36) |
| Bias: Fractional Bias (FB) | $FB = \frac{2\left(\overline{C_p} - \overline{C_m}\right)}{\overline{C_p} + \overline{C_m}}$ | -0.25< FB< 0.25 | (5.37) |

where $C_p$ = predicted concentration (g $m^{-3}$),

$C_m$ = measured concentration (g $m^{-3}$),

$\overline{C}_p$ = mean predicted concentration (g $m^{-3}$),

$\overline{C}_m$ = mean measured concentration (g $m^{-3}$),

n = number of data pairs.

## 5.8 RESULTS AND DISCUSSION

### 5.8.1 Measured data

Figure 5.6 shows the actual inlet and exhaust $NH_3$ concentrations collected over a period of seven weeks as well as the removal efficiency (RE) in one of the treatment units. The average maximum removal efficiency of $NH_3$ ranged from 49 to 68% (Table 5.4; Girard et al. 2013) while the daily average $NH_3$ inlet concentrations ranged between 1 to 16 $ppm_v$. Results from the analysis of variance (ANOVA) conducted by Girard et al. (2013) showed that the EBRT had a significant influence ($P = 0.0101$) on the removal efficiency; however, it was observed only at an EBRT of 9 s. No significant difference was observed between the EBRT of 3 and 6 s. The $NH_3$ removal efficiency only increased from 57 to 65% when the volume of the filter media was tripled. Further, no significant effect on the $NH_3$ removal efficiency was observed from the type of filter media and the liquid recirculation rate.

**Table 5.4 Average removal efficiency of $NH_3$ for each treatment.**

| Media | $U_L$ ($m\,h^{-1}$) | $NH_3$ removal efficiency (%) | | | | | |
|---|---|---|---|---|---|---|---|
| | | EBRT 3 s | | EBRT 6 s | | EBRT 9 s | |
| | | Mean | SD | Mean | SD | Mean | SD |
| S | 2.15 | 49.0 | 4.0 | 60.1 | 4.0 | 64.8 | 4.0 |
| | 4.31 | 63.5 | 4.0 | 59.0 | 4.0 | 67.8 | 4.0 |
| NS | 2.15 | 55.5 | 4.0 | 58.2 | 4.0 | 66.3 | 4.0 |
| | 4.31 | 59.2 | 4.0 | 61.6 | 4.9 | 61.8 | 4.0 |

Source: Girard et al. (2013); S: structured media; NS: non-structured media; $U_L$: liquid superficial velocity; EBRT: Empty bed residence time; SD: standard error.

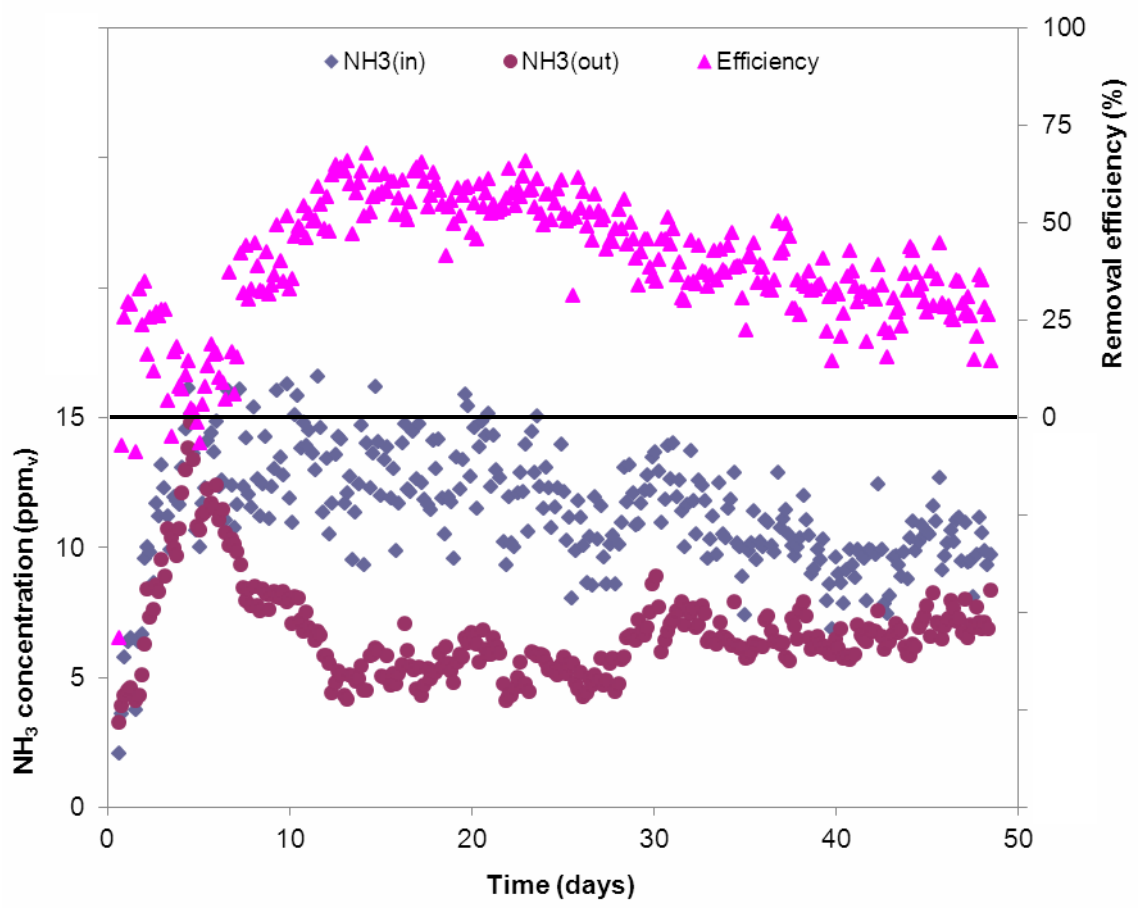


**Figure 5.6 The measured inlet and exhaust $NH_3$ concentrations and removal efficiency.**

In most of the trials, the maximum removal efficiency was attained after 2 to 3 weeks of operation when biofilm was already observed on the filter media. This condition remained stable for a period of about 1 to 2 weeks, after which the efficiency dropped, which might have been due to free $NH_3$ and $HNO_2$ inhibition. Several studies have reported that nitrification reactions are mainly inhibited by free $NH_3$ and $HNO_2$ (Baquerizo et al. 2005; Melse and Mol 2004). Since no amount of the recirculating liquid was removed during the trials, which was done on purpose to standardize the trials, the $NH_4^+$-N and $NO_2^-$-N concentrations increased over time. One has to take note that concentrations of $NH_3$ and $HNO_2$ in solution are directly proportional to the

$NH_4^+$-N and $NO_2^-$-N concentrations. The reported inhibitory concentration of free $NH_3$ for *Nitrosomonas* (ammonium oxidizing bacteria) starts at 10 to 150 mg $L^{-1}$, while that for *Nitrobacter* (nitrite oxidizing bacteria) is at 0.1 to1 mg $L^{-1}$; moreover, both types of microorganisms are inhibited by free $HNO_2$ starting at concentrations from 0.2 to 2.8 mg $L^{-1}$ (Scholtens and Demmers 1991). In the trial shown in Figure 5.6, the $NH_4^+$-N, $NO_2^-$-N and $NO_3^-$-N concentrations in the liquid after the fourth week of operation were 2100; 2200; and 90 mg $L^{-1}$ N, respectively. Assuming equilibrium between $NH_4^+$ and $NH_3$ and between $NO_2^-$ and $HNO_2$, the free $NH_3$ and $HNO_2$ concentrations at the measured pH and temperature (7 and 16°C, respectively) were 1.23 and 0.59 mg N $L^{-1}$, respectively. The free $NH_3$ was estimated using equations 5.12 and 5.13 presented earlier while the free $HNO_2$ was estimated using equations 5.38 and 5.39 given below (EIFAC 1984), where $NO_2^-/HNO_2$ represents the relative amounts of $NO_2^-$ and $HNO_2$ in solution and $pK_a$ in equations 5.38 and 5.39 is the logarithmic constant for the ionization of $HNO_2$.

$$\frac{NO_2^-}{HNO_2} = antilog\left(pH - pKa\right) \tag{5.38}$$

$$pKa = \left(\frac{655.586}{T + 273.16}\right) + 1.148 \tag{5.39}$$

The estimated values for free $NH_3$ and $HNO_2$ indicate that inhibition have already occurred in the system; the nitrite oxidizing bacteria was inhibited by the free $NH_3$ while both ammonium and nitrite oxidizing bacteria by the free $HNO_2$. According to Chen et al. (2005), $NO_3^-$ should be the dominant product of complete $NH_3$ conversion in solution. The relatively high concentrations of $NH_4^+$ and $NO_2^-$ and relatively low concentration of $NO_3^-$ in the system indicate that there were low conversions of $NH_4^+$ to $NO_2^-$ and $NO_2^-$ to $NO_3^-$, which were probably caused by free $NH_3$ and $HNO_2$ inhibitions as discussed above. However, the relatively high

concentrations of $NH_4^+$ and $NO_2^-$ measured in this study were not uncommon in waste treatment units. High build-up of $NH_4^+$ and $NO_2^-$ were also reported in some waste treatment operations (Nielsen et al. 2008; Melse and Mol 2004). Accumulation of $NH_4^+$, $NO_2^-$, and other dissolved salts could have been avoided by regular replacement of the recirculation liquid with fresh water, which in turn could help maintain high removal efficiency as reported in other studies (Chou and Wang 2007; Melse and Mol 2004). However, as mentioned earlier, this was not conducted in this study to standardize the trials.

The measurements showed that the overall process concerning the removal of ammonia in biotrickling filters was limited by the microbial degradation in the biofilm. Since $NH_3$ gas is very soluble in water, it was readily absorbed in the liquid; however, the absorbed $NH_3$ was not efficiently biodegraded. Having a stable biofilm already attached to the packing media before the start of the operation could help reduce the start-up time. Regular replacement of the recirculating liquid with fresh water could also help reduce accumulations of $NH_4^+$ and $NO_2^-$ (Chou and Wang 2007; Melse and Mol 2004).

The pressure drop across the biotrickling filter units was negligible in all trials (0.03 to 0.05 in. $H_2O$). The measured pH values were in the range of 5.9 to 8.3, while liquid temperatures were in the range of 15 to 22$^oC$. The dissolved oxygen ranged between 1 to 12 mg $L^{-1}$. Based on the reported critical value for dissolved oxygen which is 0.5 to 1 mg $L^{-1}$ for the biodegradation of organic materials and 1 to 2 mg $L^{-1}$ for nitrification (van Haandel and van der Lubbe 2012), there could have been instances that anaerobic condition existed in the system.

### 5.8.2 Model parameters

The model parameters that were used for both structured and non-structured packing media are presented in Table 5.5. As indicated in the table, these parameters were either

calculated in this study or from published literature. Although some of these parameters are temperature dependent, the values did not vary considerably when they were calculated using empirical equations at the measured temperatures in the biotrickling filters. Thus, only one value was used for each of these parameters and the values used by Sharvelle et al. (2008a) were the ones adopted for they were found closer to the values calculated at 20$^{o}$C (the average temperature of the air exhausted from the pig chambers and that of the liquid recirculating over the filter bed). The other parameters, which were obtained from the calibration process, are discussed in section 5.8.4.

**Table 5.5 Parameter values applied for both structured and non-structured media.**

| Parameter | Symbol | Value | Unit | Reference |
|---|---|---|---|---|
| Dynamic air viscosity | $\mu_G$ | 0.061 | kg m$^{-1}$ h$^{-1}$ | Sharvelle et al. (2008a) |
| Dynamic water viscosity | $\mu_L$ | 3.6 | kg m$^{-1}$ h$^{-1}$ | Sharvelle et al. (2008a) |
| Air density | $\rho_G$ | 1.2 | kg m$^{-3}$ | Sharvelle et al. (2008a) |
| Water density | $\rho_L$ | 998.2 | kg m$^{-3}$ | Sharvelle et al. (2008a) |
| Water surface tension | $\sigma_L$ | 0.073 | N m$^{-1}$ | Sharvelle et al. (2008a) |
| Packing material surface tension | $\sigma_p$ | 0.031 | N m$^{-1}$ | Aranberri-Askargorta et al. (2003) |
| Nominal packing diameter | $d_p$ | 0.003[a]; 0.0124[b] | m | Calculated in this study |
| Gravitational constant | $g_c$ | 1.3x10$^{8}$ | m h$^{-2}$ | Sharvelle et al. (2008a) |
| Diffusion coefficient in air | $D_G$ | 0.0792 | m$^2$ h$^{-1}$ | Sharvelle et al. (2008a) |
| Diffusion coefficient in water | $D_L$ | 6.12x10$^{-6}$ | m$^2$ h$^{-1}$ | Sharvelle et al. (2008a) |
| Biofilm density | $X_v$ | 7.5x10$^{4}$ | g m$^{-3}$ | Mpanias and Baltzis (1998) |

[a] structured media; [b] non-structured media.

### 5.8.3 Sensitivity analysis

The default values for the parameters (both intrinsic and design) used in the sensitivity analysis are listed in Tables 5.6 and 5.7. These values are typical for a biotrickling filter operation. The removal efficiency at the default condition was 71.2%. The removal efficiencies

when the parameters were altered from the lower to the upper limit, with the corresponding sensitivity coefficients, are also shown in the same tables.

**Table 5.6 Sensitivity analysis for the intrinsic parameters.**

| Parameter | Unit | Default value | Removal efficiency* (%) | | Sensitivity Coefficient (-) | |
|---|---|---|---|---|---|---|
| | | | UL | LL | UL | LL |
| Diffusion coefficient in water ($D_{L)}$) | $m^2 h^{-1}$ | $6.12x10^{-6}$ | 71.2 | 71.2 | 0.000 | 0.001 |
| Diffusion coefficient in air ($D_G$) | $m^2 h^{-1}$ | 0.079 | 75.3 | 66.0 | 0.290 | 0.368 |
| Effective Henry's law constant ($k_{Heff}$) | - | $1.58x10^{-6}$ | 71.2 | 71.2 | -0.001 | -0.001 |
| Wetted surface area fraction ($f_w$) | - | 0.130 | 77.6 | 63.3 | 0.446 | 0.554 |
| Gas mass transfer coefficient ($k_G$) | $m h^{-1}$ | 5.998 | 77.3 | 63.3 | 0.430 | 0.554 |
| Liquid mass transfer coefficient ($k_L$) | $m h^{-1}$ | 0.004 | 71.2 | 71.2 | 0.001 | 0.001 |
| Biofilm density ($X_v$) | $g m^{-3}$ | $7.5x10^4$ | 71.2 | 71.2 | 0.000 | 0.000 |
| Correction factor ($f_{Xv}$) | - | 0.254 | 71.2 | 71.2 | 0.000 | 0.000 |
| Maximum specific growth rate ($\mu_m$) | $h^{-1}$ | 0.020 | 71.2 | 71.2 | 0.000 | 0.000 |
| Yield coefficient (Y) | $g g^{-1}$ | 0.300 | 71.2 | 71.2 | 0.000 | 0.000 |
| Half-saturation constant ($K_s$) | $g m^{-3}$ | 5 | 71.2 | 71.2 | 0.000 | 0.000 |
| Inhibition constant ($K_i$) | $g m^{-3}$ | 15 | 71.2 | 71.2 | 0.000 | 0.000 |
| Biofilm thickness ($B_t$) | µm | 75 | 71.2 | 71.2 | 0.000 | 0.000 |

*Removal efficiency at the default condition was 71.2%; UL – upper limit; LL – lower limit.

**Table 5.7 Sensitivity analysis for the design parameters.**

| Parameter | Unit | Default value | Removal efficiency* (%) | | Sensitivity Coefficient (-) | |
|---|---|---|---|---|---|---|
| | | | UL | LL | UL | LL |
| Liquid flow rate ($Q_L$) | $m^3 h^{-1}$ | 2.4 | 73.6 | 68.3 | 0.164 | 0.206 |
| Gas flow rate ($Q_G$) | $m^3 h^{-1}$ | 302.4 | 69.3 | 73.5 | -0.135 | -0.162 |
| Bed length (L) | m | 0.610 | 75.1 | 66.3 | 0.273 | 0.347 |
| Total specific surface area ($a_t$) | $m^{-1}$ | 980 | 64.6 | 78.8 | -0.464 | -0.533 |
| Nominal packing diameter ($d_p$) | m | 0.003 | 58.3 | 85.2 | -0.910 | -0.981 |
| $NH_3$ gas inlet concentration ($C_{Gin}$) | $g m^{-3a}$ | 0.00595 | 71.2 | 71.2 | 0.000 | 0.000 |
| $NH_3$ liquid inlet concentration ($C_{Lin}$) | $g m^{-3b}$ | 1000 | 71.2 | 71.2 | 0.000 | 0.000 |
| pH | - | 7 | 61.2 | 71.3 | -0.705 | -0.006 |
| Temperature (T) | $^oC$ | 17 | 71.2 | 71.3 | -0.004 | -0.002 |

*Removal efficiency at the default condition was 71.2%; [a] is g $NH_3$ $m^{-3}$; [b] is g $NH_4^+$-N $m^{-3}$; UL – upper limit; LL – lower limit.

The results indicate that among the intrinsic parameters, the physico-chemical parameters that affect the gas mass transfer (i.e. gas diffusion coefficient, wetted surface area fraction, and gas mass transfer coefficient) had the most notable impact on the removal of $NH_3$ from the gas phase. These results are consistent with those cited in the literature (Baquerizo et al. 2005). This was expected because these parameters are directly involved in the transfer of the contaminant from the gas phase into the liquid phase. The sensitivity of the removal efficiency to the gas diffusion coefficient and gas mass transfer coefficient and the insensitivity to the liquid mass transfer coefficient indicate that the mass transfer is controlled by the gas phase rather than the liquid phase, which is due to the high solubility of ammonia. As previously mentioned (Tchobanoglous et al. 2003), for gases which are highly soluble, the mass transfer is controlled by the gas phase. The removal efficiency is highly sensitive to the wetted portion of the surface area of the packing media indicating the gas-liquid mass transfer to be a very significant process in the removal of $NH_3$ from the gas phase. The removal efficiency seems to be insensitive to the Henry's law constant. Again, this could be due to the high solubility of ammonia as indicated by its low Henry's law constant value. Sharvelle et al. (2008b) found the $NH_3$ gas removal to be highly insensitive to intrinsic parameters, which was probably due to the high solubility of $NH_3$.

None of the biokinetic parameters had a significant influence on the removal of $NH_3$ from the gas phase as indicated by a constant removal efficiency shown in Table 5.6 when these parametes were changed from upper to lower limit. However, these parameters have shown influences on the removal of the contaminant in the liquid phase (data not shown). This means that their direct impact is on the removal of ammonia in the liquid phase, which in turn, affects the removal in the gas phase when liquid concentration becomes comparatively higher than the equilibrium concentration.

Among the design parameters, the gas and liquid flow rates, residence time (or bed length), specific surface area, nominal packing diameter, and pH of the recirculating liquid showed the greatest influence on the removal efficiency (Table 5.7). The pH is expected to influence the removal efficiency since it affects the equilibrium between the un-ionized $NH_3$ and $NH_4^+$ as shown in equations 5.8 and 5.9. A higher impact was observed at higher pH where ammonia tends to stay in the un-ionized form providing a higher tendency to escape into the gas phase as described in equation 5.7, which could reduce the removal efficiency. However, the effects of pH and temperature on the microbial growth have not been accounted for in this study. Impacts of these two parameters on microbial growth have been reported in several studies (Chou and Wang 2007; Chung and Huang 1998; Gullicks and Cleasby 1990).

The gas and liquid flow rates, nominal packing diameter, and specific surface area affect the mass transfer coefficients, which in turn influence the removal efficiency. Increases in gas and liquid flow rates enhance the convective transport, thereby increasing mass transfer. The significance of the nominal packing diameter can be attributed to its effect on the gas mass transfer coefficient, where a lower value results in a higher mass transfer coefficient. It was also observed that a higher surface area results in a lower removal efficiency. This indicates that a higher liquid flow rate is required to achieve the same wetted surface area fraction when the specific surface area of the packing material is high. This observation is consistent with that of Sharvelle et al. (2008b).

The removal efficiency was not sensitive to the gas and liquid inlet concentrations, similar to what have also been observed by Sharvelle et al. (2008a). This could be again due to the high solubility of ammonia.

### 5.8.4 Calibration

As mentioned earlier, the calibration was performed only on the intrinsic parameters that showed significant influence on the removal of $NH_3$. This means that based on the results of the sensitivity analysis, only the gas diffusion coefficient, gas mass transfer coefficient, and wetted fraction of the surface area were calibrated. Since both the gas diffusion coefficient and the gas mass transfer coefficient are in the same equation (Eq. 5.33) with the correction factor $\xi_l$, it was deemed sufficient to calibrate only $\xi_l$ to account for the effects of the other two parameters. The calibration of $\xi_l$ was initiated using the value used by Baltzis et al. (2001). Due to the difference of configuration, the two types of packing media had different values for $\xi_l$ as shown in Table 5.8. Since the two types of media resulted in almost similar removal efficiencies based on the experimental results, the higher surface area of the structured media was compensated by a lower gas mass transfer coefficient; hence, $\xi_l$ for structured media was higher than with that of the non-structured media.

**Table 5.8 Parameters adjusted during calibration using structured and non-structured media.**

| Parameter | Symbol | Unit | Starting value for calibration | Calibrated value | |
|---|---|---|---|---|---|
| | | | | S | NS |
| Correction factor | $\xi_l$ | - | 2.5 | 27 | 7 |
| Maximum specific growth rate | $\mu_m$ | $h^{-1}$ | 0.174 | 0.02 | 0.02 |
| Half-saturation constant | $K_s$ | $g\ m^{-3}$ | 11.9 | 5.0 | 5.0 |
| Inhibition constant | $K_i$ | $g\ m^{-3}$ | 618.0 | 15.0 | 15.0 |
| Yield coefficient | Y | $g\ g^{-1}$ | 0.5 | 0.3 | 0.3 |
| Biofilm thickness | $B_t$ | μm | 100 | 75 | 75 |

S: structured media; NS: non-structured media.

Since the wetted fraction of the packing media varies with the changes in liquid flow rates, this parameter was not held constant, and thus, was not calibrated. Additionally, since the

removal efficiency was not sensitive to the liquid mass transfer coefficient, $\xi_2$ was set to 1 for it would be irrelevant to calibrate this parameter. The biokinetic parameters ($\mu_m$, $K_s$, $K_i$, Y, and $B_t$), though they did not show any influence on the removal of $NH_3$ from the gas phase, were also adjusted to satisfy the boundary condition given in equation 5.26. The initial values used to calibrate $\mu_m$, $K_s$, $K_i$, and Y were obtained from the shake-flask experiment presented in section 4.5.3.3, while for $B_t$ the value used was from Baquerizo et al. (2005). As shown in Table 5.8, the calibrated values for the biokinetic parameters (i.e. $\mu_m$, $K_s$, $K_i$, and Y) were relatively smaller in comparison with those obtained from the shake-flask experiment. The possible reason for this was the utilization of glucose as a carbon source in the shake-flask experiment. The calibrated value for $B_t$ was similar to the effective biofilm thickness found by Baltzis et al. (2001).

Figures 5.7 and 5.8 show the measured removal efficiencies used in the calibration process as well as the removal efficiencies predicted by the model at different EBRT and superficial liquid velocities using the structured and non-structured media.

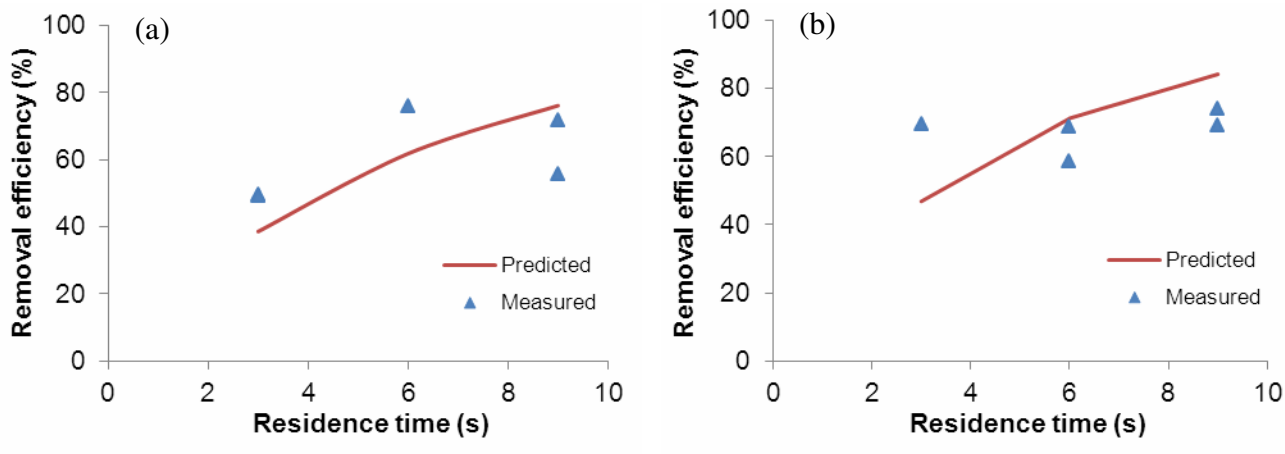


**Figure 5.7 The measured and predicted $NH_3$ removal efficiencies from the calibration process at different levels of empty bed residence time using the structured packing media with (a) 2.2 m $h^{-1}$; (b) 4.3 m $h^{-1}$ superficial liquid velocities.**

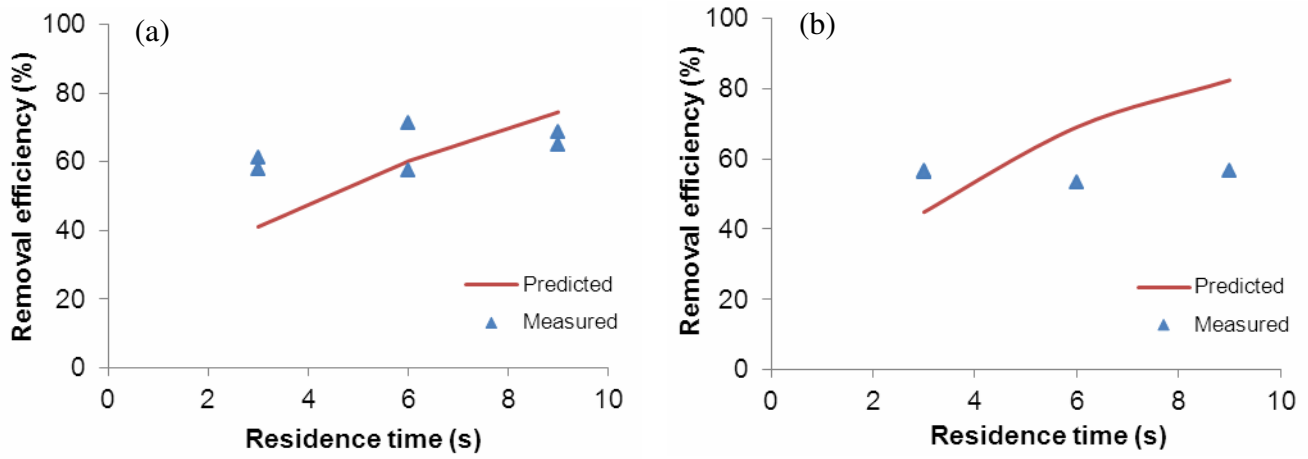


**Figure 5.8 The measured and predicted $NH_3$ removal efficiencies from the calibration process at different levels of empty bed residence time using the non-structured packing media with (a) 2.2 m $h^{-1}$; (b) 4.3 m $h^{-1}$ superficial liquid velocities.**

The predicted removal efficiencies were not different from the two types of media, consistent to what were observed in the experimental results. The model results also showed increasing removal efficiencies with residence time. Although this observation was not very evident in the measured data presented in Figures 5.7 and 5.8, this partly agreed to the general findings presented in Table 5.4. Contrary to the experimental results, the predicted removal efficiencies increase with the liquid superficial velocities. The experimental results might have been affected by the uneven liquid distribution in the system. Moreover, better predictions were obtained for lower superficial velocities.

The evaluation results for the calibration of the model (Table 5.9) were within the suggested evaluation limits presented in Table 5.3. The FB results, which are normalized values, indicated that the model applied to the structured media under-predicted (on average) the mean measured values by 4%, while when applied to the non-structured media under-predicted by 1%. The results show that there was a good agreement between the measured and predicted values for the removal efficiency.

**Table 5.9 Evaluation results for model calibration.**

| Evaluation parameter | Evaluation result | |
|---|---|---|
| | Structured media | Non-structured media |
| NMSE | 0.14 | 0.16 |
| FB | -0.04 | -0.01 |

### 5.8.5 Validation

Figures 5.9 and 5.10 show the measured and predicted $NH_3$ removal efficiencies at the different levels of residence time for both the structured and the non-structured media using liquid superficial velocities of 2.2 and 4.3 m $h^{-1}$. The model and experimental results presented relationships similar to those obtained from the calibration. Consistent with the experimental results, there was no remarkable difference in the predicted removal efficiencies from the two types of media. The experimental removal efficiencies shown in Figure 5.10b appear stable despite the increase in residence time probably due to the uneven liquid distribution in the treatment system. The standard error of the measured data utilized in the calibration and validation ranged from 0.1 to 9.1. Further, the model predicted an increase in removal efficiency as residence time and velocity were increased.

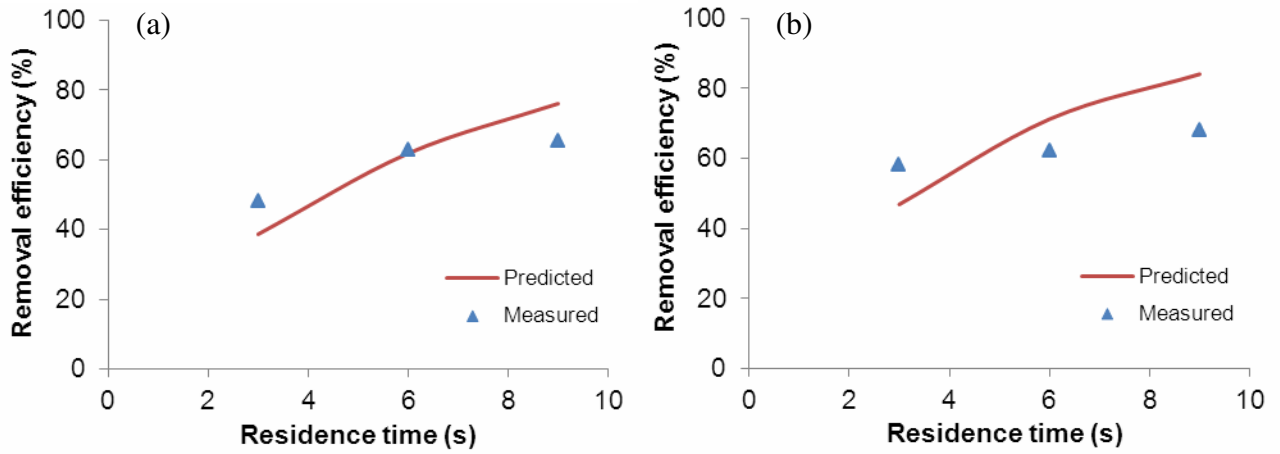


**Figure 5.9 The measured and predicted $NH_3$ removal efficiencies (RE) at different levels of residence time using the structured packing media with (a) 2.2 m $h^{-1}$; (b) 4.3 m $h^{-1}$ liquid superficial velocities.**

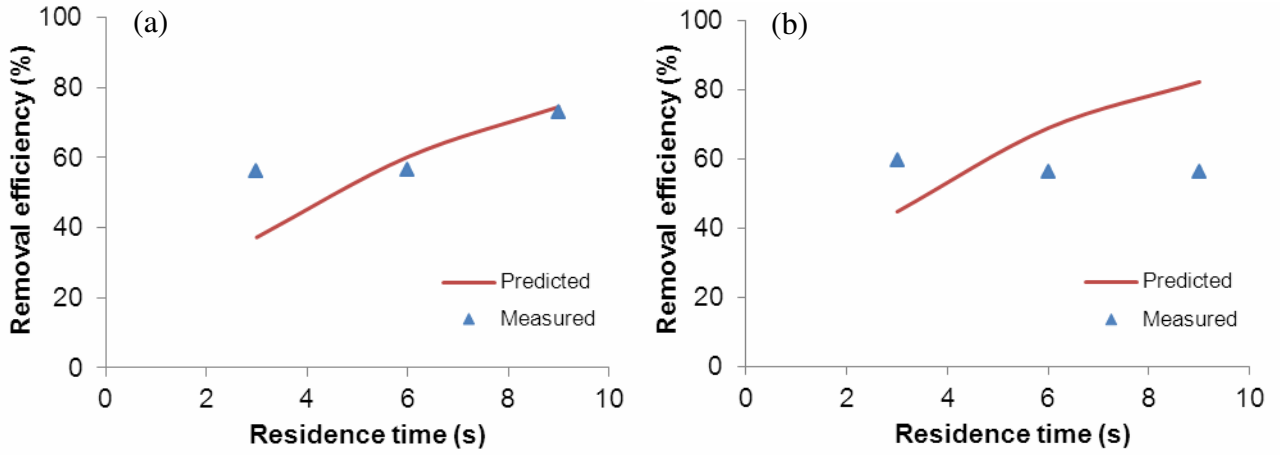


**Figure 5.10 The measured and predicted $NH_3$ removal efficiencies (RE) at different levels of residence time using the non-structured packing media with (a) 2.2 m $h^{-1}$; (b) 4.3 m $h^{-1}$ liquid superficial velocities.**

The evaluation results for the model validation using both the structured and the non-structured media are presented in Table 5.10. Again, the results were within the suggested evaluation limits listed in Table 5.3. A relatively better prediction was obtained for the structured media than for the non-structured media. Based on the FB results, the model under-predicted (on

average) the mean measured data by 1% for the structured media and under-predicted the measured values by 7% for the non-structured media. Cortus (2006) obtained NMSE values from 0.02 to 1.74 and FB values from -0.01 to 0.68 in her ACES model.

**Table 5.10 Evaluation results for model validation.**

| Evaluation parameter | Evaluation result | |
|---|---|---|
| | Structured media | Non-structured media |
| NMSE | 0.07 | 0.12 |
| FB | -0.01 | -0.07 |

The results showed that the calibrated and validated model can be potentially used to simulate the performance of biotrickling filters in removing ammonia from pig barn air. The difference between the measured and model results would not be significant if one considers the many assumptions made in the model equations as well as on the probable errors made in determining the model parameters.

## 5.9 SUMMARY AND CONCLUSIONS

A mathematical model used to simulate the removal of ammonia from swine facility air by a cross-flow biotrickling filter was developed. A sensitivity analysis was conducted to identify the governing processes and the relevant parameters affecting the treatment process. The results of the sensitivity analysis showed that the gas diffusion coefficient, wetted fraction of the surface area, gas mass transfer coefficient, gas and liquid flow rates, residence time (bed length), total surface area, nominal packing diameter, and the pH significantly influence the removal of $NH_3$ from the gas phase. The results indicate that the removal of $NH_3$ in biotrickling filters is greatly influenced by the factors that affect the gas-liquid mass transfer.

The evaluation parameters for both calibration and validation were within the suggested evaluation limits specified in the Standard Guide for Statistical Evaluation of Indoor Air Quality Models. When model predicted results were compared with the measured data, the model's prediction errors were within ±1 to 4% for the structured media and ±1 to 7% for the non-structured media. The results indicate that the model can be used to predict the performance of biotrickling filters in removing $NH_3$ from the air exhausted from pig buildings.

## 5.10 REFERENCES


Aranberri-Askargorta, I., T. Lampke and A. Bismarck. 2003. Wetting behavior of flax fibers as reinforcement for polypropylene. *Journal of Colloid and Interface Science* 263: 580-589.

Armeen, A., J.J.R. Feddes, J.J. Leonard and R.N. Coleman. 2008. Biofilters to treat swine facility air: Part 1. Nitrogen mass balance. *Canadian Biosystems Engineering* 50: 6.21-6.27.

ASTM. 2003. Standard guide for statistical evaluation of indoor air quality models. D5157-97 (Reapproved 2003). West Conshohocken, PA: ASTM International.

Baltzis, B.C., C.J. Mpanias and S. Bhattacharya. 2001. Modeling the removal of VOC mixtures in biotrickling filters. *Biotechnology and Bioengineering* 72(4): 389-401.

Baquerizo, G., X. Gamisans, D. Gabriel and J. Lafuente. 2007. A dynamic model for ammonia abatement by gas-phase biofiltration including pH and leachate modelling. *Biosystems Engineering* 97: 431-440.

Baquerizo, G., J.P. Maestre, T. Sakuma, M.A. Deshusses, X. Gamisans, D. Gabriel and J. Lafuente. 2005. A detailed model of a biofilter for ammonia removal: Model parameters analysis and model validation. *Chemical Engineering Journal* 113: 205-214.

Bettelheim, F.A., W.H. Brown, M.K. Campbell and S.O. Farrell. 2010. *Introduction to General, Organic, and Biochemistry*, 9th edition. California, USA: Cengage Learning, Inc.

Blattberg, R.C., B.D. Kim and S.A. Neslin. 2008. Statistical issues in predictive modeling. In *Database Marketing: Analyzing and Managing Customers,* ed. J. Eliashberg, 291-322. New York, USA: Spinger Science + Business Media.

Chen, Y.X., J. Yin and K.X. Wang. 2005. Long-term operation of biofilters for biological removal of ammonia. *Chemosphere* 58: 1023-1030.

Chou, M.S. and C.H. Wang. 2007. Treatment of ammonia in air stream by biotrickling filter. *Aerosol and Air Quality Research* 7(1): 17-32.

Chung, Y.C. and C. Huang. 1998. Biotreatment of ammonia in air by an immobilized *Nitrosomonas europaea* biofilter. *Environmental Progress* 17: 70-76.

Clark, O.G., S. Moehn, J.D. Price, Y. Zhang, W.C. Sauer, B. Morin, J.J. Feddes, J.J. Leonard, J.K.A. Atakora, R.T. Zijlstra, I. Edeogu and R.O. Ball. 2006. Diet manipulation to control odor and gas emissions from swine production. In *Climate Change and Managed Ecosystems*, ed. J.S. Bhatti, R. Lal, M.J. Apps and M.A. Price, 295-316. Florida, USA: CRC Press Taylor and Francis Group.

Clugston, M. and R. Flemming. 2000. *Advanced Chemistry*. New York, USA: Oxford University Press.

Cortus, E.L. 2006. A dynamic model of ammonia production within grow-finish swine barns. Unpublished Ph.D. dissertation. Saskatoon, Saskatchewan: Department of Agricultural and Bioresource Engineering, University of Saskatchewan.

Cox, H.H.J. and M.A. Deshusses. 1998. Biological waste air treatment in biotrickling filters. *Current Opinion in Biotechnology* 9: 256-262.

Devinny, J.S., M.A. Deshusses and T.S. Webster. 1999. *Biofiltration for Air Pollution Control.* USA: CRC Press LLC.

Devinny, J.S. and J. Ramesh. 2005. A phenomenological review of biofilter models. *Chemical Engineering Journal* 113: 187-196.

Dvorak, B.I., D.F. Lawler, J.R. Fair and N.E. Handler. 1996. Evaluation of the Onda correlations for mass transfer with large random packings. *Environmental Science and Technology* 30(3): 945-953.

Dunn, I.J. 2003. *Biological Reaction Engineering: Dynamic Modelling Fundamentals with Simulation Examples*. Germany: Wiley-VCH.

Dutta, B.K. 2007. *Principles of Mass Transfer and Separation Processes.* New Delhi, India: Prentice-Hall of India Private Limited.

EIFAC (European Inland Fisheries Advisory Commission). 1984. Water quality criteria for European freshwater fish: Report on nitrite and freshwater fish. EIFAC Technical paper 46. Rome, Italy: Food and Agriculture Organization of the United Nations.

EPA (Environmental Protection Agency). 1998. 1998 Update of ambient water quality criteria for ammonia. EPA 822-R-98-008. Washington, D.C., USA: Office of Water.

Fan, L.S., R. Leyva-Ramos, K.D. Wisecarver and B.J. Zehner. 1990. Diffusion of phenol through a biofilm grown on activated carbon particles in a draft-tube three-phase fluidized-bed bioreactor. *Biotechnology and Bioengineering* 35: 279-286.

Girard, M., M. Belzile, S.P. Lemay, J. Feddes, R. Hogue and S. Godbout. 2013. Innovative air treatment unit for swine exhaust air – Laboratory-scale tests. Paper No. CSBE13-116. Saskatchewan, Canada: CSBE/SCGAB.

Gullicks, H.A. and J.L. Cleasby. 1990. Cold-climate nitrifying biofilters: Design and operation considerations. *Water Environment Federation* 62(2): 50-57.

Guo, Z. and N.F. Roache. 2003. Overall mass transfer coefficient for pollutant emissions from small water pools under simulated indoor environmental conditions. *The Annals of Occupational Hygiene* 47(4): 279-286.

Hagedorn, C., A.R. Blanch and V.J. Harwood. 2011. *Microbial Source Tracking: Methods, Applications, and Case Studies*. USA: Spinger Science + Business Media.

Halder, G. 2009. *Introduction to Chemical Engineering Thermodynamics*. New Delhi, India: PHI Learning Private Limited.

Hekmat, D. and D. Vortmeyer. 1994. Modelling of biodegradation processes in trickle-bed bioreactors. *Chemical Engineering Science* 49(24A): 4327-4345.

Jensen, T.L. and M.J. Hansen. 2006. A biotrickling filter for removing ammonia and odour in ventilation air from a unit with growing-finishing pigs. In *Proceedings Workshop on Agricultural Air Quality*, 844-846. Washington, D.C., USA. June 5-8.

Jorio, H., G. Payre and M. Heitz. 2003. Mathematical modeling of gas-phase biofilter performance. *Journal of Chemical Technology and Biotechnology* 78: 834-846.

Kim, S. and M.A. Deshusses. 2003. Development and experimental validation of a conceptual model for biotrickling filtration of $H_2S$. *Environmental Progress* 22(2): 119-128.

Kim, S. and M.A. Deshusses. 2008. Determination of mass transfer coefficients for packing materials used in biofilters and biotrickling filters for air pollution control – 2: Development of mass transfer coefficients correlations. *Chemical Engineering Science* 63: 856-861.

Korner, S., S.K. Das, S. Veenstra and J.E. Vermaat. 2001. The effect of pH variation at the ammonium/ammonia equilibrium in wastewater and its toxicity to *Lemna gibba*. *Aquatic Botany* 71: 71-78.

Lantec Products, Inc. 2013. Plastic packing. http://www.lantecp.com/products/ (2013/09/06).

Martin, R.W.J, H. Li, J.R. Mihelcic, J.C. Crittenden, D.R. Lueking, C.R. Hatch and P. Ball. 2002. Optimization of biofiltration for odor control: Model calibration, validation, and applications. *Water Environment Research* 74 (1): 17-27.

Melse, R.W. and G. Mol. 2004. Odour and ammonia removal from pig house exhaust air using a biotrickling filter. *Water Science and Technology* 50(4): 275-282.

Melse, R.W., N.W.M. Ogink and W.H. Rulkens. 2009. Air treatment techniques for abatement of emissions from intensive livestock production. *The Open Agriculture Journal* 3: 6-12.

Mpanias, C.J. and B.C. Baltzis. 1998. An experimental and modeling study on the removal of mono-chlorobenzene vapor in biotrickling filters. *Biotechnology and Bioengineering* 59: 328-343.

Neilsen, D.R., A.J. Daugulis and P.J. McLellan. 2007. Dynamic simulation of benzene vapor treatment by a two-phase partitioning bioscrubber – Part 1: Model development, parameter estimation, and parametric sensitivity. *Biochemical Engineering Journal* 36: 239-249.

Neilsen, L.P., S. Juhler, N.P. Revsbech, L.B. Guldberg, K. Soerensen and L.D.M. Ottosen. 2008. Function of biofilters removing ammonia from pig house ventilation air. In *Proceedings of the 31August-4 September 2008 ASABE Conference: Livestock Environment VIII*, 63-66. Iguassu Falls, Brazil. August 31-September 4.

Okkerse, W.J.H., S.P.P. Ottengraf, B. Osinga-Kuipers and M. Okkerse. 1999. Biomass accumulation and clogging in biotrickling filters for waste gas treatment. Evaluation of a dynamic model using dichloromethane as a model pollutant. *Biotechnology and Bioengineering* 63(4): 418-430.

Onda, K., H. Takeuchi and Y. Okumoto. 1968. Mass transfer coefficients between gas and liquid phases in packed columns. *Journal of Chemical Engineering of Japan* 1: 56-62.

Ozis, F., A. Bina, and J.S. Devinny. 2005. Future prospects of biotechnology for odor control. In

*Biotechnology for Odour and Air Pollution Control*, ed. Z. Shareefdeen and A. Singh, 383-399. Germany: Springer-Verlag.

Pavlostathis, S.G. 2006. Basic concepts of biological processes. In *Advanced Biological Treatment Processes for Industrial Wastewaters: Principles and Applications*, ed F.J. Cervantes, S.G. Pavlostathis and A.C. Van Haandel, 16-46. UK: IWA Publishing.

Roustan, M. 2006. Wet scrubbing for the removal of $NH_3$ from waste gases. In *Waste Gas Treatment for Resource Recovery*, ed. P.N.L. Lens, C. Kennes, P. Le Cloirec and M.A. Deshusses, 305-319. London, UK: IWA Publishing.

Sanchez, O., E. Aspe, M.C. Marti and M. Roeckel. 2005. Rate of ammonia oxidation in a synthetic saline wastewater by a nitrifying mixed-culture. *Journal of Chemical Technology and Biotechnology* 80: 1261-1267.

Schnelle, K.B. and C.A. Brown. 2002. *Air Pollution Control Technology Handbook*. Florida, USA: CRC Press LLC.

Scholtens, R. and T.G.M. Demmers. 1991. Biofilters and air scrubbers in the Netherlands. In *Odour and Ammonia Emissions from Livestock Farming*, ed. V.C. Nielsen, J.H. Voorburg and P. L'Hermit, 100-105. New York, USA: Elsevier Science Publishing Co. Inc.

Shareefdeen, Z., B. Herner and A. Singh. 2005. Biotechnology for air pollution control – An overview. In *Biotechnology for Odour and Air Pollution Control*, ed. Z. Shareefdeen and A. Singh, 3-15. Germany: Springer-Verlag.

Sharvelle, S., M. Arabi, E. McLamore and M.K. Banks. 2008a. Model development for biotrickling filter treatment of graywater simulant and waste gas. I. *Journal of Environmental Engineering* 134(10): 813- 824.

Sharvelle, S., M. Arabi, E.M.K. Banks, and F. Mannering. 2008b. Model sensitivity analysis for biotrickling filter treatment of graywater simulant and waste gas. II. *Journal of Environmental Engineering* 134(10): 826- 834.

Tchobanoglous, G., F.L. Burton, H.D. Stensel and Metcalf & Eddy. 2003. *Wastewater Engineering: Treatment and Reuse*. USA: McGraw-Hill.

Trucano, T.G., L.P. Swiler, T. Igusa, W.L. Oberkampf and M. Pilch. 2006. Calibration, validation, and sensitivity analysis: What's what. *Reliability Engineering and System Safety* 91: 1331-1357.

van Haandel, A.C. and J.G.M. van der Lubbe. 2012. *Handbook of Biological Wastewater Treatment: Design and Optimisation of Activated Sludge Systems*, 2nd edition. London, UK: IWA Publishing.

Vayenas, D.V., S. Pavlou and G. Lyberatos. 1997. Transient modeling of trickling filters for biological ammonia removal. *Environmental Modeling and Assessment* 2: 221-226.

Werth, C.J. 2005. Equilibrium partitioning and mass transfer of organic chemicals leached from recycled hazardous waste materials. In *Environmental Impact Assessment of Recycled Wastes on Surface and Ground Waters – Engineering Modeling and Sustainability*, ed. T.A. Kassim, 1-30. Germany: Springer-Verlag.

Zhang, R.H., D.L. Day, L.L. Christianson and W.P. Jepson. 1994. A computer model for predicting ammonia release rates from swine manure pits. *Journal of Agricultural Engineering Research* 58: 223-229.

# Chapter 6
# Simulation Study on Ammonia Removal in a Cross-flow Biotrickling Filter using a Steady-state Model

## 6.1 VERSION PRESENTED IN A CONFERENCE

A similar version of this chapter was presented at the conference of the Canadian Society for Bioengineering (CSBE) in July 7-10, 2013 in Saskatoon, Saskatchewan, Canada.

- Martel, M., S.P. Lemay, B. Predicala, M. Girard, R. Hogue, M. Belzile, J. Feddes and S. Godbout. 2013. Simulation study on ammonia removal in a biotrickling filter using a steady-state model. CSBE Paper No. 13-081. Presented at the CSBE Technical Conference. Saskatoon, Saskatchewan, Canada. July 7-10, 2013.

## 6.2 CONTRIBUTION OF THE PH.D. CANDIDATE

This present study identified the governing processes involved in the removal of ammonia in biotrickling filters, which are important in process design and optimization. Interpretation of results and manuscript writing were performed by the candidate while editorial inputs were provided by Dr. Stéphane P. Lemay and Dr. Bernardo Predicala as well as by Dr. Matthieu Girard of the Research and Development Institute for the Agri-Environment (IRDA).

## 6.3 CONTRIBUTION OF THIS PAPER TO THE OVERALL STUDY

Using the calibrated and validated model discussed in Chapter 5, this simulation study was conducted to evaluate the behaviour of biotrickling filters in removing ammonia from swine facility air when various process and design parameters vary in a certain range. As mentioned earlier, results from this study helped identify the governing processes involved in the removal of

ammonia in biotrickling filters, and thus, were relevant to the realization of the overall research objective.

## 6.4 ABSTRACT

A simulation study was conducted using a calibrated and validated model for ammonia removal in a cross-flow biotrickling filter. Simulation runs were performed to evaluate the relationships of some of the process and design parameters (i.e. gas flow rate, liquid flow rate/superficial velocity, gas and liquid inlet concentrations, empty bed residence time (EBRT), wetted fraction of the surface area, and pH) with reactor performance. Ammonia removal in the gas phase was found to increase with the liquid flow rate and EBRT. However, there seems to be an optimum liquid flow rate that must be applied to biotrickling filters since further increases in flow rate did not improve the removal efficiency. Removal efficiency also increased with EBRT and gas flow rate; however, the increases were more significant at lower EBRT. Since ammonia is a very soluble gas, the removal efficiency was not affected by the gas and liquid inlet concentrations in the studied range. In addition, the removal efficiency was found to increase with the wetted fraction of the surface area of the packing media. Under similar operating conditions, two types of packing media (with different total specific surface area) obtained similar removal efficiencies when both were equally wetted. Further, lower removal efficiencies were obtained at higher pH values, particularly at pH above 8.

## 6.5 INTRODUCTION

One of the advantages of using a mathematical model is the ability to easily perform simulations to evaluate how various process and design parameters relate to reactor performance or how these parameters relate to each other. Mathematical models are cost effective and rapid in

conducting virtual experiments (Deshusses and Shareefdeen 2005), and they are particularly important in processes such as optimization and scaling-up.

There are a number of simulation studies published in the literature, however, only a few of them (Baquerizo et al. 2005; Sharvelle et al. 2008b) deal with ammonia ($NH_3$) removal in biofilters and biotrickling filters. In the study conducted by Baquerizo et al. (2005), the physico-chemical parameters (e.g. specific surface area of the packing media, gas mass transfer coefficient, and pH) were found to have notable impacts on ammonia removal in biofilters. On the other hand, Sharvelle et al. (2008b) found that the removal of ammonia from the gas phase would not be a challenge to biotrickling filter operations due to its high solubility in water. However, they observed that the wetted fraction of the packing media is highly significant in the removal of ammonia from the liquid phase. In addition, they also found that, though the liquid recirculation flow rate had little effect on liquid contaminant removal, it is important to maintain adequate liquid recirculation through the reactor to increase the wetted area within the system and improve gas contaminant removal.

This study presents the simulation runs performed using the model discussed in Chapter 5, which was developed, calibrated, and validated for the removal of ammonia from pig barn exhaust air using a cross-flow biotrickling filter. The objective of this study was to evaluate how the system behaves in relation to changes in process and design parameters and to understand how these parameters may affect the performance of the system or influence its design. This information can be useful in designing a new treatment system or in improving the performance of an existing one.

## 6.6 METHODS

Simulations were performed to evaluate the behaviour of biotrickling filters in removing ammonia from swine exhaust air when various process and design parameters are changed. The parameters evaluated in this simulation study were gas flow rate, liquid flow rate/superficial velocity, gas and liquid inlet concentrations, empty bed residence time (EBRT), wetted surface area of the packing media, and pH. All these parameters (except the wetted surface area) are important design parameters. The wetted surface area, which is an intrinsic parameter, was included in the simulation because it has been found in the sensitivity analysis conducted in Chapter 5 as well as in other related studies that this parameter significantly affects the performance of biotrickling filters. A simulation study to evaluate the impact of temperature was not conducted since the sensitivity analysis showed that temperature does not have a significant impact on ammonia removal; it should be noted, however, that the model considered only the impact of temperature on ammonia-ammonium equilibrium and ammonia dissociation and not on microbial activity.

The ranges of the values applied in the simulations were within ± 25% of the values used in the model calibration and validation; however, the simulations involving the gas inlet concentration, liquid superficial velocity, EBRT, and wetted surface area fraction were conducted in a wider range of values to see the effects or variations on a larger scale. Only two values were chosen for the liquid inlet concentration (120 and 1800 g $NH_4^+$-N $m^{-3}$) since their results did not have any remarkable difference. These values represent the lower and higher liquid concentrations used in the calibration and validation of the model. Table 6.1 shows the parameters, with their corresponding values, used in the simulations. This study was applied to two types of packing media: (1) structured packing media with a specific surface area of 984 $m^2$ $m^{-3}$ and (2) non-structured packing media with a specific surface area of 242 $m^2$ $m^{-3}$.

**Table 6.1 Parameters used in the simulation study.**

| Parameter | Unit | Value | |
|---|---|---|---|
| | | Calibration/Validation | Simulation |
| Gas flow rate | $m^3\ h^{-1}$ | 302 | 200 - 400 |
| Liquid superficial velocity | $m\ h^{-1}$ | 2.2 and 4.3 | 0.6 - 5.4 |
| Gas inlet concentration | $ppm_v$ | 5 - 10 | 1 - 45 |
| Liquid inlet concentration | $g\ NH_4^+\text{-}N\ m^{-3}$ | 150 - 1500 | 120 and 1800 |
| Wetted surface area | % | 10 - 15[a]; 15 - 30[b] | 0.01 - 100 |
| Specific surface area | $m^{-1}$ | 242 and 984 | 242 and 984 |
| EBRT | s | 3 - 9 | 1 - 13 |

[a] structured media; [b] non-structured media.

It should be noted that the bed length was adjusted to obtain the same EBRT for the different gas flow rates or to obtain different EBRT for the same gas flow rate. This means that as the gas flow rate or the EBRT was increased, the bed length was correspondingly increased.

The removal of ammonia from the gas phase at different simulation runs were evaluated in terms of removal efficiency (RE; %) and elimination capacity (EC, $g\ m^{-3}_{bed}\ h^{-1}$) given in equations 6.1 and 6.2, respectively:

$$RE = \frac{C_{Gin} - C_{Gout}}{C_{Gin}} \times 100 \tag{6.1}$$

$$EC = \frac{(C_{Gin} - C_{Gout}) \times Q_G}{V_f} \tag{6.2}$$

where $C_{Gin}$, $C_{Gout}$ = ammonia gas inlet and exhaust concentrations, respectively ($g\ m^{-3}$),

$Q_G$ = gas flow rate ($m^3\ h^{-1}$),

$V_f$ = filter bed volume ($m^3$).

## 6.7 RESULTS AND DISCUSSION

### 6.7.1 Concentration profiles

The concentration profiles of ammonia in the gas phase along the length (L) of the bed and in the liquid phase along the height ($H_t$) of the bed are shown in Figure 6.1. These are the simulation results using a gas inlet concentration of 8.5 $ppm_v$, liquid inlet concentration of 1000 g $N\text{-}NH_4^+$ $m^{-3}$ (1000.63 g TAN [total ammonia nitrogen] $m^{-3}$), gas flow rate of 302.4 $m^3$ $h^{-1}$, liquid superficial velocity of 4.3 m $h^{-1}$, EBRT of 9 s, pH 7, temperature of 17°C, and a structured packing media. These values were within the ranges used in the calibration of the model.

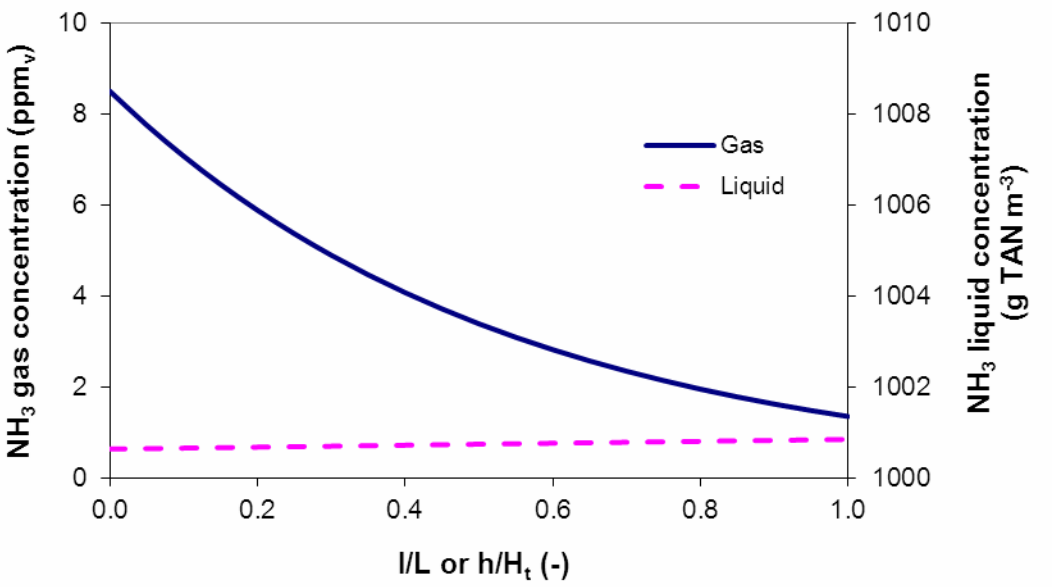


**Figure 6.1 $NH_3$ concentration profiles along the length and height of the filter bed (*l* is any position along the length *L* and *h* is any position along the height $H_t$ of the bed).**

As expected, ammonia concentration in the gas phase decreases as the air moves through the length of the bed. At these simulated conditions, the model predicts 84% ammonia removal as can be seen from Figure 6.1. On the other hand, the ammonia concentration in the liquid phase

is almost constant as it flows down the filter bed. This is due to the cross flow direction of the gas and liquid streams as well as on the boundary condition set for the mass balance in the liquid phase, where the exit and inlet liquid concentrations are assumed equal since the liquid is recirculated in the system. Since the gas and liquid streams are in cross-flow configuration, the liquid concentration profile looks different from that of the co-current and counter-current configurations (Sharvelle et al. 2008a; Ockeloen et al. 1996).

Figure 6.2 shows the concentration profiles within the biofilm at the top-exit and bottom-entrance sections of the filter bed.

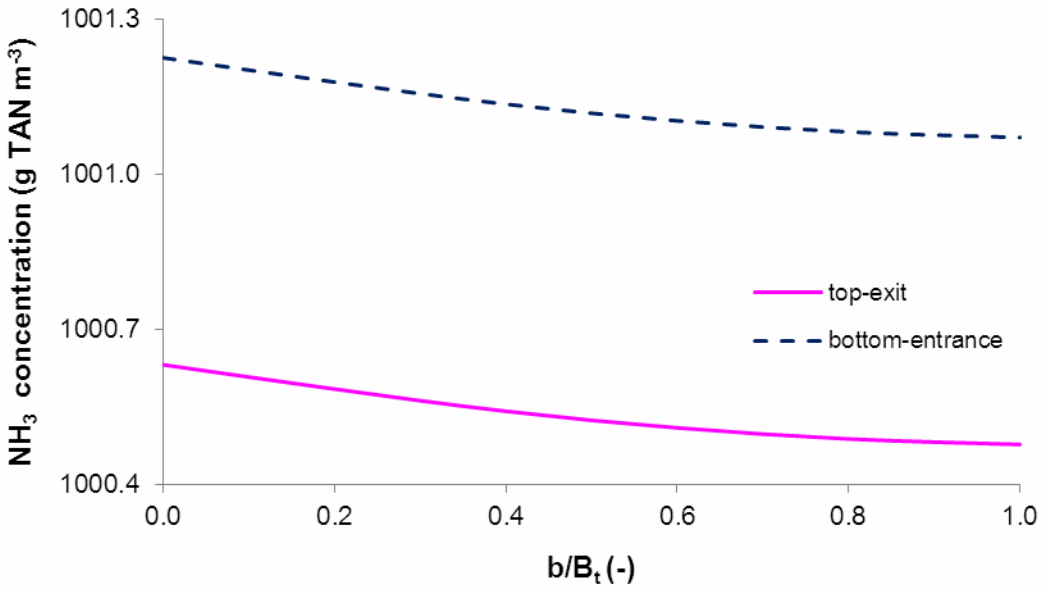


**Figure 6.2 $NH_3$ concentration profiles within the biofilm at the top-exit and bottom-entrance sections of the filter bed (*b* is any position along the biofilm depth; $B_t$ is the biofilm thickness).**

As shown in Figure 6.2, the concentration decreases within the biofilm depth, i.e. from the liquid-biofilm interface (at position $b = 0$) to the media support (at position $b = B_t$). Moreover, the degradation rate at the top-exit section looks similar to the degradation rate at the

bottom-entrance section. Since there is only little variation in liquid concentration at any section in the bed, as shown in Figure 6.1, and also due to the model assumption that all the biokinetic parameters are constant within the system including biofilm thickness, the degradation rate is the same at any parallel section in the biofilm.

### 6.7.2. Liquid flow rate

Figures 6.3 and 6.4 are the simulation results for both structured and non-structured media, respectively, using a gas inlet concentration of 8.5 $ppm_v$, liquid inlet concentration of 1000 g $N\text{-}NH_4^+$ $m^{-3}$, gas flow rate of 302.4 $m^3\ h^{-1}$, pH 7, temperature of 17°C, and liquid flow rates varying from 0.5 to 4.5 $m^3\ h^{-1}$ (0.6 to 5.4 m $h^{-1}$ superficial velocities).

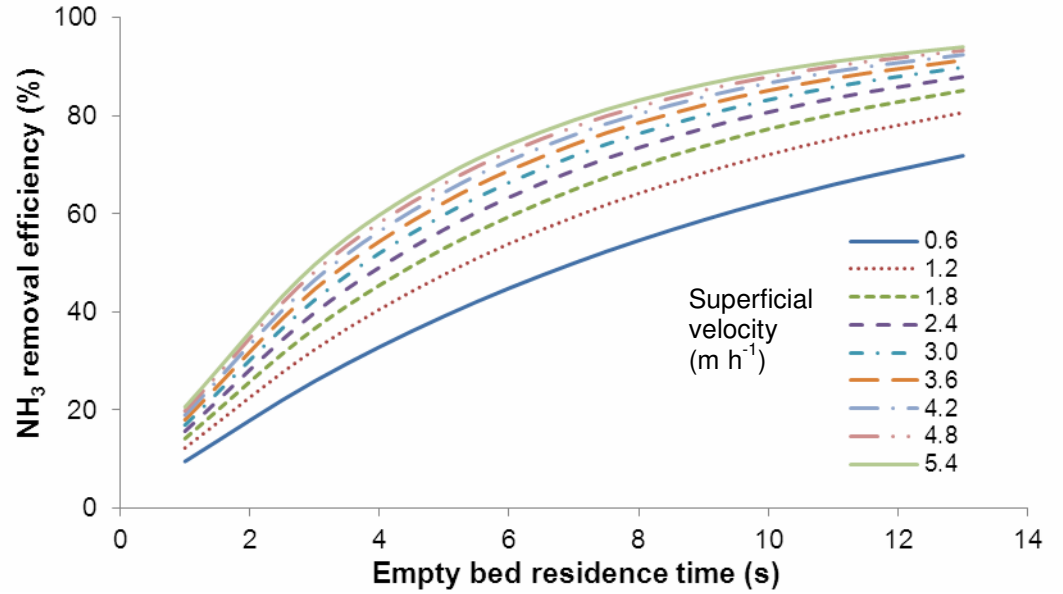


**Figure 6.3 $NH_3$ removal efficiency at different superficial liquid velocities and levels of residence time using structured packing media.**

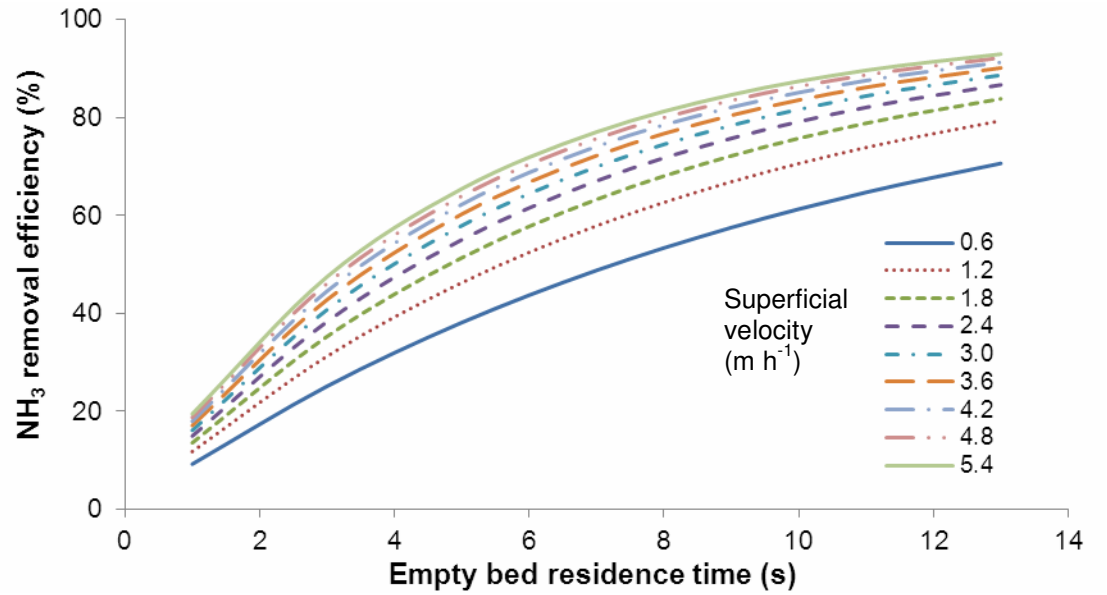


**Figure 6.4 $NH_3$ removal efficiency at different superficial liquid velocities and levels of residence time using non-structured packing media.**

Figures 6.3 and 6.4 show no remarkable difference in the results between the structured and non-structured media despite the difference in their characteristics (e.g. specific surface area, nominal packing diameter, packing configuration). It should be noted that the model was calibrated with data where both types of media showed no significant difference in removal efficiencies. At the same liquid flow rate and residence time, a packing material which has a higher total surface area has an almost similar removal efficiency with one which has lower surface area (four times lower). This means that at similar operating conditions, total surface area may not be a critical factor to achieve higher efficiencies.

As shown in the figures, ammonia removal increases with liquid velocity and EBRT. These results are expected because higher EBRT allows longer contact between the gas and liquid phase and higher liquid velocity results in greater convective transport. Since the liquid flow rate is directly related to the wetted surface area as shown in equation 5.19, higher liquid

velocity would enhance the wetting of the system. However, further increases in liquid velocity did not significantly improve the removal efficiency. A similar observation was also obtained by Popat and Deshusses (2010) in their biotrickling filtration study on trichloroethene removal. According to these authors, relatively higher liquid velocities could lower the contact area for the gas and liquid because both streams may follow preferential flow paths at these conditions. Further, liquid velocity influences the wetted fraction of the packing media, thereby affecting the path at which the pollutant is transferred (Kim and Deshussses 2003). Increases in liquid flow rates could also result in thicker liquid film at the gas-liquid interface, thereby limiting the gas-liquid mass transfer.

In addition, at higher liquid velocities, increasing the EBRT did not remarkably improve the removal efficiency. This could be due to the mass transfer limitations (e.g. preferential gas and liquid flow paths, decreased interfacial area for the gas-liquid mass transfer or decreased wetted surface area, thicker liquid film) that could occur at higher liquid flow rates. Further, the results also show that incremental increase in removal efficiency was more significant when EBRT was increased from 1 to 3 s. One has to be aware that the model was validated at EBRT from 3 to 9 s, and that applying the model outside this range could possibly affect the accuracy of the results. This also applies to liquid velocities outside the 2.2 to 4.3 m $h^{-1}$ range.

Further, simulation results also show that when both media were subjected to same liquid flow rate, the non-structured media obtained higher wetted surface area fraction. Sharvelle et al. (2008b) stated that if the specific surface area of a packing material is high, a higher liquid flow rate is required to achieve the same wetted surface area fraction. This means that in order to obtain similar wetted surface area fraction for both media, the structured media would require higher liquid flow rate.

One important implication that can be derived from the results of this simulation is that to achieve a certain level of removal efficiency, one could either choose a higher EBRT and lower liquid flow rate or a lower EBRT and higher liquid flow rate. However, one has to consider also that there might be an optimum liquid flow rate and EBRT that must be applied to the system. In addition, factors such as cost of the packing media, available land area for the treatment unit, and pumping cost to recirculate the liquid would also have to be considered in the decision making process. Further, it is important to note that the liquid flows through the bed by gravity, and that excessive liquid volume could possibly cause flooding in the system.

### 6.7.3 Gas flow rate

Figures 6.5 and 6.6 show the resulting removal efficiencies using the structured and non-structured packing media, respectively, at constant gas inlet concentration but at various EBRT as the gas flow rate was varied. These are the results of using a gas inlet concentration of 8.5 $ppm_v$, liquid inlet concentration of 1000 g $N\text{-}NH_4^+$ $m^{-3}$, liquid superficial velocity of 2.2 m $h^{-1}$, pH 7, temperature of 17°C, and gas flow rates varying from 200 to 400 $m^3$ $h^{-1}$. Again, almost similar results were obtained from both types of packing media.

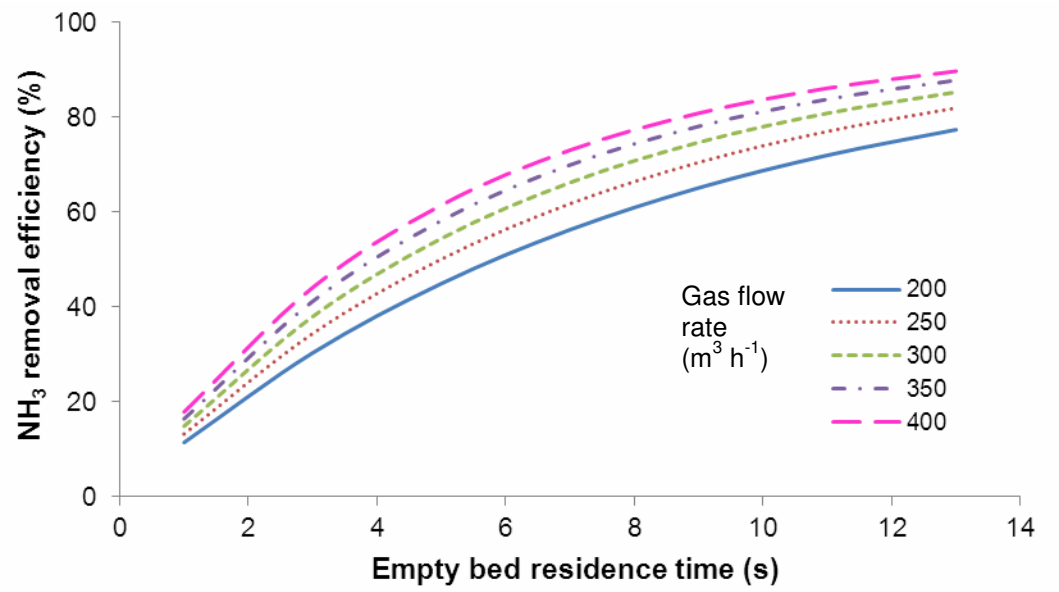


**Figure 6.5 $NH_3$ Removal efficiency at various gas flow rates and levels of residence time using structured packing media.**

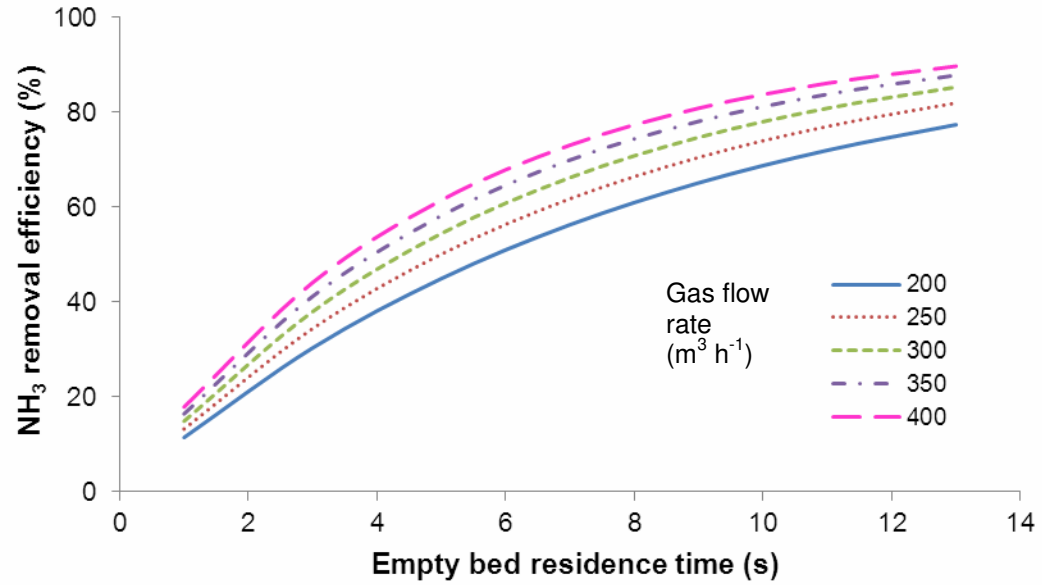


**Figure 6.6 $NH_3$ Removal efficiency at various gas flow rates and levels of residence time using non-structured packing media.**

As expected, the removal efficiency increases with EBRT and gas flow rate. For the same reason as in the effect of the liquid flow rate given above, higher EBRT allows longer contact between the gas and liquid phase and higher gas flow rate enhances convective transport, thus improving mass transfer. However, the increases in the removal efficiency were more significant at lower EBRT (1 to 3 s). Results of the study conducted by Chou and Wang (2007) showed a rapid increase of ammonia removal in a biotrickling filter when the EBRT was increased from 0.5 to 0.98 min; however, beyond this range the removal efficiency became stable. This could be due to ammonia's high solubility in water where almost all of the ammonia is already dissolved at the sections near the inlet of the bioreactor as it comes in contact with the trickling liquid. The experimental results obtained by Chou and Wang (2007) showed that almost all of the ammonia in the incoming air was absorbed at the first one-fifth of the height of the column.

In a real barn system, EBRT varies as air of variable flow rates flows through a fixed reactor volume. Thus, Figures 6.7a and 6.7b compare the removal efficiencies and elimination capacities, respectively, of three reactors with three different bed sizes (length of 0.3, 0.6, and 0.9 m) each treating air of variable flow rates (200 to 400 $m^3$ $h^{-1}$). The results show that the 0.9 m-long bioreactor had the highest removal efficiency, though the trend indicates that the increases in the removal efficiency become smaller as the reactor becomes longer. In terms of the elimination capacity, the 0.3 m-long bioreactor provided the highest elimination capacity than the other two reactors. Furthermore, the increases in the elimination capacity at higher gas flow rates were more significant in the 0.3 m-long bioreactor than in the other two reactors. Since ammonia is a very soluble gas, most of its amount in the gas phase was already absorbed in the first few sections of the reactor, consistent with observations by Chou and Wang (2007). However, it is also important to realize that even if a shorter bed is more favourable in terms of elimination capacity, the bed could not be made shorter to achieve the same removal efficiency

since adequate surface area is required to support sufficient amount of biomass to oxidize the substrate and keep the liquid-phase concentration low (Ockeloen et al. 1996). Moreover, one has to consider that the air exhausted from pig barns are also composed of less soluble components that may favour longer filter beds (or EBRT).

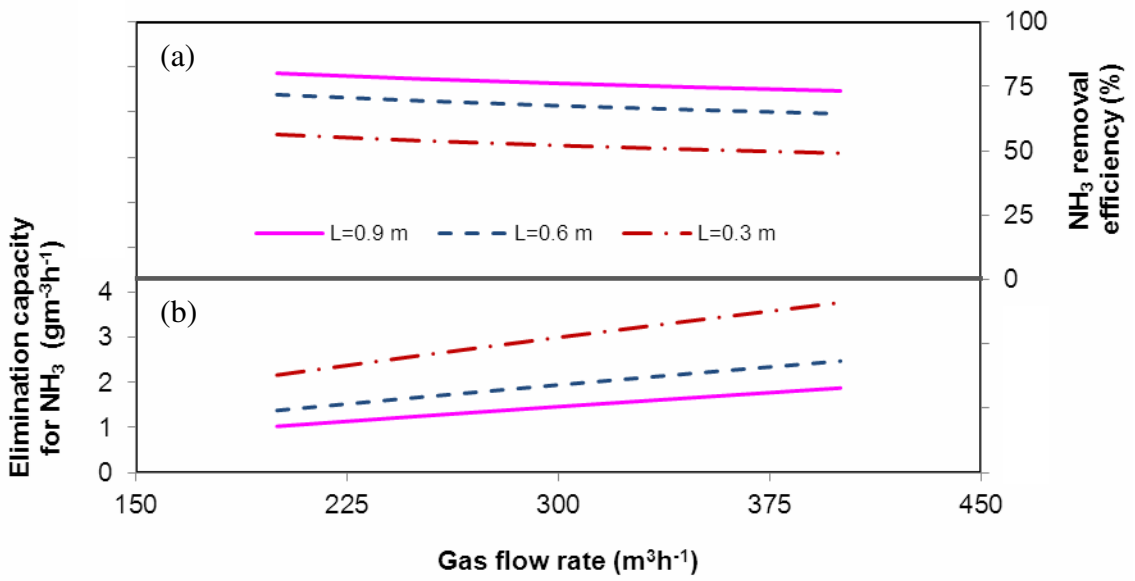


**Figure 6.7 (a) Removal efficiency; (b) elimination capacity for $NH_3$ at various gas flow rates and bed lengths.**

The predicted elimination capacities shown in Figure 6.7b may be smaller compared with those obtained from other reported biofiltration studies (Taghipour et al. 2008; Sorial et al. 2001); however, it should be noted that this simulation study was conducted at 8.5 $ppm_v$ gas inlet concentration, which is a lot lower compared than those applied in the above-mentioned related studies. Taghipour et al. (2008) obtained a maximum elimination capacity of 9.85 g $NH_3$ $m^{-3}$ $h^{-1}$ at an inlet concentration of 236 $ppm_v$. Furthermore, elimination capacity increases with loading rate or inlet concentration until maximum efficiency is reached, beyond which removal rate starts to decline.

The information obtained from these results can be useful in designing a biotrickling filter when removal efficiency, elimination capacity, and reactor size need to be optimized at the same time for a given range of gas flow rate. However, the model was calibrated and validated with only one value of gas flow rate (302 $m^3$ $h^{-1}$) and at EBRT of 3 to 9 s, and simulations with values other than these could probably affect the accuracy of the results.

### 6.7.4 Gas and liquid inlet concentrations

The effects of gas and liquid inlet concentrations on ammonia removal are presented in Figure 6.8. These are the results of using a gas flow rate of 302.4 $m^3$ $h^{-1}$, liquid superficial velocity of 2.2 m $h^{-1}$, EBRT of 6 s, pH 7, temperature of 17°C, gas inlet concentration varying from 1 to 45 $ppm_v$, two liquid inlet concentrations (120 and 1800 g $N\text{-}NH_4^+$ $m^{-3}$), and a structured packing media. These gas inlet concentrations are within the typical range of ammonia concentrations encountered in pig barns.

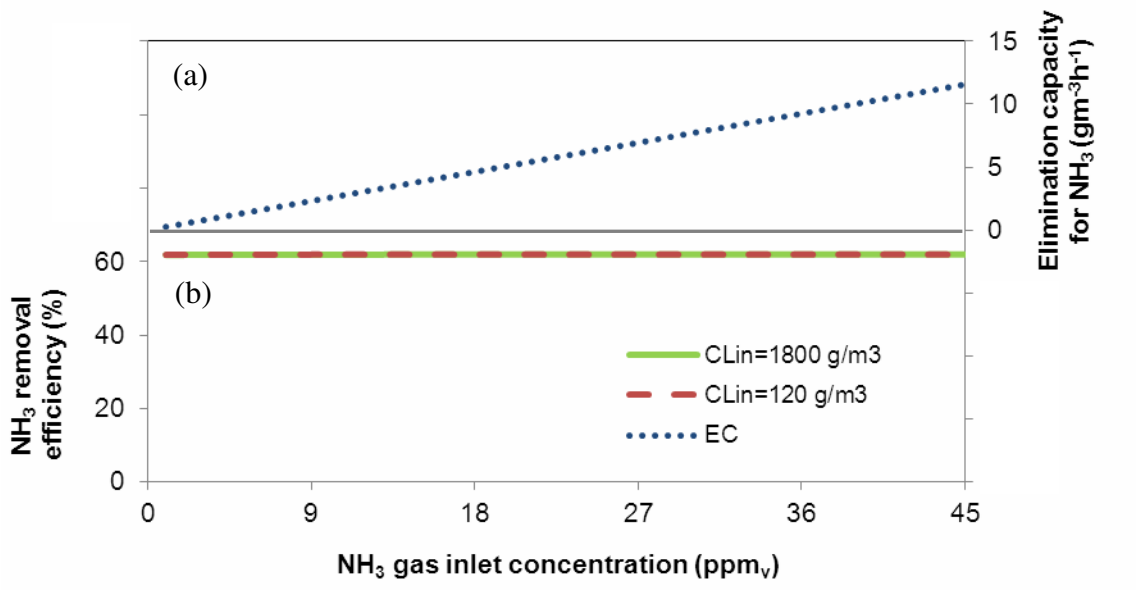


**Figure 6.8 (a) Elimination capacity for $NH_3$ with 1800 g $NH_4^+$-N $m^{-3}$ liquid inlet concentration; (b) $NH_3$ removal efficiency at various $NH_3$ gas and liquid inlet concentrations.**

The result shows that neither the gas nor the liquid concentration affect the removal efficiency (Figure 6.8b). A gas inlet concentration of 45 $ppm_v$ ammonia had almost the same removal efficiency than that of 1 $ppm_v$. Chung and Huang (1998) only observed a significant reduction in the removal efficiency when concentrations were above 100 $ppm_v$.

Liquid concentrations of 1800 and 120 g $NH_4^+$-N $m^{-3}$ also resulted in almost similar ammonia removal efficiency. This means that as long as the liquid concentration is below the equilibrium concentration, it does not greatly affect the removal efficiency. The results also indicate that factors other than the gas and liquid inlet concentrations have the most influence on the removal efficiency. Similar observations were also obtained by Sharvelle at al. (2008b).

In terms of elimination capacity, Figure 6.8a shows that within the simulated range of the gas inlet concentration, the maximum elimination capacity was not reached. This supports the previous observation that gas inlet concentration is not a limiting factor to the removal of ammonia. This is again due to the high solubility of ammonia in water.

### 6.7.5 Wetted surface area

Figure 6.9 shows the relationship between the wetted surface area of the packing media and the removal efficiency. These are the results of using a gas inlet concentration of 8.5 $ppm_v$, liquid inlet concentration of 1000 g N-$NH_4^+$ $m^{-3}$, gas flow rate of 302.4 $m^3\ h^{-1}$, liquid superficial velocity of 2.2 $m\ h^{-1}$, EBRT of 6 s, pH 7, temperature of 17$^oC$, and wetted surface area from 0.01 to 100%.

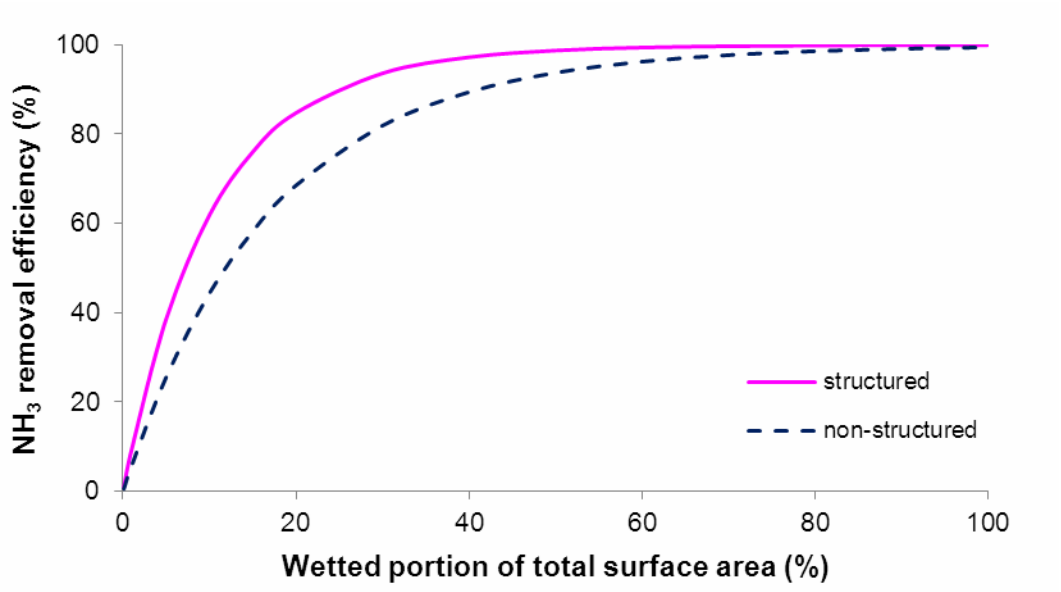


**Figure 6.9 Removal efficiency at various wetted surface area fraction using structured and non-structured media.**

The results show that when the wetted surface area was within 20% of the total surface area for the structured media or 40% for the non-structured media, the removal efficiency increased rapidly with increases in wetted surface area for both types of packing media. However, beyond these values, increases in the wetted surface area only produced very small improvements in the removal efficiency. Though at certain values of wetted surface area the removal efficiency using structured media was relatively higher than that of the non-structured media, the trend was almost similar for both media. The removal efficiencies from both types of packing media were not very different despite the big difference in their total specific surface area (specific surface area of the non-structured media was only 25% of that of the structured media). As discussed in Chapter 5, the higher surface area of the structured media was compensated by a lower gas mass transfer coefficient.

Baquerizo et al. (2005) and Sharvelle et al. (2008b) also observed significant impact of the wetted fraction of the packing media on ammonia removal. Due to ammonia's high solubility

in water, the primary removal mechanism from the gas phase is mass transfer; thus, wetting ratio is very significant. This implies that in the context of reactor design, the factors that affect the wetting of the packing media are extremely important.

One has to be aware also that the results could be affected by the fact that the model was calibrated at wetted surface area fraction from 0.1 to 0.3 as well as by the limitations of the empirical equations used to estimate the mass transfer parameters.

### 6.7.6 pH

The pH of the trickling liquid is also significant for the removal of ammonia because it affects the equilibrium of ammonia in the liquid phase and eventually, in the gas phase. As shown in Figure 6.10, the effect of pH on the removal of ammonia was more evident at higher pH values since in alkaline solutions, ammonia tends to exist in its un-ionized form ($NH_3$) than in ionized form ($NH_4^+$). This affects the $NH_3$ equilibrium in the liquid phase, which in turn affects the equilibrium in the gas phase resulting in a higher probability of the un-ionized form to escape into the gas phase, and thus reducing removal efficiency.

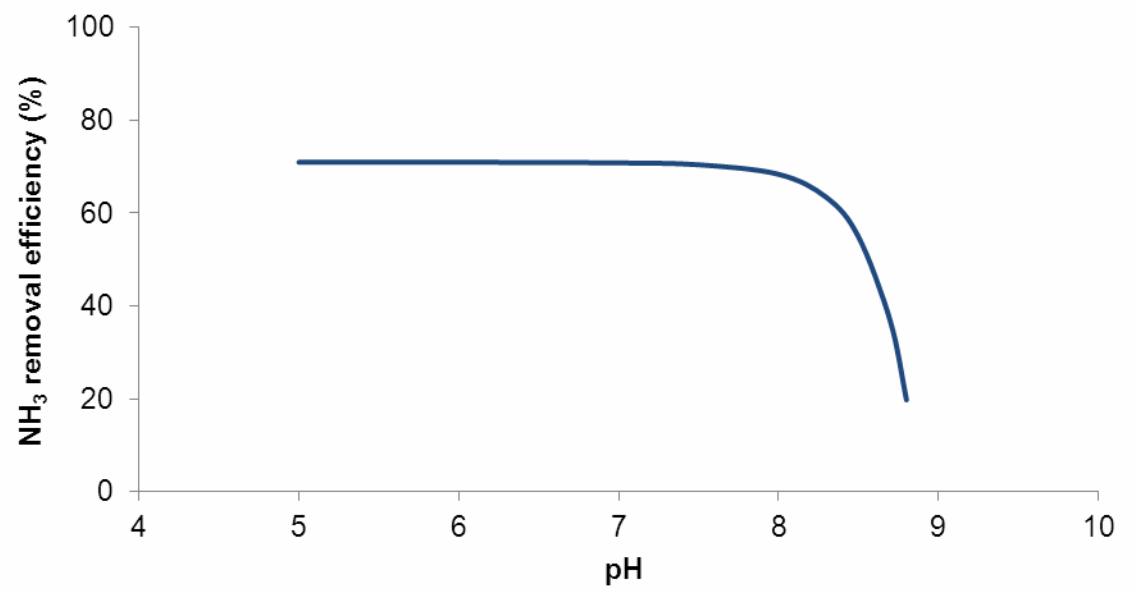


**Figure 6.10 Effect of pH on $NH_3$ removal efficiency.**

Under the conditions (gas inlet concentration of 8.5 $ppm_v$, liquid inlet concentration of 1000 g $N\text{-}NH_4^+$ $m^{-3}$, and temperature of 17°C) utilized in this simulation, it was important to keep the pH below 8. Once the pH reached close to 9, production of ammonia started to occur due to stripping. Instead of absorbing ammonia from the gas phase, the un-ionized ammonia in the liquid phase was stripped out from the solution because its concentration became comparatively higher than the equilibrium concentration. However, it is important to note that the optimum pH changes as operating conditions are changed. Further, only the effect of pH on mass transfer was considered in this study; those that pertain to microbial growth rate were not accounted for.

## 6.8 SUMMARY AND CONCLUSIONS

Simulations using the calibrated and validated model for ammonia removal were performed to evaluate the relationships between the model parameters (i.e. gas flow rate, liquid flow rate/superficial velocity, gas and liquid inlet concentrations, wetted fraction of the surface

area, and pH) and the reactor's performance. Ammonia removal increased with liquid flow rate and EBRT; however, further increases in liquid flow rate did not improve the removal efficiency. Increasing the liquid flow rate might result in preferential flow paths for the gas and liquid, thus, lowering the interfacial area for the gas and liquid mass transfer. Increases in the liquid flow rate could also result in thicker liquid film at the gas-liquid interface, thereby limiting the gas-liquid mass transfer. In addition, at higher liquid flow rates, increasing the EBRT did not improve the removal efficiency. Mass transfer limitation taking place at higher liquid flow rates could be a possible reason for this.

Since ammonia is very soluble in water, the gas and liquid inlet concentrations in the studied range did not affect the removal efficiency. Although a longer filter bed (or a higher EBRT) resulted in higher removal efficiency, a shorter filter bed (or a lower EBRT) was more favourable in terms of elimination capacity. In terms of the wetted surface area, once a minimum fraction of the surface area was wetted, further increases in this parameter provided only very little improvements in the removal efficiency. Furthermore, with similar operating conditions, the two types of packing media resulted in similar removal efficiencies when both had a similar fraction of wetted surface area. In terms of pH, its effect on ammonia removal was more evident at higher pH values. This is because ammonia tends to exist in the un-ionized form ($NH_3$) than in the ionized form ($NH_4^+$) in alkaline solutions. This results in a higher tendency of ammonia to escape into the gas phase, thereby reducing removal efficiency.

Even if some of the values used in the simulations were outside the range of the values used in the model calibration and validation, which might have affected the accuracy of the results, this study still provides useful information in designing a new treatment system or in improving the performance of an existing one.

## 6.9 REFERENCES


Baquerizo, G., J.P. Maestre, T. Sakuma, M.A. Deshusses, X. Gamisans, D. Gabriel and J. Lafuente. 2005. A detailed model of a biofilter for ammonia removal: Model parameters analysis and model validation. *Chemical Engineering Journal* 113: 205-214.

Chou, M.S. and C.H. Wang. 2007. Treatment of ammonia in air stream by biotrickling filter. *Aerosol and Air Quality Research* 7(1): 17-32.

Chung, Y.C. and C. Huang. 1998. Biotreatment of ammonia in air by an immobilized *Nitrosomonas europaea* biofilter. *Environmental Progress* 17: 70-76.

Deshusses, M.A. and Z. Shareefdeen. 2005. Modeling of biofilters and biotrickling filters for odour and VOC control applications. In *Biotechnology for Odour and Air Pollution Control*, ed. Z. Shareefdeen and A. Singh, 213-231. Germany: Springer-Verlag.

Kim, S. and M.A. Deshusses. 2003. Development and experimental validation of a conceptual model for biotrickling filtration of $H_2S$. *Environmental Progress* 22(2): 119-128.

Ockeloen, H.F., T.J. Overcamp and C.P.L. Grady Jr. 1996. Engineering model for fixed-film bioscrubbers. *Journal of Environmental Engineering* 122(3): 191-197.

Popat, S.C. and M.A. Deshusses. 2010. Analysis of the rate-limiting step of an anaerobic biotrickling filter removing TCE vapors. *Process Biochemistry* 45:549-555.

Sharvelle, S., M. Arabi, E. McLamore and M.K. Banks. 2008a. Model development for biotrickling filter treatment of graywater simulant and waste gas. I. *Journal of Environmental Engineering* 134(10): 813- 824.

Sharvelle, S., M. Arabi, E. M.K. Banks and F. Mannering. 2008b. Model sensitivity analysis for biotrickling filter treatment of graywater simulant and waste gas. II. *Journal of Environmental Engineering* 134(10): 826-834.

Sorial, G.A., F.L. Smith, M.T. Suidan and R.C. Brenner. 2001. Removal of ammonia from contaminated air by trickle bed air biofilters. *Journal of the Air & Waste Management Association* 51: 756-765.

Taghipour, H., M.R. Shahmansoury, B. Bina and H. Movahdian. 2008. Operational parameters in biofiltration of ammonia-contaminated air streams using compost–pieces of hard plastics filter media. *Chemical Engineering Journal* 137: 198-204.

# Chapter 7
# General Discussion, Summary, and Conclusions

## 7.1 INTRODUCTION

There is an increasing interest in the application of biotrickling filters for odour and gas emission reductions from pig buildings. Several studies that have been conducted involving pilot and full-scale biotrickling filters units showed the promising potential of this technique. However, despite its advantages, this technique has not yet been efficiently incorporated into barn systems (Ozis et al. 2005), and is still limited by some operational problems. Non-uniform biomass distribution, biomass accumulation, inhibition of microorganisms, and mass transfer limitations are some of the impediments to its effective performance. Despite the research conducted related to the operation as well as to the feasibility of this technique, the complexities of the processes occurring within the system as well as the impact of each of these processes to the overall effectiveness of the system are not yet fully understood. Mathematical models such as the one developed in this study can help better understand these processes as well as identify the factors that have the greatest influence on the reactor's performance. Knowledge of these governing processes and influential factors provides useful information for optimizing the performance of the system.

This chapter discusses the impacts of my thesis research. The discussion on the future work in some areas that may help understand the mechanisms of the system in a more holistic way is also presented here.

## 7.2 GENERAL DISCUSSION

This dissertation work focused on the development of a model describing the removal of ammonia from swine exhaust air using biotrickling filters as well as on the application of the developed model to identify the governing processes, the significant influencing parameters, and their impacts on the removal of ammonia. It would have been desirable to develop a model that could capture the removal of several contaminants, particularly those that were found in Chapter 2 as key odour indicators (i.e. *p*-cresol, dimethyl sulphide, and ammonia); however, choosing ammonia alone as the model contaminant was viewed as adequate to describe the performance of biotrickling filters since ammonia has been reported to account for more than 50% of the odorants in pig barn (Armeen et al. 2008).

The model calibration and validation results presented in Chapter 5 showed the potential applicability of the model in simulating the removal of ammonia in biotrickling filters, despite the several assumptions made in the model equations as well as the probable errors in the experimental data and those made in determining the model parameters.

The predicted values of removal efficiency showed no difference between the two types of packing media used in this study, consistent with the observations from the experimental results. It was surprising that the structured media with a total specific surface area of 984 $m^2 m^{-3}$ had almost the same performance with the non-structured media having a specific surface area of 242 $m^2 m^{-3}$ when both were subjected to similar operating conditions. Results of the sensitivity analysis showed an inverse relation between total surface area and removal efficiency since a higher surface area resulted in a lower removal efficiency when liquid flow rate was held constant. Though it had not been verified in the experimental trials, modelling results showed that the structured media had a lower wetted surface area fraction than with the non-structured media at the same liquid flow rate. This means that if the specific surface area of a packing

material is high, a higher liquid flow rate is required to achieve the same wetted surface area fraction. This implies that though a high specific surface area is important to provide a higher mass transfer area, its wetted portion is more important since the transfer of the contaminants occurs only in the wetted portion. Using the specific surface area as the sole criterion in choosing a packing material is not adequate. Geometry of the packing material that promotes high wetting efficiency should also be considered, so that lower liquid flow rates would be required to achieve adequate wetted surface area. Although increasing liquid flow rates and promoting better liquid distribution could also help achieve high wetting efficiency, distributing liquid at different layers of the bed rather than at the top only could also be a potential solution to improve wetting.

Although the removal efficiency increased with the wetted portion of the packing media, the simulation results showed that the impact was significant only when the wetted portion was within 20% of the total surface area for the structured media or within 40% for the non-structured media. Beyond these values, the impact of the wetted surface area became less significant and the removal efficiencies using both types of media were almost the same. This means that there is a critical wetted surface area that exists that would result in maximum removal efficiencies.

Apart from the packing material's surface area and its wetted fraction, the removal efficiency was also found sensitive to the other factors affecting gas-liquid mass transfer such as the gas diffusion coefficient, gas mass transfer coefficient, gas and liquid flow rates, and the nominal packing diameter. The sensitivity of the removal efficiency to these factors indicates that the gas-liquid mass transfer is a prime mechanism in the removal of ammonia in biotrickling filters. The sensitivity of the removal efficiency to the gas diffusion coefficient and gas mass transfer coefficient and insensitivity to the liquid mass transfer coefficient indicate that the mass

transfer is mainly controlled by the gas phase rather than the liquid phase, an expected mechanism for very soluble gases such as ammonia.

The simulations conducted employing various liquid and gas flow rates showed no remarkable difference in the removal efficiencies between structured and non-structured media, consistent with the observations in the actual experimental trials. The wetted surface area discussed above could be the reason for this observation. Liquid and gas flow rates, as well as empty bed residence time, were found to positively affect ammonia removal due to increased convective transport enhancing mass transfer at higher flow rates and longer gas-liquid contact at higher residence time; however, the impacts of the flow rates were more significant at lower empty bed residence time and became less at higher residence time. This observation could be due to the high solubility of ammonia in water, where most of the influent ammonia is already absorbed at the first few sections of the filter bed resulting to a higher removal at lower residence time (or bed length). However, even if a shorter filter bed seems favourable for the removal of ammonia due to its high solubility, the bed could not be made shorter to achieve the same removal efficiency since adequate surface area is required to support sufficient amount of biomass to oxidize the substrate and keep the liquid-phase concentration low. Further, in a pig barn air where poorly-soluble components are also present, optimum removal of these components must also be taken into consideration.

While the model predicted increasing removal efficiency with the empty bed residence time, the experimental data showed no significant difference ($P = 0.0101$) among the residence times tested (3, 6, and 9 s) except for 9 s (Girard et al. 2013). This was probably caused by the uneven liquid distribution in the experimental trials.

Although a high liquid velocity, as mentioned earlier, would promote high wetting efficiency, there seems to be an optimum liquid velocity that must be delivered to filter beds for

it was found that further increases in liquid velocity did not improve the removal efficiency. A relatively high liquid velocity would probably result in preferential flow paths for the gas and liquid, thus, lowering the interfacial area for the gas and liquid mass transfer. It could also result in thicker liquid film at the gas-liquid interface, thereby limiting the gas-liquid mass transfer.

The simulation results also showed the influence of pH on the removal of ammonia from the gas phase. This was expected since the pH of the liquid affects the equilibrium between the un-ionized ammonia and the ammonium ion in the solution. A higher impact was observed at higher pH where ammonia tends to stay in the un-ionized form, promoting higher possibility to escape into the gas phase, and thereby reducing the removal efficiency. This means that at relatively high pH, stripping would probably occur. The effect of pH on the microorganisms was not accounted for in the model; however, the shake-flask experiment conducted in Chapter 4 using suspension of mixed microbial cultures showed that nitrification was optimum at pH 7.

Due to the high solubility of ammonia, the gas and liquid inlet concentrations did not show significant influence on the removal efficiency. A gas inlet concentration of 45 $ppm_v$ ammonia had almost the same removal efficiency than that of 1 $ppm_v$. In addition, liquid concentrations of 1800 and 120 g $NH_4^+$-N $m^{-3}$ resulted to almost similar ammonia removal efficiency. This means that as long as the liquid concentration is below the equilibrium concentration, it should supposedly not affect the removal efficiency. However, the inhibiting effect of high liquid ammonia concentration to the microorganisms should not be disregarded. Experimental results showed a decrease in removal efficiency when ammonium and nitrite concentrations became relatively high.

None of the biokinetic parameters showed significant impact on the removal of ammonia from the gas phase. However, these parameters have demonstrated significant influences on the removal of ammonia in the liquid phase. This means that they could have an indirect impact on

the removal of ammonia from the gas phase when liquid concentration becomes saturated, and could occur when there is low degradation of ammonia in the liquid phase.

In summary, a model that could describe the removal of ammonia from swine exhaust air using biotrickling filters was successfully developed, calibrated, and validated. Although the model cannot simulate the varying ammonia concentrations in pig barn exhaust air as well as the accumulation of reaction products in the liquid phase of biotrickling filters, the steady-state model developed in this study was able to describe the removal of ammonia in biotrickling filters. The application of the model adequately identified the processes and parameters that significantly affect the performance of biotrickling filters. Further, the model can sufficiently predict ammonia removal profiles and outlet concentrations under certain conditions.

It would have been interesting to correlate the performance of the model on ammonia removal with odour as expressed in the objectives of this study; however, such attempt was not initiated in this study due to a relatively low correlation found in Chapter 2 between ammonia and odour concentrations. Further, the odour emitted from swine buildings is not caused by ammonia alone. Perhaps correlating predicted removal profiles of several key odorants with odour will give meaningful results. Although this was one of the initial plans of this study, it was not fully accomplished due to problems encountered in monitoring the other components and to the overall work required.

## 7.3 GENERAL SUMMARY AND CONCLUSIONS

The ultimate goal of this research was to obtain insights on how to optimize the performance of biotrickling filters in removing odorous gases from swine exhaust air. A hypothesis was formulated that if the processes and the parameters that play important roles in the removal of these contaminants could be properly identified and their effects clearly

understood, then a better understanding of the treatment process could be achieved, which could eventually lead to a better design and process optimisation. Thus, a mathematical model was developed to realize this objective.

Since it is impossible to simulate the removal of all the gaseous odorants in swine facility air, key odor components were chosen to serve as model pollutants. The model pollutants chosen were *p*-cresol, dimethyl sulphide, and ammonia, as presented in Chapter 2. Since different substances are degraded at different rates by different types of microorganisms, the best inoculum to degrade the three model pollutants was selected. The best performing inoculum found in Chapter 3 was the complex inoculum taken from an existing biotrickling filter. Due to known significant impacts of pH on microbial activity, the effect of pH on the degradation of the key odorants with the complex inoculum was evaluated in Chapter 4. The optimum pH found was pH 7. Thus, the biokinetic parameters for the degradation of *p*-cresol and ammonia at various concentrations were determined at this pH. Though the values found for ammonia were relatively higher compared to those published in the literature, these values were used as starting points for a modelling study where more accurate values were determined by fitting the kinetic model to the experimental data.

Chapter 5 discussed the development, sensitivity analysis, calibration, and validation of the model. Though it was originally planned to develop a model for the removal of two or three key odorants, due to problems encountered in monitoring the contaminants, the model was finally developed, calibrated, and validated for ammonia removal only. Based on the calibration and validation results, the model developed can be potentially used to describe the removal of ammonia in biotrickling filters from swine exhaust air. Results of the sensitivity analysis showed that the removal of ammonia from the gas phase is highly sensitive to the parameters related to the gas-liquid mass transfer. Using the calibrated and validated model, simulations were

conducted in Chapter 6 to further evaluate the extent of the impacts of the significant parameters on ammonia removal.

Model and experimental results showed that ammonia removal using the structured media had no significant difference from the non-structured media, which has lower specific surface area and less expensive than the structured media. The wetted portion of the packing material was found more relevant than the total surface area. Further, experimental results showed that removal efficiencies obtained from lower residence time (3 s) or shorter filter bed and lower liquid flow rate (1.8 m $h^{-1}$) were not significantly different from those obtained from higher residence time (6 s) or longer filter bed and higher liquid flow rate (3.6 m $h^{-1}$). This means that filter bed may not be necessarily long or liquid flow rate may not be necessarily high to obtain adequate ammonia removal efficiency. Better liquid distribution promoting high wetting efficiency was regarded more important.

Below are the general conclusions of this study:

1. Ammonia was considered to be the most abundant odorous gas in the air exhausted from swine facilities. Further, *p*-cresol and dimethyl sulphide were found to have high odour indices. In addition, among the pig barn air key odorants identified, *p*-cresol, ammonia, and dimethyl sulphide were found to be not completely removed in biotrickling filter operations. Thus, optimizing the removal of these three odorants could further improve the performance of biotrickling filters in reducing swine odour.
2. Among the three groups of inocula tested in this study, the mixed microbial culture taken from an existing biotrickling filter unit showed the best performance in degrading both *p*-cresol and ammonia. Further, among the microbial strains present in the mixed culture, the *Arthrobacter sp.*, a heterotrophic nitrifier, was found to be the most important in the

biodegradation of *p*-cresol and ammonia. The optimum pH for the oxidation of *p*-cresol and ammonia was observed at pH 7.

3. The biodegradation of *p*-cresol was best described by the Monod equation ($\mu_m$ = 0.1 $h^{-1}$ and $K_s$ = 103.4 mg $L^{-1}$) while that of ammonia was best described by the Haldane equation ($\mu_m$ = 0.17 $h^{-1}$, $K_s$ = 11.9 mg $L^{-1}$, and $K_i$ = 618 mg $L^{-1}$). Though the biokinetic parameters for ammonia were relatively higher compared to those published in the literature, these values were found to be good starting points for a modelling study where more accurate values were determined by fitting the kinetic model to the experimental data.
4. A model that could describe the removal of ammonia from swine exhaust air in biotrickling filters was successfully developed. The model can adequately predict ammonia removal profiles and outlet concentrations as well as identify the governing processes and significant parameters affecting ammonia removal.
5. Since ammonia is a very soluble gas, gas-liquid mass transfer has been found as an important process in the removal of ammonia from the waste air. However, experimental results showed that the limiting process in the overall removal of ammonia in biotrickling filters is the microbial degradation.
6. Due to the high solubility of ammonia in aqueous solution, its removal from the gas phase may not necessarily need a higher residence time or a longer filter bed. However, even if a shorter filter bed seems favourable for the removal of ammonia due to its high solubility, the bed could not be made shorter to achieve the same removal efficiency since adequate surface area is required to support sufficient amount of biomass to oxidize the substrate and keep the liquid-phase concentration low. Further, the presence of the

poorly-soluble components in pig barn air has to be also taken into consideration in the design of the treatment units.

7. Gas and liquid inlet concentrations did not present a challenge to the removal of ammonia from the waste gas at the studied range.
8. The wetted portion of the packing media is a critical factor in the success of ammonia removal in biotrickling filters. Thus, the specific surface area should not be the sole criterion of choosing a packing material. The geometry of the packing material that promotes high wetting efficiency is also important. Moreover, optimizing liquid distribution could help improve wetting efficiency.
9. There is an optimum liquid flow rate that must be delivered to filter bed. Though removal efficiency increases with liquid flow rate due to enhanced convective transport and wetting of the packing media, mass transfer limitations seem to occur at relatively high liquid flow rates.
10. The pH of the liquid has significant impact on the removal of ammonia from the gas phase. Aside from the known negative effects of extreme pH to the growth of the microorganisms, ammonia tends to exist in un-ionized form at higher pH values, thus promoting higher tendency to escape into the gas and thereby lowering the removal efficiency.

## 7.4 CONTRIBUTIONS OF THE RESEARCH WORK

The objective of this study was successfully achieved and its contributions are summarized below:

1. Though there are a few models that have been developed to describe removal of ammonia in biofilters and biotrickling filters, none were calibrated and validated using conditions

that exist in swine production. Thus, the model developed in this study is a useful tool in identifying the governing processes and relevant factors affecting ammonia removal in biotrickling filters from the air emitted from pig production.

2. The information obtained from using the developed model can help optimize system performance.
3. The model developed in this study can be used to predict the impact of certain operating conditions and system designs to ammonia removal that may be applied to existing or new biotrickling filter units in the near future.

## 7.5 RECOMMENDATIONS FOR FUTURE WORK

In this study, different areas have been found where more research could promote better understanding of the removal of ammonia in biotrickling filters. These include:

1. Optimization of ammonia removal in the recirculating liquid

   Since the ultimate goal of ammonia removal is not only in the gas phase but also in the liquid phase, studies to optimize the removal of ammonia in the liquid phase should also be conducted. Several biotrickling filter operations have shown that accumulation of total ammonia and reaction products such as nitrite and nitrate has adverse effects on the microorganisms, which in turn adversely affects ammonia gas removal efficiency. It is therefore equally important to conduct a thorough investigation on the biofilm kinetics so that appropriate solutions can be laid out to enhance biodegradation of contaminants in the liquid phase.

2. Modelling transient condition of pig barn gas emissions

   The flow rate and concentration of the gas emitted from pig barns vary according to the barn's indoor and outdoor conditions. Although the model developed in this study was

calibrated and validated at only one air flow rate, simulation results showed that this parameter has significant influence on ammonia removal. Thus, it is recommended to validate the model at other flow rates to obtain more confidence in the results. Further, although it has been found in this study that the ammonia concentration does not present a challenge to biotrickling filter design and operation in terms of removal efficiency, a model that depicts this variability may help illustrate its impact to microbial growth, and eventually to the contaminant degradation in the liquid phase. By doing this, the factors that cause accumulation of contaminants in the liquid phase may be identified.

3. Model calibration and validation using several key odour indicators

   It has been found that the odour emitted from swine facilities is caused by hundreds of substances. Modelling the removal of more odour components, including their interactions, would deepen and widen the understanding of the application of biotrickling filters on the treatment of swine facility odour, and would provide more concrete solutions for a more effective performance. This, in fact, was the initial plan of this research, but due to circumstances was not fully accomplished.

4. Correlating predicted contaminant removal profiles with odour reduction

   It would be interesting to also apply the model to predict odour reduction as expressed in the objectives of this study. However, since swine odour is caused by many substances, a more meaningful result might be obtained if a correlation is made between removal profiles of several odour components and odour reduction.

## 7.6 REFERENCES

Armeen, A., J.J.R. Feddes, J.J. Leonard and R.N. Coleman. 2008. Biofilters to treat swine facility air: Part 1. Nitrogen mass balance. *Canadian Biosystems Engineering* 50: 6.21-6.27.

Girard, M., M. Belzile, S.P. Lemay, J. Feddes, R. Hogue and S. Godbout. 2013. Innovative air treatment unit for swine exhaust air – Laboratory-scale tests. Paper No. CSBE13-116. Saskatchewan, Canada: CSBE/SCGAB.

Ozis, F., A. Bina and J.S. Devinny. 2005. Future prospects of biotechnology for odor control. In *Biotechnology for Odour and Air Pollution Control*, ed. Z. Shareefdeen and A. Singh, 383-401. Germany: Springer-Verlag.

# Appendices

## Appendix A: Growth media of the pure bacterial strains.

### A.1 DSM medium 756a for *Nitrobacter vulgaris* (Mixotrophic *Nitrobacter*):

Yeast extract……...1.50 g

Peptone ……..1.50 g

Na-pyruvate ……...0.55 g

$NaNO_2$ ……...2.00 g

Trace element solution ……1.00 ml

Stock solution ……..…....100.00 ml

Distilled water ……...……..…….899.00 ml

*pH was adjusted to 7.4 with NaOH or KOH and autoclaved at 115 $^{o}$C for 20 min.*

Stock solution:

$CaCO_3$ ……...……..……..0.07 g

NaCl ……...…….…….5.00 g

$MgSO_4.7\ H_2O$ ……..…….…….……..0.50 g

$KH_2PO_4$ ……....…….……1.50 g

Distilled water ……..……..1000.00 ml

Trace element solution:

$MnSO_4.H_2O$ ……...…….……33.80 mg

$H_3BO_3$ ……..……..…….49.40 mg

$ZnSO_4.7H_2O$……..……..…….....43.10 mg

$(NH_4)_6Mo_7O_{24}$ ……..…….…….37.10 mg

$FeSO_4.7H_2O$ ……..……..…….....97.30 mg

$CuSO_4.5H_2O$ ……..…….……..…....25.00 mg

Distilled water ……..…….……..…...1000.00 ml

*Growth conditions: 28$^oC$.*

**A.2 ATCC medium 2265 for *Nitrosomonas europaea*:**

Solution 1:

$(NH_4)_2SO_4$ (for 50 mM $NH_4^+$).....4.95 g

$KH_2PO_4$.....0.62 g

$MgSO_4.7H_2O$.....0.27 g

$CaCl_2.2H_2O$.....0.04 g

$FeSO_4$ (30 mM in 50 mM EDTA at pH 7.0).....0.5 ml

$CuSO_4.5H_2O$.....0.2 mg

Distilled water.....1.2 L

*Filter sterilized.*

Solution 2:

$KH_2PO_4$.....8.2 g

$NaH_2PO_4$.....0.7 g

Distilled water.....300.0 ml

*Brought to pH 8.0 with 10N NaOH. Filter sterilized.*

Solution 3 (buffer):

$Na_2CO_3$ anhydrous.....0.6 g

Distilled water.....12.0 ml

*Filter sterilized.*

Complete medium:

*Solutions 1, 2, and 3 were combined and dispensed aseptically into desired aliquots. Growth conditions: 26$^{o}$C.*

**A.3 DSM medium 36 for *Thiobacillus thioparus*:**

$(NH_4)_2SO_4$…….…….0.10 g

$K_2HPO_4$…….…… 4.00 g

$KH_2PO_4$…….……..…….. 4.00 g

$MgSO_4.7H_2O$……..…….. 0.10 g

$CaCl_2.2H_2O$…….……..0.10 g

$FeCl_3.6H_2O$…….…….. 0.02 g

$MnSO_4.H_2O$…….…….…… 0.02 g

$Na_2S_2O_3.5H_2O$……..…….. 10.00 g

Distilled water …….……..1000.00 ml

*All ingredients were dissolved in distilled water; pH was adjusted to 6.6; autoclaved at 115 $^{o}$C for 20 min. Growth conditions: 26$^{o}$C.*

**A.4 DSM medium 1 for *Pseudomonas putida*:**

Peptone …….…….. 5.0 g

Meat extract …….……3.0 g

Distilled water …….……1000.0 ml

*pH was adjusted to 7.0; autoclaved at 115 $^{o}$C for 20 min. Growth conditions: 26 $^{o}$C.*

**Appendix B: Silanization procedure.**

1. The glass surface was coated with 5% dimethyldichlorosilane by rinsing with the reagent for 10 to 15 s;
2. The surface was rinsed with toluene two times;
3. The surface was rinsed three times with methanol;
4. The surface was dried with air instead of nitrogen gas.

**Appendix C: Calibration curves.**

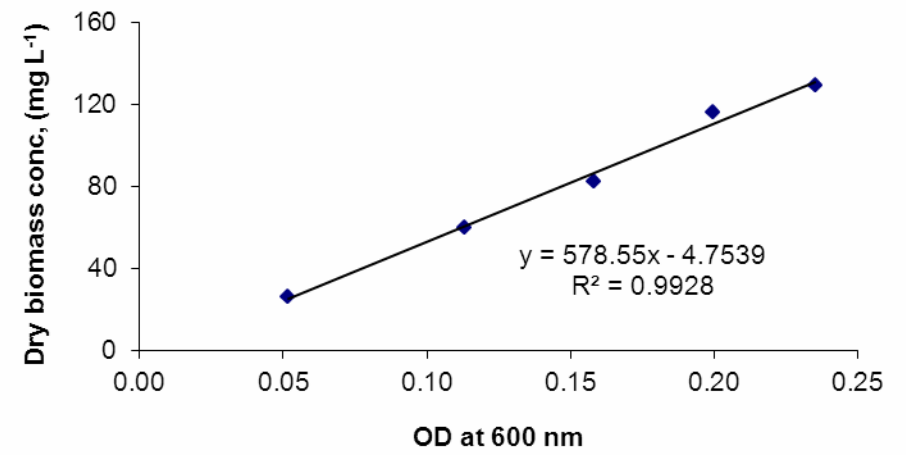


**Figure C.1 Calibration curve for biomass concentration using *p*-cresol as carbon source.**

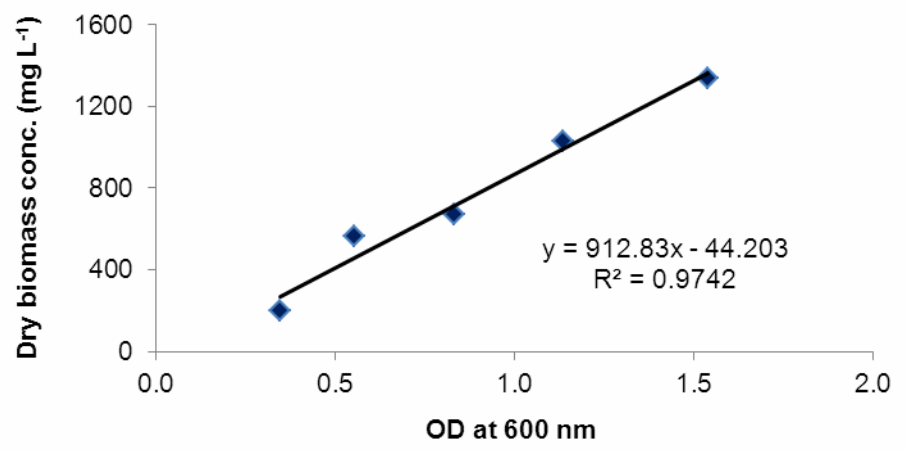


**Figure C.2 Calibration curve for biomass concentration using *p*-cresol and glucose as carbon sources.**

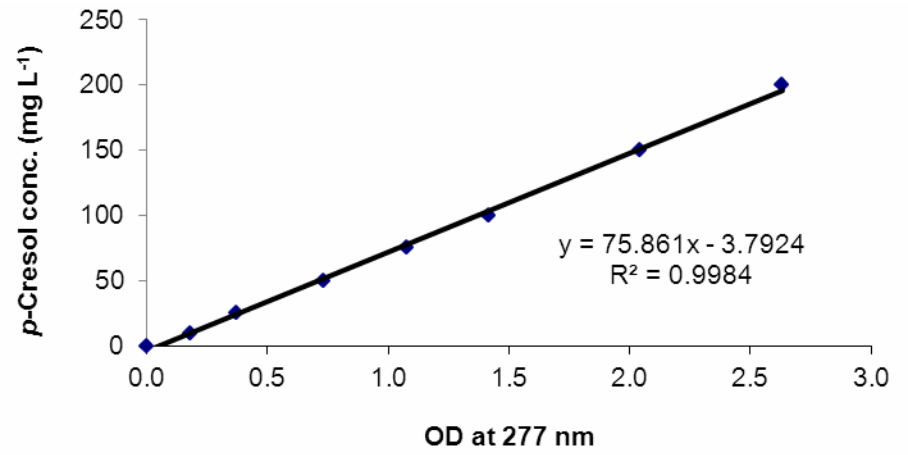


**Figure C.3 Calibration curve for *p*-cresol concentration.**

**Appendix D: $NH_3$, $H_2S$, and odour concentrations measured at the inlet and outlet of the three biotrickling filters during the dates indicated.**

| Date | $NH_3$ concentration ($ppm_v$) | | $H_2S$ concentration ($ppb_v$) | | Odour concentration ($OU\ m^{-3}$) | |
|---|---|---|---|---|---|---|
| | In | Out | In | Out | In | Out |
| 26 Nov 2008[a] | 10 | 4.2 | 29 | 18.2 | 430 | 142 |
| (day 7) | 8.4 | 3.5 | 31.3 | 23.7 | 430 | 352 |
| | 6.6 | 3 | 55.2 | 24.1 | 236 | 157 |
| 03 Dec 2008[a] | 12.2 | 4 | 29.4 | 28.4 | 268 | 55 |
| (day 14) | 9.3 | 3.5 | 44.3 | 33.7 | 328 | 165 |
| | 8 | 3.4 | 34 | 29 | (-) | 126 |
| 10 Dec 2008[a] | 14.1 | 4.7 | 42.7 | 36.5 | 175 | 18 |
| (day 21) | 12.6 | 4 | 68.2 | 60.5 | 474 | 69 |
| | 10.9 | 3.9 | 63.4 | 41.3 | 271 | 50 |
| 17 Dec 2008[a] | 17 | 5.9 | 47 | 36.4 | 348 | 29 |
| (day 28) | 16 | 4.2 | 103.6 | 83 | 357 | 87 |
| | 10.3 | 4 | 91.9 | 37.8 | 356 | 42 |
| 20 May 2009[b] | 5.7 | 2.4 | 13.4 | 6.4 | 161 | 20 |
| (day 7) | 9.1 | 3.6 | 9.6 | 15.8 | 178 | 26 |
| | 6.2 | 2.4 | 105.6 | 8.1 | 186 | 45.6 |
| 27 May 2009[b] | 6.1 | 1.6 | 14.6 | 12.6 | 163 | 75 |
| (day 14) | 9.2 | 1.8 | 13.6 | 10.8 | 152 | 27 |
| | 5.9 | 2 | 13.6 | 9.9 | 100 | 31.7 |
| 03 Jun 2009[b] | 10.6 | 2.2 | 90.7 | 24.9 | 276 | 548 |
| (day 21) | 12.6 | 2.7 | 20.5 | 22.4 | 238 | 37 |
| | 8.3 | 2.1 | 14.1 | 18.8 | 238 | 27.2 |
| 10 Jun 2009[b] | 6.8 | 2.4 | 116 | 26.8 | 343 | 154 |
| (day 28) | 11.8 | 4.7 | 59 | 23.2 | 192 | 89 |
| | 8.5 | 2.1 | 121.5 | 46.9 | 197 | 44.6 |

In: inlet of bioreactors (air directly coming from the pig chambers);
Out: outlet of bioreactors;
(-) means data not available;
[a]Fall/winter trial;
[b]Spring/summer trial.

**Appendix E: VBA program for the simulation of ammonia removal in biotrickling filters.**

A model was developed to simulate the removal of ammonia from swine facility air using biotrickling filters. To carry out the calculation process, a computer program was designed using Visual Basic for Applications (VBA).

VBA is a version of Visual Basic (VB) 6.0 that is used as an internal programming language in many other systems such as Microsoft Office programs like Word and Excel. Unlike VB which can run standalone program, VBA can only run code within a host application. In this study, the code was written in Excel 2010. Thus, the program comes as an Excel (.xlsm) file, which can be run on any computer that is installed with Excel 2010.

Upon opening the file, a main page similar to the one shown in Figure E.1 will appear. The main page has four input command buttons that once they are clicked will open windows that allow input for different types of information, i.e. design parameters, physico-chemical parameters, biokinetic parameters, and simulation options.

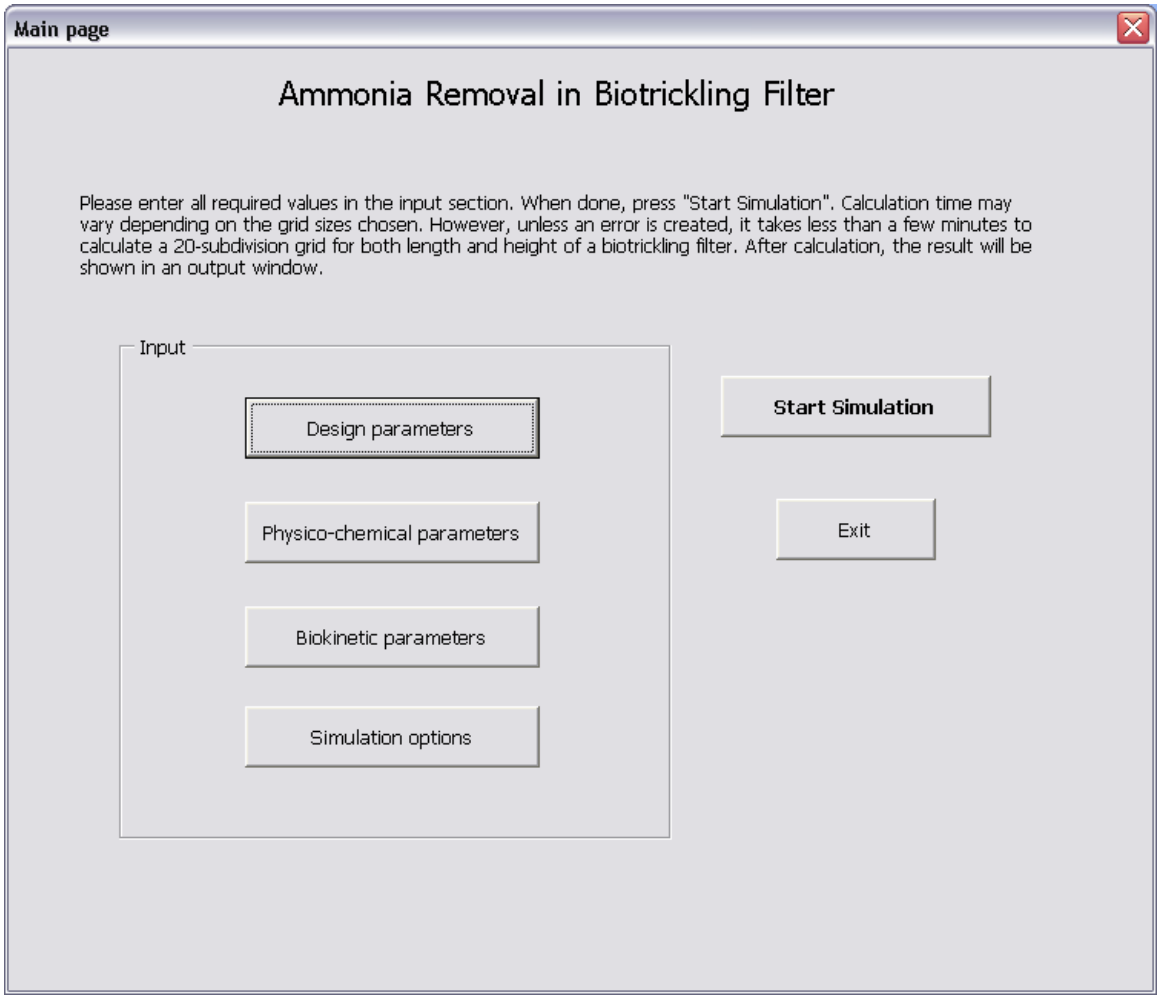


**Figure E.1 Main page of the model.**

When the ″Design parameters″ command button is clicked, a window shown in Figure E.2 will crop up that allows the user to choose the type of packing media utilized. One has to take note that the model was calibrated using these two types of packing media, and that the two media had different model parameters, particularly on the correction factor related to the mass transfer coefficient. After choosing the media and once the ″Okay″ button is clicked, a window shown in Figure E.3 will appear where the design parameters can be entered. Pressing the ″Cancel″ button in Figure E.2 will close the Excel file.

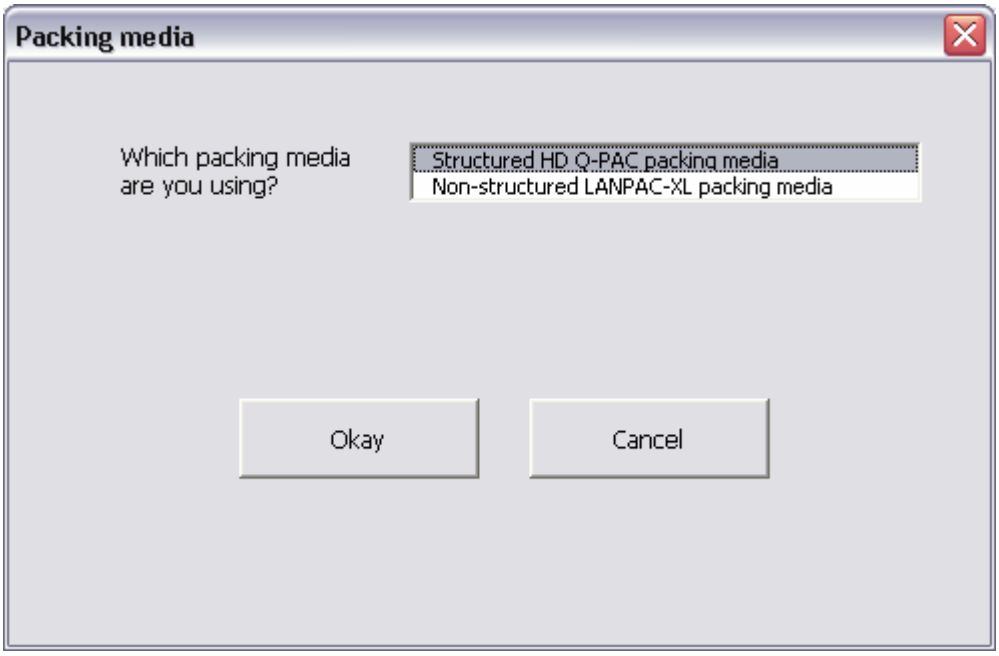


**Figure E.2 Packing media choice form.**

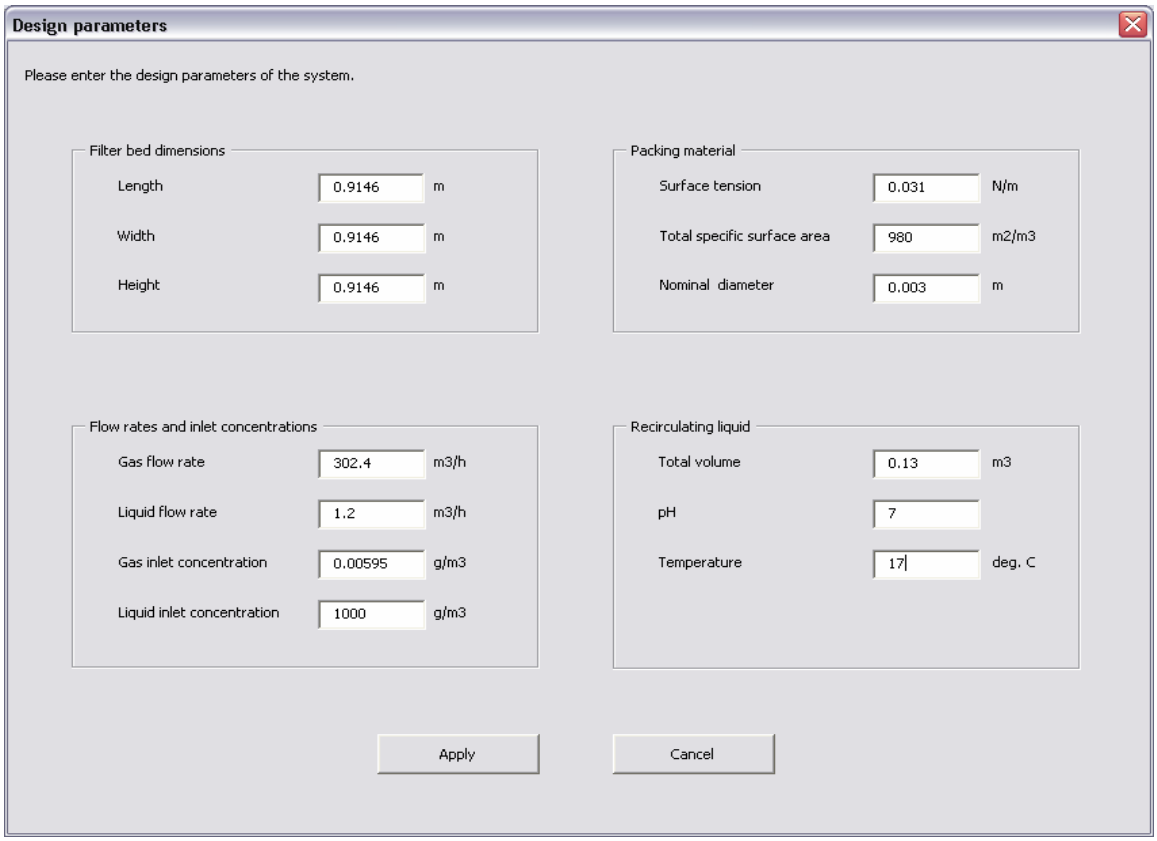


**Figure E.3 Design parameters input form.**

The ″Design parameters″ input form will appear with default values. New values specific to the design of the system under study should be entered. The default values for the packing material need not be changed since the ones provided are for the packing media chosen. Once all the values are entered, the “Apply” button should be pressed to update the values and to return to the Main page. Clicking the other input command buttons in the Main page (i.e. Physico-chemical parameters, Biokinetic parameters, and Simulation Options will show the forms shown in Figures E.4, E.5, and E.6, respectively. These forms will also appear with default values. All these values can be changed except the number of subdivisions in the biofilm thickness (Figure E.5), which was fixed at five. Similarly, after entering the values, the “Apply” button in each of these forms should be pressed to update the values and to bring back to the Main page. Pressing “Cancel” in Figures E.3 to E.6 will cancel the data entered, close the window, and bring back to the Main page.

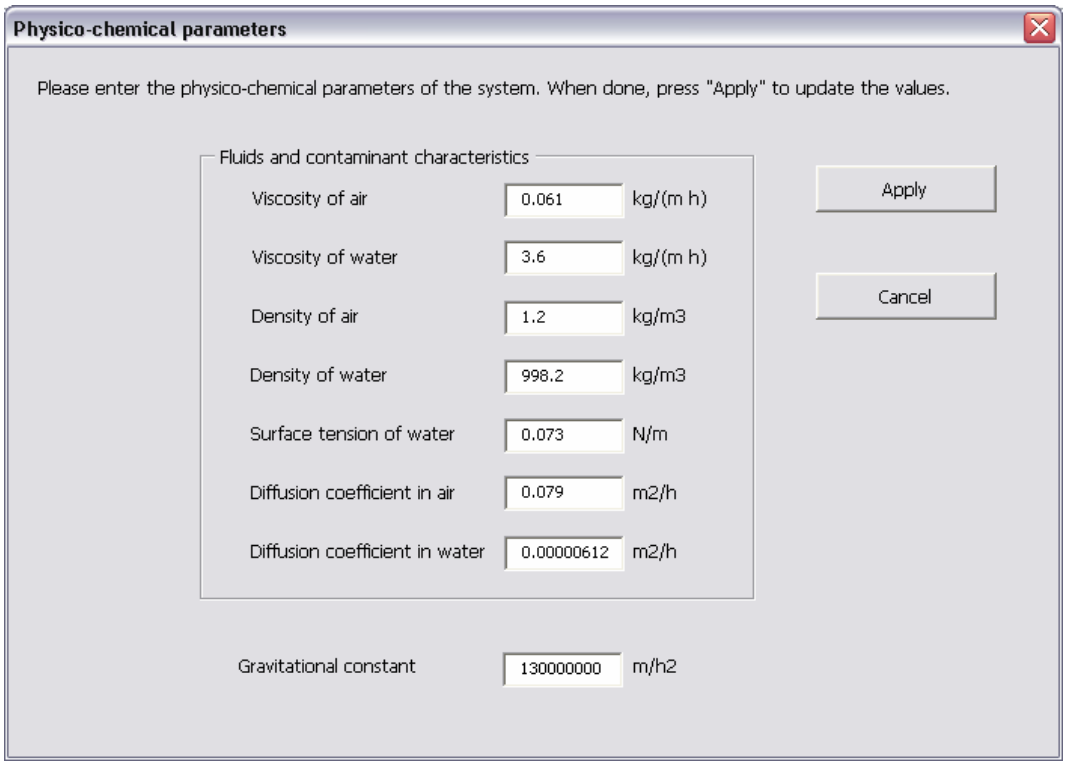


**Figure E.4 Physico-chemical parameters input form.**

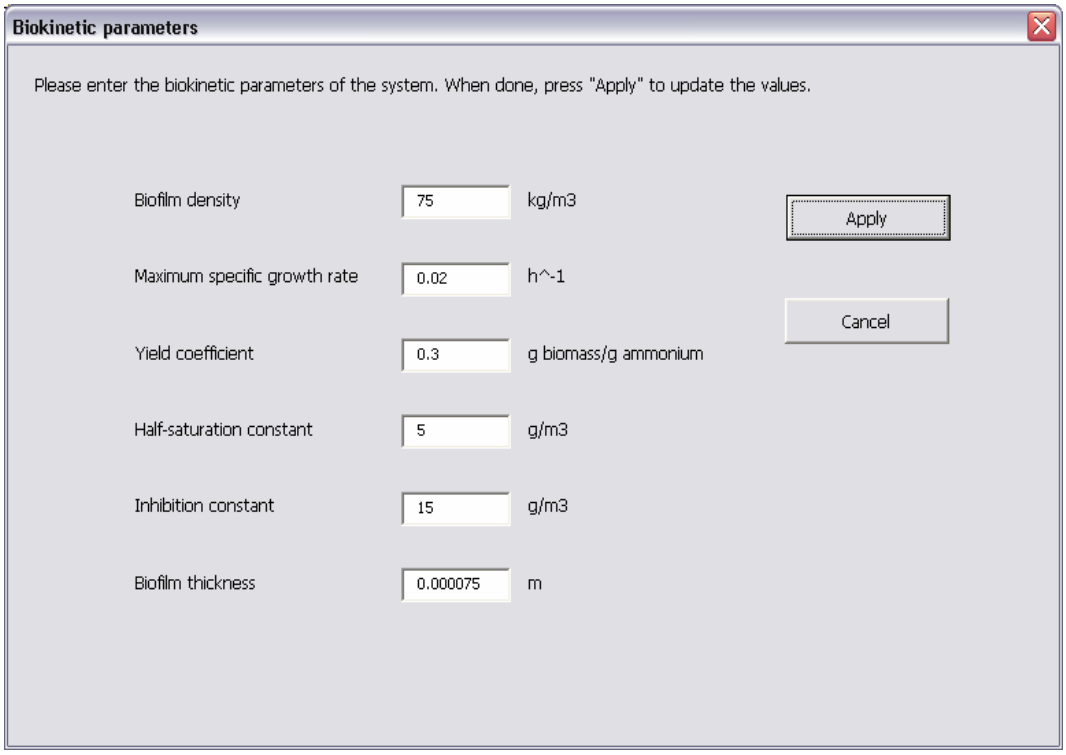


**Figure E.5 Biokinetic parameters input form.**

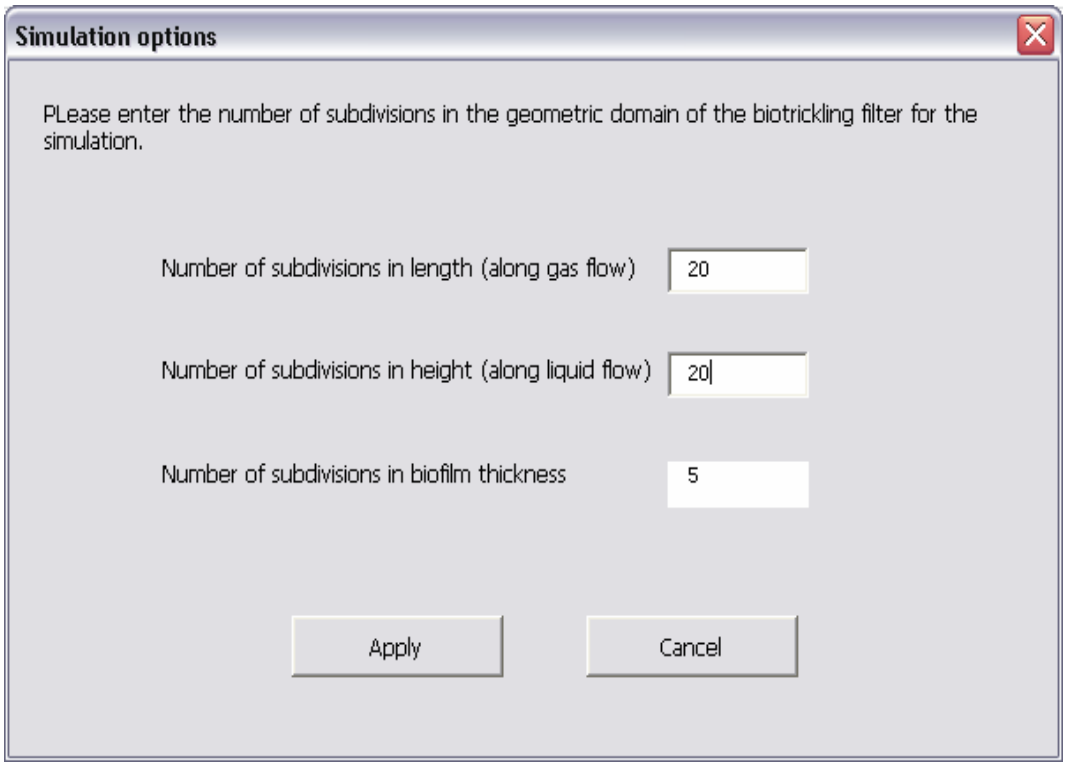


**Figure E.6 Simulation options input form.**

When all the input values are already entered, the “Start Simulation” button can then be pressed to start the calculation. Calculation time may vary depending on the grid sizes chosen. However, unless an error is created, it will take less than a few minutes to calculate a 20-grid size for both length and height of a biotrickling filter. When calculation is completed, an output window similar to the one presented in Figure E.7 will appear showing the percent removal efficiency. Clicking the “Exit” buttons in Figures E.1 and E.7, as well as the red “X” buttons in the upper right hand of all the forms, will close the Excel file. Clicking the “Return to the Main page” button in Figure E.7 will bring to the Main page to start another simulation.

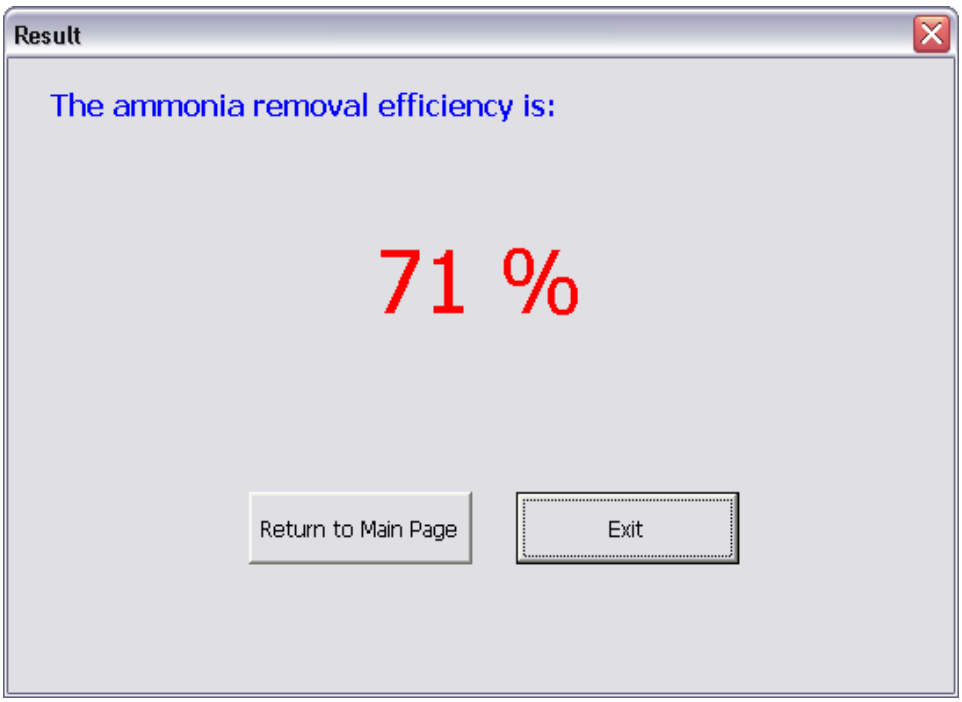


**Figure E.7 Output window.**

The flowchart of the program is presented in figure E.8. To protect the code, it is hidden from the user. The user only interacts with the model by entering the input values and by viewing the results. As long as all the values entered are positive (greater than zero), the program should work without any problem; hence, values verification is implemented in the program.

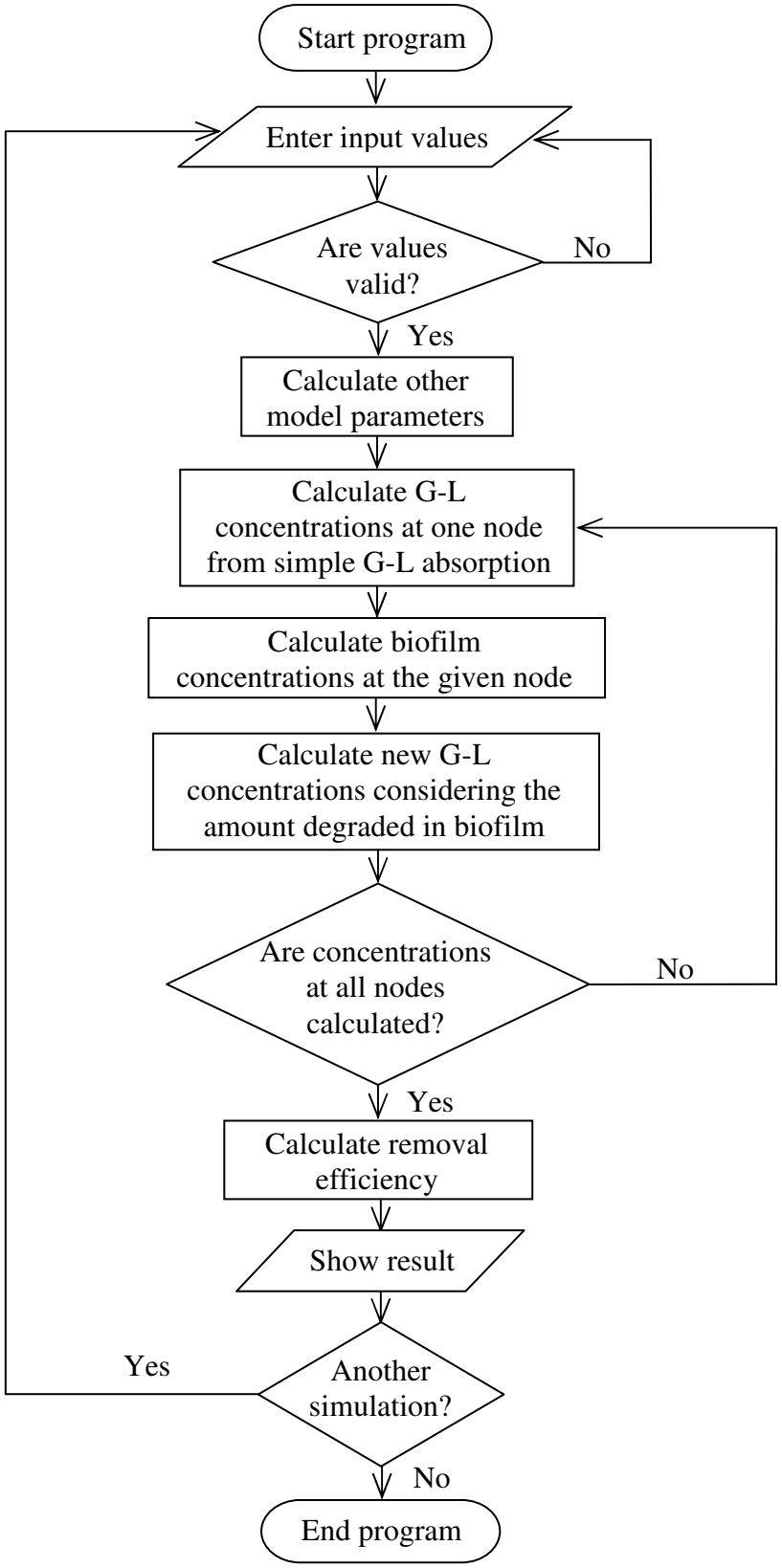


**Figure E.8 Program flowchart.**